THREE PHASE POWER SYSTEM

HARMONIC PENETRATION

A thesis
presented for the degree of
Doctor of Philosophy in Electrical Engineering
in the
University of Canterbury,
Christchurch, New Zealand

by

T.J. Densem B.E. (Hons)

1983

Harmony would lose its attractiveness if it did not have a background of discord.

TEHYI HSIEH

TABLE OF CONTENTS

LIST OF FIGURES

LIST OF TABLES

LIST OF PRINCIPAL SYMBOLS

a	transformer tap ratio
abc	phase components
ABCD	transmission line parameters
AC	alternating current
AC/DC	alternating to direct current conversion
C	capacitance
$[C]$	connection matrix
DC	direct current
EPM	equivalent PI model
f	frequency
G	generator
GMR	geometric mean radius
h	harmonic order
HVDC	high voltage direct current
I_h	current at harmonic h
L	inductance
$[M]$	matrix of normalized eigenvectors
NPM	nominal PI model
p	primary
PCC	point of common coupling
P	real power
POI	point of injection
POS	point of supply
prim	primitive
pu	per unit
Q	reactive power
r	radius
R	resistance
RYB	red, yellow and blue phases
s	secondary
t	thickness
V_h	voltage at harmonic h
x	length
$[Y]$	shunt admittance matrix
Y'	shunt admittance of a transmission line per unit length
Y_h	admittance at harmonic h

$[Z]$	series impedance matrix
Z'	series impedance of a transmission line per unit length
Z_{fh}	filter impedance at harmonic h
Z_{sh}	AC system impedance at harmonic h
Zo	characteristic impedance
+ - o	sequence components
α	attenuation constant
β	phase constant
γ	propagation constant
γ_j	jth eigenvalue

ABSTRACT

Three phase harmonic penetration software is developed and tested using measured results from the New Zealand power system.

The unbalanced nature of the impedances, currents and voltages usually present in a power system is illustrated. The versatility of the algorithm to provide accurate information for studies of convertor interaction and single phase traction supplies is clearly indicated.

Practical problems encountered in harmonic modelling are discussed, particularly the adequacy of available component data and the validity of models using this data.

Harmonic spillover interference to load management equipment operating above fundamental power frequencies is of practical significance, and the levels of such interference for a proposed frequency change are investigated.

A commitment to three phase modelling must be justified, and situations are determined where simpler single phase modelling is acceptable.

ACKNOWLEDGEMENTS

I wish to express my sincere thanks to my supervisors, Professor J. Arrillaga, Dr P. Bodger and Dr B. Harker for their advice, assistance and loyalty throughout the course of this research.

Special recognition is due to my employer, New Zealand Electricity. The wholehearted technical and financial support of this research is deeply appreciated.

The intial financial help of the University Grants Committee is gratefully acknowledged as is the technical assistance given by Chris Currie, John Baird, Hermann Dommel and Neville Ross. Their experience and helpful advice has been invaluable.

Thanks are due to my postgraduate colleagues for their useful comments and words of encouragement. The computer results in this thesis would not have been possible without the tireless efforts of Bill Kennedy and the graphics software written by Steve Gellen.

Christine McEntee's typing of this thesis has been excellent.

Finally, to those family and friends who cared, I offer my warmest thanks.

CHAPTER 1

INTRODUCTION

Problems associated with the propagation of harmonic currents in electric power systems are extensive, affecting both the economics of operation and security of supply. The cost of interference with load management equipment and telephone circuits is large, and the solutions expensive. Also, the failure of power system components and the maloperation of equipment as a result of high levels of harmonic voltages and currents causes less secure system operating conditions. These wide repercussions, coupled with increasing levels of harmonics, have prompted interest in analysis of the penetration of harmonics in power systems.

An understanding of harmonic penetration requires the coordinated development of both measurement and digital computer simulation techniques. This thesis discusses the simulation aspect, combining the techniques used in fundamental frequency three phase power flow and single phase harmonic modelling, to develop three phase harmonic penetration software. The use of unbalanced analysis in three phase systems leads to more accurate simulation of the propagation of harmonics.

In Chapter 2 some fundamental concepts of harmonic analysis in power systems are discussed and the limitations of present modelling techniques are illustrated using comparisons with measured data. Often measurement is not practical at harmonic frequencies, and simulation is presented as a complementary tool to measurement techniques in this situation.

Chapter 3 discusses the development of harmonic modelling leading to the present work in three phases. Requirements for harmonic software are stated, and the need for a different approach to that used in single phase modelling is indicated. The purpose of the individual programs is explained and the development of the penetration program, HARMAC, is described. Admittance matrix techniques are utilized and the inclusion of system elements into these matrices using phase components is detailed.

Chapter 4 includes the three phase harmonic frequency modelling of shunt capacitors, filters, generators, loads and transformers. The wide range of models available is presented together with the evidence for the validity of each representation.

Chapter 5 details the modelling of three phase transmission lines including skin effect. The ability of the three phase model to match known unbalanced conditions is confirmed and the effect on system harmonic levels of convertor transformer connection is investigated.

In Chapter 6 a small test system is progressively developed to assist in the understanding of harmonic penetration, without the complications of a large interconnected grid. The damping and resonant effects of the transformers, generators and loads are discussed. The connection of unbalanced harmonic loads is simulated showing the ability of three phase techniques to accurately model such situations.

Chapter 7 utilises test results to confirm modelling techniques on a large power system. The sensitivity of system voltages to variations in individual component impedances is used to determine the adequacy of present data. Single phase and three phase analysis techniques are also compared and a number of different cases are tested to illustrate the versatility of the software.

Chapter 8 studies the problem of ripple control spillover, where load management signals from a distribution authority penetrate, via the transmission system, to other distribution authorities. If the ripple relays are sensitive to these signals then unscheduled load switching can occur. The differences between single phase and three phase modelling techniques are illustrated on the complete system of the South Island of New Zealand.

Finally in Chapter 9 the main conclusions to this thesis are discussed along with directions for further endeavour.

CHAPTER 2

REVIEW OF POWER SYSTEM HARMONICS

2.1 BASIC CONCEPTS

A number of terms are commonly referred to in the field of power system harmonics. A harmonic is defined as a sinusoid whose frequency is an integral multiple of the actual system frequency. The order of a harmonic is the ratio of the harmonic frequency to the fundamental frequency. Harmonic analysis is described as the process of measuring or calculating the magnitude and phase of the harmonic components contained in a waveform. The full set of harmonics present forms a Fourier series which, when summated, replicates the original waveform.

When a non-sinusoidal waveform is viewed on an oscilloscope its shape is observed in the time domain. That is, for any given instant in time, the amplitude of the waveform is displayed. Time is normally drawn on the horizontal axis with increasing time to the right. This waveform can also be described in the frequency domain. If the basic repetition frequency of a square wave was say 50 Hz, and it was applied to a hi-fi amplifier, then the ear would hear the resultant sound as a mixture of many frequencies. That is, it would sound like a full musical chord. The waveform may therefore be described by its time domain data or its frequency domain data. The transfer from the time domain to the frequency domain is accomplished by a Fourier transformation.

The function of a power system is to provide consumers with a purely sinusoidal voltage supply of constant amplitude and frequency. The presence of harmonics causes the character of the supply to deviate from this ideal by introducing distortion into the wave shape.

Power system harmonics are not new phenomena. As a form of power system pollution harmonics have been present since the inception of alternating current systems, generated by components such as transformers. The non-linearity of transformer magnetic circuits results in a non-sinusoidal magnetising current being drawn from the system. This current distortion consists principally of harmonics below the 10th harmonic. Transformer non-linearity is not treated in this thesis. It is however becoming more important because the increasing flux densities used in modern transformers increase the likelihood of transformer saturation and hence harmonic production (Lopez et al 1977).

The major contribution to system harmonic content comes from the various non-linear loads connected to the transmission network, of which the most important are the various forms of static power convertor. Harmonics are introduced into the power system by these devices due to the non-linear frequency relationship between voltage and current. The proliferation of non-linear HVDC plant and domestic appliances (Blommaent et al 1977, Carroll et al 1977, Evers 1980 and Orr et al 1982) is on the increase, and will lead to increased harmonic levels.

The alternating current waveform associated with an HVDC convertor may be considered to be the smooth direct current distributed between the three phases of the AC system in the form of rectangular blocks. In turn, this rectangular wave shape can be considered as being composed of a fundamental sinusoid and harmonic components. Only the fundamental is of prime interest in the transfer of power between the AC and DC systems. The harmonics are generally an unwanted product of the conversion process.

The study of harmonic currents and voltages propagating in the AC power system, is termed harmonic penetration. This thesis is concerned with harmonic penetration in the transmission system, which includes modelling from the harmonic sources through the transmission lines to the generators and load centers.

2.2 HARMONIC POWER FLOWS

To analyse harmonic power flows, the system equivalent circuit as depicted in Figure 2.1 has been used by Tschappu (1981). The generator G constitutes a fundamental sinusoidal voltage source and it supplies a resistive load controlled with a static convertor via the system impedance Zs.

Figure 2.2 illustrates the equivalent circuit diagram for the fundamental frequency. The generator supplies, via the point of common coupling (PCC), the fundamental power Pg1, which flows to a large extent as P&1, to the load and to a lesser extent, as Pc1 to the convertor. This portion is transformed into harmonic power. In addition to this, the system losses Ps1 in the resistance Rs of the system impedance are supplied.

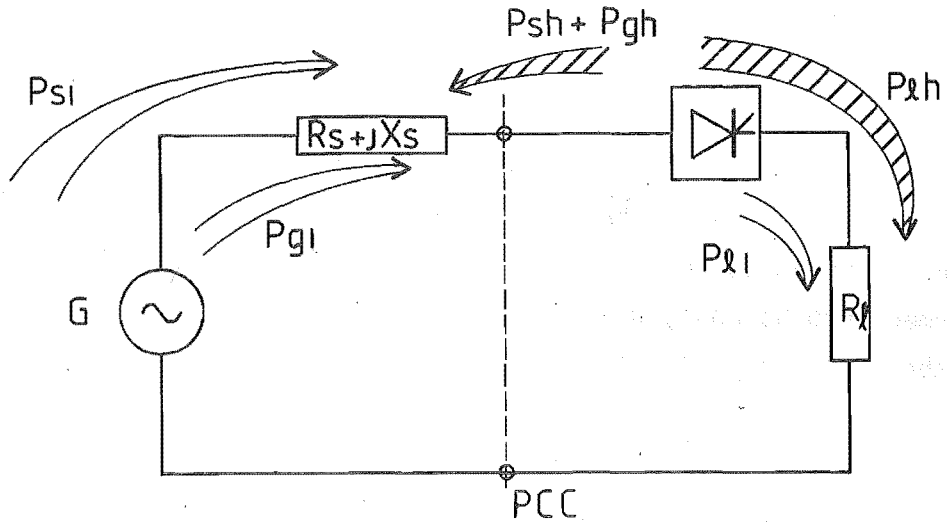

FIGURE 2.1: Schematic of Power Flow in the AC System

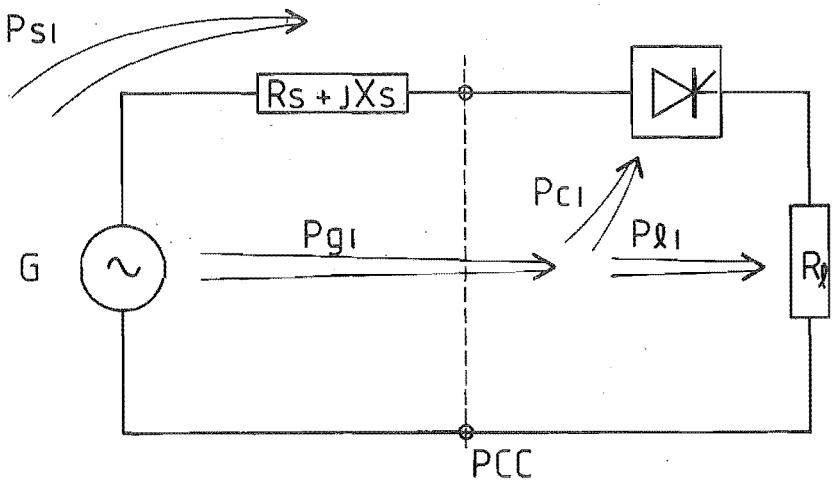

FIGURE 2.2: Schematic of Fundamental Frequency Power Flow

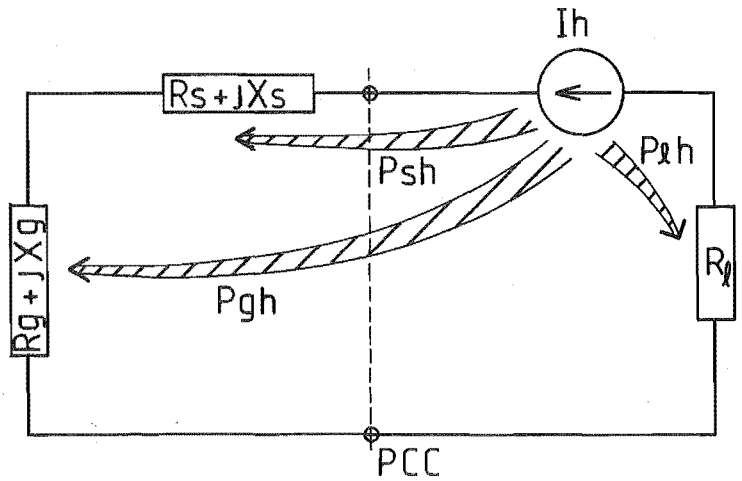

FIGURE 2.3: Schematic of Harmonic Power Flow

In Figure 2.3 the equivalent circuit diagram for the harmonic power flow is depicted. Since the generator voltage is sinusoidal it can only supply fundamental power and it is included in this diagram as a harmonic impedance. The convertor appears in place of the generator as an impressed harmonic current source. A small portion of the fundamental power Pc1, transformed into harmonic power, is fed as Psh and Pgh back to the resistance of the system and the generator, and the large portion, Pℓh, to the load. Since Rs and Rℓ are connected in series, the ratio of Pℓh/(Psh + Pgh) can also be expressed as Rℓ/(Rs + Rg). In practice, Rℓ/(Rs + Rg) is very large, and for this reason, the portion of harmonic power propagating in the AC system remains small even when the current is badly distorted.

The total losses in the system impedance are composed of the fundamental power Ps1, supplied from the generator, and the harmonic power of the convertor, Psh + Pgh. The harmonic loss in the system incurred on the generator side of the point of common coupling, is debited to the supply authority. This loss in the system is larger by the ratio (Psh + Pgh)/Ps1 than with linear loading.

2.3 HARMONIC EFFECTS ON POWER SYSTEM PLANT

Whether or not the harmonic power is considered as useful or unwanted, is dependent upon the type of load. If the harmonic power serves to produce heat in a heating load, then it constitutes useful energy. However, when converting electrical power into mechanical work, e.g. when using an induction motor, the harmonic power gives rise to additional heating in the stator and rotor windings. The efficiency of the motor is thereby reduced. In this case, the harmonic content of the supplied power is considered to be detrimental.

Other effects on power system equipment of a distorted supply are also documented. They include telephone interference where lines run in close proximity to power transmission lines (Klewe 1958), protection maloperation (IEEE Working Group 1981), metering inaccuracies (Baggott 1974), losses (Klingshirn and Jordan 1968), capacitor failure (Gates 1979), ripple control spillover (Ross 1972) and unstable operation of static convertors (Yacamini and de Oliveira 1980a).

More general material can be found in Kendall and Johnson 1977, Arrillaga 1981 and Owen et al 1980. It is not the purpose of this thesis to discuss this work in any detail.

2.4 HARMONIC MODELLING

2.4.1 Introduction

There are a number of areas where harmonic modelling can be usefully employed. The major assumptions in each area, the limitations and the extent to which more investigations are required, will be discussed.

2.4.2 Balanced Harmonic Penetration

Figure 2.4 illustrates two sets of balanced harmonic currents, $I1_h$ and $I2_h$, of order h, injected into any busbar of an AC system. A large power system is likely to have a number of such injections. The resultant system harmonic voltages are calculated by direct solution of the linear equation:

$$[I_h] = [Y_h][V_h] \qquad (2.1)$$

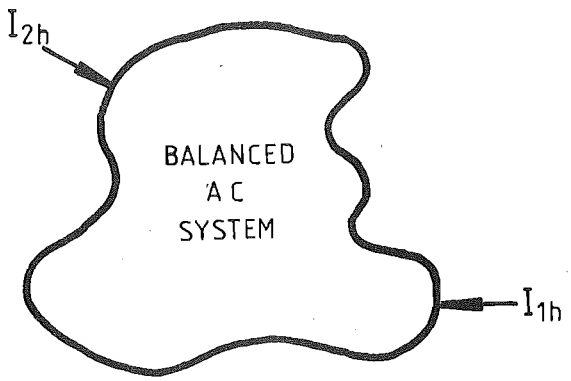

FIGURE 2.4: Balanced Current Injection into a Balanced AC System

An assumption generally made is that the AC system is balanced and can therefore be modelled by the positive sequence component impedances (McGranaghan et al 1981 and Breuer et al 1982). The validity of this assumption will be examined in Chapters 7 and 8.

One limitation of this algorithm inherent in all modelling to a lesser or greater extent is the accuracy of the data. The adequacy of presently available data needs to be determined.

The above algorithm models the steady state behaviour of a power system. Unfortunately the harmonic behaviour of a physical system changes as loads, generators and line configuration alter. It is difficult with a steady state model to obtain more than a few "snap shots" of a continuously varying system.

A power system is three phase and will have imbalance between phases due to transmission line conductor assymetry and load imbalance. By modelling these imbalances, illustrated in Figure 2.5, more accurate simulations will be possible. In such a system the current injections, I1h-I3h and I4h-I6h, can be unbalanced in magnitude and phase angle. In a similar manner to the balanced system the current injections for each frequency are presumed constant and known and the linear equation (2.1) is solved directly to obtain the three phase harmonic voltages. Investigating three phase harmonic penetration forms the bulk of the work in this thesis.

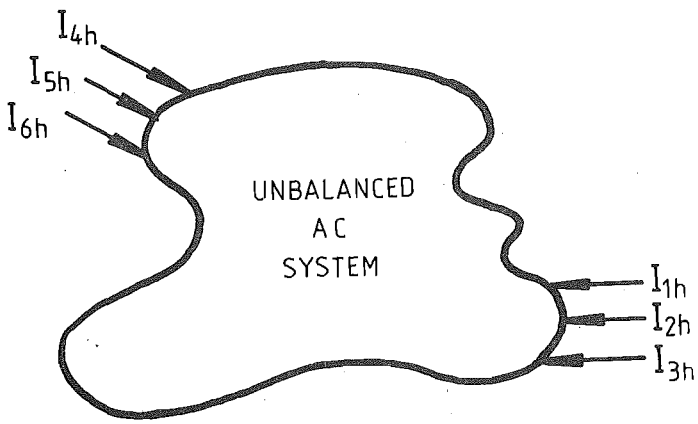

FIGURE 2.5: Unbalanced Current Injection into an Unbalanced AC System

2.4.3 System Impedances for Filter Design

AC harmonic filters play an important role in limiting harmonic levels on the AC system to acceptable values. While the cost of filters represents a minor part, 10-15%, of a DC terminal, requirements for DC system performance and compatibility with the AC system are dependent on sound AC filter design (Breuer 1983).

To achieve adequate performance levels requires information on characteristic and non-characteristic harmonic generation of the convertor, harmonic impedances of the AC system, frequency swings, voltage swings and VAR requirements of the AC system (Lacoste et al 1979). This then allows the selection of a harmonic filter configuration, (Steeper and Stratford 1976, Pileggi and Emanuel 1982 and Szabados 1982).

In steady state operation, harmonic currents are determined by the convertor configuration and by the system parameters. Characteristic harmonics are produced by an ideal convertor (i.e. for a 12 pulse convertor these will be 12k +/- 1, where k is a positive integer).

The Fourier series for the normalized current waveform of an ideal 12 pulse convertor is:

$$\frac{4\sqrt{3}}{\pi}\left[\cos(wt) - \frac{1}{11}\cos(11wt) + \frac{1}{13}\cos(13wt) + \ldots.\right] \qquad (2.2)$$

The harmonic magnitudes are equal to that of the fundamental current divided by the harmonic order (Arrillaga 1983).

All other harmonics are termed noncharacteristic and are produced by AC system voltage magnitude and phase imbalance, convertor transformer reactance differences and control firing angle assymmetry. The injection of harmonic currents into the AC system results in harmonic voltages which are a function of the AC system harmonic impedance and harmonic current flow throughout the AC network.

To mitigate the harmonic current flow into the network, filters are applied on the convertor bus as shown in the single line diagram of Figure 2.6. The model representation of Figure 2.6 shows the harmonic current flow into the combination of filter, Z_f, in parallel with the system including generation and loads, Z_s, which permits calculation of individual harmonic voltages, V_h.

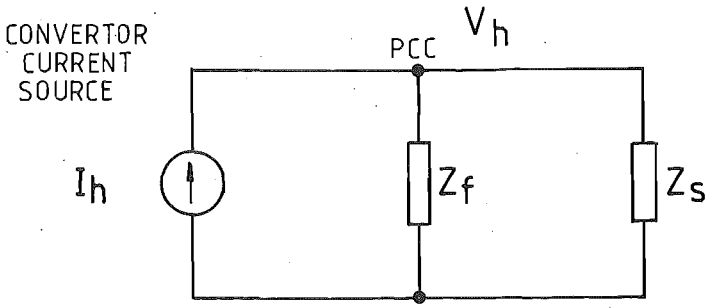

FIGURE 2.6: Filters Connected to a Convertor Busbar

Accurate system impedances are required because of the possibility of resonance between the filters and system impedances, and the need to meet both voltage and current specifications at the point of common coupling.

Initial design of filters for HVDC applications proved to be unsatisfactory (Gunn 1966, Jarrett and Csuros 1966 and Huddart and Brewer 1966), a major reason being poor system impedance representation at harmonic frequencies. Subsequent design concepts became conservative because of these experiences and the inability to match measured with simulated system impedances (Laurent et al 1962 and Melvold 1972). After successful filter installations (Vithayathil 1973), attention has focussed on more appropriate filters by utilising better system impedance representation (Breuer et al 1982 and Abramovich et al 1982). The attainment of more accurate system impedances will be investigated in Chapter 7.

2.4.4 Unbalanced Convertor Operation

Figure 2.7 illustrates an equivalent circuit suitable for the analysis of unbalanced convertor operation. The convertor generates harmonic currents, I_h, which propagate in the parallel system and filter impedances causing harmonic voltages to be present at the convertor terminal busbar. A number of convertors may be attached to the same busbar.

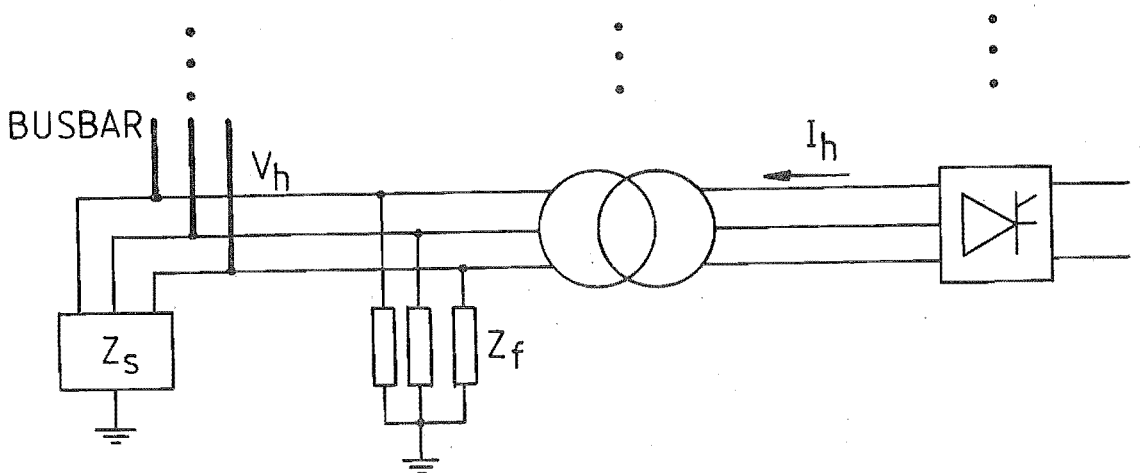

FIGURE 2.7: Three Phase Convertor with Approximate System Impedances

Early convertor investigations involving fundamental frequency imbalance were performed by Phadke and Harlow (1966). Considerable work on improved control strategies to solve harmonic instabilities was initiated by Ainsworth (1967). Further investigations were performed on digital computers for harmonic voltage and firing angle imbalance by Reeve and Krishnayya (1968), Phadke and Harlow (1968) and Reeve et al (1969).

The interaction of convertor current injections with system voltages, leading to a more accurate convertor representation, was undertaken by Reeve and Baron (1970). It was not until Yacamini and de Oliveira (1980a) that convertor interaction was generalised for any configuration at the injection bus. Transformer saturation was included in this study. The complete range of interactions including accurate DC system impedance modelling was discussed by Yacamini and de Oliveira (1980b) and Yacamini and Smith (1983).

The AC system in the above studies has been represented in an approximate form by either an impedance based on the short circuit ratio, a tee equivalent circuit Bowles (1970) or a balanced impedance locus, Reeve and Baron (1970). The first approach using the short circuit ratio is an unsatisfactory representation (Kauferle et al 1970), and only by using measured or simulated impedances calculated for the whole network can realistic studies be performed. Results using unbalanced AC systems have not been investigated. The provision of three phase impedance modelling will make this possible.

The situation with a single injection point into the AC system can be generalised to a number of injection points, each point being connected to a separate busbar. This is represented in Figure 2.8. The calculation of three phase system impedances will also enable such studies to be performed.

A basic premise of the convertor analysis discussed, is that the fundamental frequency power flow is unaltered by the superposition of harmonic voltages at the point of harmonic injection into the AC system. Initial studies of the operating state of a convertor with harmonic power flow included have been performed by Xia and Heydt (1982). These studies were however restricted to characteristic harmonics and no three phase results were presented.

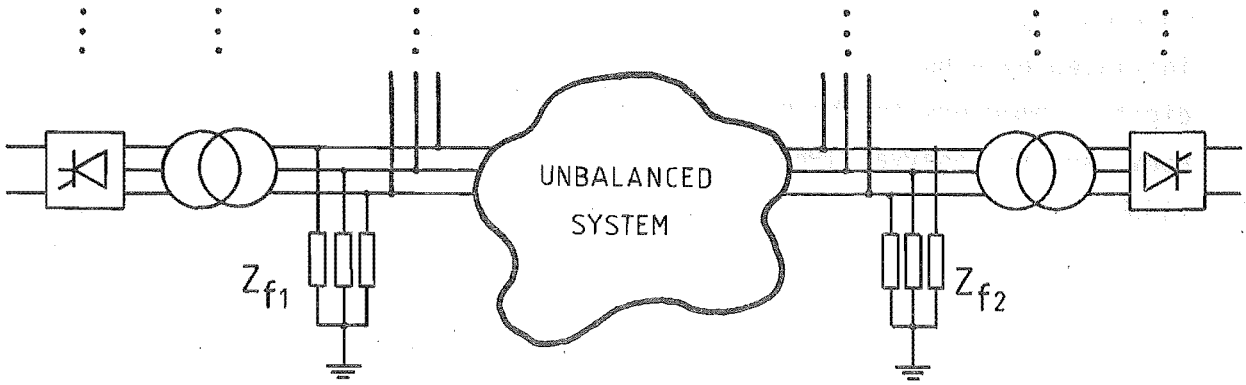

FIGURE 2.8: Convertors Attached to Different Busbars of the Unbalanced AC System

2.5 MEASUREMENT OF HARMONICS

Measurement of harmonics is carried out for a number of reasons; to provide background levels for planned installation of plant, to provide impedance data for filter design, to enforce harmonic limits, to determine the propagation of audio frequency control signals or to determine solutions to harmonic problems on installed plant. Measuring in these different areas requires different equipment and can be achieved to varying degrees of success.

Multiple frequency measurement is often required, but because transducer calibration and instrumentation accuracy is difficult, this is an exacting task (Pesonen et al 1981).

Figure 2.9 indicates the components of a harmonic measurement system. The transducers are either for measuring current or voltage and give replicas of system conditions. They may be connected to a number of instruments to record the waveform, analyse the harmonic content or display the time domain information to an operator, for example. Measuring the small quantities of harmonics in the presence of 50 Hz power flow is also difficult, without consideration of the electromagnetic environment the measuring system is required to perform in. Measurement systems have not yet been developed that allow accurate reliable measurements to be made at a number of locations simultaneously.

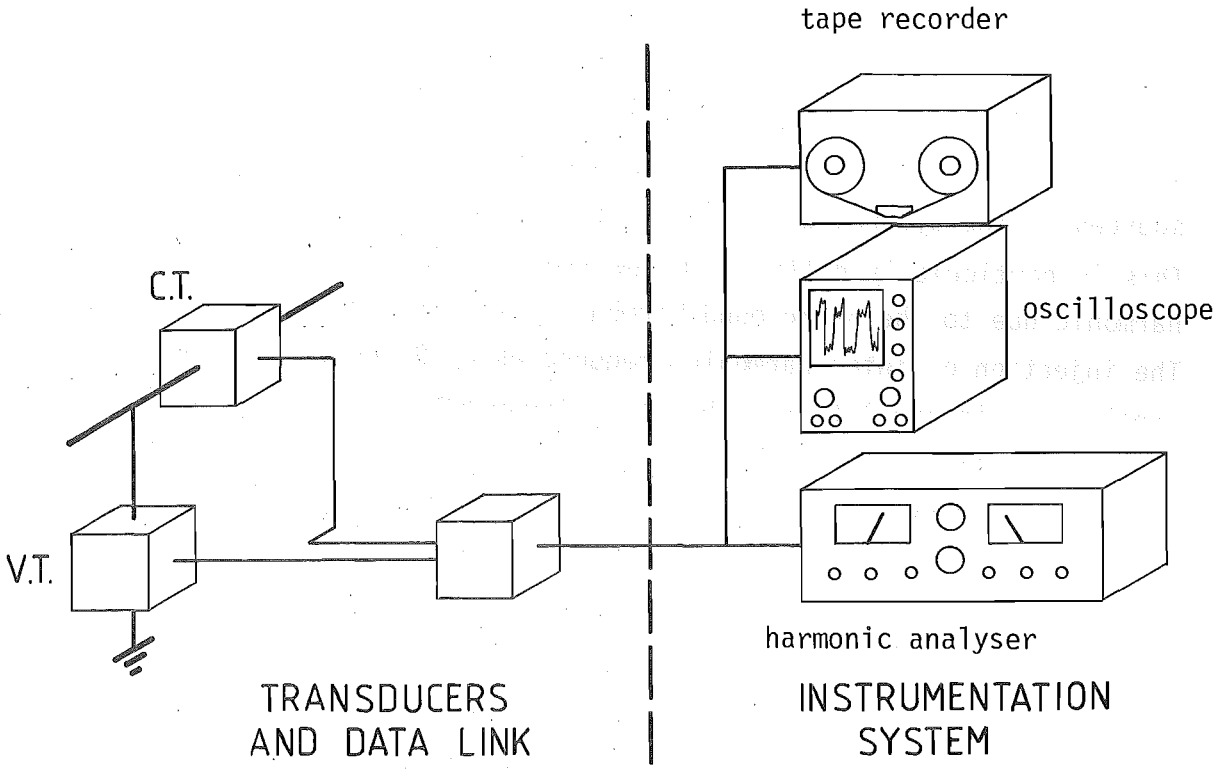

FIGURE 2.9: Schematic of Harmonic Measurement System

Three phase measurement is not simply a duplication of single phase techniques. Voltage and current phase angles must be obtained to a single reference angle, say red phase fundamental. The phase angle at each harmonic in the Plessey instrument (Edward et al 1981) is the angle between the voltage and the current at that harmonic and thus no reference is possible. Although the instrumentation system of Breuer et al (1982) included a phase angle reference the phase information was not as accurate as the magnitude, due to equipment resolution. The method of Crevier and Mercier (1978) was used and assumed a balanced system. Because this method gives only an approximate representation of an unbalanced system the accurate three phase instrumentation with a dynamic range of 100 dB was not utilized to its potential. Although three phase measurement is technically feasible it has yet to be achieved to a satisfactory level. Without accurate phase angles three phase simulation comparisons require the assumption of balanced phase angles to be made. This does not give accurate results.

Derivation of system impedance is an onerous task for a measurement system. It is not possible to obtain useful impedances with multiple sources on the system, a situation often encountered in practice. This is particularly difficult below the 10th harmonic due to the background harmonic levels (Kidd and Duke 1974). The injection of inter-harmonic frequencies by Baker (1981) avoids this problem but interpolation to harmonic frequencies is required. A range of harmonic impedances likely to be found with varying system configurations at each frequency is usually necessary. Often however, it is not possible to study the numerous outage conditions required (Huddart and Brewer 1966).

The ability of measuring equipment to determine accurate harmonic impedances is restricted. The cost of measurement is high and the availability of suitable equipment and personnel is often limited. Simulation can overcome these problems and reduce the need for measuring under varying system configurations and multiple source injection conditions. With known or measured current injections from one source and measured voltages at one bus agreeing with simulated voltages at that bus, model results can be used at other locations with confidence. Using measurement and modelling in this way reduces the need to measure simultaneously at large numbers of busbars; a daunting task.

2.6 MEASUREMENT AND MODELLING CORRELATION

An agreement between harmonic measurements on a system, and computer simulation of the same system, would confirm the validity of both the measurement equipment and the computer model. However until this is achieved full confidence in both areas of endeavour cannot be guaranteed.

However, in dealing with a physical power system, it is not possible to achieve exact agreement of modelled and measured quantities. The New Zealand Limits (New Zealand Electricity 1983) specify the measurement accuracies necessary for the determination of the small signal levels usually associated with harmonics. They are:

- the error in measuring constant harmonic voltage current shall not exceed 0.1% phase to earth system voltage.
- the error in measuring a constant harmonic current shall not exceed 0.2 amps.

The extent that present harmonic modelling meets quantitative accuracies can be assessed from the work of Owen et al (1980):

- Resonant frequencies were predicted to within 5% of the measured values.
- Magnitudes at resonance were predicted to within 50% of measured values.
- Magnitudes at frequencies not near a resonance were predicted to within 20% of measured values.

A second comprehensive study performed under EPRI guidance (Breuer et al 1982), on the Bonneville Power Administration System, produced the average measured and simulated impedances of Figure 2.10.

Both of these studies would be unacceptable if the above measurement limits were applied to modelling.

At present, modelling is therefore not accurate enough to be used for quantitative studies. The reasons for modelling deficiencies will be isolated in Chapters 7 and 8.

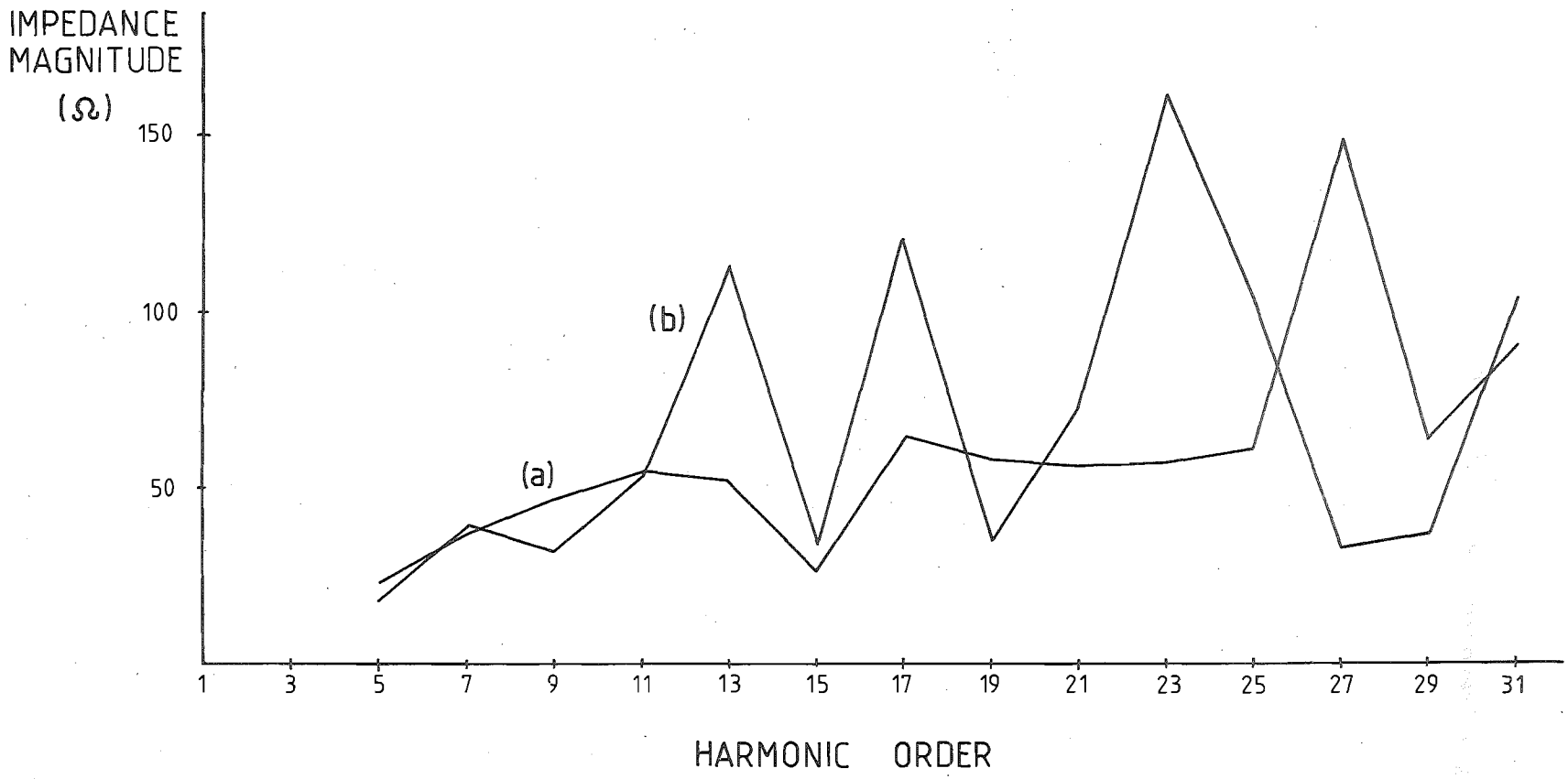

FIGURE 2.10: Harmonic Impedances of the Bonneville Power Administration System from Celilo HVDC Substation

(a) measured

(b) simulated

CHAPTER 3

ALGORITHM DEVELOPMENT

3.1 INTRODUCTION

There is little difference in the basic approach to harmonic investigations when using either single or three phase models. However, the complexity and data requirements for three phase studies are much greater. Because of this the development of three phase software necessitates more effort on data preparation and output display.

Some early understanding of harmonic penetration was obtained in relation to HVDC convertors (Robinson 1966) and using analogue simulation. Laurent et al (1962), at the French end of the cross-channel HVDC link, found simulation results did not match those measured. System impedances were not accurately modelled and considerable imbalance between phases in measured voltages was reported. Brewer et al (1974) also reported difficulty in matching predictive computer studies with measured results on the Kingsnorth HVDC scheme.

Digital computer models at harmonic frequencies have been developed which have the capability to represent more of the elements of the transmission system. Campbell and Murray (1970), Kaban and Parten (1970), Northcote-Green et al (1973a), Frosch and Schultz (1978), Mahmoud and Shultz (1982), and Breuer et al (1982) all used balanced transmission line parameters and loads, reducing the transmission system to a single phase positive sequence equivalent. Linear, passive elements allowed analysis at individual harmonic frequencies. Only the single phase model of Breuer et al (1982) has been used to compare harmonic impedances of a network with measured test data. There were frequencies where the comparison was poor and again unbalanced impedances were reported.

Harmonic penetration studies have been undertaken for distribution systems, (Pileggi et al 1981 and McGranaghan et al 1981). In the former, the low order unbalanced characteristic and non-characteristic harmonics were injected from a convertor load. Symmetrical component matrix analysis was used to obtain harmonic voltages at specific network buses. In the latter paper, multiphase analysis was applied when coupling existed between double circuits. While the above studies discuss representation of three phase unbalanced networks, the presentation of results and significance of these has not been conveyed.

Kitchin (1981) proposed that a time domain solution using transient simulation would give accurate steady state harmonic levels where the voltage waveform was affecting convertor current generation. This approach however does not include accurate transmission line frequency dependence. The ability of frequency domain techniques to allow this facility was a major reason for its use in this thesis.

This chapter describes an algorithm to model three phase harmonic penetration. An essential feature is that multiconductor transmission lines cannot be modelled with fundamental frequency data. The algorithm encompasses convertor harmonic interaction as well as harmonic penetration modelling, and while the results being presented only relate to the latter, the structuring of the programs has been made general to permit developments in both areas.

3.2 REQUIREMENTS FOR HARMONIC MODELLING

The requirements to be met for accurate harmonic modelling are:

- transmission lines must be represented with provision for skin effect and standing wave phenomena.
- load, transformer, generator, shunt capacitor and filter models should be included.
- provision must be made for editing of data to allow for different system configurations.
- nodal admittance matrices should be formed for a range of frequencies and not restricted to harmonic multiples of the fundamental.
- it should be possible to calculate system impedances at any busbar.
- the possibility of current injections at multiple locations in the system needs to be considered.
- the network (assumed linear and passive) must be solved to obtain system voltages at all nodes for all frequencies.
- line current flows should be calculated at each frequency.
- output data needs to be plotted to facilitate interpretation.

These requirements utilise standard power system techniques involving solution of simultaneous linear equations. Different applications mean that not all the above features will be used in any one study.

3.3 SINGLE PHASE MODELLING

The structure of the single phase algorithm is illustrated in Figure 3.1. This corresponds to the program ELAFANT (Baird 1981), used by New Zealand Electricity, and indicates the simplicity and efficiency of this software. Features of the program include:

- fundamental frequency system component data is used at harmonic frequencies. This data is held in system data bases which means very little work is required in preparation for studies.
- editing facilities can retain changes for future runs, i.e. only one set of data is needed which can easily be reconfigured for a desired system.
- storage for a single admittance matrix only is required and this is reformed for each frequency.

Low requirements for storage combined with efficient solution techniques and ease of data preparation makes the program fast and easy to operate. ELAFANT meets all the requirements of the previous section, except that of multiple injection locations, although this can be performed if necessary by vector summation of the results of each separate injection.

The single phase algorithm has been presented to illustrate that the design of three phase software is necessarily different.

FIGURE 3.1 Structure Diagram of Single Phase Modelling

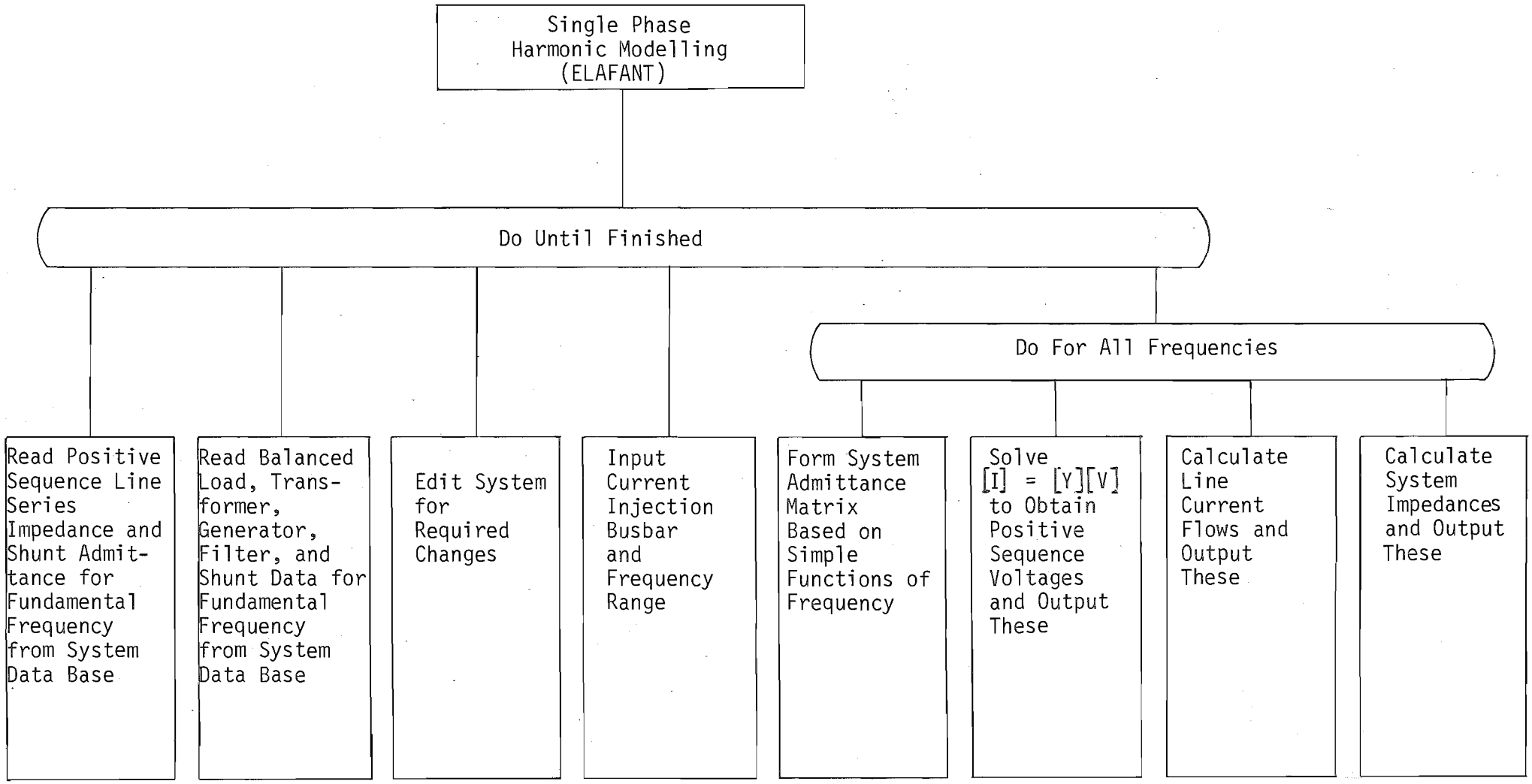

3.4 THREE PHASE ALGORITHM

Unbalanced transmission lines and to a lesser extent other system components, have led to the proposed development from single phase to three phase analysis. The structure of the three phase algorithm developed is illustrated in Figure 3.2. The harmonic penetration program, HARMAC (abbreviation of AC HARMonics), is only one part of this diagram indicating that three phase modelling is not a direct extension of single phase techniques. This structure is however very similar to that used in three phase power flow studies.

Data preparation is not trivial in three phase harmonic modelling. Reasons for data complexity are:

- unbalanced three phase load data.

- three phase transmission line frequency dependence.

The volume of data and the need for practical program blocks are central to the algorithm developed; not speed or efficiency of computation as has been the case in development of power flow or transient stability simulation. The need for separate program blocks is a function of multiple use of software and practical program debugging and maintenance.

The first block of Figure 3.2, program TL (Transmission Line), calculates the transmission line parameters for each frequency over a required range using an Equivalent PI model. This is the subject of Chapter 5. Program INTER (INTERactive) completes the data base by reading line data from TL in unformatted form and adding it to the unbalanced load and other component data required in the network. Use of unformatted data is a method of data compression to save storage. Both programs were obtained from New Zealand Electricity and extended from fundamental to harmonic frequencies. These two programs are unnecessary in single phase studies due to low data requirements and smaller software size. Data necessary for a network need not be reformed each time a study is contemplated.

The volume of output data for a practical study is such that ordinary tabular techniques are inadequate to understand the phenomena of harmonic penetration and also to detect significant results. Instead graph plotting software, program GRAPH1 (Gellen 1982), is used throughout this thesis.

FIGURE 3.2 Structure Diagram of Three Phase Modelling

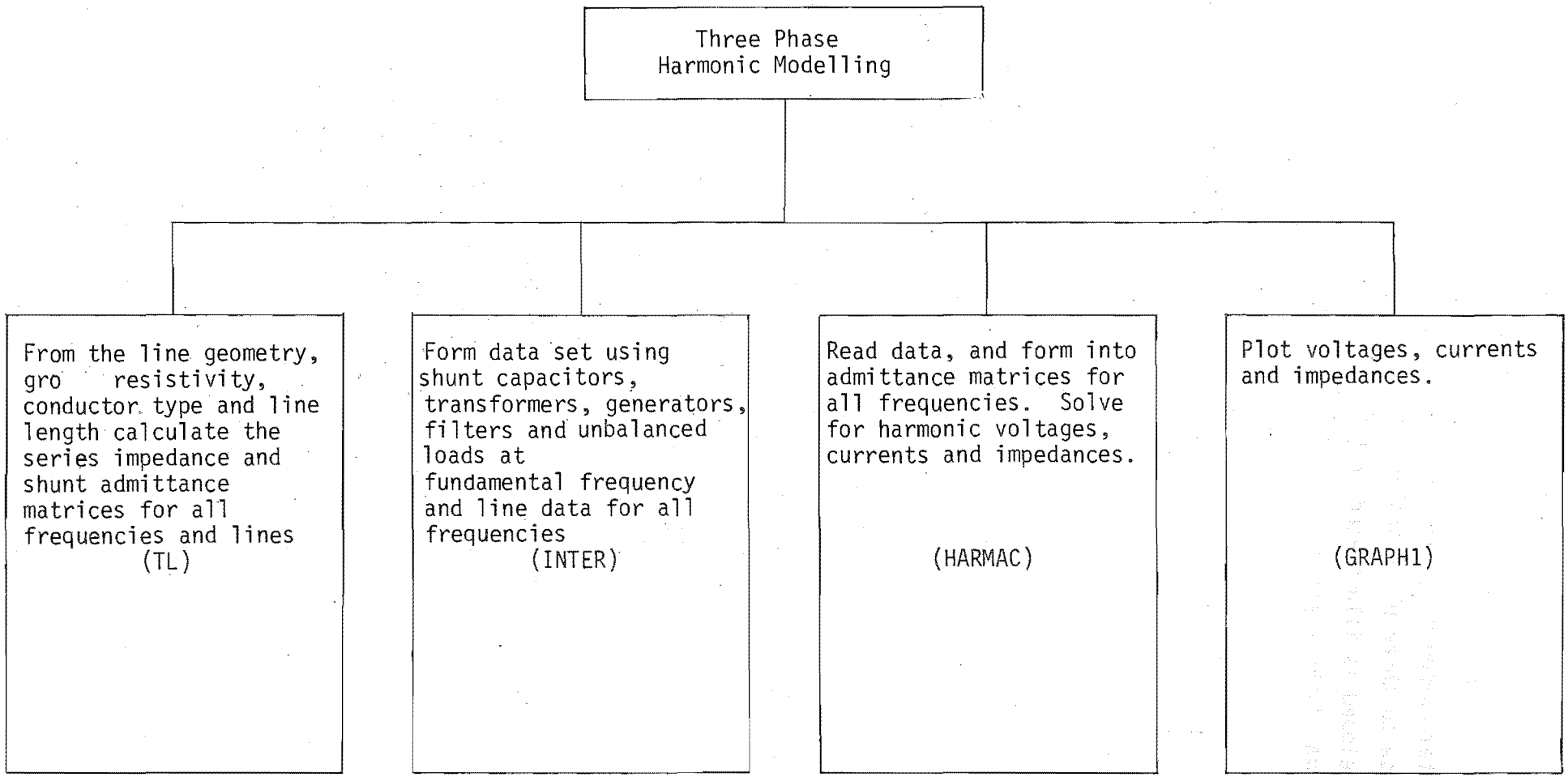

NOTE: Program name is in brackets

The data flow diagram of Figure 3.3 indicates the individual programs and major data files that form the basis of the three phase steady state solution technique. Data formation for both the harmonic penetration software, and three phase power flow (Harker and Arrillaga 1979) is performed by the same software. This ensures that the system configuration used to supply data to program HARMCO (COnvertor HARMonics) by the harmonic penetration and power flow programs is the same. It also avoids the duplication of data preparation software, particularly for the transmission lines where similar analysis techniques can be used for fundamental and harmonic frequencies. The disadvantage of this structure is that line data for all the desired frequencies needs to be stored as data for HARMAC.

The three phase AC/DC power flow supplies fundamental frequency data and the convertor operating state (Harker 1980) to the convertor interaction software, HARMCO. This software uses the three phase system impedances calculated by HARMAC to solve the non-linear convertor equations obtaining harmonic voltages and currents at the convertor terminals. Current data from any number of convertors connected at any busbars in an AC system is then available for calculation of the harmonic penetration of these currents into the AC system. The interaction of convertors due to distortion of the commutating voltages is a field of on-going research, and not part of this thesis. Both the harmonic penetration and convertor interaction programs have similar output presentation requirements and utilise the graphics software, GRAPH1.

FIGURE 3.3 Data Flow Diagram

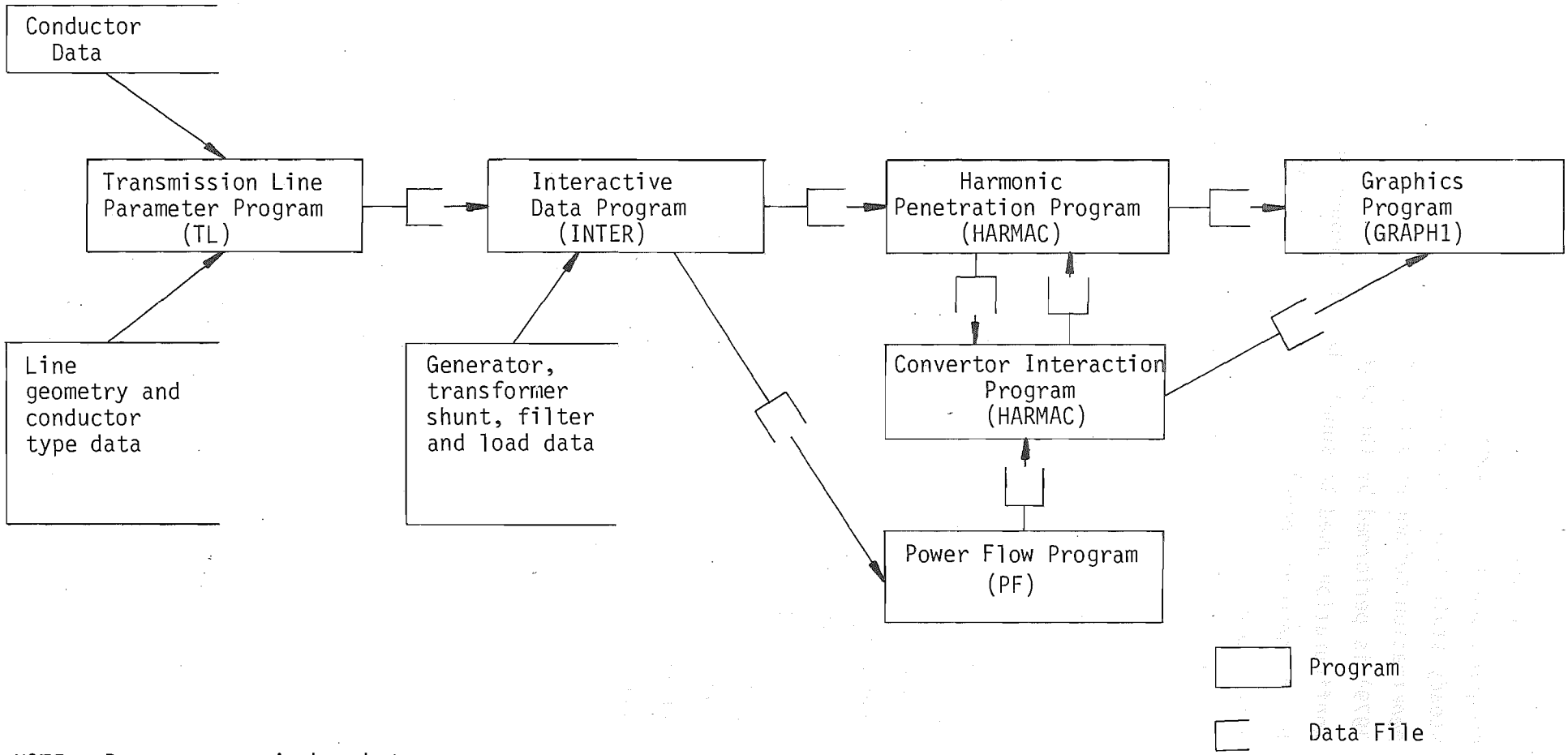

NOTE: Program name in brackets

3.5 THREE PHASE HARMONIC PENETRATION

The three phase harmonic penetration program HARMAC is illustrated in the structure diagram of Figure 3.4. Features of the algorithm include:

- three phase mutually coupled transmission line data can be utilized.
- three phase unbalanced loads and other system components are modelled.
- separate admittance matrices are formed for each frequency.
- three phase impedance matrices for a reduced portion of the network suitable for filter design or convertor interaction studies are derived.
- unbalanced current injections at a number of busbars on the system can be specified.

All the requirements previously stated for harmonic modelling have been met, although data file editing is not comprehensive.

For a three phase network, unbalanced self and mutual admittances of network elements can be modelled as well as circuit coupling. As indicated earlier, it is assumed that the AC system is linear and passive and therefore the principle of superposition may be applied to enable each harmonic to be considered independently.

In a multibranch interconnected network an admittance matrix $[Y_h]$ is formed from the individual elements, for each particular harmonic, h. Harmonic currents are injected into the buses under consideration and the voltages throughout the system calculated from the solution of:

$$[I_h] = [Y_h][V_h] \qquad (3.1)$$

For the three phase system, the elements of the admittance matrix are themselves 3x3 matrices consisting of self and transfer admittances. Figure 3.5 indicates the nature of the analysis where h sets of linear equations are solved.

FIGURE 3.4 Structure Diagram of Three Phase Harmonic Penetration Program

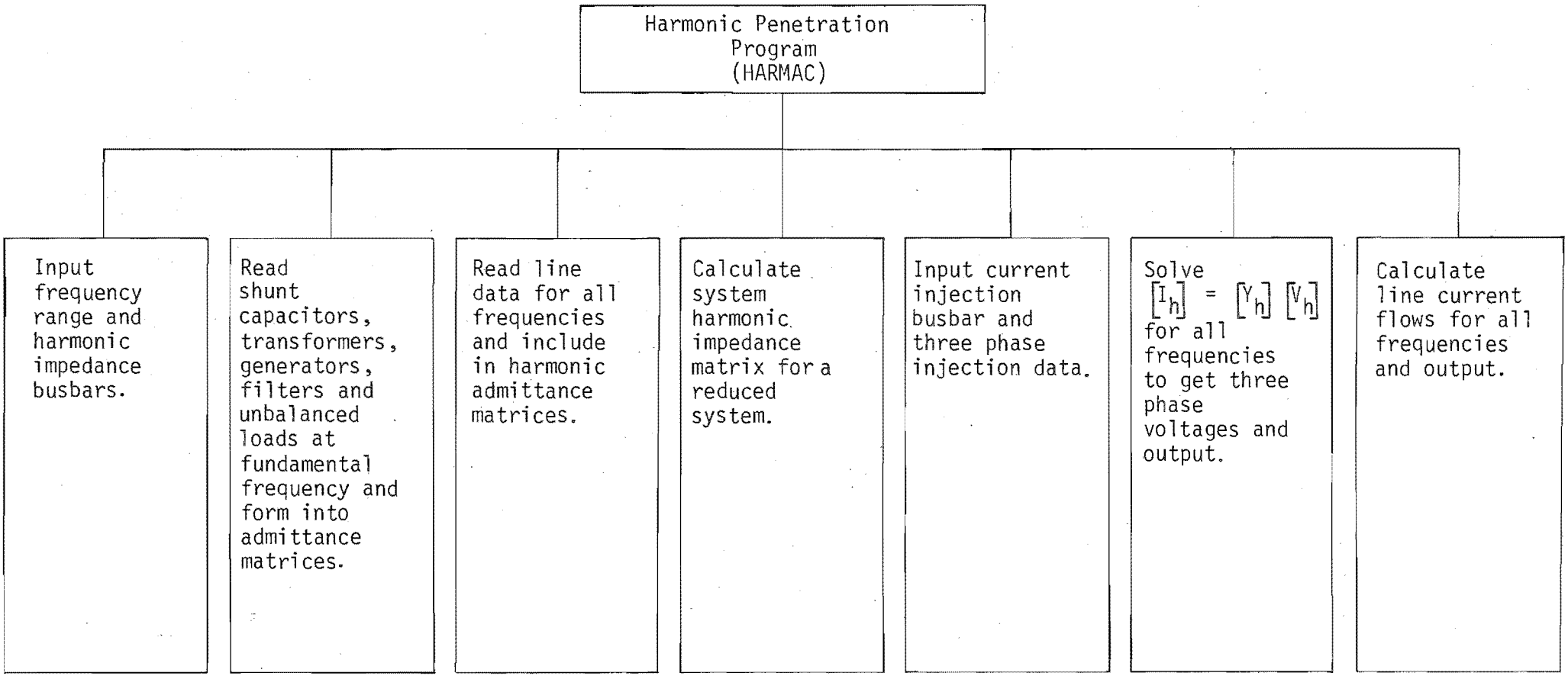

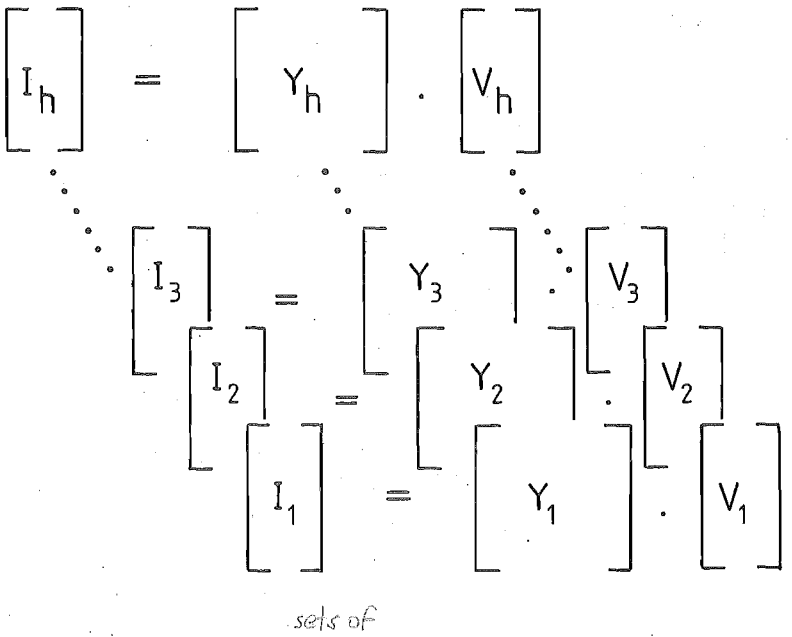

FIGURE 3.5. Solution of h Linear Simultaneous Equations

While it is usual to consider harmonic frequencies any frequencies may be solved for.

The injected currents at most AC busbars will be zero, since the sources of the harmonics considered are generally from static convertors. To calculate an impedance matrix for the reduced portion of a system comprising the injection busbars, it is necessary to form the admittance matrix with those buses at which harmonic injection occurs, ordered last. Advantage is taken of the symmetry and sparsity of the admittance matrix (Zollenkopf 1970), using row ordering techniques to reduce the amount of off-diagonal element build-up. The matrix is triangulated using Gaussian elimination, down to but excluding the rows of the specified buses. The resulting matrix equation for an n-node system with n-j+1 injection points is

$$\begin{bmatrix} 0 \\ \vdots \\ 0 \\ \hline I_j \\ \vdots \\ I_n \end{bmatrix} = \begin{bmatrix} & & \\ & & \\ & 0 & \\ & & \\ \hline & Y_{jj} \cdots Y_{jn} & \\ & \vdots \quad \vdots & \\ & Y_{nj} \cdots Y_{nn} & \end{bmatrix} \cdot \begin{bmatrix} V_1 \\ \vdots \\ V_{j-1} \\ \hline V_j \\ \vdots \\ V_n \end{bmatrix} \qquad (3.2)$$

As a consequence, $I_j \ldots I_n$ remain unchanged since the currents above these in the current vector are zero. The reduced matrix equation is:

$$\begin{bmatrix} I_j \\ \vdots \\ I_n \end{bmatrix} = \begin{bmatrix} Y_{jj} & \cdots & Y_{jn} \\ \vdots & & \vdots \\ Y_{nj} & \cdots & Y_{nn} \end{bmatrix} \cdot \begin{bmatrix} V_j \\ \vdots \\ V_n \end{bmatrix} \qquad (3.3)$$

where the admittance matrix is of order equal to 3 times the number of injection busbars. The elements are the self and transfer admittances of the reduced system as viewed from the injection busbars. An impedance matrix may be obtained for the reduced system by matrix inversion.

Reducing a system to an equivalent impedance matrix is not only useful for filter design where the system as viewed from one bus is required, but also where a number of convertors are connected to the AC system at different points, Figure 3.6. In this case the reduced admittance matrix would be of order 9.

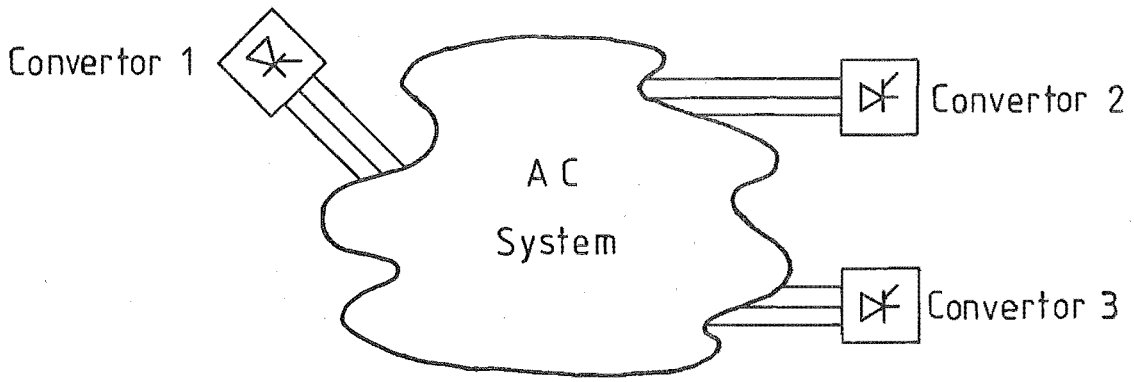

FIGURE 3.6 Three Convertors Attached to Different Busbars on the AC System

For the purposes of this thesis the currents from the convertors are assumed to be known. In general however (Yacamini and de Oliveira 1980a, b) voltage distortion at the convertor terminals affects the firing angles and hence current injection into the system. Solution of this problem is iterative and not suited to the large matrices associated with the AC system. During each iteration only the convertor terminal voltages are required. These can be obtained in the example above by reducing the AC system to a three bus equivalent system for the three

convertors indicated in Figure 3.7 below. Each of the admittances represents a 3x3 matrix.

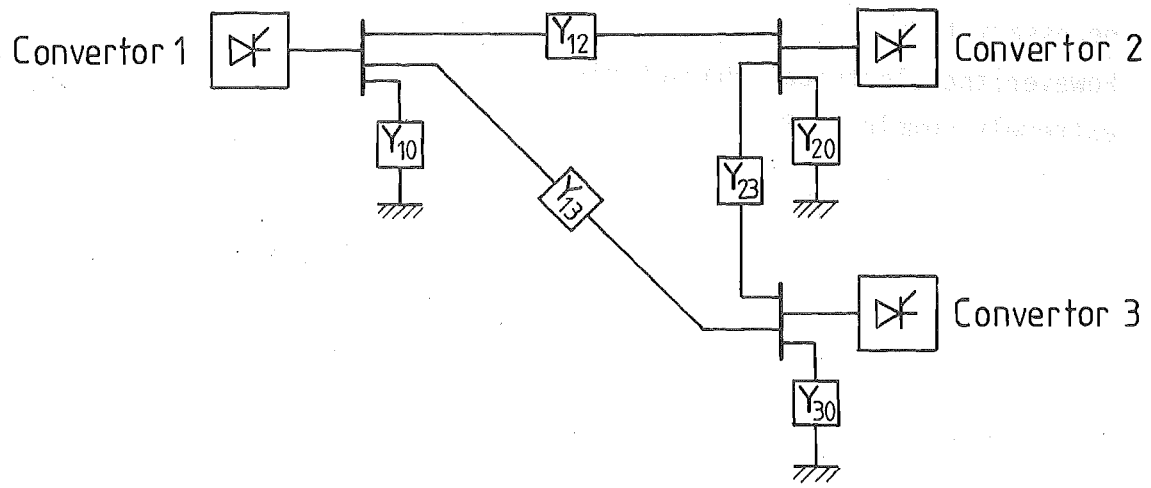

FIGURE 3.7 Reduced Three Convertor System

Restricted measurements on the physical network limit the ability to compare a three phase model with test results. Measured impedance data is obtained on live three phase systems and thus only phase voltages and currents for the coupled phases are available for impedance calculations. To compare measured and simulated impedances at a current injection busbar it is necessary to define equivalent phase impedances, derived from the 3x3 admittance matrix. Assuming $I_1 = 1\lfloor 0^o$ pu, $I_2 = 1\lfloor -120^o$ pu, $I_3 = 1\lfloor 120^o$ pu, the matrix equation:

$$\begin{bmatrix} I_1 \\ I_2 \\ I_3 \end{bmatrix} = \begin{bmatrix} Y_{11} & Y_{12} & Y_{13} \\ Y_{21} & Y_{22} & Y_{23} \\ Y_{31} & Y_{32} & Y_{33} \end{bmatrix} \cdot \begin{bmatrix} V_1 \\ V_2 \\ V_3 \end{bmatrix} \qquad (3.4)$$

solved for V_1, V_2 and V_3, yields the following equivalent phase impedances:

$$Z_1 = \frac{V_1}{I_1}, \quad Z_2 = \frac{V_2}{I_2}, \quad Z_3 = \frac{V_3}{I_3} \qquad (3.5)$$

and these can be compared with measured values.

The impedances can be plotted in their cartesian coordinates over the range of frequencies of interest. This has previously been presented for single phase impedance-frequency data (Laurent et al 1962 and Breuer et al 1982).

3.6 FORMATION OF THE NODAL ADMITTANCE MATRICES

3.6.1 Introduction

To enable harmonic penetration analysis to be performed it is necessary to form a mathematical representation of the power system. However, the electrical characteristics of an interconnected network are extremely complex. By considering the individual physical elements the parameters of which can be determined and connecting them in the manner of the physical network, this complexity can be overcome. Nodal admittance matrix techniques are presented to perform this interconnection efficiently.

Phase quantities are retained throughout the formation and solution of the harmonic admittance matrices. Symmetrical components provide no computational advantage and are only used as an aid to interpretation of results.

This section treats the interconnection of various three phase element types by the use of linear transformation techniques. It is left to the two succeeding chapters to assign the physical elements of the network to these element types.

Admittance matrices for each frequency have the same non-zero elements with values determined by element models.

3.6.2 Network Subdivision

Although an element, or branch, of a network is the basic component elements may be coupled and non-homogeneous, i.e. mutually coupled transmission lines with different tower geometries over the line length. To facilitate the inclusion of this a subsystem is defined as follows:

A subsystem is the unit into which any part of the system may be divided such that no subsystem has any mutual coupling between its constituent branches and those of the rest of the system.

The smallest unit of a subsystem is a single network element.

The subsystem unit is retained for input data organisation. Data for any subsystem is input as a complete unit, the subsystem admittance matrix is formulated and then combined in the total system admittance matrix.

Subsystem admittance matrices may be derived by finding, for each section, the ABCD or transmission parameters, then combining these by matrix multiplication to give the resultant transmission parameters. These are then converted to the required nodal admittance matrices.

This procedure involves an extension of the usual two port network theory to multi-two-port networks. Currents and voltages are now matrix quantities as defined in Figure 3.8. Dimensions of the parameter matrices correspond to those of the section being considered, i.e. 3, 6, 9, or 12 for 1, 2, 3 or 4 mutually coupled three phase elements respectively. All sections must contain the same number of mutually coupled three phase elements, ensuring that all the parameter matrices are of the same order and that the matrix multiplications are executable. Uncoupled elements need to be considered as coupled ones with zero coupling to maintain correct dimensions for all matrices.

Once the resultant ABCD parameters have been found the equivalent nodal admittance matrix for the subsystem can be calculated from:

$$[Y] = \begin{bmatrix} [D][B]^{-1} & [C] - [D][B]^{-1}[A] \\ [B]^{-1} & -[B]^{-1}[A] \end{bmatrix} \qquad (3.6)$$

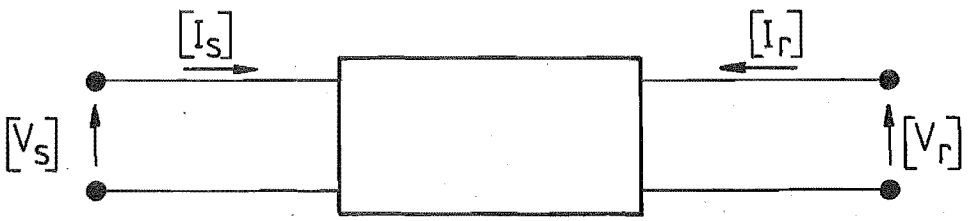

(b) Multi-two port network

$$\begin{bmatrix} [V_s] \\ [I_s] \end{bmatrix} = \left[\begin{array}{c|c} [A] & [B] \\ \hline [C] & [D] \end{array}\right] \begin{bmatrix} [V_r] \\ [I_r] \end{bmatrix}$$

(a) Matrix transmission parameters

FIGURE 3.8 Two Port Network Transmission Parameters

Two-port network theory is not the only way a number of sections can be reduced to a branch equivalent. Matrix reduction introduced for systems impedance calculation in the previous section could also have been used (Alvarado 1982).

3.6.3 Linear Transformation

Linear transformation techniques enable the admittance matrix of any network to be found in a systematic manner (Kron 1965 and Brameller et al 1969). Steps needed to form the network admittance matrix by linear transformation are:

- label the nodes in the original network.
- number in any order the branches and branch admittances.
- form the primitive network admittance matrix $[Y_{prim}]$ by inspection.
- form the connection matrix $[C]$.
- calculate the element nodal admittance matrix using
  $[Y_{abc}] = [C]^T [Y_{prim}] [C]$

Examples of this technique can be found in Harker (1980).

Representation of three phase elements by the use of compound admittances will be used extensively. Formation of both the primitive and actual network admittance matrices using three phase compound admittances is covered in detail in Arrillaga et al (1983a).

For the models developed in this section, the intermediate steps in forming the element nodal admittance matrices have been neglected, similar to the program implementation.

3.6.4 Shunt and Series Elements

Coupled admittances to ground at bus k are formed into the 3x3 admittance matrix shown in Figure 3.9, and this reduces to the compound admittance representation indicated.

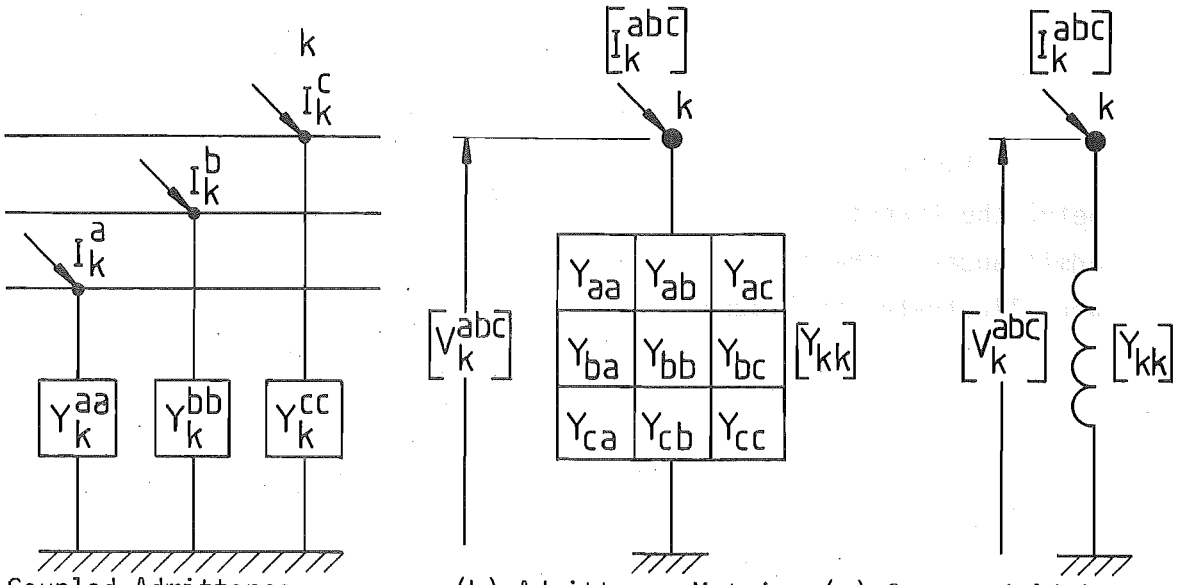

(a) Coupled Admittance (b) Admittance Matrix (c) Compound Admittance

FIGURE 3.9 Representation of a Shunt Element

The admittance matrix is usually diagonal as there is normally no coupling between the components of each phase. It is incorporated directly into the system admittance matrix, contributing only to the self admittance of the particular bus. Shunt elements represent the simplest subsystem, being composed of only one busbar.

Coupled series admittances between busbars i and k in Figure 3.10 reduce to the nodal admittance matrix and compound admittance indicated.

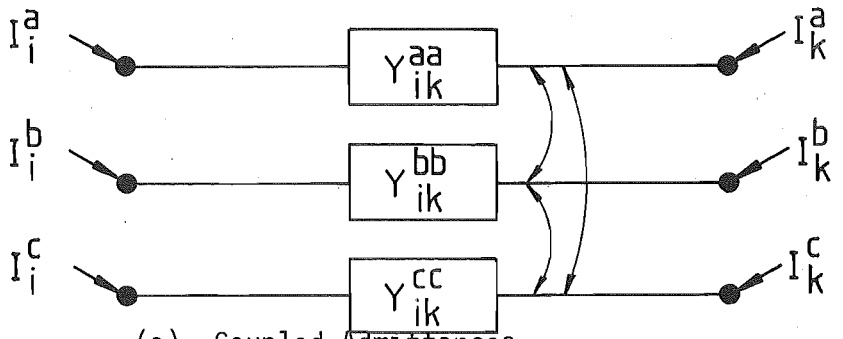

(a) Coupled Admittances

$$\begin{bmatrix} [I_i] \\ \hline [I_k] \end{bmatrix} = \begin{bmatrix} [Y_{ik}] & -[Y_{ik}] \\ \hline -[Y_{ik}] & [Y_{ik}] \end{bmatrix} \begin{bmatrix} [V_i] \\ \hline [V_k] \end{bmatrix}$$

(b) Admittance Matrix

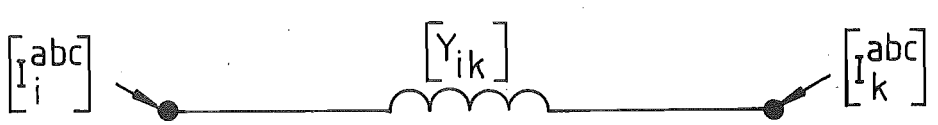

(c) Compound Admittance

FIGURE 3.10: Representation of a Series Element

3.6.5 Coupled Shunt Elements

Two three phase shunt branches coupled together, a common example being the transformer, may be represented using two coupled compound admittances. The admittance matrix and compound admittance representation are illustrated in Figure 3.11.

$$\begin{bmatrix} [I_p] \\ [I_s] \end{bmatrix} = \begin{bmatrix} [Y_{pp}] & [Y_{ps}] \\ [Y_{sp}] & [Y_{ss}] \end{bmatrix} \begin{bmatrix} [V_p] \\ [V_s] \end{bmatrix}$$

(a) Admittance Matrix

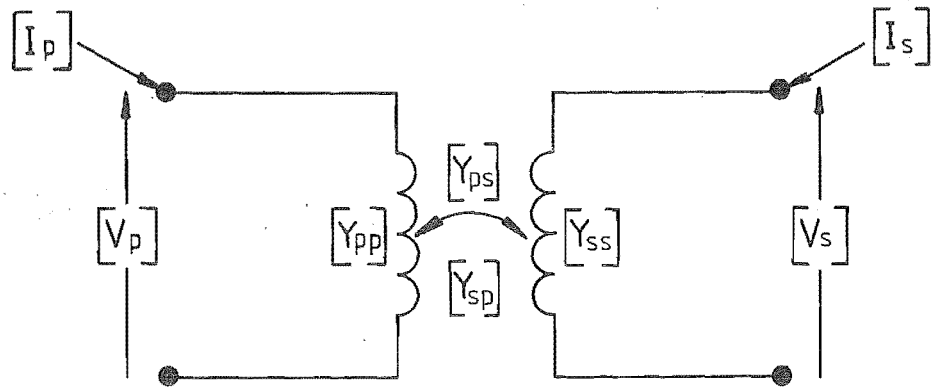

(b) Compound Admittance

FIGURE 3.11 Two Winding Three Phase Transformer as Two Coupled Compound Admittances

It should be noted that:

$$[Y_{sp}] = [Y_{ps}]^T \tag{3.7}$$

as the coupling between the two compound admittances is bilateral.

Practical details of the different coupling arrangements possible are discussed in Laughton (1968) and Dillon and Chen (1972).

3.6.6 Combined Series and Shunt Connected Elements

For this element representation in single phase analysis, the usual example being the transmission line, half of the total shunt admittance is connected to earth at each terminal and the series impedance for the total element is placed in series between the busbars as shown in Figure 3.12.

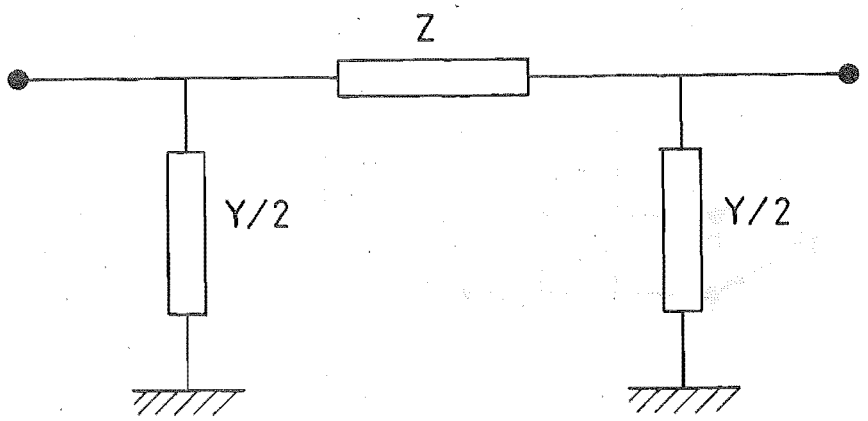

FIGURE 3.12 Series and Shunt Connected Element

The same model can be used in the three phase case. The process by which Z and Y become 3x3 matrix quantities is illustrated in Figure 3.13. In part (a) of the figure the full circuit representation is shown. This consists of three circuits (one for each phase) which are coupled together. Parts (b) and (c) show alternative and more concise circuit representations where [Z] and [Y] are written as 3x3 matrices and corresponding three phase compound admittances.

The admittance matrix for the three phase element can now be written. This is done following the rules of linear transformation for the formation of the admittance matrix using compound admittances.

The element admittance matrix relates the nodal injected currents illustrated in Figure 3.13 to the nodal voltages by the equation:

$$\underset{6 \times 1}{\begin{bmatrix} [I_i] \\ \hline [I_k] \end{bmatrix}} = \underset{6 \times 6}{\left[\begin{array}{c|c} [Z]^{-1} + [Y]/2 & -[Z]^{-1} \\ \hline -[Z]^{-1} & [Z]^{-1} + [Y]/2 \end{array}\right]} \underset{6 \times 1}{\begin{bmatrix} [V_i] \\ \hline [V_k] \end{bmatrix}} \qquad (3.8)$$

Significant coupling exists between some three phase system elements. Transmission lines often occupy the same right of way for a considerable length and the electrostatic and electromagnetic coupling between these lines must be considered.

FIGURE 3.13 Three Phase Combined Series and Shunt Connected Elements

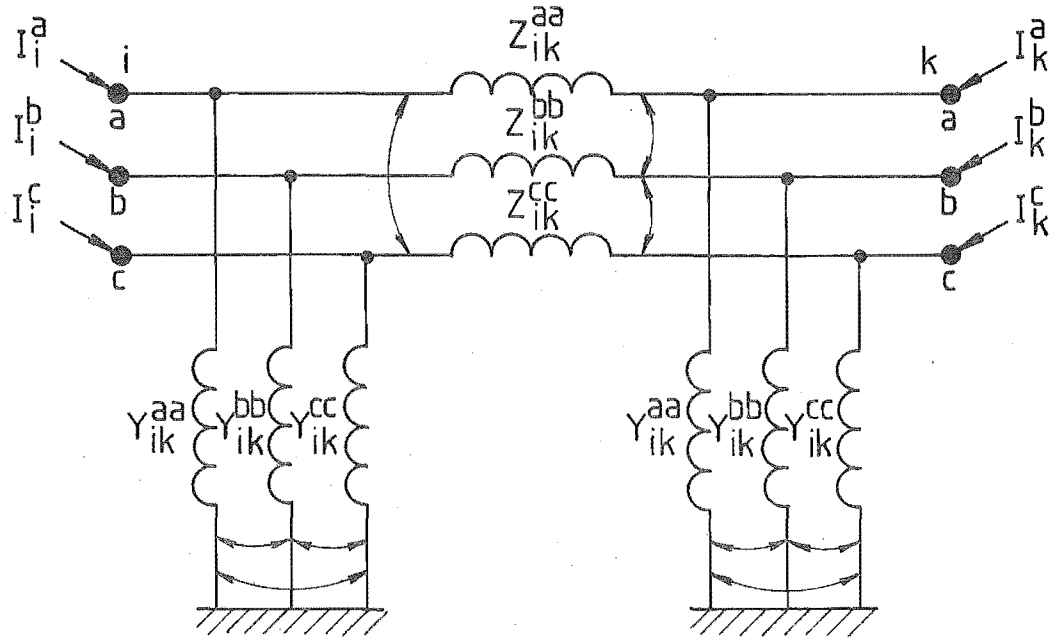

(a) Full Circuit Representation

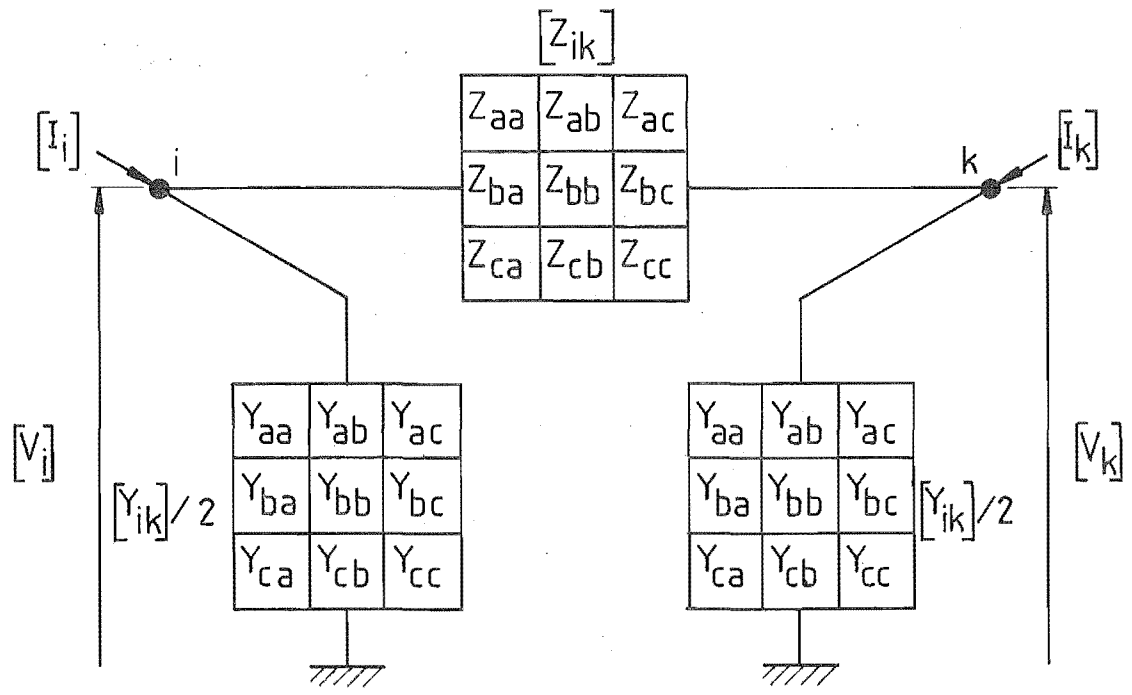

(b) Matrix Equivalent

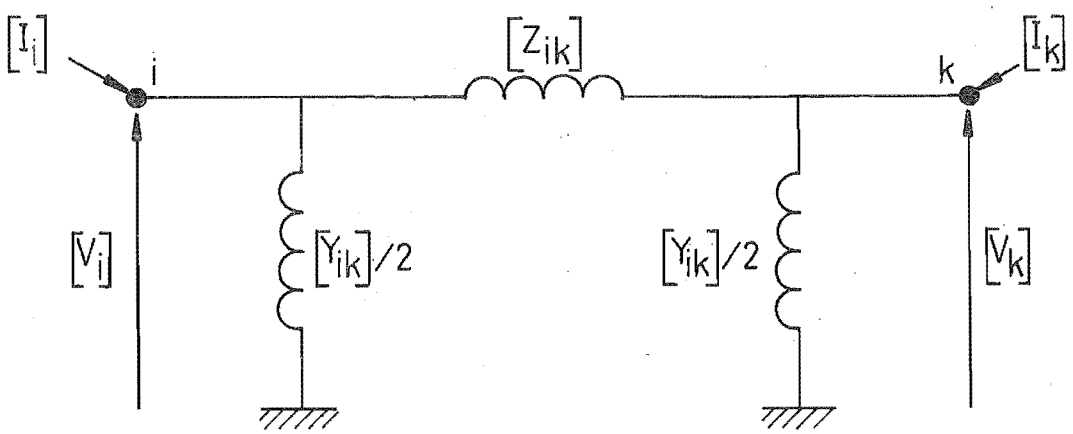

(c) Using Three Phase Compound Admittances

In the simplest case of two mutually coupled three phase elements, the two elements are considered to form one subsystem, composed of four busbars. This is represented in the equation below:

$$\begin{bmatrix} \begin{bmatrix} I_A \\ I_B \end{bmatrix} \\ \hline \begin{bmatrix} I_C \\ I_D \end{bmatrix} \end{bmatrix} = \left[\begin{array}{c|c} [Z_s]^{-1} + [Y_s] & -[Z_s]^{-1} \\ \hline -[Z_s]^{-1} & [Z_s]^{-1} + [Y_s] \end{array}\right] \begin{bmatrix} \begin{bmatrix} V_A \\ V_B \end{bmatrix} \\ \hline \begin{bmatrix} V_C \\ V_D \end{bmatrix} \end{bmatrix} \qquad (3.9)$$

$12 \times 1 \qquad\qquad 12 \times 12 \qquad\qquad 12 \times 1$

where $[Z_s]$ and $[Y_s]$ are the 6x6 compound series impedance and shunt admittance matrices respectively.

This is similar to the equation for an uncoupled element with the appropriate matrix partitioning.

Data which must be input to the program to enable coupled elements to be treated in a similar manner to single elements, are the series impedance and shunt admittance matrices. These matrices are of order 3x3 for a single element, 6x6 for two coupled elements, 9x9 for three and 12x12 for four coupled elements. Once the matrices $[Z]$ and $[Y]$ are available, the admittance matrix for the subsystem is formed.

When all the busbars of the coupled lines are distinct, the subsystem may be combined directly into the system admittance matrix. However, if the busbars are not distinct then the subsystem admittance matrix must be modified. This is simply a matter of adding appropriate rows and columns and is referred to as network collapsing by Alvarado (1982).

It should be noted that the admittance matrix of each individual branch must also be stored to facilitate calculation of individual element current flows after the solution of the harmonic penetration has been completed.

3.6.7 Forming the System Admittance Matrix

It has been shown that the element (and subsystem) admittance matrices can be derived and manipulated efficiently if the three nodes at a busbar are associated together. This association proves equally helpful when forming the admittance matrix for the total system.

A subsystem may have common busbars with other subsystems, but may not have mutual coupling terms to the branches of other subsystems. Therefore the subsystem admittance matrices can be combined to form the overall system admittance matrix as follows:

- the self admittance of any busbar is the sum of all the sub-system self-admittance matrices at that busbar.
- the mutual admittance between any two busbars is the sum of the individual mutual admittance matrices from all the subsystems containing those two nodes.

3.7 CONCLUSIONS

An algorithm for three phase steady state harmonic penetration studies has been introduced. Modelling in phase co-ordinates with emphasis on the essential components present in the input routine for any three phase harmonic penetration alaysis, have been described. Transmission lines are represented by non-linear functions of frequency, thus parameters cannot be determined from fundamental frequency data.

While the user requirements for harmonic penetration software are similar for single and three phase modelling, the programs are structured differently. The complexity of three phase system modelling requires the programmer to devote comparable effort on formulation of the three phase data and the penetration program itself.

Data flow is central to the algorithm and the main file transfers have been illustrated. Sparsity storage has been used together with efficient solution techniques to enable actual transmission systems to be modelled.

CHAPTER 4

MODELLING OF NEAR BALANCED COMPONENTS

4.1 INTRODUCTION

The design of shunt capacitors, filters, generators, loads and transformers is reasonably balanced and so is the information normally provided for their modelling. However, the models derived in this thesis allow for unbalanced parameters wherever available.

There is some disagreement regarding which harmonic models are best for generators, transformers and loads (Pesonen et al 1981), and because of this, the various proposed models are discussed.

4.2 SHUNT CAPACITORS

Shunt capacitors are represented as elements contributing to the shunt admittance of the busbar to which they are connected, illustrated in Figure 4.1. Usually the element admittance matrix will be diagonal and proportional to frequency. The MVA rating at 50 Hz, Q_{50} and the nominal voltage, V, are used to calculate the capacitive reactance. The presence of any series inductance in the capacitor banks is ignored.

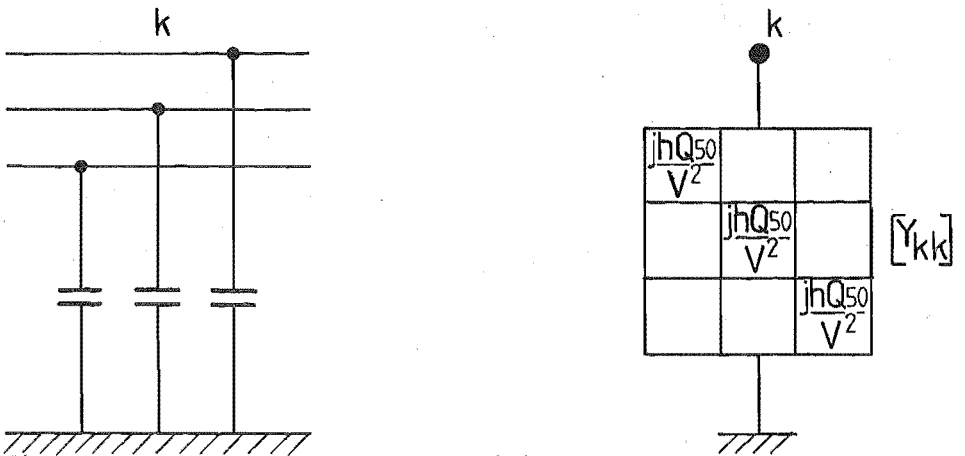

(a) Shunt Capacitors (b) Admittance Matrix

FIGURE 4.1: Shunt Capacitor Representation

4.3 FILTERS

Single tuned, and high pass, shunt filters are usually connected to the terminal busbars of high power AC/DC convertor installations. The filters are represented as uncoupled LRC branches, contributing to the shunt admittance of the convertor busbar to which they are connected.

Typical equivalent circuits for each phase of single tuned and high pass filters are illustrated in Figure 4.2.

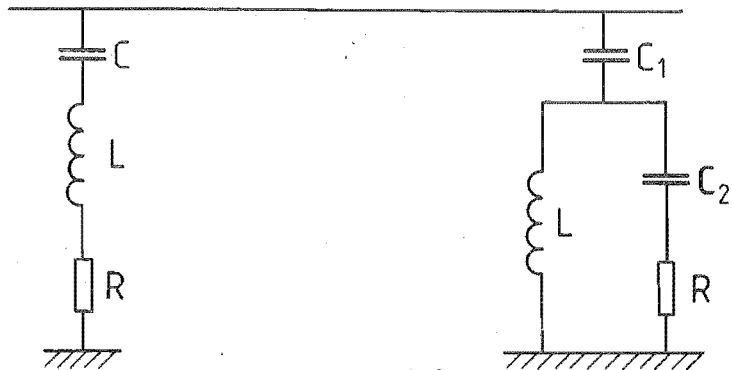

(a) Single tuned filter (b) High Pass Filter

FIGURE 4.2: HVDC Shunt Filter Types

4.4 SYNCHRONOUS GENERATORS

In general, it may be assumed that synchronous generators produce no harmonic voltages, and they can therefore be modelled by a shunt connected impedance, at the generator terminal busbar.

Ross and Smith (1948) and Easton (1966) conclude that alternators can be treated as having a constant harmonic impedance, irrespective of the power delivered by the machine.

The literature is not however in agreement, regarding appropriate impedances at audio frequencies. Ross and Smith (1948), Easton (1966), Northcote-Green et al (1973a) and Clarke (1973), propose a frequency dependent resistance, with most authors suggesting a linear relationship. However Pesonen et al (1981) proposes a constant resistance while Campbell and Murray (1970) and Breuer et al (1982) use none at all.

A number of authors (Ross and Smith 1948, Pesonen et al 1981, and Breuer et al 1982) use a linear reactance derived from either the subtransient or negative sequence inductances; both having similar values, or in the case of Campbell and Murray (1970) the transient inductance. There is disagreement with this approach by Clarke (1973) and Northcote-Green et al (1973b) who suggest second order equations that give lower values of impedance at higher frequencies, however no reasons for this approach are given.

Arseneau et al (1979) conducted tests on a laboratory size synchronous motor, with measured impedances and the subtransient reactances agreeing to within 15%. No confirmation using power system synchronous generators, was attempted however.

With no generally accepted model, and no comprehensive published tests, the model of Ross and Smith (1948) with linear subtransient reactance and resistance will be used in two forms as below:

A. 100% of the subtransient reactance with a power factor of 0.2.

B. 80% of the subtransient reactance with a power factor of 0.2.

Conversion to a form suitable for inclusion into the harmonic admittance matrices is straight forward.

4.5 LOAD MODELLING

The transmission system program, HARMAC, lacks the capability to represent the system from generators right through to individual customer loads. At some point on the network the elements at lower voltages have to be aggregated into an equivalent circuit. In New Zealand there is one organisation responsible for generation and transmission to load centers, and a number of power supply authorities who reticulate power to individual customers within the load centers. In this thesis equivalent circuits are used at the boundaries of the transmission system, i.e. at the points of supply (POS) to supply authorities.

This is justified for the following reasons:

- generally lines within distribution authorities are much shorter than those in the transmission system, and therefore standing wave effects at harmonic frequencies are less likely.

- transformers at the point of supply have reactances which reduce the effect of supply authority system harmonic impedance variation, caused by the combined effects of reticulation and individual customer load impedances.

The methods available for determining the equivalent harmonic impedance of supply authority networks are:

- direct measurement can be performed at a sufficient number of frequencies to enable satisfactory interpolation. This has been discussed in Chapter 2. The limitations of measurement technique make this method very time consuming and difficult, especially for a number of authorities.

- component characteristics, i.e. motors and industrial plant, can be derived by using statistical diversity data. This approach, while difficult, is under consideration for system stability studies (Concordia and Ihara 1982) and could be extended to harmonic studies.

- known fundamental frequency real and reactive power flow at the point of supply can be used.

Wide variation in impedance with frequency and load level has been reported (Ross 1972, Baker 1981 and Barnes and Kearley 1981), for industrial and domestic customers. Industrial loads often have capacitors installed for power factor compensation which can cause series and parallel resonances.

There is a correspondingly large number of models useful for customer loads (McGranaghan et al 1981, Pesonen et al 1981 and Pileggi et al 1981). All are designed as component or as component aggregate models.

However, transformation to higher voltage levels and reticulation to the point of supply tends to reduce the effect of individual consumer harmonic impedance variation. A typical supply authority network indicating this is shown in Figure 4.3.

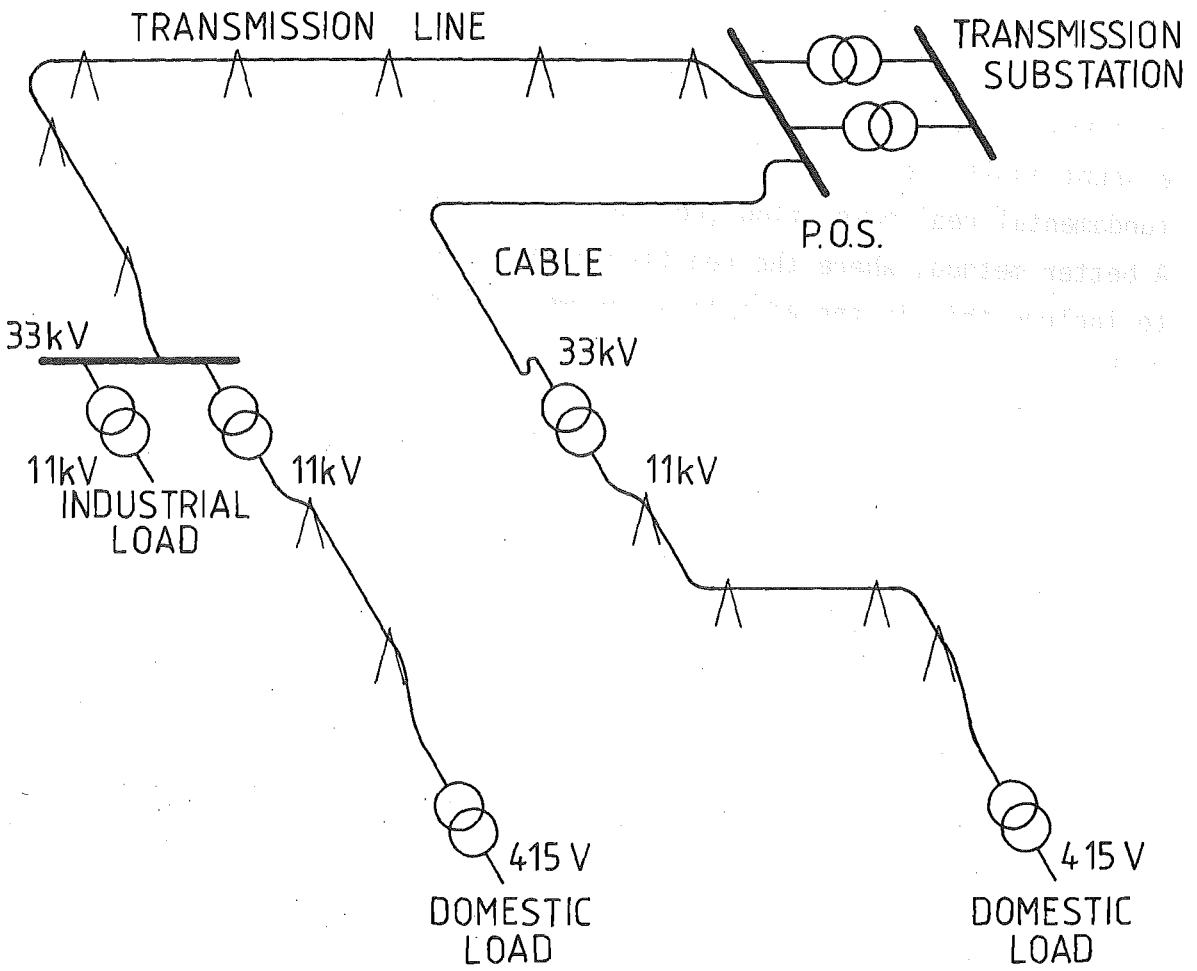

FIGURE 4.3: Schematic Representation of Supply Authority Distribution Network

Some measured data for the Central Canterbury Electric Power Board (CCEPB) confirming the insensitivity of harmonic impedances to customer loads is documented in Table 4.1. The impedance at 520 Hz is inductive and not substantially greater than that at 50 Hz for both the points of supply at Springston and Islington.

	SPRINGSTON	ISLINGTON
520 Hz impedance (Ω)	$57.0 \lfloor 35.5^{o}$	$21.3 \lfloor 37.5^{o}$
50 Hz impedance (Ω)	$47.0 \lfloor 18.2^{o}$	$19.2 \lfloor 18.2^{o}$

TABLE 4.1: Measured Impedances for Central Canterbury Electric Power Board Points of Supply

From this information, the use of fundamental frequency data at the point of supply is reasonable and no individual customer loads need be considered. On first investigation it would appear simple to include a shunt admittance at the point of supply busbar that gives the correct fundamental real power flow (Ross and Smith 1948 and Pesonen et al 1981). A better method, where the reactive power consumption is available, is to include this in the admittance as well (Campbell and Murray 1970 and Harker 1980).

Various combinations of the real and reactive power demand at 50 Hz, P_{50} and Q_{50}, have been suggested. Those considered are:

A

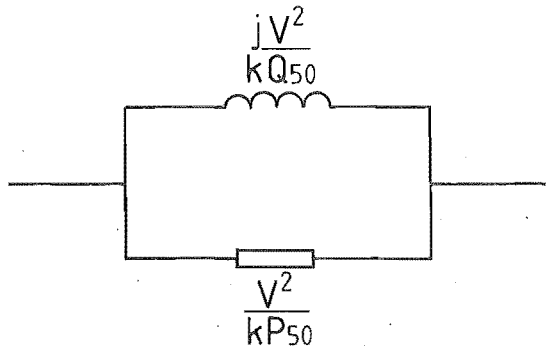

where k = 0.1 h + 0.9, h is the harmonic order and V is the nominal voltage. This model is based on that of Pesonen et al (1981).

B

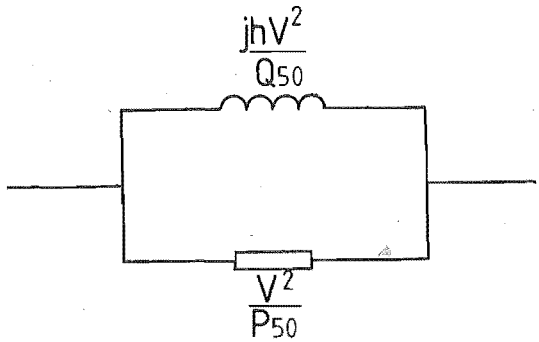

The reactance is assumed to be frequency dependent with a constant parallel resistance.

C

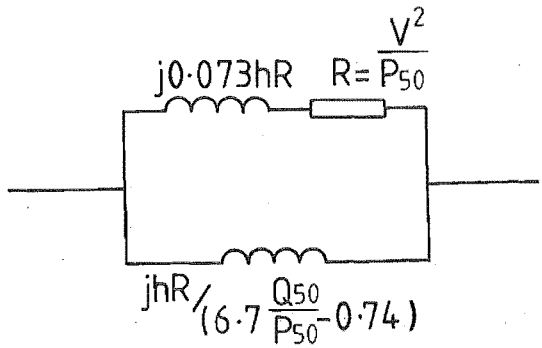

This model was derived by measurements performed on medium voltage loads using audio-frequency ripple control generators (Pesonen et al 1981).

D

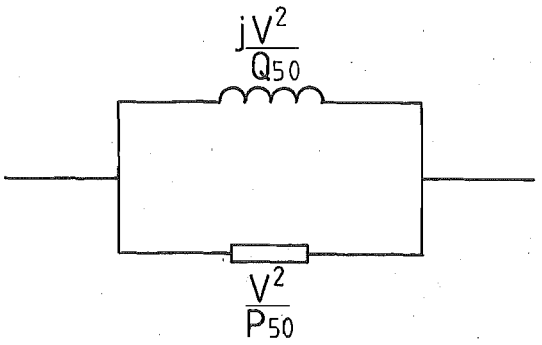

The load impedance calculated at 50 Hz remains constant for all frequencies (Ross 1972).

Converting the above models from impedance into a suitable form for inclusion into the system admittance matrices is straight forward.

Load modelling for transmission studies will become more difficult as supply authorities install filters at the points of supply, to remove ripple control signals from the distribution networks. If the point of supply harmonic impedances are capacitive, then series resonance with the supply transformer occurs, and assumptions made for these supply authorities need to be re-examined.

4.6 TRANSFORMER MODELLING

In general a two-winding, three phase transformer has a primitive, or unconnected, network consisting of six coupled coils, and is thus modelled as a six by six admittance matrix.

The transformer nodal admittance matrix is, in each case, derived from the primitive admittance by the expression

$$[Y_{node}] = [C]^T [Y_{prim}] [C] \qquad (4.1)$$

where $[C]$, the connection matrix, is derived from consideration of the actual transformer connections.

The star-g/delta transformer, one of the two common convertor transformer connections, does not provide a path for any zero sequence currents to flow from one voltage level to another. The nodal admittance matrix for this transformer connection, on the assumption of single phase units, is:

$$
[Y_{node}] = \left[\begin{array}{ccc|ccc}
\frac{Y_{t1}}{a_1^2} & & & -\frac{Y_{t1}}{\sqrt{3}\,a_1} & \frac{Y_{t1}}{\sqrt{3}\,a_1} & \\
& \frac{Y_{t2}}{a_2^2} & & & -\frac{Y_{t2}}{\sqrt{3}\,a_2} & \frac{Y_{t2}}{\sqrt{3}\,a_2} \\
& & \frac{Y_{t3}}{a_3^2} & \frac{Y_{t3}}{\sqrt{3}\,a_3} & & -\frac{Y_{t3}}{\sqrt{3}\,a_3} \\
\hline
\frac{-Y_{t1}}{\sqrt{3}\,a_1} & & \frac{Y_{t3}}{\sqrt{3}\,a_3} & \frac{Y_{t1}+Y_{t3}}{3} & -\frac{Y_{t1}}{3} & -\frac{Y_{t2}}{3} \\
\frac{Y_{t1}}{\sqrt{3}\,a_1} & \frac{-Y_{t2}}{\sqrt{3}\,a_2} & & -\frac{Y_{t1}}{3} & \frac{Y_{t2}+Y_{t1}}{3} & -\frac{Y_{t2}}{3} \\
& \frac{Y_{t2}}{\sqrt{3}\,a_2} & \frac{-Y_{t3}}{\sqrt{3}\,a_3} & -\frac{Y_{t3}}{3} & -\frac{Y_{t2}}{2} & \frac{Y_{t2}+Y_{t3}}{3}
\end{array}\right] \qquad (4.2)
$$

which is sufficiently general to investigate the effect of small asymmetries in single phase transformer units due either to leakage admittances, Y_t, or off-nominal tap ratios, a. If the three single phase units are perfectly symmetrical, the equivalent circuit for the star-g/delta connection, unity tap ratio, is as shown in Figure 4.4

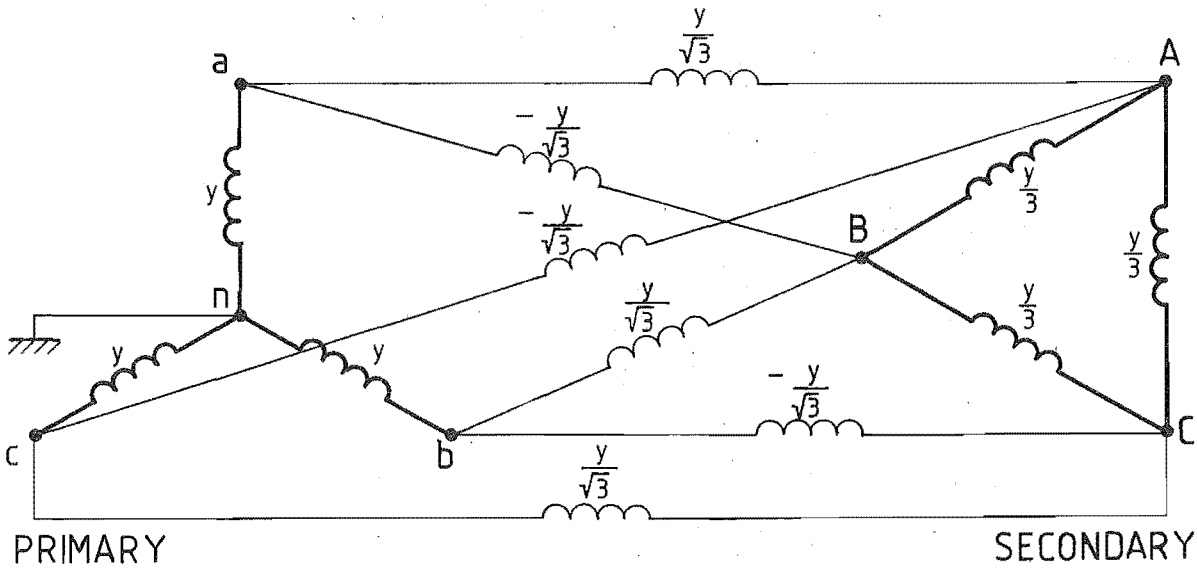

FIGURE 4.4: Equivalent Circuit for Symmetrical Star-g/delta Transformer (unity tap ratio)

The only information required is the leakage reactance, which is readily available, and transformer type, e.g. star-g/delta or star-g/star-g, being the common connections in New Zealand.

Transformer models developed at fundamental frequency are also used in harmonic studies, except for provision for damping due to winding losses as skin effect increases with frequency. Adielson et al (1981) and Degeneff et al (1982) confirm this approach with measured and simulated data. Transformer impedance is shown to be proportional to the leakage reactance and linear with frequency, up to 10 kHz where the interturn capacitances produce internal resonance. Since harmonic frequencies considered here are less than this, the magnetising inductance and stray capacitances can be neglected.

Avila-Rosales and Alvarado (1982) introduce a method for calculating eddy current losses, by solving the electromagnetic field theory problem in the transformer core. Such an approach is too detailed for the requirements of harmonic modelling, where a simple model applicable for all transformers, without knowledge of core or winding dimensions, is needed. Fortunately eddy current effects are considered small at harmonic frequencies and this approach is not required.

Szabados and Lee (1981) disagree with the assumption that transformers always operate in the linear region of the magnetisation curve. With less steel in transformer cores to reduce costs, and thus operation closer to the saturation region, they argue the need for non-linear modelling (Brandwajn et al 1982). There is considerable background harmonic content on the system, especially 3rd, 5th and 7th harmonics (Hyland 1981), due to the non-linear nature of transformers, indicating that this is an area for future endeavour.

Assuming that transformers are not operated in saturation, various impedance representations have been suggested to replace the leakage reactance:

A.

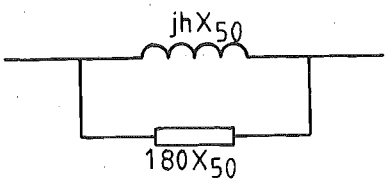

where X_{50} is the leakage reactance at 50 Hz (Harker 1980).

B.

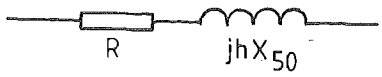

where $R = .1026\ kh\ X_{50}(J+h)$ (Baird 1981),
and J is the ratio of hysteresis to eddy current losses, taken as 3 for silicon steels and:

$$k = \frac{1}{J+1}$$

C. As for B except R and X are scaled to 80% of the 50 Hz values (Baird 1981).

D.

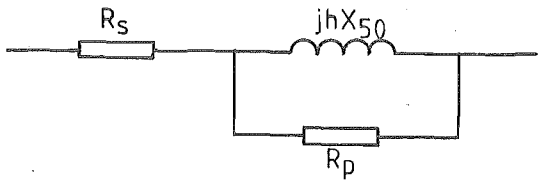

where, $90 < V^2/SR_s < 110$

$13 < SR_p/V^2 < 30$

with S being the rated power of the transformer (Pesonen et al 1981). For this case, R_s = 0.04 pu and R_p = 60 pu which corresponds to a 30 MVA rating.

E. As for D but with R_s = 0.01 pu and R_p = 20 pu, corresponding to a 100 MVA rating.

The last two models are the same except for transformer ratings and all transformers in the network were assumed to have the same rating.

4.7 CONCLUSIONS

While near balanced components such as capacitors, filters, generators, loads and transformers have been considered as balanced, provision in the models is available for any imbalance for which data is available.

The validity in assuming a simple equivalent circuit for distribution authority networks at harmonic frequencies has been investigated.

A number of practical models for loads, generators and transformers have been determined. The adequacy of the representations will be discussed in Chapter 7 using measurements taken on a transmission network, and by conducting sensitivity tests on each element model.

CHAPTER 5

TRANSMISSION LINE MODELLING

5.1 INTRODUCTION

Although the bridge convertor produces only positive and negative sequence harmonic currents, the coupling between sequence networks resulting from AC transmission system asymmetries can cause considerable zero sequence interference in nearby power or communications lines (Whitehead and Radley 1949 and Kuussaari and Pesonen 1976). The modelling of transmission lines connected to large convertor plant needed to assess the level of zero sequence harmonic current penetration, is discussed in this chapter. No attempt is made to model coupling into the communication network, the determination of which can only be achieved in simple situations (Meyer and Dommel 1969).

In fundamental frequency AC/DC power flow, the effect of line asymmetry can only be assessed by detailed representation of the AC transmission network in the phase frame of reference, with mutual effects included, as well as three phase analysis of the convertor operation (Arrillaga and Harker 1978, Harker and Arrillaga, 1979). Even when the analysis is restricted to purely sinusoidal voltages, the line and convertor voltage asymmetry are shown to produce phase currents of varying widths containing unbalanced, uncharacteristic harmonic frequencies, for which filtering is not normally provided.

Measurements of the harmonic currents at the rectifier end of the New Zealand DC link have shown deviations between phases of up to 56% (at 450 Hz) with an average deviation of 35% (Robinson 1966). The combined effect of the current imbalance and any system impedance imbalance is reflected in the phase voltages, which are shown in Table 5.1 for the Benmore 220 kV busbar. All harmonic voltages are unbalanced, with the most severe imbalance occurring at the non-characteristic third and ninth harmonics.

TABLE 5.1: Harmonic Voltage Measurements during Back-to-Back Testing of the New Zealand DC Link While Commissioning in 1966.

Harmonic	400 A dc (one third full load current) Phase-to-neutral voltages At Benmore 220 kV		
	Red phase (%)	Yellow phase (%)	Blue phase (%)
1	100	100	100
2	0.5	0.7	1.0
3	2.9	0.3	1.0
4	0.6	0.3	0.4
5	0.25	0.15	0.25
6	0.25	0.30	0.35
7	0.15	0.15	0.1
8	0	0.05	0.1
9	0.05	0.05	0.15
10	0.05	0.05	0.05
11	0.1	0.15	0.1
12	0.15	0.05	0.15
13	0.05	0.05	0.05
14	0.05	0.05	0.05
15	0.15	0	0.2
16	0	0.1	0.15
17	0.3	0.3	0.3
18	0	0.05	0.1
19	0.3	0.3	0.7

In this chapter, balanced current injections at the convertor illustrate the effects of a single transmission line configuration on the propagation of unbalanced harmonics. While the line distance may not be sufficient to cause unacceptable fundamental frequency voltage imbalance, the "electrical distance" at harmonic frequencies will increase in proportion to the harmonic order. Consequently the line is expected to exhibit standing wave effects.

5.2 SINGLE PHASE LINE MODEL

A physical understanding of the impedances, voltages and currents is difficult with a three phase mutually coupled ground return model. Moreover, much of the reference material (Clarke 1943, Kimbark 1950 and Chipman 1968) is primarily concerned with single phase balanced systems. Because of this an understanding of standing wave effects is approached from the single phase transmission line model. Three phase lines are illustrated as a progression from this.

Transmission line parameters are expressed as a series impedance, Z', and shunt admittance, Y', per unit length of line. Nominal PI models are of general use in fundamental frequency studies to represent single phase transmission lines, illustrated in Figure 5.1.

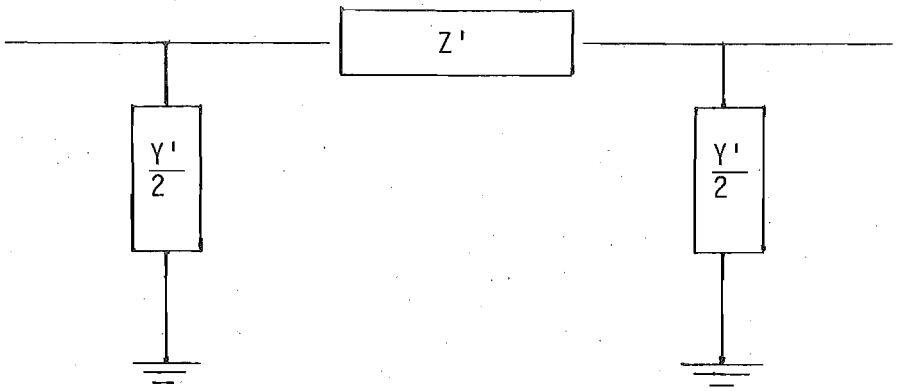

FIGURE 5.1: Nominal PI Transmission Line Model

When this model is used at harmonic frequencies a number of sections need to be cascaded. This depends on the frequency and line length; e.g. a 1500 km line at 50 Hz (1/4 wavelength) requires 3 cascaded Nominal PI sections to provide approximately 1% accuracy. As the frequency increases, the number of Nominal PI sections to maintain this accuracy increases proportionally; e.g. a 300 km long line requires 30 Nominal PI sections to maintain the above accuracy for the 50th harmonic.

The computational effort can be reduced and the accuracy improved with the use of an Equivalent PI model derived from the solution of the second order linear differential equations describing wave propagation along transmission lines (Kimbark 1950). Such a model, illustrated in Figure 5.2, is obtained from the Nominal PI model by using two correction factors:

$$\frac{\sinh(x\sqrt{Z'Y'})}{x\sqrt{Z'Y'}} \quad \text{for the series impedance} \qquad (5.1)$$

$$\frac{\tanh(x\sqrt{Z'Y'}/2)}{x\sqrt{Z'Y'}/2} \quad \text{for the shunt admittance} \qquad (5.2)$$

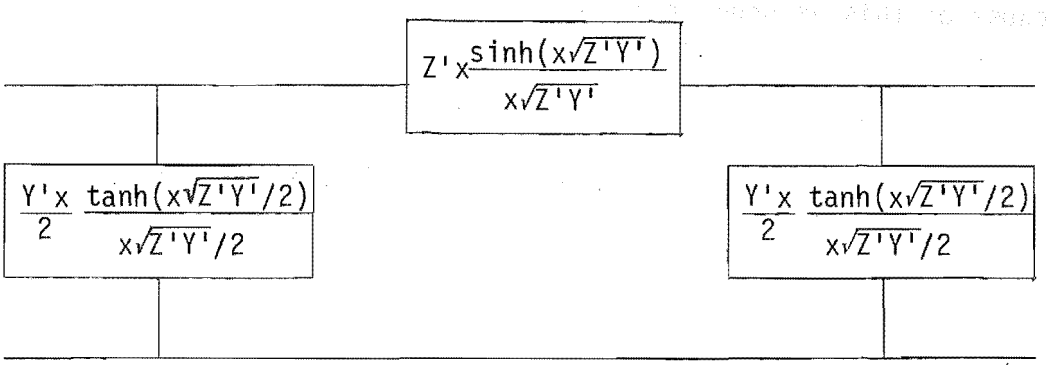

FIGURE 5.2: The Equivalent PI Model of a Long Transmission Line

Impedances in the diagram of Figure 5.3, obtained for a 230 km line, are plotted in Figure 5.4 against frequency. The impedances were calculated using geometric mean distances and three equal length transposition sections (Elgerd 1971). The shunt resistance and shunt reactance are formed by inverting the shunt admittance.

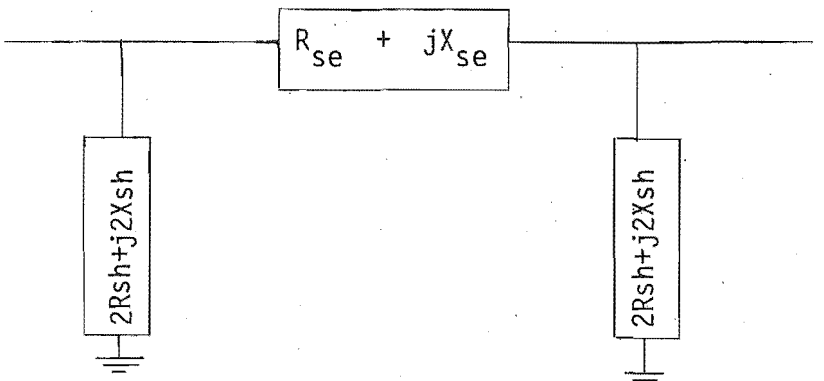

FIGURE 5.3: Equivalent PI Impedances

Predominant impedances can be observed as the series and shunt reactances, both of which have a period of 1300 Hz. The line length of 230 km is 1 wavelength at this frequency. The series reactance increases from its 50 Hz value, up to a maximum at 325 Hz, the ¼ wavelength frequency and then decreases, passing through zero at 650 Hz, the ½ wavelength frequency. The shunt reactance is capacitive and large at

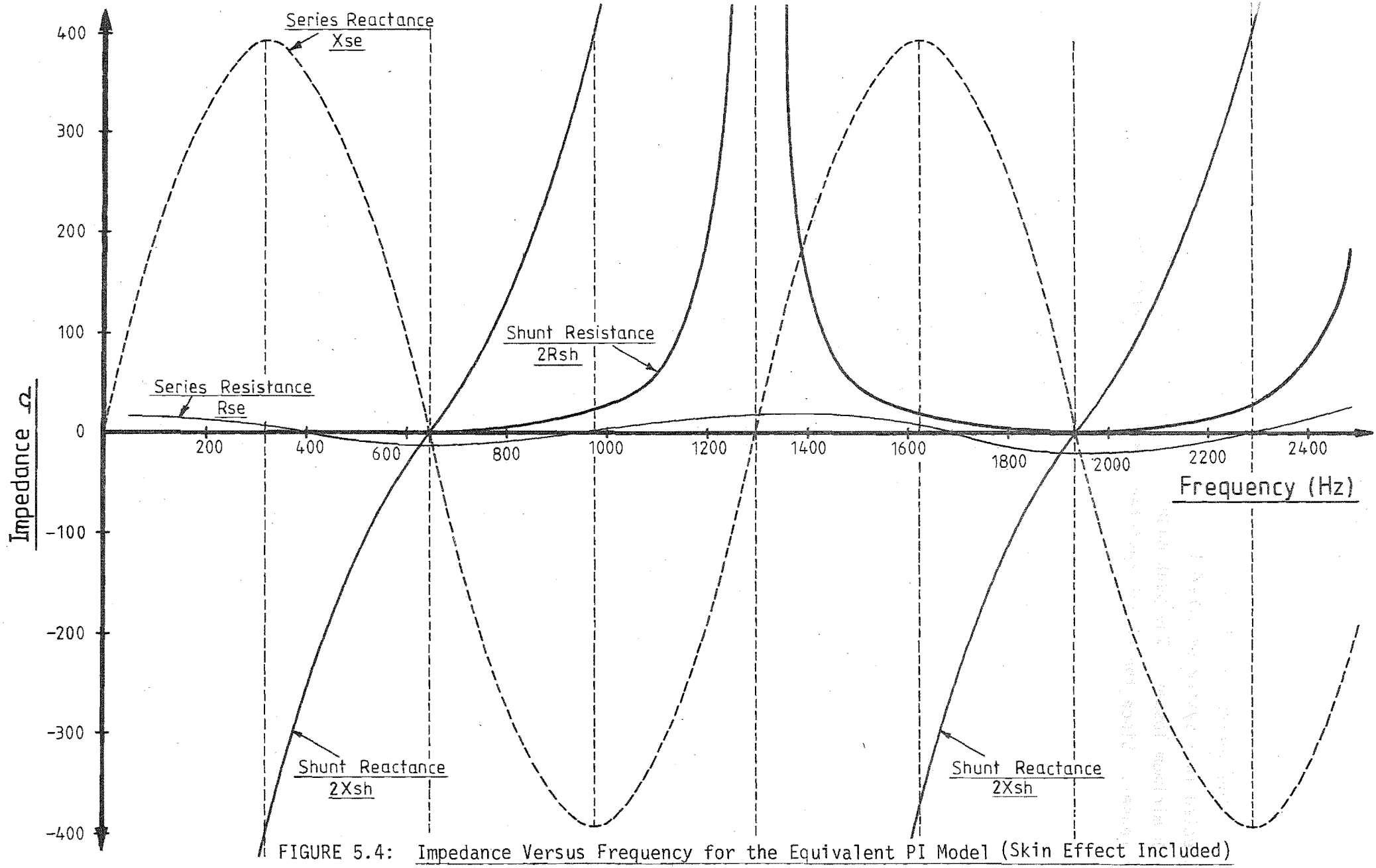

FIGURE 5.4: Impedance Versus Frequency for the Equivalent PI Model (Skin Effect Included)

fundamental frequency, reducing in magnitude until the ½ wavelength frequency, beyond which it becomes inductive.

The series resistance is small at audio frequencies. This is expected in a system designed to transmit power at fundamental frequency with minimum losses. The peak magnitudes increase slowly as frequency increases. Since the series resistance does not get appreciably larger over the audio frequency range, the attenuation does not increase significantly. Frequencies in this range will propagate large distances on the power system. The negative resistances are a mathematical artifice and are not physically measurable. They give the correct terminal conditions for a distributed parameter transmission line.

The shunt resistance, which is normally considered to be zero in a Nominal PI model, has considerable effect at resonant frequencies and, as can be observed from Figure 5.4, becomes very large as the wavelength frequency is approached.

The conditions of a transmission line at resonance can be considered similar to an alternately series and parallel resonating tuned circuit. In Figure 5.4 the series and shunt reactance are equal in magnitude but of opposite sign at 325 Hz, i.e. a series resonance (or node) with a purely resistive low impedance. This can be seen in Figure 5.5 where the impedance of the open circuited line is plotted.

Although at 650 Hz both the series and shunt reactances are small, the transmission line has a high impedance equivalent to a parallel resonating tuned circuit. This condition is called an antinode and can also be observed on Figure 5.5. Low impedance magnitudes at series resonance occur for an open circuited line at the odd ¼ wavelength frequencies, as well as at the parallel resonances of the ½ wavelength frequencies.

At series resonance the impedance of the line comprises only the series and shunt resistances. The low impedance at these frequencies and the large impedance at the ½ wavelength frequencies, indicate the low level of attenuation of audio frequency signals. The addition of other system components such as loads and generators must provide the harmonic damping.

FIGURE 5.5: Impedance Versus Frequency for the Open Circuited Islington to Kikiwa Transmission Line (Skin Effect Included)

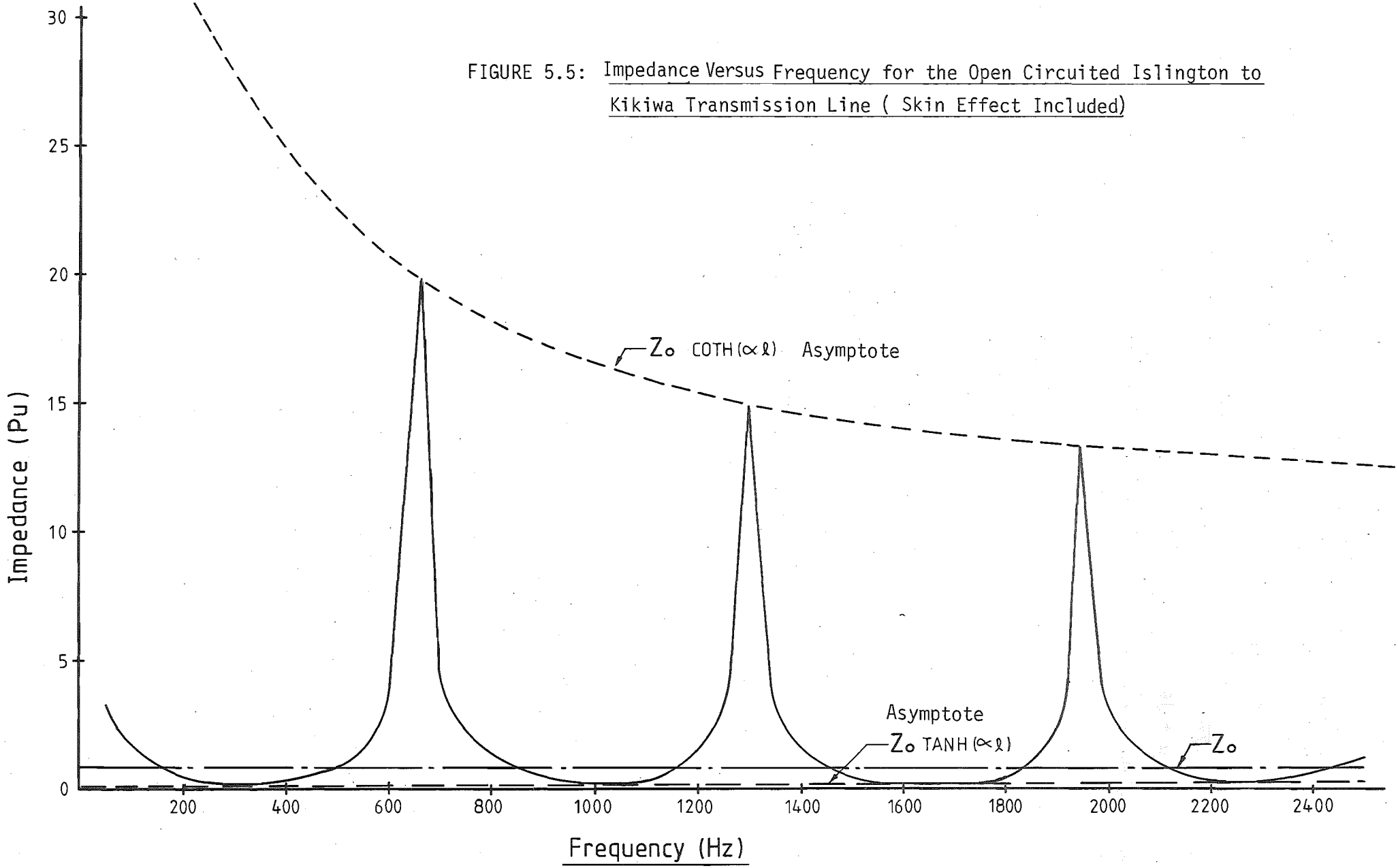

The asymptotes of Figure 5.5 are calculated from a knowledge of the total series impedance, Z, and shunt reactance, Y, of the line, (Kimbark 1950). The propagation constant γ is:

$$\gamma = \sqrt{ZY} = \alpha + j\beta \tag{5.3}$$

where α is the attenuation constant and β is the phase constant. The characteristic impedance Zo is:

$$Zo = \sqrt{\frac{Z}{Y}} \tag{5.4}$$

The upper asymptote or maximum impedance is:

$$Zo \coth(\alpha x) \tag{5.5}$$

and the lower asymptote or minimum impedance is:

$$Zo \tanh(\alpha x) \tag{5.6}$$

The lower asymptote is small in value and slowly increases with frequency, while the upper asymptote decreases from an infinite value as frequency increases. For large frequencies these two asymptotes approach a value equal to the characteristic impedance.

5.3 MULTICONDUCTOR TRANSMISSION LINE MODELLING

Multiconductor transmission line modelling uses the known and readily obtainable line geometry and conductor types to calculate electrical parameters. These parameters are not easily measured on the EHV network. With ground return, the resistances and inductances are frequency dependent.

Initial work in developing computer transmission line models at fundamental frequency was done by Coleman et al (1958), Thomas (1959), Hesse (1963) and Shipley et al (1963) and is summarised in Appendix 4.

Their work was based on that of Carson (1926) who solved the equations for a transmission line in the presence of the earth. The approximate series of Clarke (1943) are in general use, with little reference being made to the original infinite series.

Long line high frequency modelling was proposed by Wedepohl (1963) for travelling wave effects and implemented by Galloway et al (1964). Bowman and McNamee (1964) developed the correction factors for the model, and this material was adapted for harmonic frequencies in Arrillaga et al (1983 included in Appendix 4.

A program written by New Zealand Electricity to calculate the Nominal PI multiconductor parameters, has been extended here to include the Equivalent PI model and skin effect.

In the case of multiconductor transmission lines, the Nominal PI series impedance and shunt admittance matrices per km, $[Z']$ and $[Y']$ respectively, are square, their size being fixed by the number of mutually coupled conductors.

The derivation of the Equivalent PI model from the Nominal PI matrices, is similar to that of the single phase lines, except that it involves the evaluation of hyperbolic functions of a matrix. This can be achieved by series expansion or by transformation into a diagonal matrix. The latter method was chosen and this avoided determining the number of terms in the expansion, although there is no reason why series expansion would not be acceptable.

The use of eigenvalue analysis results in the following expressions for the Equivalent PI Model (Bowman and McNamee 1964):

$$[Z]_{EPM} = x[Z'][M]\left[\frac{\sinh(\gamma x)}{(\gamma x)}\right][M]^{-1} \tag{5.7}$$

where x is the transmission line length

$[Z]_{EPM}$ is the EquivalentPI series impedance matrix

$[M]$ is the matrix of normalized eigenvectors

$$\left[\frac{\sinh(\gamma x)}{(\gamma x)}\right] = \begin{bmatrix} \frac{\sinh(\gamma_1 x)}{(\gamma_1 x)} & 0 & \cdots & 0 \\ 0 & \frac{\sinh(\gamma_2 x)}{(\gamma_2 x)} & & 0 \\ \vdots & & & \\ 0 & 0 & & \frac{\sinh(\gamma_j x)}{(\gamma_j x)} \end{bmatrix} \tag{5.8}$$

and γ_j is the jth eigenvalue for $\frac{j}{3}$ mutually coupled circuits. Similarly

$$[Y]_{EPM} = x[M]\left[\frac{\tanh(\gamma x/2)}{(\gamma x/2)}\right][M]^{-1}[Y'] \tag{5.9}$$

where $[Y]_{EPM}$ is the Equivalent PI shunt admittance matrix.

An illustration of the relative accuracies achieved by the Equivalent PI and Nominal PI models is displayed in Figure 5.6.

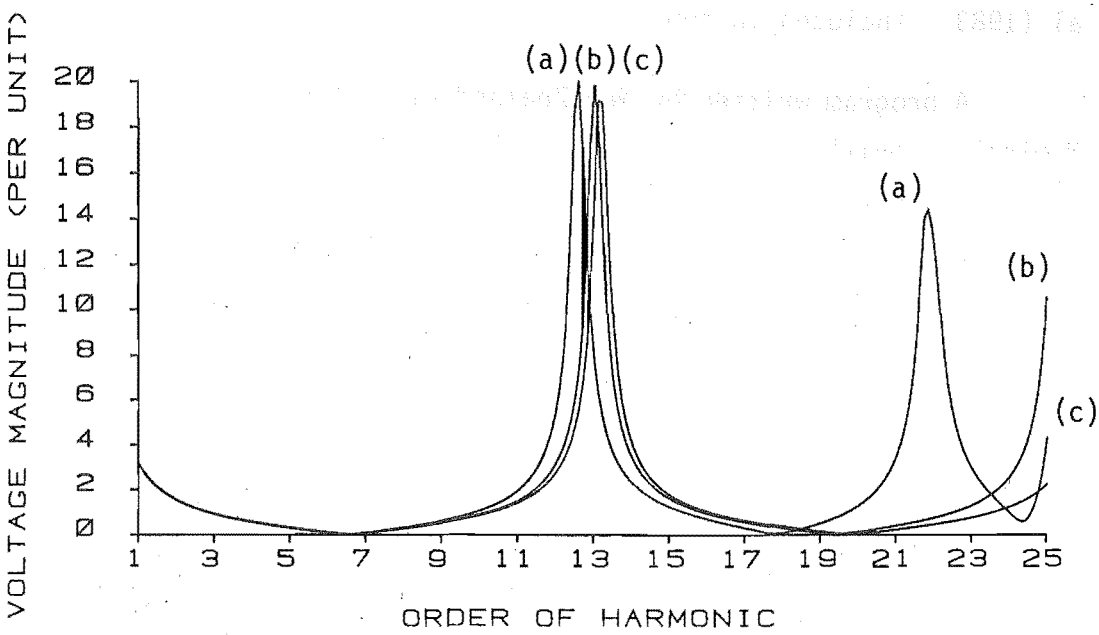

FIGURE 5.6: Comparison of the Equivalent and Nominal PI Transmission Line Models at 5 Hz Intervals (a) 3 sections, (b) 6 sections (c) Equivalent PI

This figure shows the per unit positive sequence voltages of a 230 km, 220 kV line (for parameter information refer to Figure 5.7). Standing wave effects show the different accuracies provided by the two models, with the resonant frequencies of the Nominal PI model approaching those of the Equivalent PI model as the number of sections increases from 3 to 6. Accuracy of the Nominal PI model decreases as the frequency increases and this can be observed at the wavelength frequency.

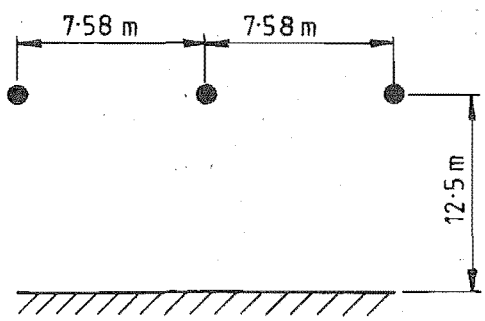

Conductor type Zebra (54/3.18 + 7/3.18)
Length = 230 km, resistivity 100 Ωm

FIGURE 5.7: Conductor Information for the Islington to Kikiwa Line

Cascading of Nominal PIs requires a large number of sections for long lines at higher frequencies, to achieve acceptable accuracy. The Equivalent PI model avoids the problems of determining the number of sections needed and round-off error that accumulates in this situation.

Derivation of correction factors for conversion from the Nominal PI to Equivalent PI model, and their incorporation with the series impedance and shunt admittance matrices, is carried out as indicated in the structure diagram of Figure 5.8. The LR2 algorithm of Wilkinson and Reinsch (1971) is used with due regard for accurate calculations in the derivation of the eigenvalues and eigenvectors.

5.4 SKIN EFFECT MODELLING

Change in conductor parameters due to the non-uniform current distribution inside a conductor is termed "skin effect". Current tends to flow on the surface or skin of a conductor and this effect increases as frequency increases. The consequence of skin effect is an increase in the resistance of the conductor and a decrease in its internal inductance (Chipman 1968). The solution of the field theory equations for skin effect have been summarised in Appendix 4.

Changes in the internal inductance have little effect on the geometric mean radius and therefore on the conductor component of self inductance and on the self inductance with ground return. Therefore the inductive skin effect is usually ignored (Kimbark 1950).

When conductors are separated by small distances, the magnetic field inside the conductor is not circular. Current density is not symmetrical about the conductor axis and the net effect is an increase in series resistance and a decrease in inductive reactance. This phenomenon is called "proximity effect". In solid round wires, this effect is much less significant than skin effect, and Kennelly et al (1915) conclude that it can be neglected for separations greater than 20 cm. Since bundled conductors are generally spaced slightly further apart than this, proximity effects have been neglected. This is not the case for cable parameters however.

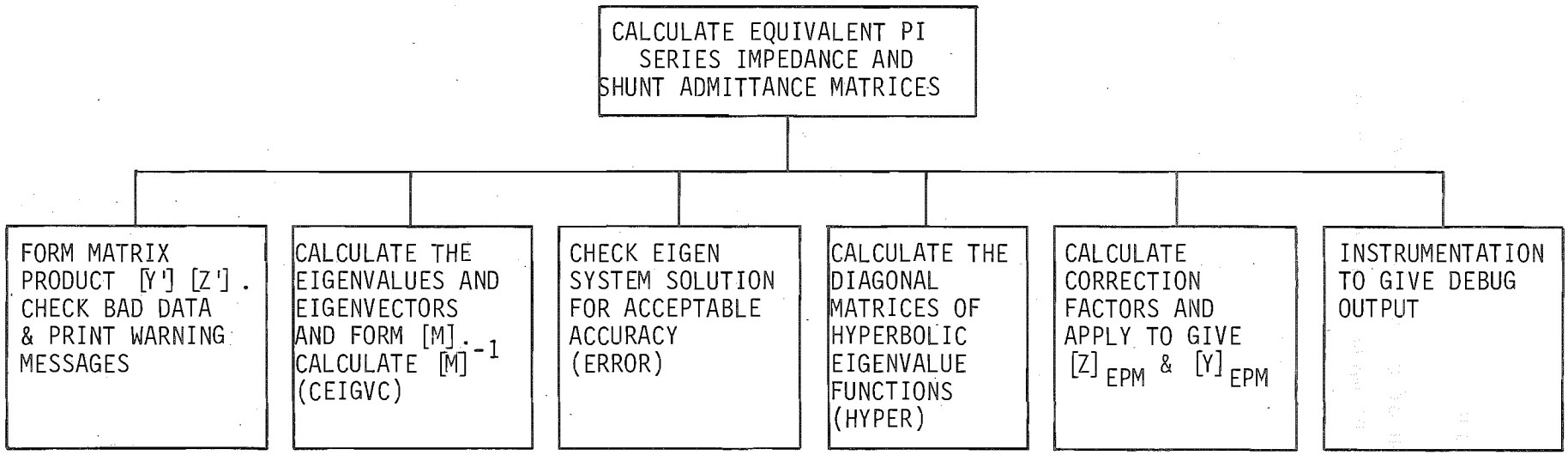

FIGURE 5.8: Structure Diagram for the Equivalent PI Model. Subroutine Names are in Brackets.

Kennelly et al (1915) conducted tests on solid copper and aluminium wires and simple stranded wires at various separations, up to 5 kHz. It was observed that stranded conductors without spiralling had similar skin effect ratios to solid conductors of the same cross-sectional area. Unfortunately, ACSR cables (Aluminium Conductor Steel Reinforced) used in power system transmission lines have steel cores and multiple layers of aluminium strands with different lays. Some current leaks from strand to strand and this leakage will vary depending upon the condition of the strand surface, the conductor tension, and length of lay and will change over the time of service. These non-ideal parameters make calculation of the skin effect ratio over a range of frequencies difficult. A number of authors (Zaborszky 1953, Silvester 1969, King 1970 and Comellini et al 1973) have developed accurate models for various combinations of these effects at power frequencies, by dividing the conductors into a number of sub-conductors. However, the amount of data and computation required to do this for each conductor prohibits its use for a general transmission line model.

Simpler relationships developed for solid conductors, valid for various frequency ranges (Westinghouse 1950 and Breuer et al 1982), do not give completely accurate results for ACSR cables as can be seen from Figure 5.9.

These approximate relationships have been applied to the resistance of the series impedance in single phase models, i.e. the skin effect ratio is applied to the resistance of an equivalent conductor and not to each conductor individually.

Lewis and Tuttle (1958) presented a practical method of calculating the skin effect resistance ratios by approximating ACSR conductors to uniform tubes having the same inside and outside diameters as the aluminium conductors, see Figure 5.10. The assumption is that little current flows in the steel core.

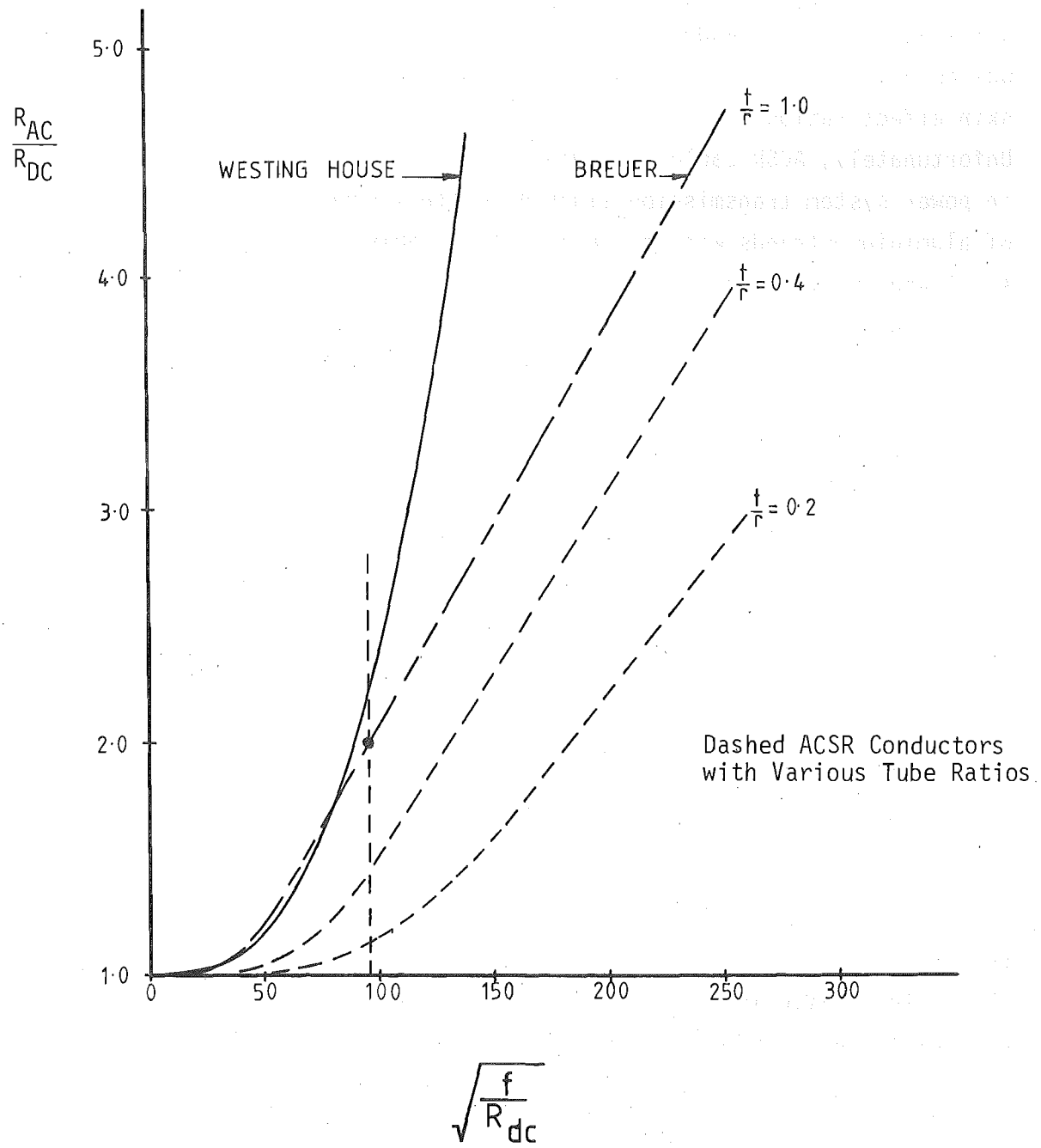

FIGURE 5.9: Skin Effect Resistance Ratios for Different Models

• Skin Effect Ratio for Islington to Kikiwa Line at the ½ Wavelength Resonant Frequency.

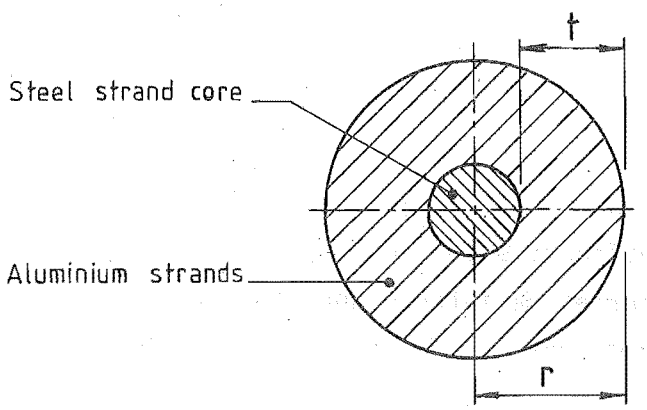

FIGURE 5.10: ACSR Hollow Tube Conductor Representation

These relationships involve Bessel functions given in a suitable form for computer applications by Abramowitz and Segun (1968). Values are most accurate for an even number of layers of aluminium, the longitudinal magnetic field for each layer induced in the core almost cancelling. The worst case is for a single layer cable where the skin effect resistance ratio is current dependent. At transmission voltages single layered cables are used infrequently.

Thickness to radius ratios for some common conductors are presented in Table 5.2 and a range of values plotted in Figure 5.9.

TABLE 5.2: Tube Ratios for Commonly Used Conductors

Conductor	$\frac{t}{r}$
Chukar	.73
Special (2)	.67
Special (3)	.77
Pheasant	.66
Zebra	.66
Goat	.57
Coyote	.64

To avoid errors in resonant peaks the more rigorous Bessel function relationships for tubular conductors have been used. There is a trade-off between accuracy and computation cost; the necessary solution being an acceptance of some inaccuracy for practical computability. It is however doubtful if more accurate skin effect ratios are justified in a practical power system.

For long lines, skin effect ratios and their effect on the resonant voltage magnitudes, are important. Because the series resistance of a transmission line is a small component of the series impedance when the transmission line is not at resonance, the harmonic voltages do not change to any significant extent when skin effect is included, Figure 5.11. At resonance the series resistance and shunt conductance become the dominant system components. Changes in the series resistance magnitude change the voltage peaks but do not affect the resonant frequency.

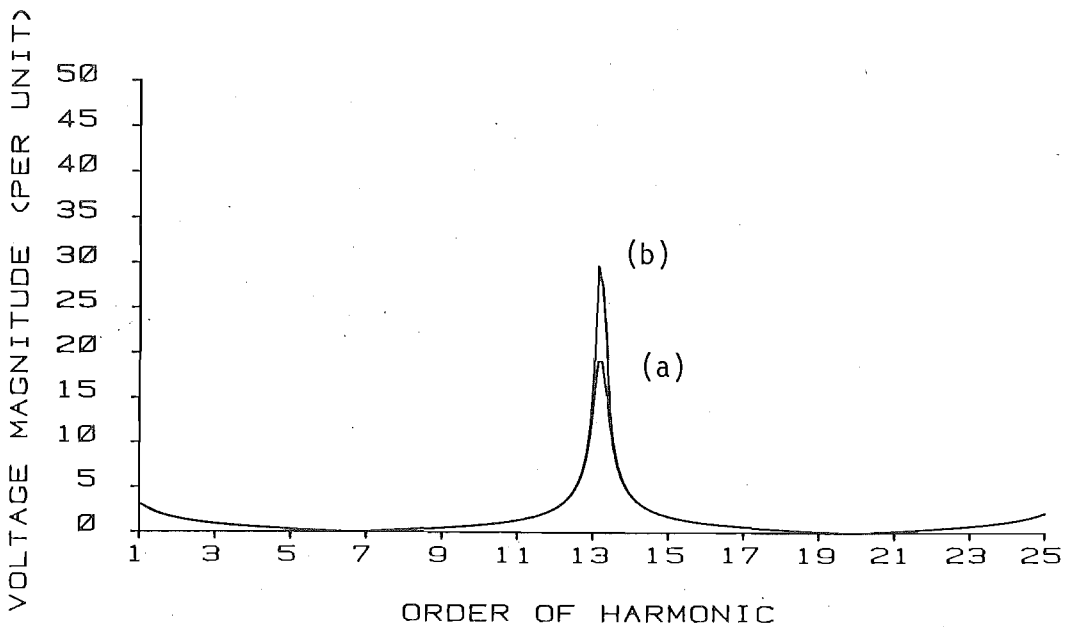

FIGURE 5.11: The Effect of Skin Effect Modelling
(a) Skin Effect included (b) No Skin Effect

Referring to Figure 5.11, the voltage ratio at resonance between cases with and without skin effect is 1.5. The skin effect ratio calculated from Figure 5.9 is 2.0. In a single phase model without ground return the ratio of voltages at resonance, with and without skin effect, is the same as the skin effect ratio. In a three phase model the presence of shunt conductance and series resistance coupling between phases, and the different resonant frequencies of the phases, reduces the resonant peak voltages compared with single phase modelling.

The combined effects of climate and loading on line temperatures alters line resistance. If the resistance ratio of a line is defined as:

$$\frac{R2}{R1} = \frac{T + t2}{T + t1} \qquad (5.10)$$

where t1, t2 are the temperatures in Centigrade and T is a constant dependent on conductor type, (228 for hard drawn aluminium, 241 for hard drawn copper), then with t1 = 10^{o}C and t2 = 40^{o}C for aluminium:

$$\frac{R2}{R1} = \frac{228 + 40}{228 + 10} \simeq 1.13 \qquad (5.11)$$

A thirty degree Centigrade change in line temperature is not unusual for a line with a load curve similar to that of the New Zealand system. Change in DC resistance and hence resonant peak magnitude voltage is approximately 13%. Since a transmission line forms part of a power system with variable conditions, it is not justifiable to include extremely accurate skin effect resistance ratios, valid in only a small number of controlled conditions.

5.5 APPLICATIONS OF THE COMPUTER MODEL

5.5.1 Harmonics Generated Along Transmission Lines

The Islington to Kikiwa line of the New Zealand system has been used to test the computer model described in previous sections.

A three dimensional graphic representation has been developed to provide simultaneous information of the harmonic levels along the line. At each harmonic (up to the 25th harmonic), one per unit positive sequence current is injected at the Islington end of the line. The voltages caused by this current injection are the same as the calculated impedances, where V_+ gives Z_{++}, V_- gives Z_{+-} and V_o gives Z_{+o}, (the subscripts +, -, o refer to the positive, negative and zero sequences respectively).

Figures 5.12 - 5.14 illustrate the effect of two extreme cases of line termination (at Kikiwa), the line open circuited and short circuited respectively. The differences in harmonic magnitudes along the line are due to standing wave effects and shifting of the resonant frequencies caused by line terminations.

Figure 5.12 indicates the high voltages at both ends of the open circuited line at the half wavelength frequencies. The 25th harmonic illustrates the shape of the line resonance; that of a rectified cosine wave. The minima are sharper than the maxima and although the magnitude of the minima are low they are not zero. Minima or nodes are separated by a distance of ½ wavelength at the frequency concerned and the maxima and minima alternate; separated by ¼ wavelength. High currents flow on the line at points of low voltage. Thus at a particular frequency, high harmonic voltages can be used to indicate the presence of high harmonic currents at some point (a maximum at a ¼ wavelength away) in the line.

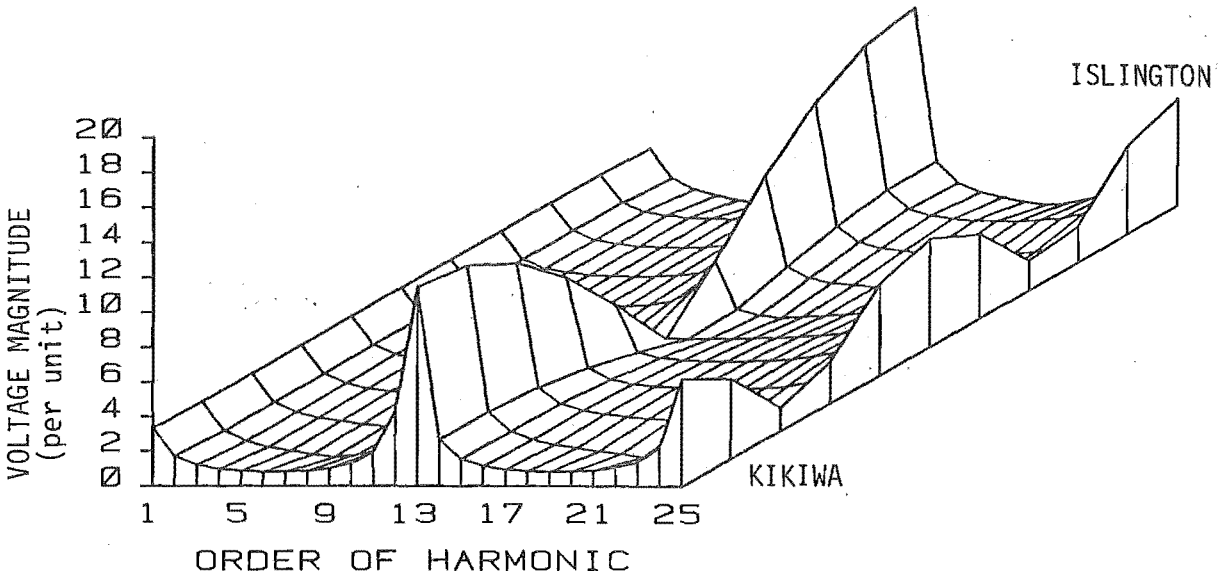

FIGURE 5.12: Positive Sequence Voltage versus Frequency Along the Open Ended Islington to Kikiwa Line

Resonant conditions of the current along the line are indicated in Figure 5.13a. Nodes and antinodes along the line correspond to the positions of voltage antinodes and nodes respectively. The one pu current injection at the Islington bus can be observed at the 25th harmonic. The incomplete ½ sine wave at this bus for the 13th harmonic is caused by the ½ wavelength frequency being slightly less than 650 Hz.

A short circuited line will resonate at odd ¼ wavelength frequencies. This is illustrated in Figure 5.14a. High current levels at the Kikiwa end of the line are due to the short circuit. Earlier in this chapter Figure 5.5 indicated that the resonant maxima decrease as frequency increases. However, this is not the case in Figure 5.14a. Points are calculated at 50 Hz intervals and if resonances do not fall on these frequencies a misleading impression of the magnitudes is obtained. It should be noted that peak magnitudes at non-harmonic frequencies may be greater than the values plotted.

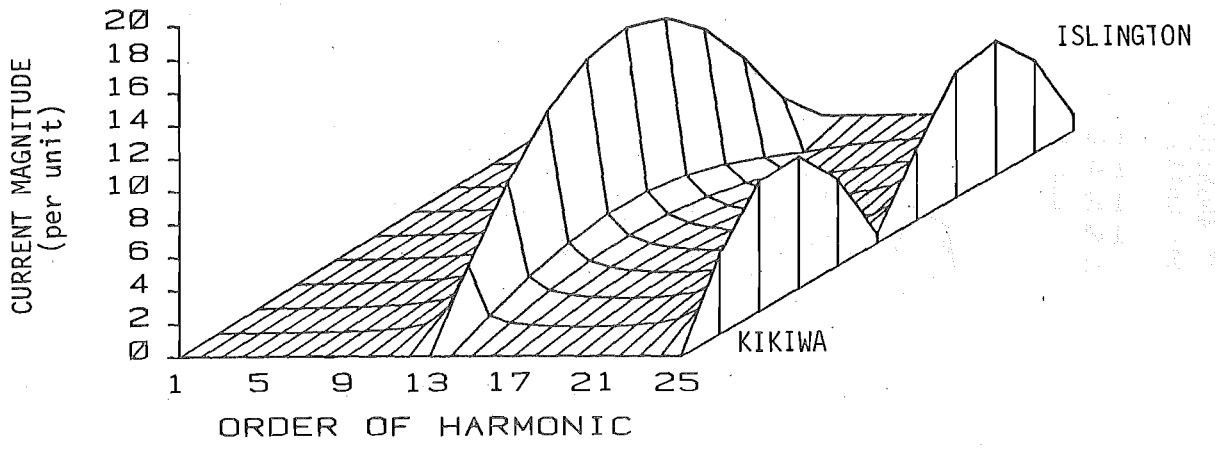

(a) Positive Sequence Current

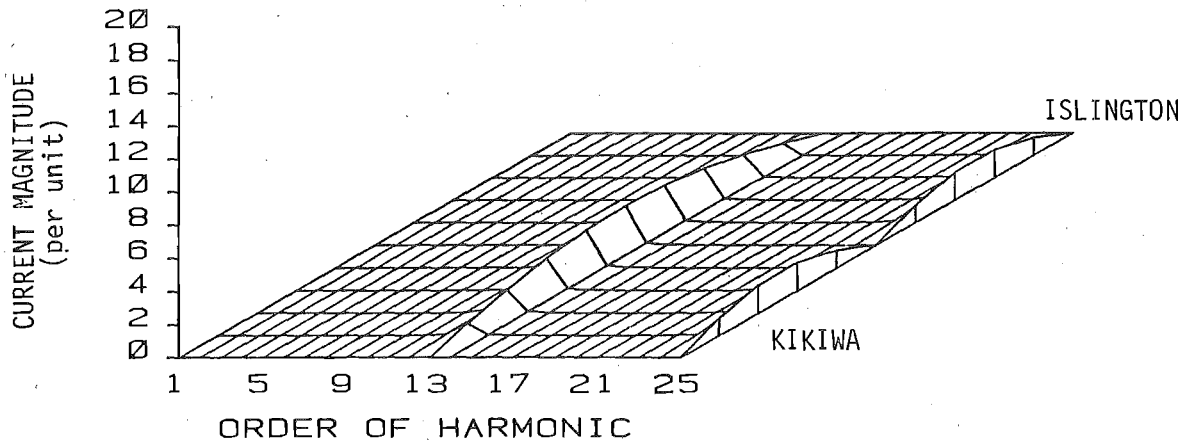

(b) Negative Sequence Current

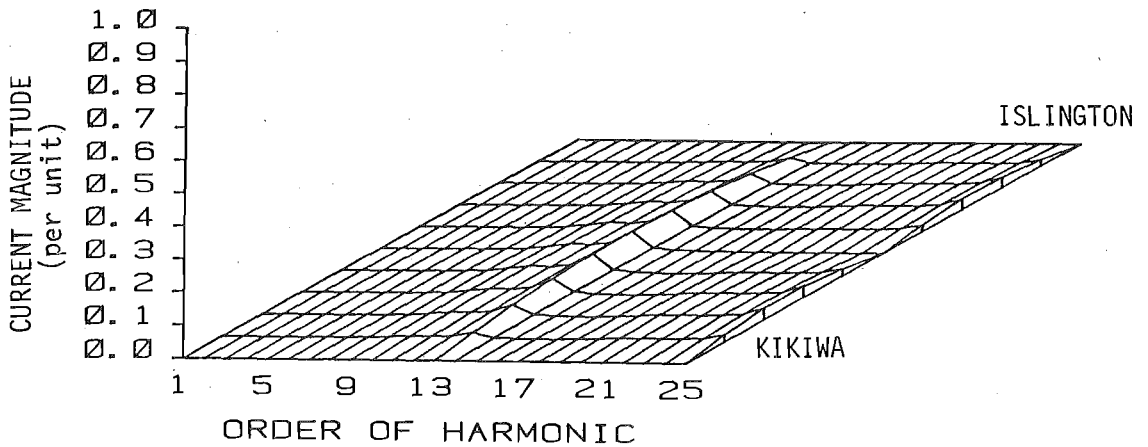

(c) Zero Sequence Current

FIGURE 5.13: Sequence Currents Along the Open Ended Line for a 1 pu Positive Sequence Current Injection

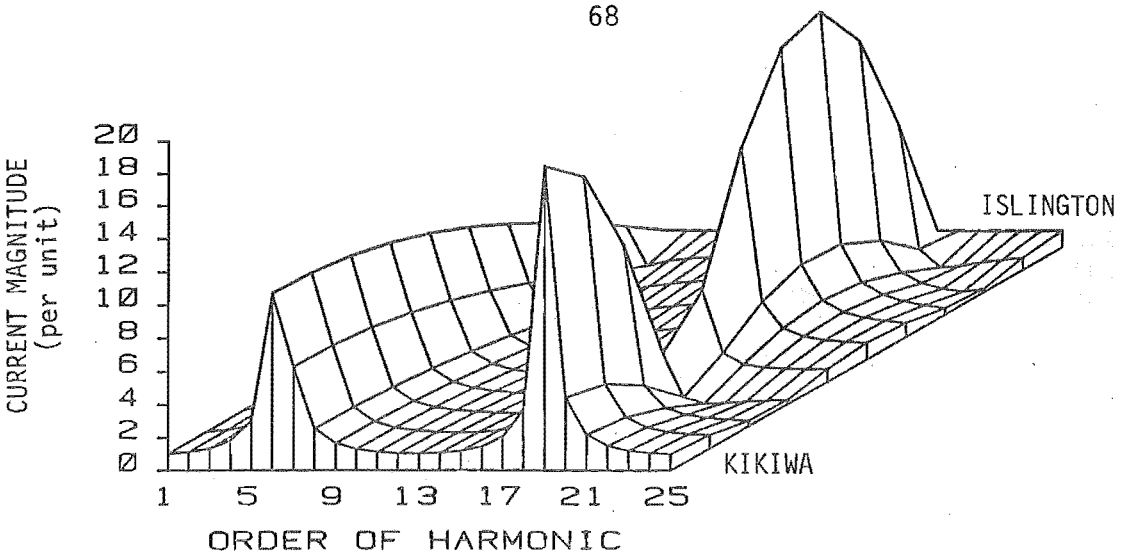

(a) Positive Sequence Current

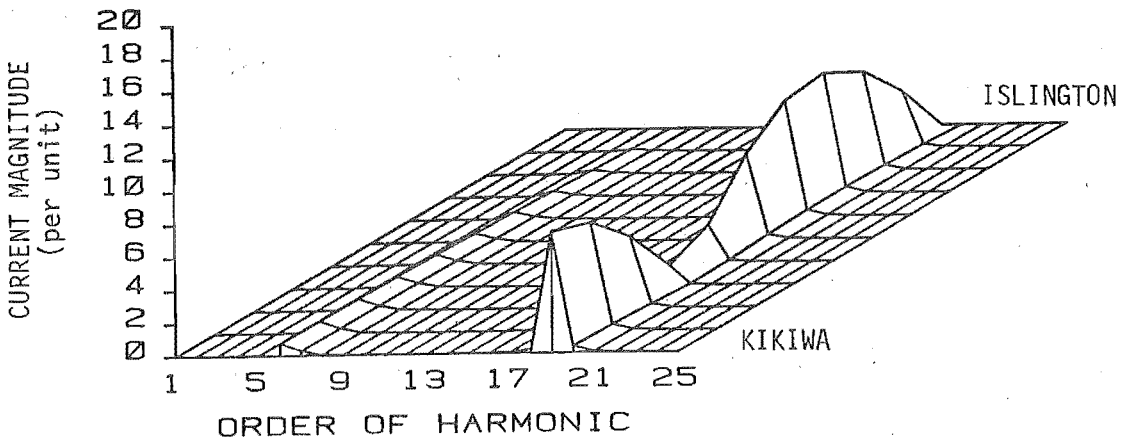

(b) Negative Sequence Current

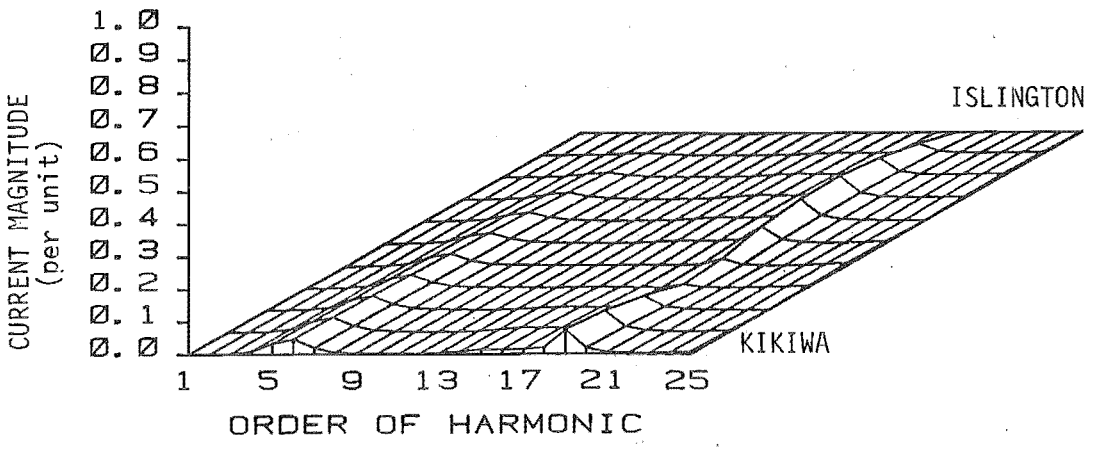

(c) Zero Sequence Current

FIGURE 5.14: Sequence Currents along the Short Circuited Line for a 1 pu Positive Sequence Current Injection

5.5.2 Zero Sequence Harmonics in Transmission Lines Connected to Static Convertors

It is the zero sequence penetration, rather than the positive sequence, that provides relevant information for the assessment of possible harmonic interference in neighbouring telephone systems. Presence of zero sequence in a transmission line connected to a convertor bridge is entirely due to asymmetries in either the convertor AC plant components or the transmission line itself.

In Figure 5.14, locations of maximum zero sequence current coincide with those of the positive sequence, and the highest level produced in the test line, about 10% of the injected positive sequence current, occurs at the 19th harmonic, at the Kikiwa end of the short circuited line. Levels of zero sequence current are low and the scale change between positive and zero sequence should be pointed out.

When 1 pu zero sequence is injected into the open circuited line, the zero sequence resonances of Figure 5.15 result. Levels of zero sequence are lower than the similar positive sequence resonance for a positive sequence current injection, and the resonant frequency at the 10th harmonic is considerably different. Attenuation is greater, indicating that the zero sequence currents will not propagate as far.

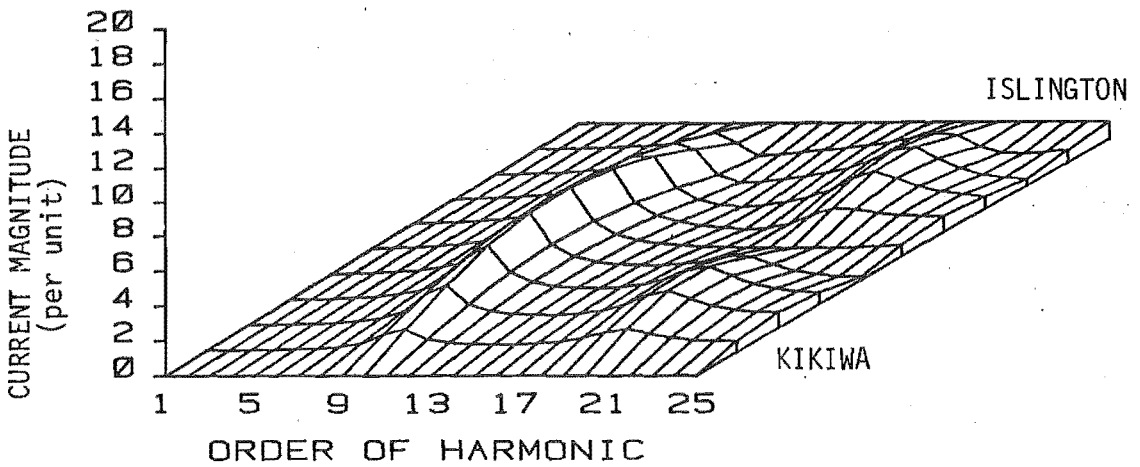

FIGURE 5.15: Zero Sequence Current versus Frequency for a 1 pu Zero Sequence Current Injection

When one per unit positive sequence harmonic current is now injected by a convertor bridge into the secondary (valve side) of a star-g/delta transformer connected to the same Islington to Kikiwa transmission line, the harmonic currents in Figure 5.16 result. Care should again be used when comparing positive and zero sequence quantities because of the scale change.

The effects of a convertor transformer can be assessed by comparing the results of Figures 5.13 and 5.16. The transformer has little effect on the positive and negative sequence harmonic currents produced by the positive sequence current injection. However, the provision of a low impedance zero sequence path, due to the transformer delta connection, increases substantially the generation of zero sequence harmonic current. This is illustrated by the larger content of 13th harmonic current in 5.16c. Also the zero sequence does not have the same resonant frequency as Figure 5.13.

In practical convertor installations filters reduce the harmonic current injection into the system considerably. Smaller current injections produce considerably less zero sequence in the AC system. This can be observed in Figure 5.17 where filters for the characteristic harmonics have been connected to the Islington bus. The levels are particularly low at 5th, 7th, 11th, 13th, and above the 17th harmonic, corresponding to the filter design frequencies.

By adding a 9th harmonic filter branch it is possible to excite a parallel resonance at the 8th harmonic. This is shown in Figure 5.18. The one per unit positive sequence current injection can be seen at the Islington bus. This is a common situation where the filters resonate with the system impedance, in this case that of the line, between the filter design frequencies.

Figure 5.19 illustrates the effect of a large imbalance, e.g. an open circuited phase in the filter bank. The pronounced coupling between sequence networks in this case, gives rise to considerable levels of zero sequence harmonic currents, with the highest level occurring at the 14th harmonic. Levels of the three sequence networks are similar.

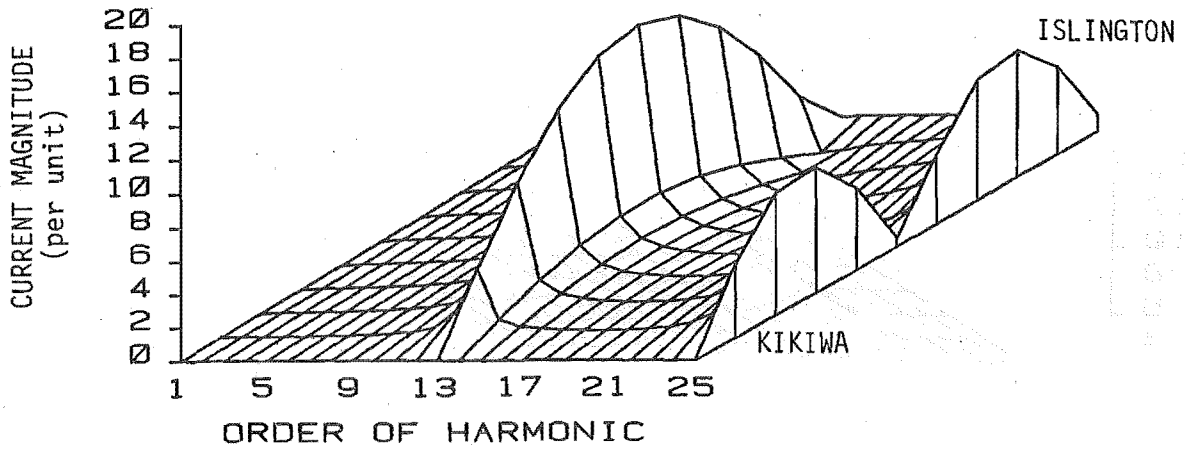

(a) Positive Sequence Currents

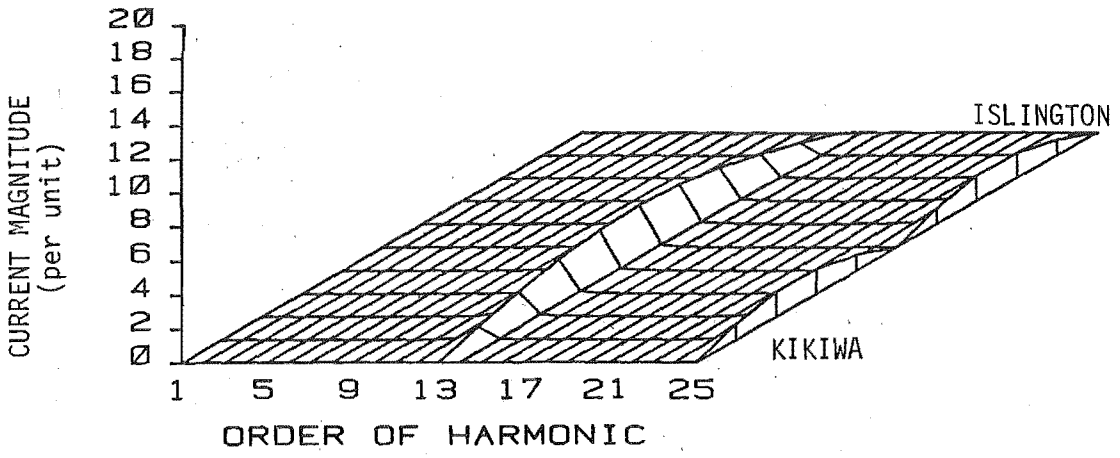

(b) Negative Sequence Currents

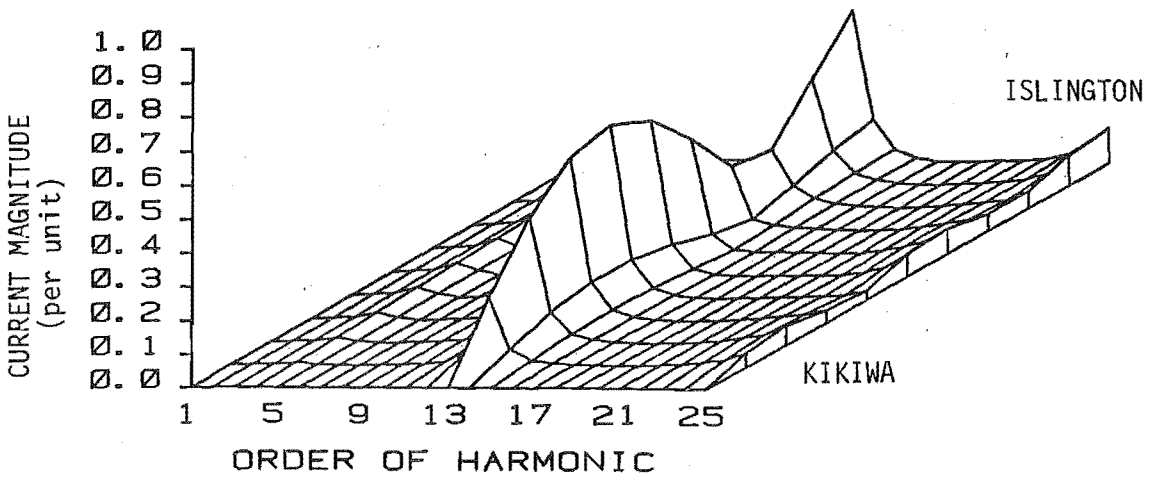

(c) Zero Sequence Current

FIGURE 5.16: Sequence Currents for a 1 pu Positive Sequence Current Injected into a Transformer and Line

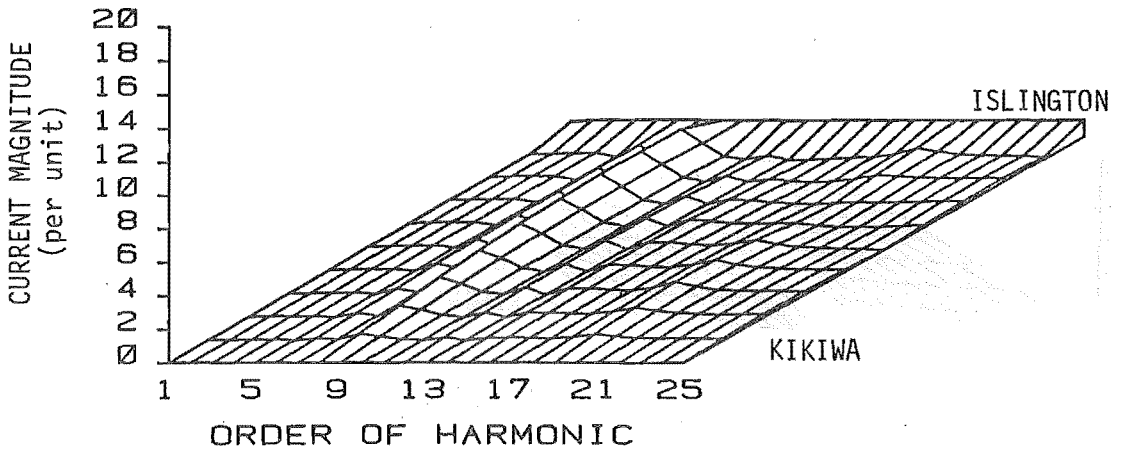

(a) Positive Sequence Current

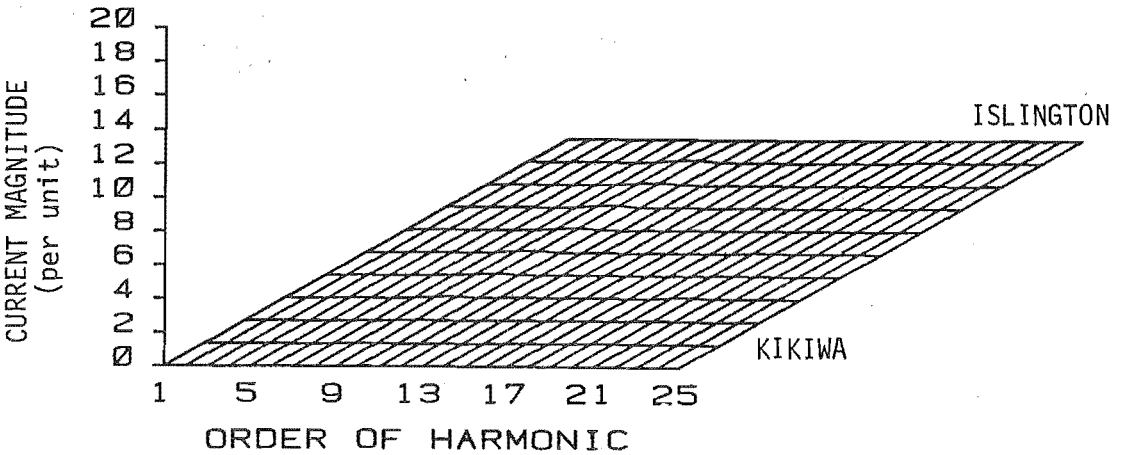

(b) Negative Sequence Current

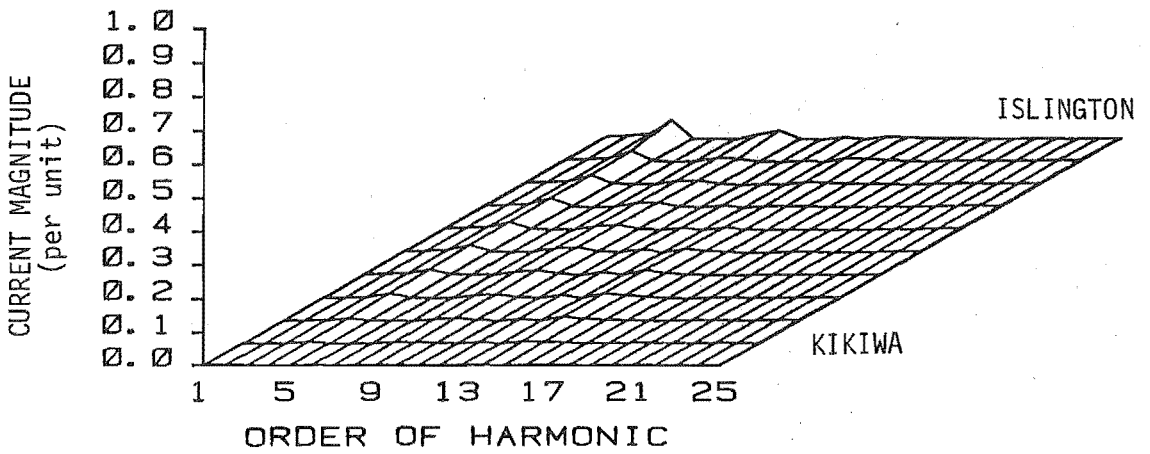

(c) Zero Sequence Currents

FIGURE 5.17: Sequence Currents for a 1 pu Positive Sequence Current Injection in the Presence of a Convertor Transformer & Filters

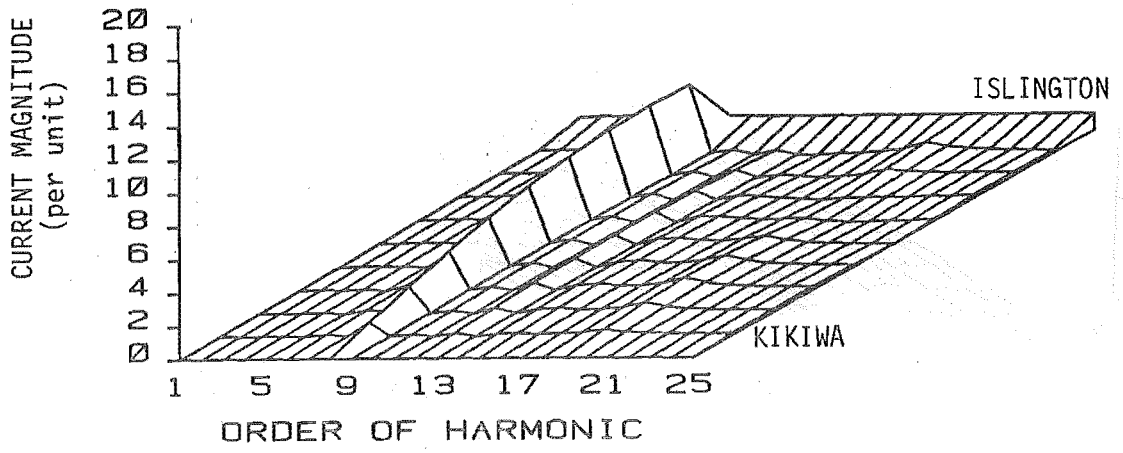

(a) Positive Sequence Current

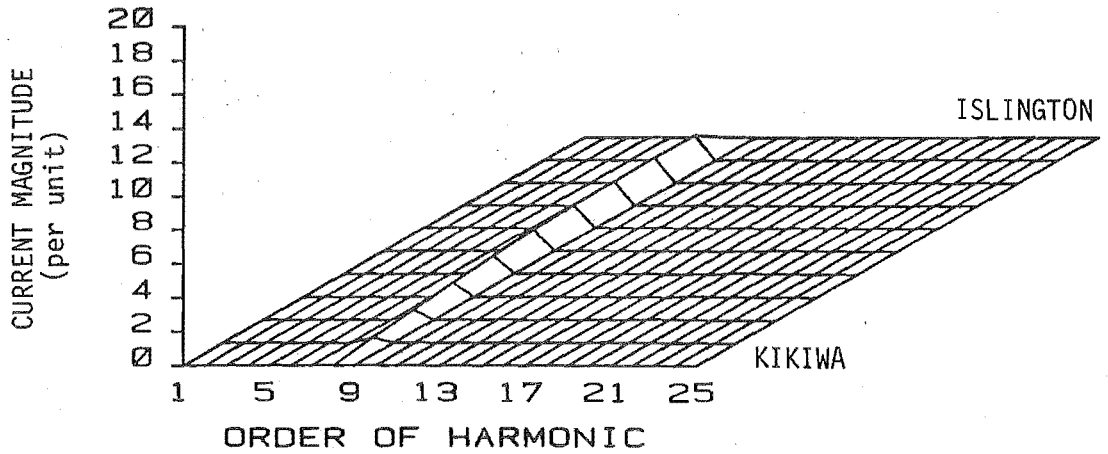

(b) Negative Sequence Current

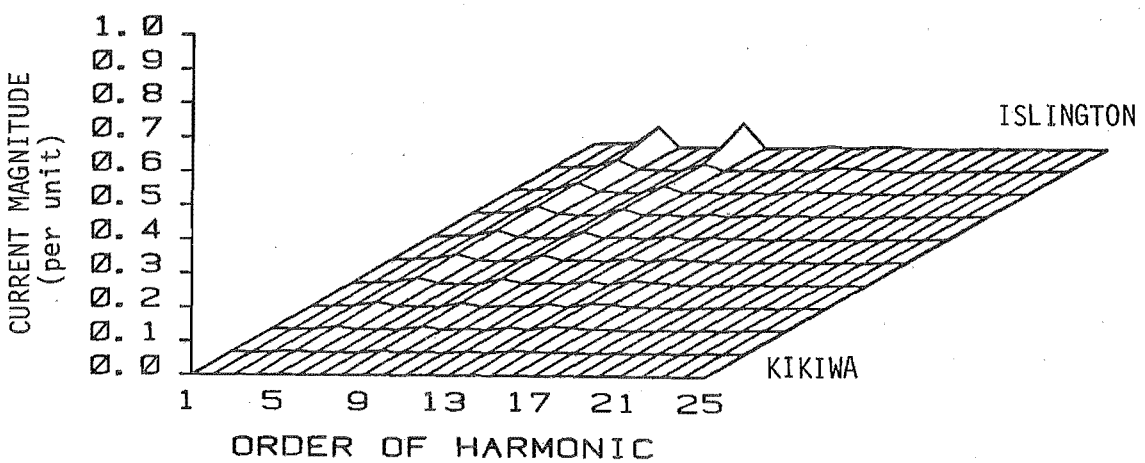

(c) Zero Sequence Current

FIGURE 5.18: Sequence Currents for a 1 pu Positive Sequence Current Injection with a Parallel Resonance between the Line and Filter

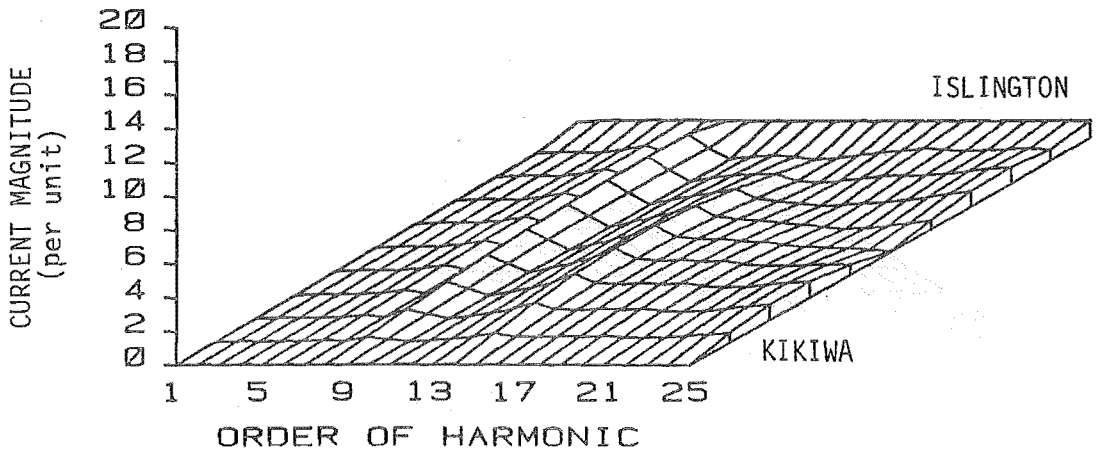

(a) Positive Sequence Current

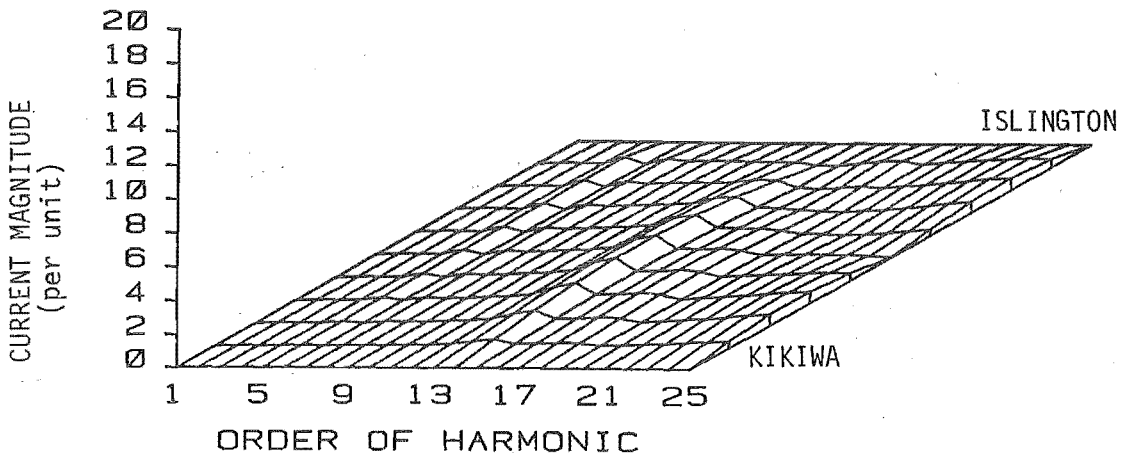

(b) Negative Sequence Current

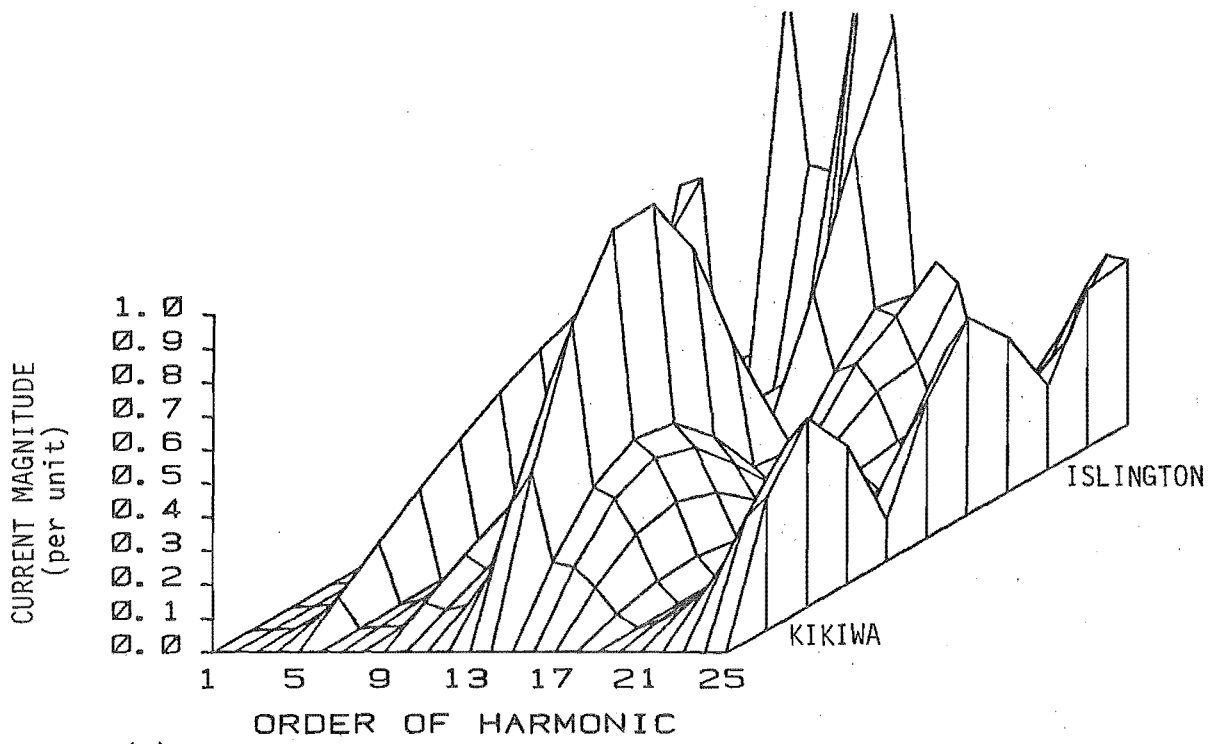

(c) Zero Sequence Current

FIGURE 5.19: Sequence Currents for a 1 pu Positive Sequence Current Injection with One Phase of the Filter Bank Open Circuited

5.6 PHASE DIFFERENCES

For conventional harmonic modelling using single phase positive sequence models (Breuer et al 1982), a transmission line is assumed to have one resonant frequency every ½ wavelength. The use of a three phase unbalanced transmission line model provides information on the individual phase voltages at resonance. The Islington to Kikiwa line has half wavelength resonant frequencies on open circuit that are different for each phase. The spread of frequencies can be seen from Figure 5.20 to be approximately 6 Hz. The irregular shape of the peaks in Figure 5.20a is caused by the frequency increment of 5 Hz used for the analysis. When this is reduced to 1 Hz in Figure 5.20b the smooth shape of the resonant peak is apparent.

The different resonant frequencies and magnitudes (up to 30%) of the three phases, partly explains the problems encountered with correlating single phase modelling and measurement on the physical network. Results indicate that harmonics in the transmission system are unbalanced and three phase in nature.

Normal transposition of a transmission line into three equal length sections to balance the line at fundamental frequency, has a detrimental effect at harmonic frequencies. Far from being balanced the line has very different phase magnitudes. Of interest is the two resonant peaks separated by almost 40 Hz for the half wavelength resonance of the open circuited line. The graph for the Islington to Kikiwa line, Figure 5.21, shows that the first peak is caused by phases 2 and 3 while phase 1 has a low level. At the second resonant peak at 656 Hz phase 1 has the maximum magnitude.

In power systems where there are no line transpositions many resonances do not fall on multiples of the fundamental frequency and are thus not harmful. However, the wide bandwidth over which the transposed line resonates creates a greater possibility that the line will resonate at harmonic frequencies and thus interact with a harmonic source to provide high harmonic voltages and currents.

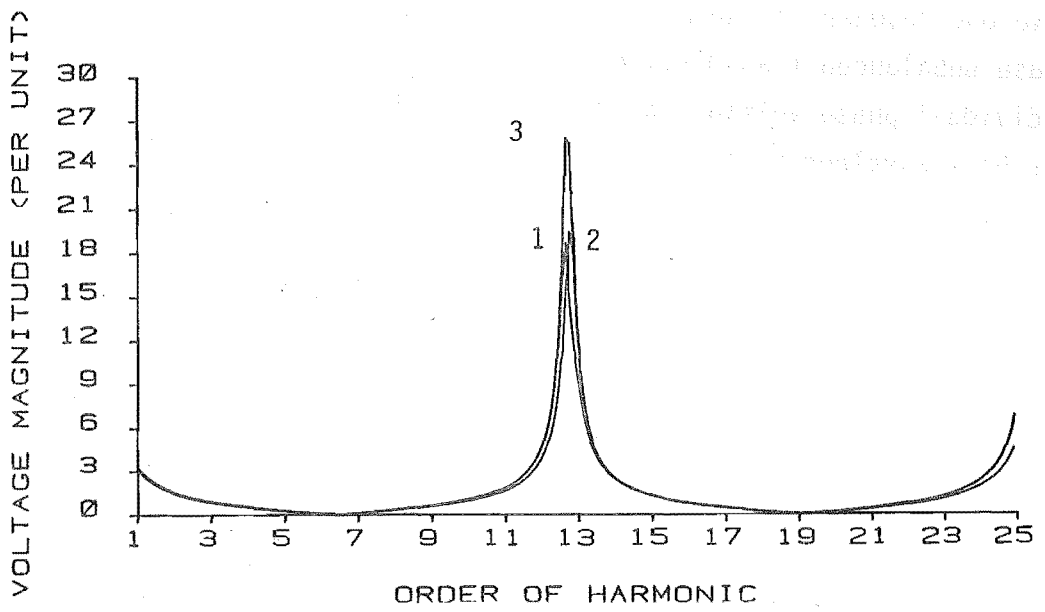

(a) Individual Phase Voltages

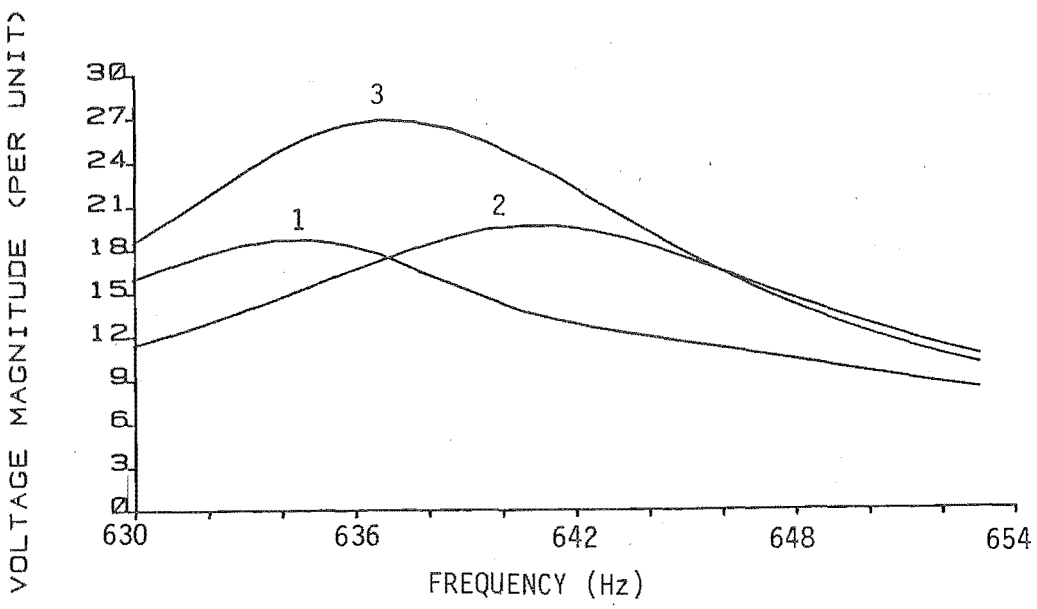

(b) Expanded Frequency Scale for 3 Phase Resonances

FIGURE 5.20: Three Phase Resonant Frequencies of the Islington to Kikiwa Line with a Balanced 1 pu Current Injection (Skin Effect Included)

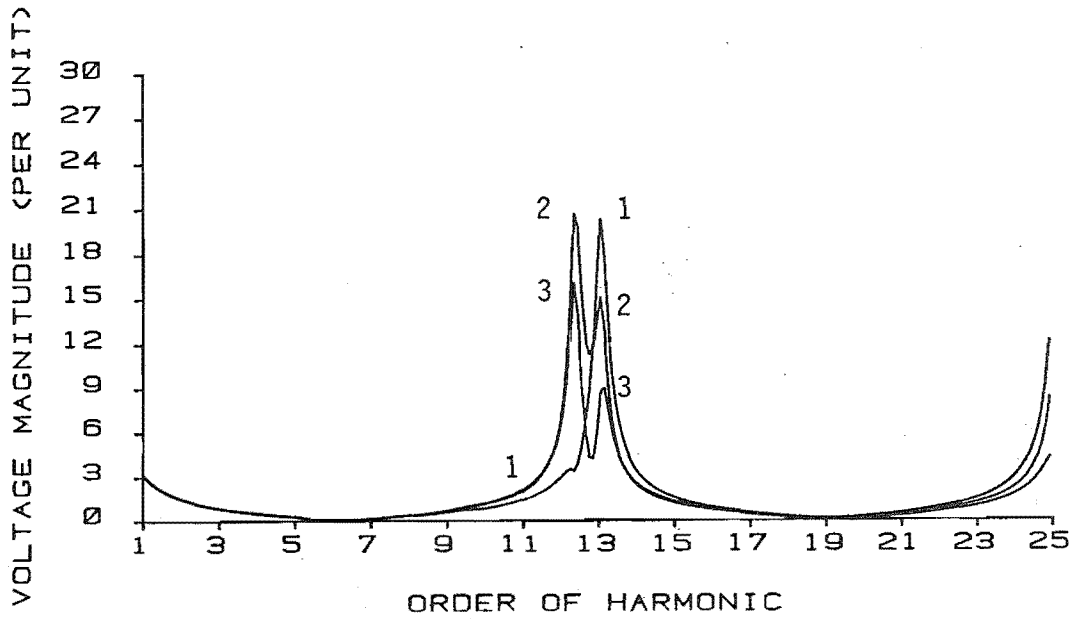

(a) Individual Phase Voltages

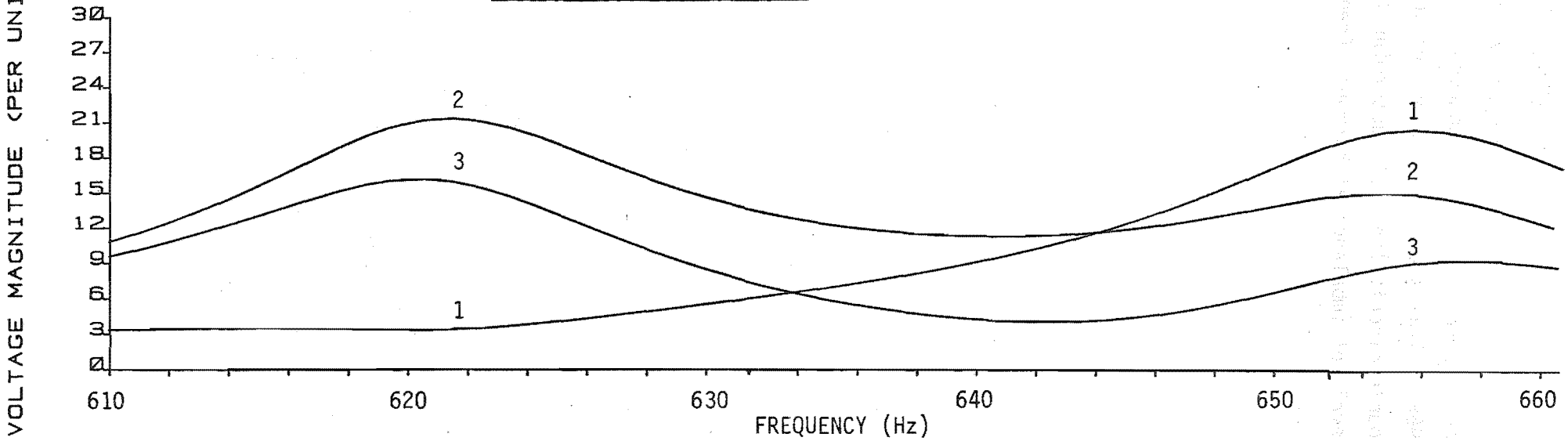

(b) Expanded Frequency Scale for Three Phase Resonances

FIGURE 5.21: Three Phase Resonant Frequencies for the Transposed Line

5.7 MUTUAL COUPLING OF DOUBLE CIRCUITS

Considerable discussion can be found on the unbalanced effects of double circuit lines at fundamental frequency (Hesse 1966 and Edison 1968). This section compares the voltages of both coupled and uncoupled double circuit lines, to determine the importance of coupling and the levels of imbalance at harmonic frequencies. The line used is shown in Figure 5.22.

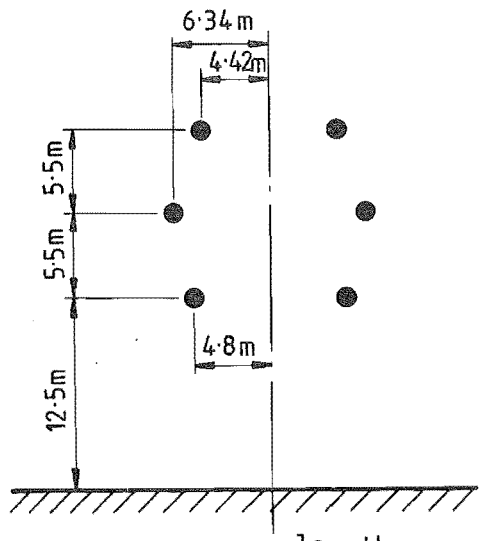

2 conductors per bundle
Bundle spacing .45m
Conductor 30/3.71+7/3.71

length	167 km
earth resistivity	100 Ωm

FIGURE 5.22: Line Geometry of Double Circuit Line

Sequence voltages for a 1 pu current injection allows investigation of symmetrical component impedances. By injecting positive sequence current, the coupling between the positive and other sequence networks can be examined; Z_{++}, Z_{+-} and Z_{+0}. Similarly with a 1 pu zero sequence current injection the voltages Vo are the same as Z_{00} impedances. Figure 5.23, for the double circuit line on open circuit, indicates the resonances of the sequence impedances. The magnitudes of Z_{+-}/Z_{++} and Z_{+0}/Z_{++} are 8% and 5% respectively. Coupling from the positive to the negative and zero sequences resonate at similar frequencies to Z_{++}. The zero sequence impedance, Z_{00}, resonates at a lower frequency, and the magnitude of Z_{00} is considerably less than Z_{++}.

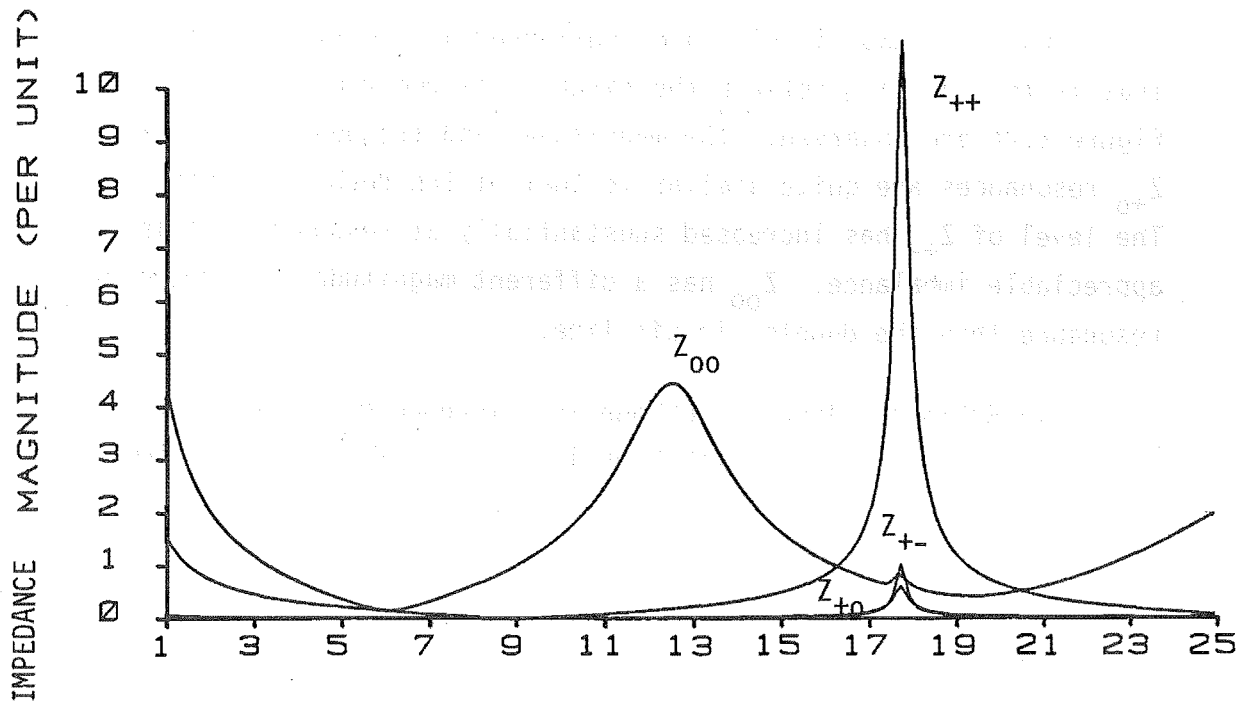

FIGURE 5.23: Sequence Impedance Magnitude versus Frequency for the Double Circuit Coupled Line

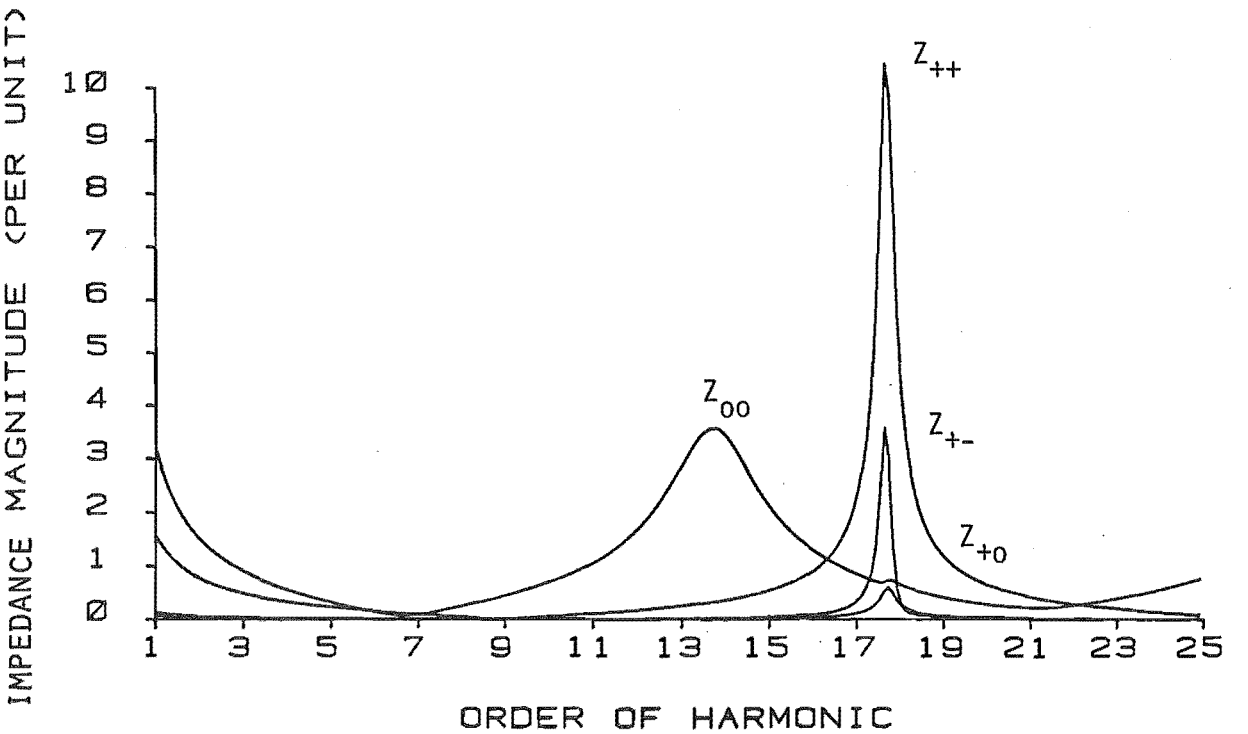

FIGURE 5.24: Sequence Impedance Magnitude versus Frequency for Two Single Circuit Lines

When the two circuits are considered as two single circuit lines; that is the coupling between the circuits is removed, the impedances of Figure 5.24 are observed. The magnitudes and frequencies of the Z_{++} and Z_{+o} resonances are quite similar to that of the double circuit line. The level of Z_{+-} has increased substantially at resonance showing appreciable imbalance. Z_{oo} has a different magnitude and frequency at resonance than the double circuit line.

In Robinson (1966) telephone interference caused by zero sequence currents did not coincide with high levels of power system harmonics. This is partly explained with the different resonant frequencies of Z_{++} and Z_{oo} observed. The levels of this imbalance are similar to those considered by Robinson (1966). The effect this has on the imbalance of a transmission network will be examined in succeeding chapters.

5.8 CONCLUSIONS

A transmission line model has been developed to investigate the coupling between the positive, negative and zero sequence circuits of asymmetrical transmission lines and also the generation of zero sequence currents from balanced convertor injected harmonic currents.

It has been shown that skin effect has considerable influence on the harmonic levels under resonant conditions. Changing line temperatures due to climatic and loading conditions mean complicated, accurate skin effect models are however not justified.

Transformer delta windings have been shown to affect the flow of zero sequence currents considerably.

The problem of resonance between convertor filters and the AC system in this case comprising a single circuit transmission line, was investigated.

Using the three phase transmission line model, different resonant frequencies and magnitudes have been observed for each phase of a single transmission line. Normal line transposition balances a line at fundamental frequency, but not at harmonic frequencies. Transposition is considered to have a detrimental effect at harmonic frequencies.

Circuit coupling affects the mutual impedance between positive and negative sequence networks for the line considered. Levels of imbalance are similar to those measured in practical tests. Zero sequence resonant frequencies and magnitudes are different to those of the positive and negative sequences, consistent with observed behaviour.

CHAPTER 6

REDUCED TEST SYSTEM

6.1 INTRODUCTION

A number of researchers have written about their findings on individual component harmonic models, the most significant of which has been discussed in the previous two chapters. There are also single phase studies of small test systems (Campbell and Murray 1970), and larger distribution systems (McGranaghan et al 1981 and Littler 1982). However, the progressive formation of the impedance of a system from the individual component characteristics has not been addressed. Using this approach gives an understanding of network modelling at harmonic frequencies, in a situation where intuitive reasoning is not possible. Such an understanding is distinctly absent in the recent work of Mahmoud and Shultz (1982).

A system with only a single source of harmonic current, which enables the measurement of system impedances, is difficult to achieve. Further, harmonic impedances calculated from the measured values of voltage and current only represent the system at the time of the test. Harmonic network modelling on the other hand uses known system components, along with their interconnections and couplings, to calculate the system impedances at any frequency. Modelling enables these impedances to be calculated at any point in the system and for any configuration.

A nine bus system is used in this chapter to illustrate a number of these advantages. It is comprised of data from the actual grid below Roxburgh in the South Island of New Zealand, and is detailed in Appendix 1. The source of harmonic interference is an aluminium smelter at Tiwai Point and the nine bus system includes the 220 kV network to two busbars away from this source. At Roxburgh the rest of the grid is ignored and because of this the term "reduced system" is an appropriate description.

This test system also serves to introduce the effects of three phase modelling. The production of non-characteristic harmonics is affected by the extent of harmonic imbalance in the AC system, and the contribution to this by system load and generation will be investigated using three phase techniques.

6.2 GENERATOR, TRANSFORMER AND LOAD IMPEDANCES

The step by step formation of the test system is initiated by examining the impedances of a number of common system components. The impedances of a generator model with constant phase angle is illustrated in the linear impedance plot of Figure 6.1a. The impedance plot of the combination of the generator and its associated transformer, illustrated in Figure 6.1b, indicates the need to include transformer modelling.

Loads are also major elements that need to be included. The presence of a 90 MW and 54 MVAR load connected to the same bus as the generator and also fed by a transformer, illustrates the damping effect of the load.

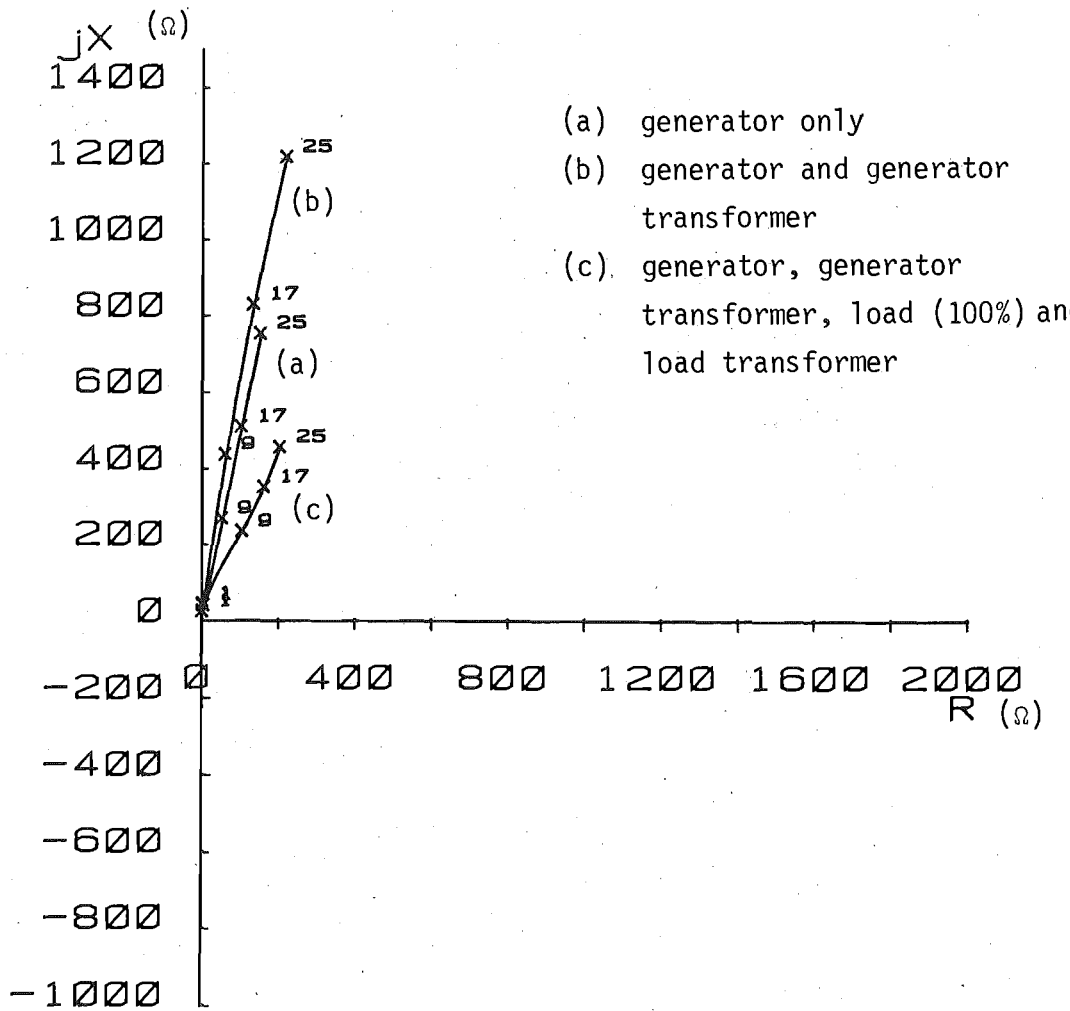

FIGURE 6.1: Polar Plot of the Generator, Transformer and Load Impedances at Roxburgh

6.3 CONNECTION OF COMPONENTS TO TRANSMISSION LINES

The standing wave effects of two separate 220 kV transmission lines between Invercargill and Roxburgh are modelled in Figure 6.2. The short and open circuited lines have quarter and half wavelength resonant frequencies as expected from discussion in the previous chapter.

When the generator and its associated transformer, from Section 6.2, are connected to the Roxburgh end of the lines, the positive sequence voltage for a 1 pu current injection at Invercargill, has a lower magnitude at resonance than the extreme cases of termination. Moreover, the resonant frequencies lie between those of the open circuit and short circuit cases. As the impedances of the generator and transformer increase with frequency, so the voltage magnitudes also increase with frequency; this is evidenced by the higher second peak at the 24th harmonic in Figure 6.2.

Connection of the load transformer and load to the Roxburgh bus reduces the resonant peaks and increases slightly the resonant frequencies.

The corresponding phase angles for the above cases are plotted in Figure 6.3. At resonance the phase angles change by approximately 180 degrees, from inductive to capacitive and vice versa. The higher the resonant peak magnitude the smaller the frequency range over which this occurs. The high rate of change of phase angles at resonance indicates that the system voltages and currents will be very sensitive to parameter variations, and explains the less accurate simulations found by Breuer et al (1982) at these points.

The polar plot of impedance in Figure 6.4 for the open circuited line shows a circular shape with very little damping. At fundamental frequency the line is capacitive although this is difficult to observe. As the frequency increases the line approaches a series resonance, a minimum impedance at which point the impedance is purely resistive and the phase angle becomes inductive. The impedance increases in magnitude, moving in a clockwise direction with increasing frequency. As the indicated parallel resonance is approached, the sensitivity observed in the phase plot becomes apparent. The line has a maximum impedance at the point it crosses the real axis, and is resistive only. As frequency increases the line again becomes capacitive.

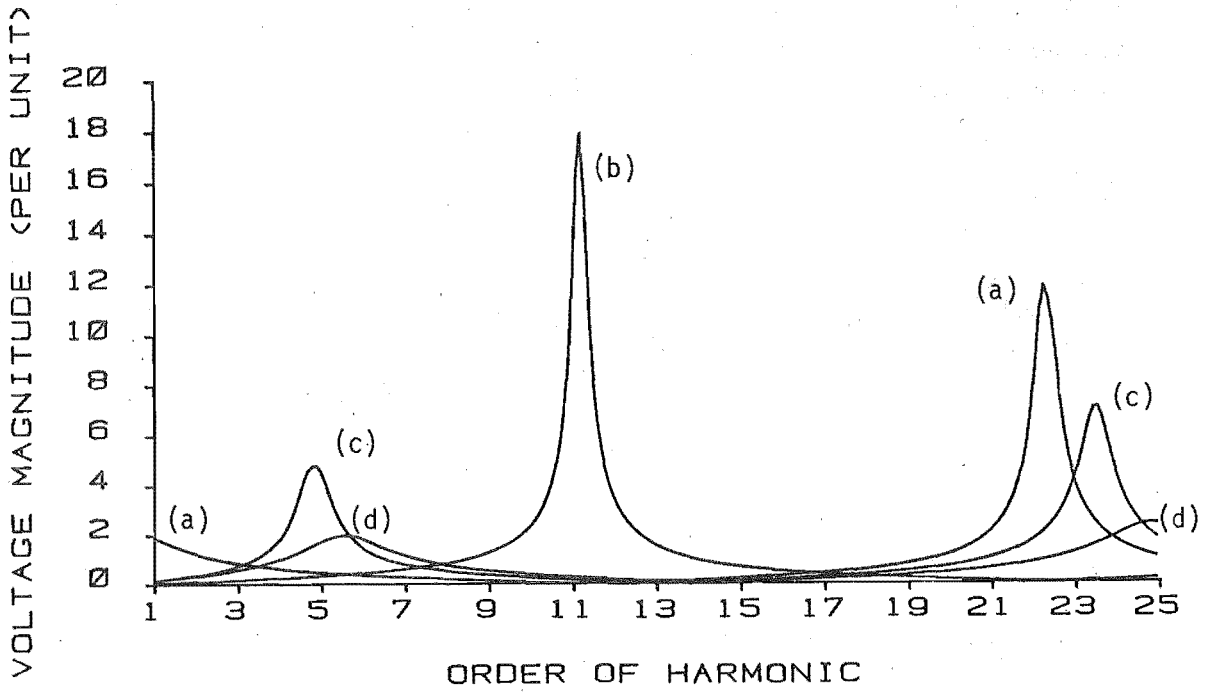

FIGURE 6.2: Positive Sequence Voltage Magnitude at Invercargill versus Frequency for Different Terminations of the Roxburgh to Invercargill lines.

(a) open circuit
(b) short circuit
(c) generator and generator transformer
(d) generator, generator transformer, load and load transformer.

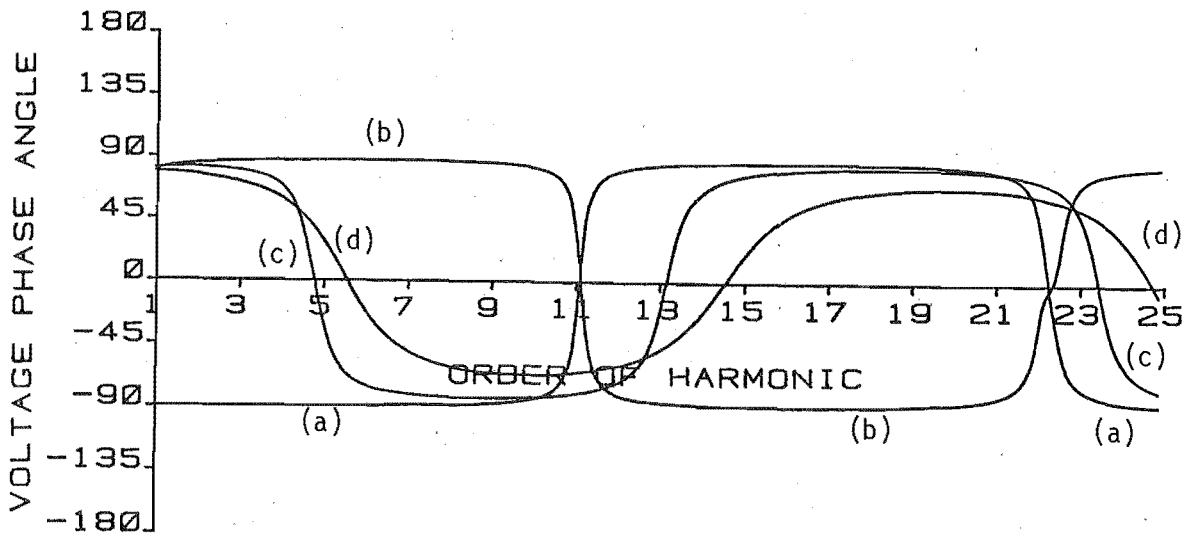

FIGURE 6.3: Positive Sequence Voltage Phase Angles at Invercargill versus Frequency for Different Terminations of the Roxburgh to Invercargill Lines.

(a) open circuit
(b) short circuit
(c) generator and generator transformer
(d) generator, generator transformer, load and load transformer.

The polar plot includes both the magnitude and the phase angle information contained in Figure 6.2 and Figure 6.3. To convert from pu voltages on a 100 MVA base with a 1 pu current injection, to impedances at 220 kV, multiply by 484.

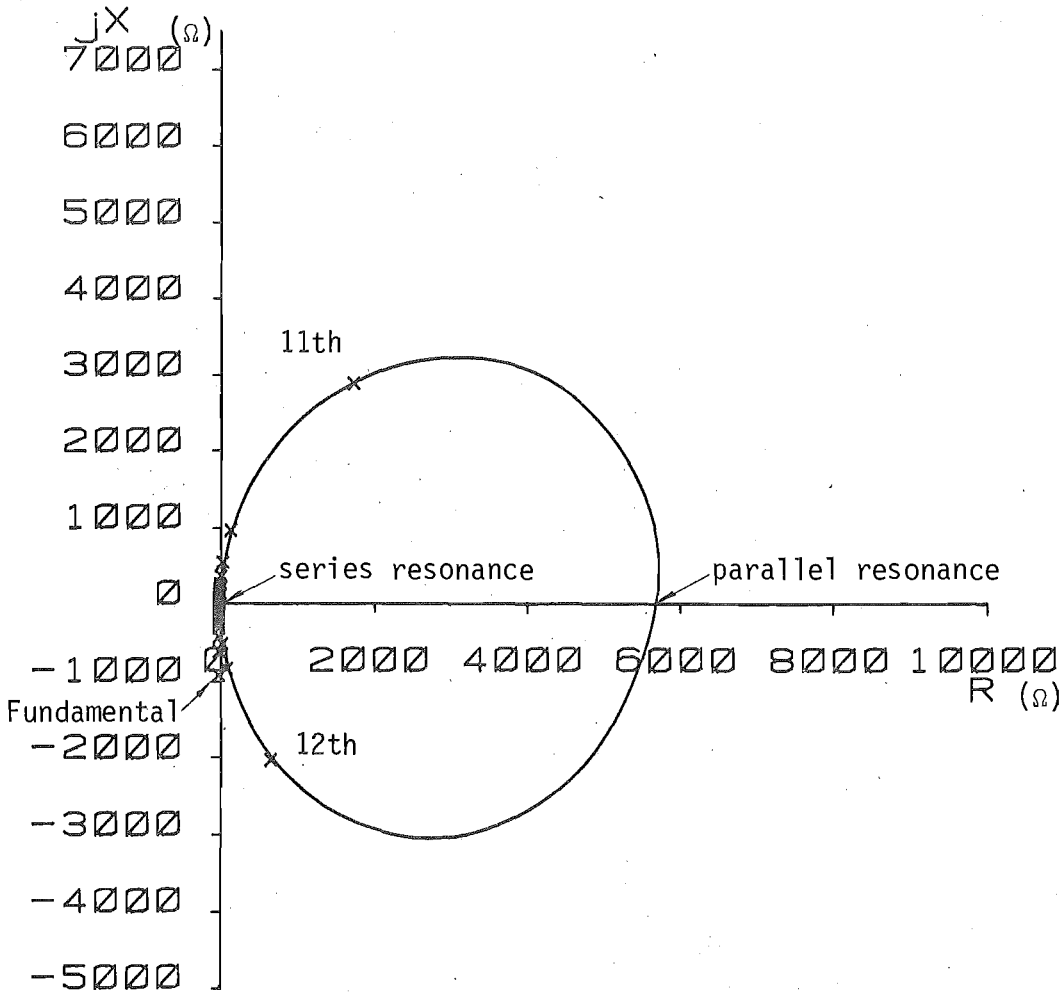

FIGURE 6.4: Polar Plot of the Impedance of the Open Circuited Invercargill to Roxburgh Lines with 50 Hz Intervals Marked.

6.4 SIX LINE SYSTEM

The six line system of Figure 6.5 was constructed as the next step in progressively increasing the complexity of the AC system.

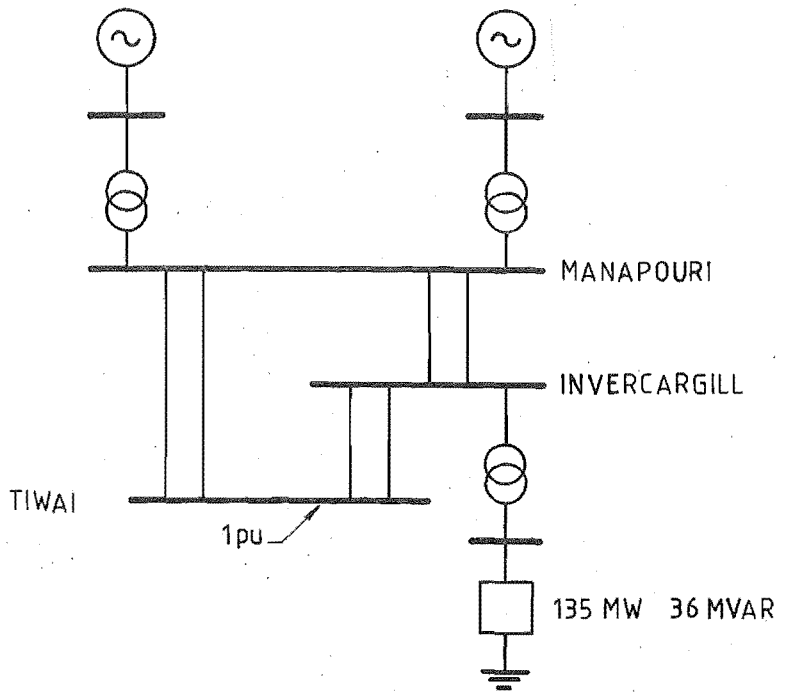

FIGURE 6.5: Six Line System Including Load and Generation

Figure 6.6 illustrates the voltages with no load or generation for a 1 pu current injection at Tiwai. Typical standing wave effects for the length of lines are shown. When first generation in Figure 6.6c and then load in Figure 6.6d are added with the associated transformers, similar effects to the previous section are observed. The resonances lie between open and short circuit resonant frequencies, with reduced magnitudes compared with the extreme cases of termination. The voltage levels at resonance in Figure 6.6 are lower than those for the Roxburgh lines in the previous section due to the increased length and number of lines.

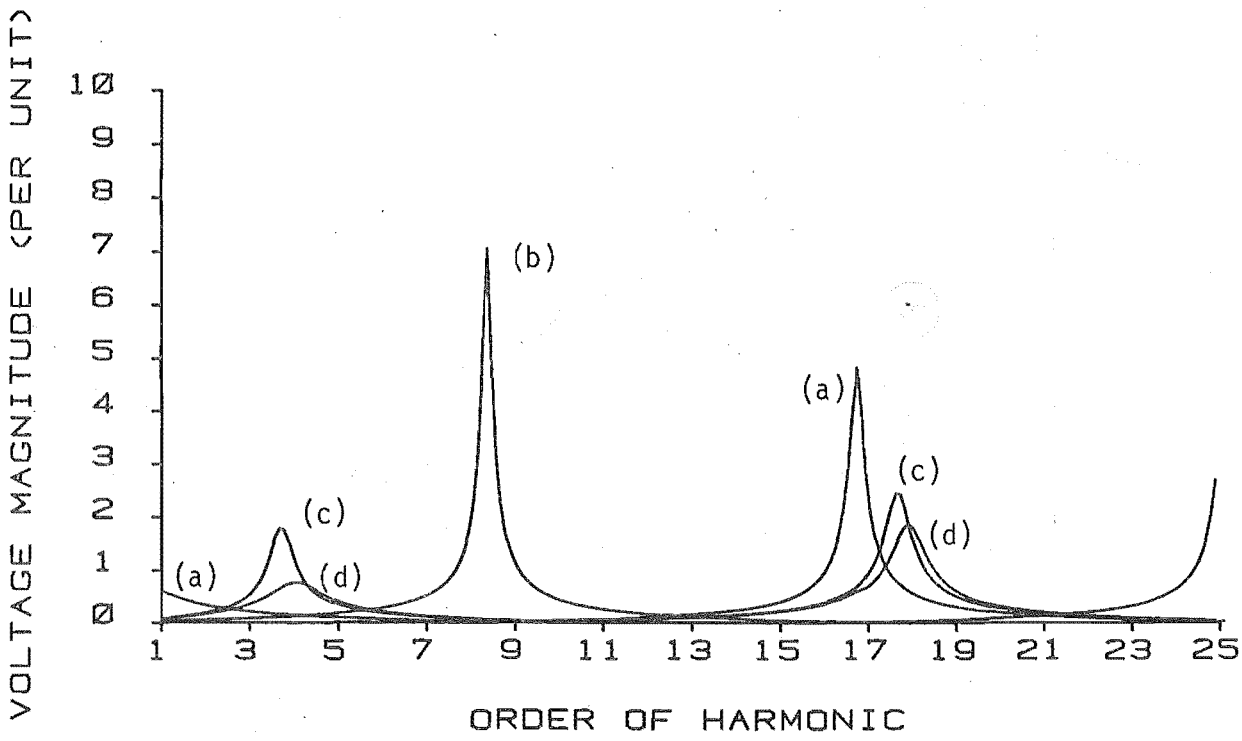

FIGURE 6.6: Positive Sequence Voltage Magnitude at Tiwai versus Frequency for Different Terminations

(a) open circuit
(b) short circuit
(c) generator and generator transformer
(d) generator, generator transformer, load and load transformer.

6.5 EIGHT LINE SYSTEM

Adding the Invercargill to Roxburgh lines to the lines between Manapouri, Invercargill and Tiwai, Figure 6.7, completes the progressive formation of the test network.

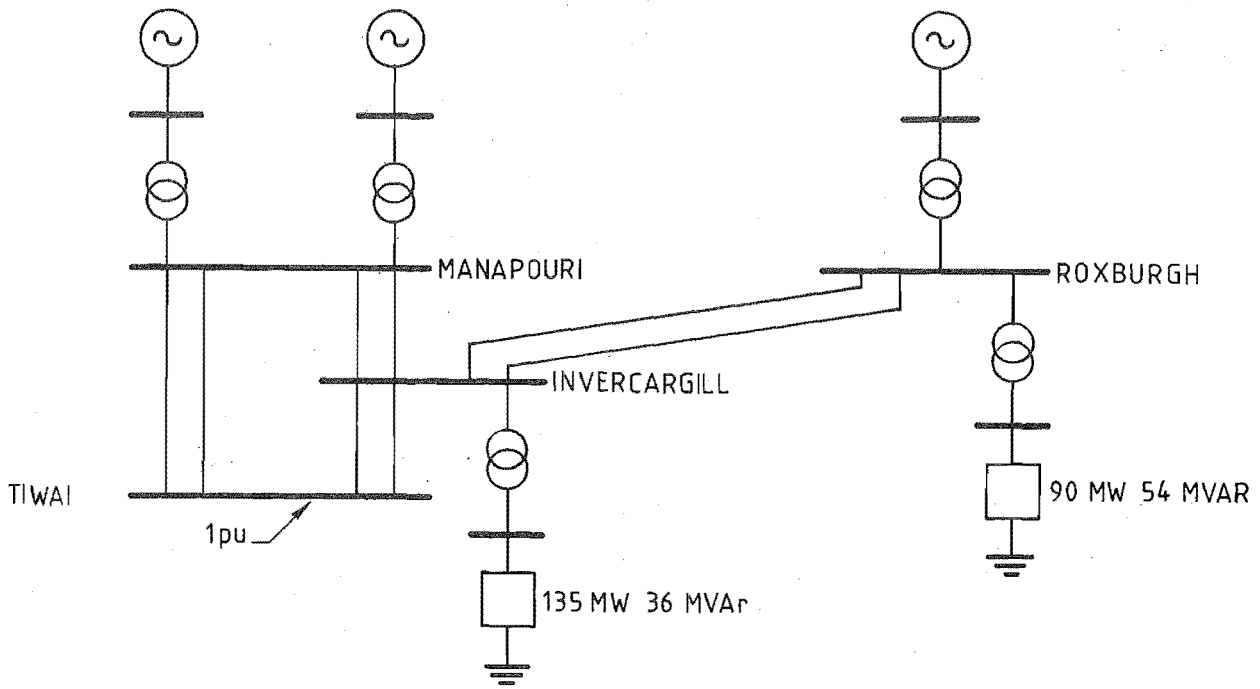

FIGURE 6.7: Reduced System Including Load and Generation

The voltages of Figure 6.8 for this system indicate resonant frequencies that do not correspond to the frequencies of the two individual systems in Section 6.3 and 6.4, that were combined together. This is an important point; the resonant frequencies of transmission lines in a network are significantly affected by the interconnections of the network. The voltage levels at Tiwai have decreased with the increase in system size, and there are now two resonances around the 18th harmonic, one of smaller magnitude than the other. The voltage phase angles for the Tiwai bus are plotted in Figure 6.9, and the smaller of the two resonances, at the 17th harmonic, is shown to cause the phase angles to drop and then recover.

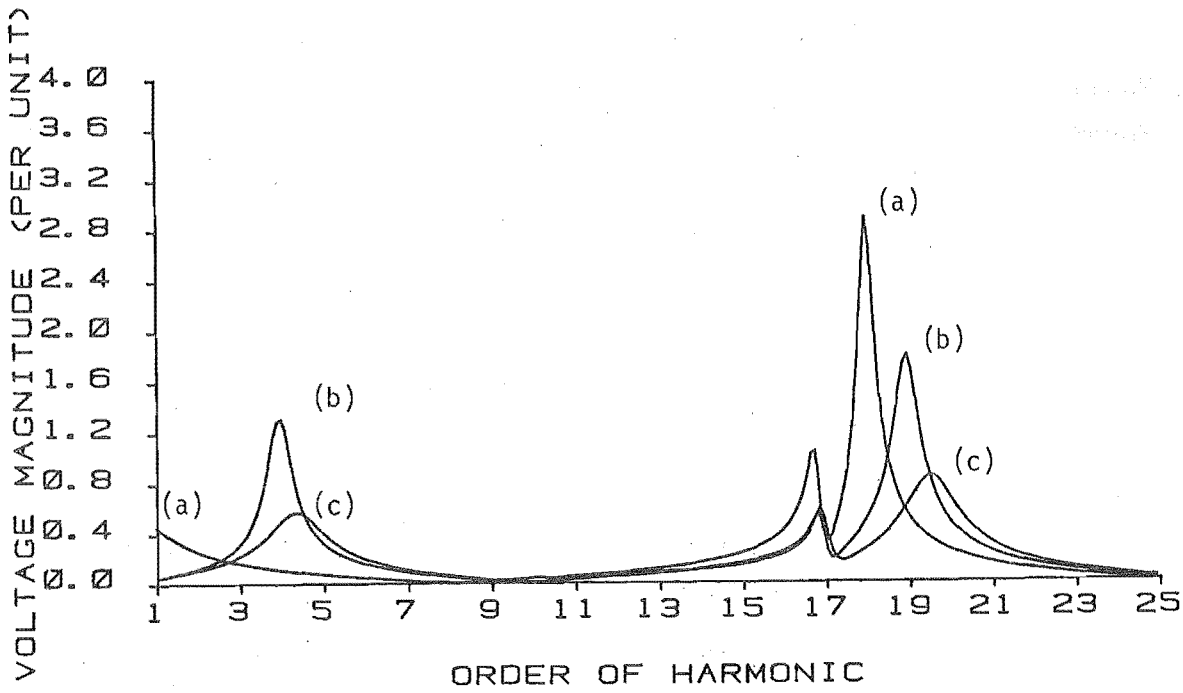

FIGURE 6.8: Positive Sequence Voltage Magnitude versus Frequency for Different Terminations

(a) open circuit

(b) generators and generator transformers

(c) generators, generator transformers, loads and load transformers.

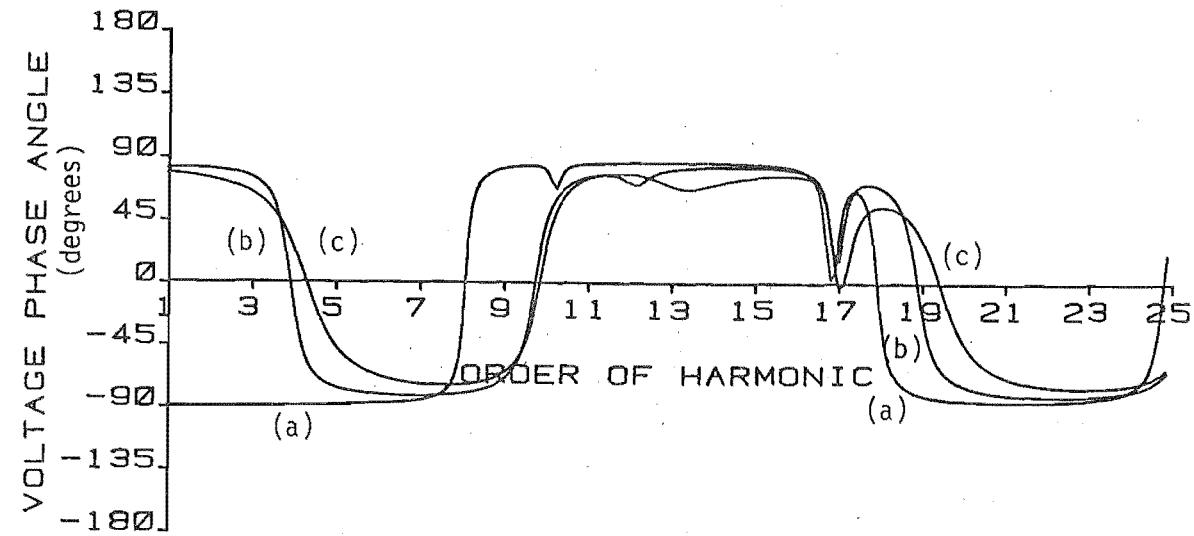

FIGURE 6.9: Positive Sequence Voltage Phase Angles at Tiwai versus Frequency for different Terminations

(a) open circuit

(b) generators and generator transformers

(c) generators, generator transformers, loads and load transformers.

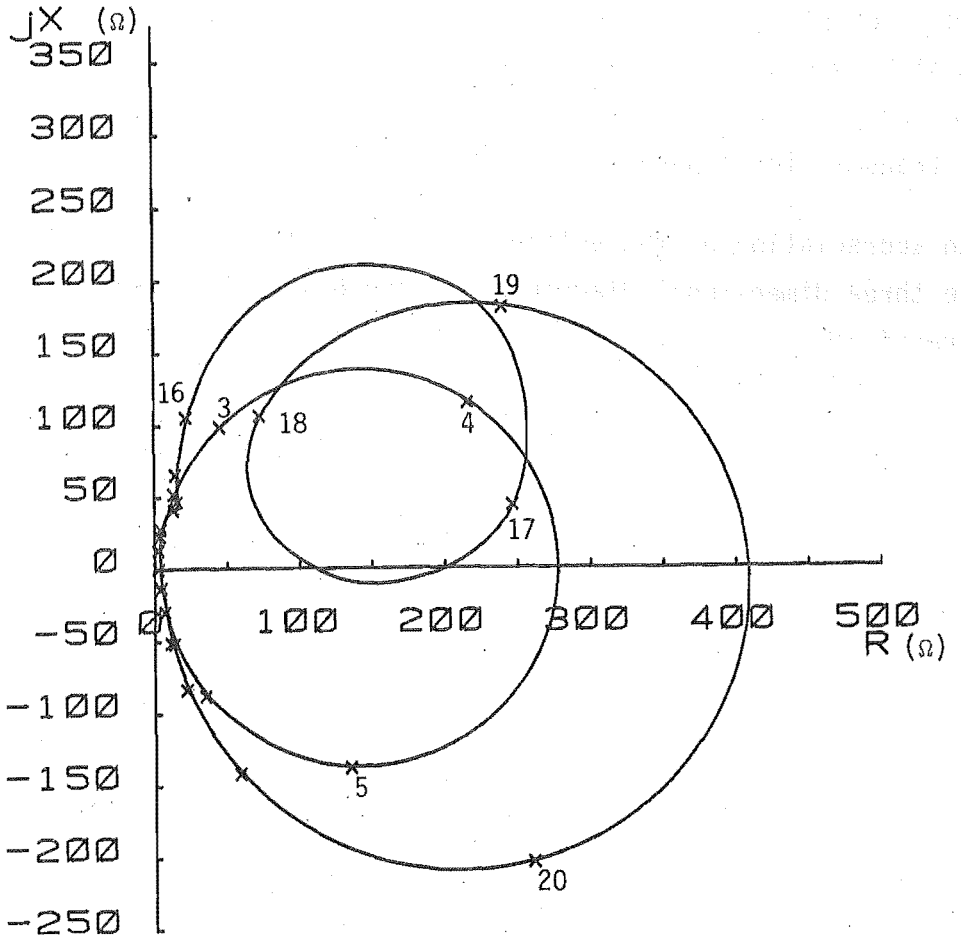

FIGURE 6.10: Positive Sequence Impedances of the Reduced System from Tiwai with Harmonic Intervals Indicated

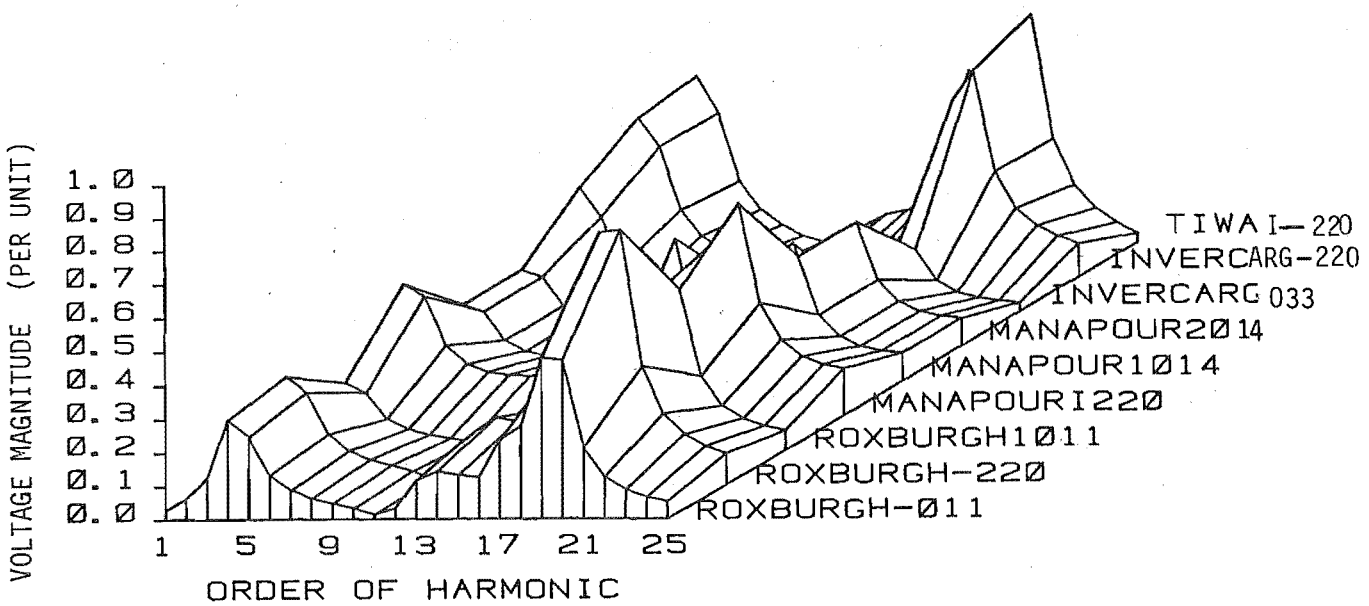

FIGURE 6.11: Positive Sequence Voltage Magnitude versus Frequency at All Reduced System Busbars.

This resonance is observed as the smaller loop, in the inductive quadrant, of Figure 6.10. As the complexity of the AC system increases, the impedance plot progressively becomes more cluttered with loops due to resonant transmission lines.

An appreciation of the voltages over a whole system is obtained using the three dimensional diagram of Figure 6.11. The lower voltages on the transformer secondaries, namely the generator and load busbars, are apparent. The two major resonances between the 4th and 5th harmonics and between the 19th and 20th harmonic observed in Figure 6.8c at Tiwai, occur at all the busbars. The smaller resonance at the 17th harmonic at Tiwai, does not however propagate in the Roxburgh region. It cannot be assumed that resonant frequencies at the point of harmonic injection will be the same at other busbars.

6.6 VOLTAGE SENSITIVITY TO LINE PARAMETER VARIATION

By selectively reducing the line lengths and observing the voltages at Tiwai, the lines which most affect resonant conditions are determined. The results are illustrated in Figure 6.12.

A 5% reduction in length in the Tiwai to Manapouri lines causes the two resonant frequencies around the 18th harmonic to shift by approximately 20 Hz. A 5% decrease in the line lengths for the lines from Roxburgh to Invercargill does not change the smaller resonant frequency, but changes that between the 19th and 20th harmonics by approximately 10 Hz.

Lines closest to the point of injection have the largest effect on system resonances. The sensitivity of the voltages to lines connected to the point of injection, indicates that line parameters for these lines will be required to a greater level of accuracy than lines more distant in the network.

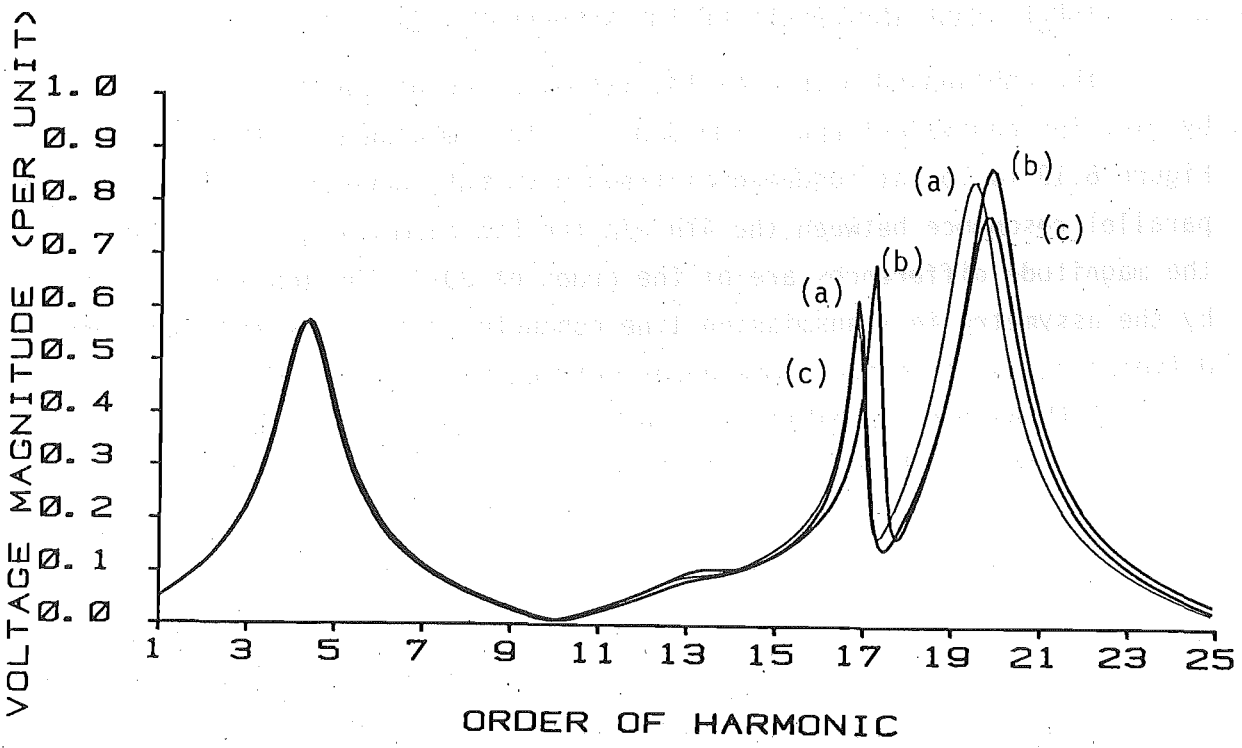

FIGURE 6.12: Positive Sequence Voltage Magnitude versus Frequency for Line Length Variations

(a) Reduced system including generation and loads

(b) Tiwai to Manapouri lines 5% shorter

(c) Invercargill to Roxburgh lines 5% shorter

6.7 THREE PHASE IMPEDANCES OF THE REDUCED SYSTEM

The unbalanced nature of the transmission network can be illustrated by plotting equivalent phase impedances. The imbalance in the phases of Figure 6.13 is low at fundamental frequency, but increases towards the first parallel resonance between the 4th and the 5th harmonics, at which point the magnitude differences are of the order of 30%. The imbalance is caused by the assymetry in transmission line conductor geometries and consequent differences in the mutual impedances between phases. The series resonance at the 11th harmonic exhibits low levels of imbalance, and the second parallel resonance between the 19th and the 20th harmonics, again shows considerable differences in the impedances between phases. High levels of imbalance at parallel resonant frequencies assist in explaining the difficulties being experienced with correlating single phase simulation results with measured tests (McGranaghan et al 1981 and Breuer et al 1982).

While most system loads are nearly balanced, this is not the case with single phase traction supplies (Winthrop 1983). This has been simulated by applying unbalanced loads of 10%; that is reducing phase 1 load by 10% and increasing phase 3 load by 10%. Results are also plotted in Figure 6.13 The imbalance in impedance at the two parallel resonant points increases with load imbalance. The three phase model can be used to determine the effect of multiple single phase injections at different locations, simulating the traction loads.

6.8 HARMONIC UNBALANCE FACTOR

Harmonic imbalance in the AC system will affect the three phase voltage waveforms, and hence the zero crossings used in convertor control. As a consequence, harmonic imbalance will affect the non-characteristic harmonics produced by this plant.

At fundamental frequency an "unbalance factor" is used to indicate the extent of unbalanced system conditions (Roper and Leedham 1974). The use of such an index at harmonic frequencies, gives a simple measure of imbalance. Table 6.1 includes the values of the unbalance factor at parallel resonances, defined as the ratio of negative sequence voltage to positive sequence voltage, for a balanced 1 pu current injection. The values of the unbalance factor are largest at parallel resonant frequencies and hence Table 6.1 represents maximum levels.

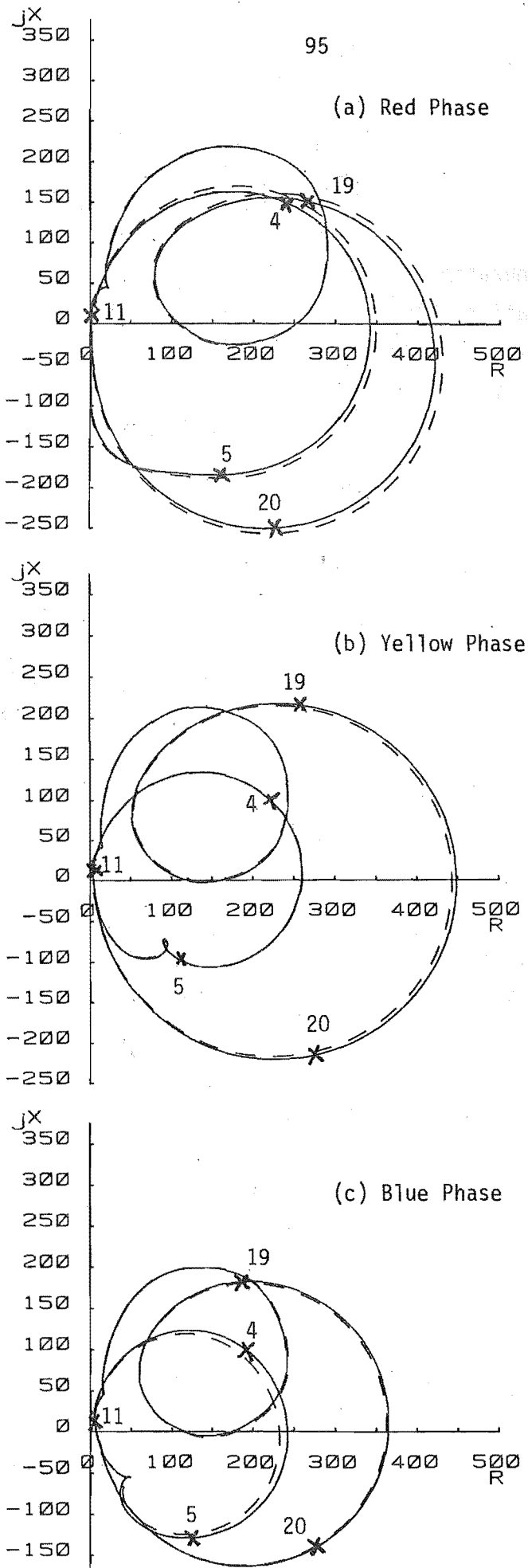

FIGURE 6.13: Equivalent Phase Impedances for the Reduced System. Solid Line Balanced, Dashed Line 10% Unbalanced

TABLE 6.1: Values of the Unbalance Factor at Parallel Resonances for Various Terminations of the Reduced System

	Harmonic	Unbalance Factor
Reduced system, no generation or load	17th	24.8%
Reduced system, generation only	19th	10.1%
Reduced system, generation and 100% load	20th	6.2%
Reduced system, generation and 100% load with phasing the same on each circuit	20th	17.2%

The unbalance factor is greatest with a network comprised of only the transmission lines. The connection of both generation and load, the models of which are balanced, reduces the unbalance factor. At periods of light load therefore, the AC system is more unbalanced than at times of high load, and the generation of convertor non-characteristic harmonics will increase accordingly. At light load however, the level of harmonics will be higher, and so imbalance is only one factor in the production of these non-characteristic harmonics.

The last entry in Table 6.1 is for the system with both load and generation, and altered line phasing as indicated in Figure 6.14. The position of phases in double circuit lines is varied in each circuit as in Figure 6.14a to minimise the fundamental frequency imbalance. When the phase positions are altered to be the same in each circuit, illustrated in Figure 6.14b, the unbalance factor rises substantially to 17.2%. Conductor geometries are thus important in unbalanced harmonic penetration analysis.

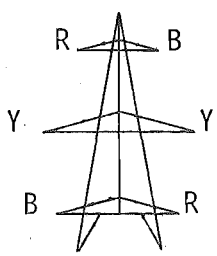

(a) common arrangement

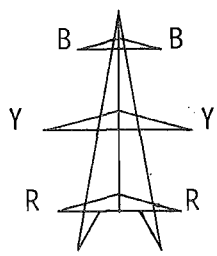

(b) phase positions the same in each circuit

FIGURE 6.14: Examples of Different Tower Conductor Arrangements

6.9 CONCLUSIONS

The unbalanced nature of the AC system at harmonic frequencies has been shown to be significant, indicating the approximation of single phase analysis. Harmonic penetration has been introduced using a simple system comprising two lines terminated in generation and load. By progressively adding more lines, transformers, generators and loads to this case, the complicated network response of a large interconnected power system is avoided.

As the intricacy of the network increases, the harmonic voltage and impedance plots show a corresponding increase in complexity. The resonant frequencies which occur in an intricate system have been shown to be dependent on all the components of the power system, not just the transmission lines.

CHAPTER 7

THREE PHASE HARMONIC PENETRATION

7.1 INTRODUCTION

In fault studies symmetrical component analysis is used to determine the fault currents, and generally the sequence networks in these studies are considered as uncoupled. Previous attempts to consider the unbalanced nature of harmonic problems (Howroyd 1977 and Littler 1977) have used this approach. It is the purpose of this chapter to perform studies in the phase frame of reference where this coupling is inherent, and show that phase analysis accurately and simply duplicates unbalanced conditions.

By comparing measured impedances with simulated impedances, a best fit of models from the alternatives available can be chosen and these models used for studies where there are no corresponding measurements.

Such studies include investigating the sensitivity of a network to changes in component impedances. This enables the critical components needed to assure model validity to be isolated. The importance of three phase techniques can be put in perspective by duplicating single phase results and comparing the voltage variations in the network.

There are a number of practical restrictions in modelling due to the temperature variation of line conductors and ground resistivity inconsistencies. These limitations indicate an accuracy which modelling cannot hope to better.

7.2 TEST SYSTEM

The interconnections for the New Zealand South Island electric power transmission system used for simulation in this chapter are presented in Figure 7.1. Appendix 2 includes details of the modelled system including generation, maximum loadings, transformer reactances and line geometry data. The transmission network above Bromley is represented by a single load of 500 MW, .95 power factor. Similarly at Timaru, on the 110 kV network, a 50 MW, .95 power factor load was added as an equivalent for the network at this busbar.

FIGURE 7.1: New Zealand South Island Transmission System Below Bromley

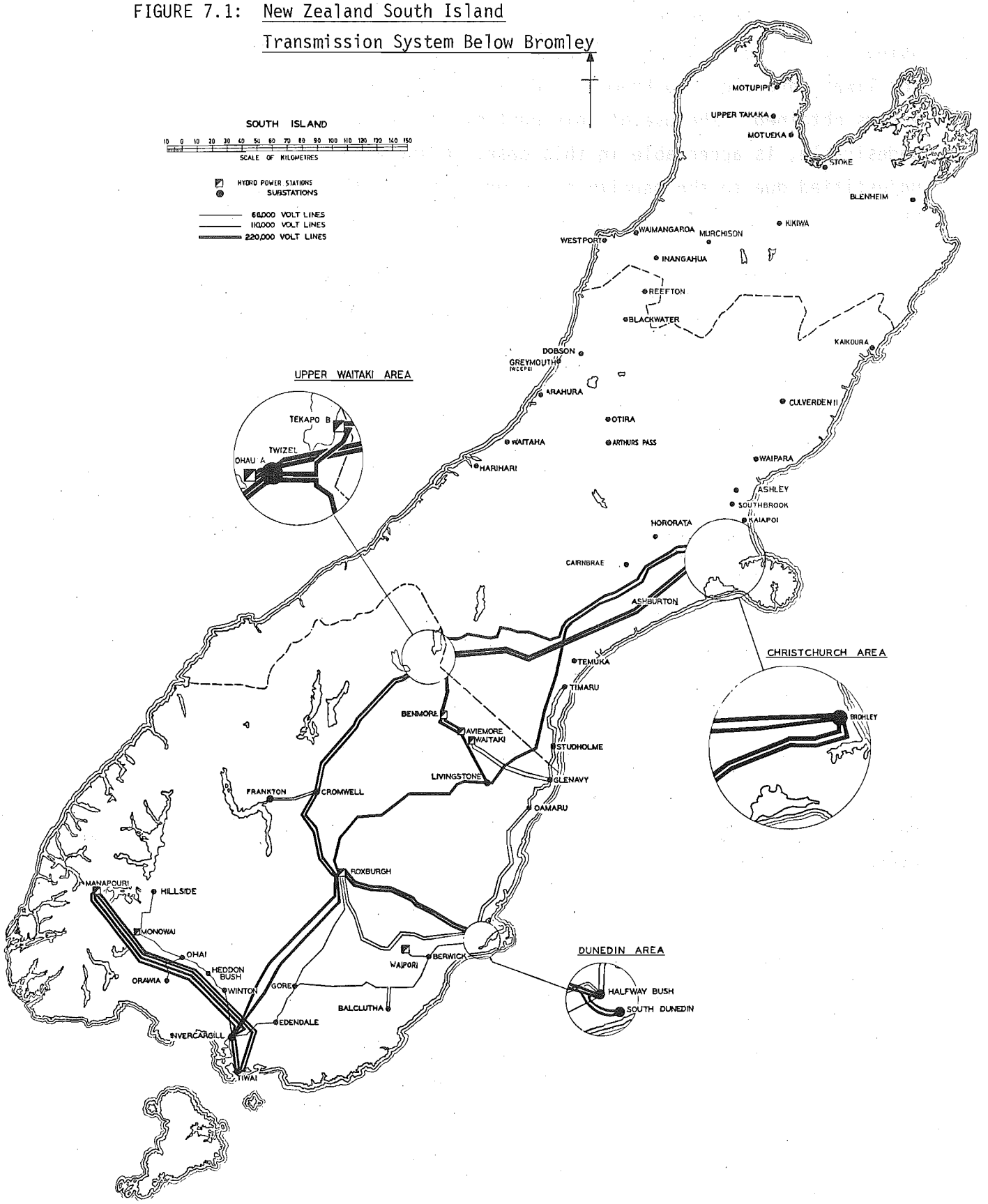

The values in Table 7.1 compare the simulated results of this network with modelling the whole South Island grid. These results were obtained using the single phase program ELAFANT. The busbars in the table, except for Tiwai, are close to Bromley and Timaru and represent the largest errors obtained. The use of only part of the South Island network, while undesirable, is acceptable in this case. Using a larger network is unjustified due to the paucity of records kept at the time of the tests. This will be discussed in more detail in Section 7.5.

TABLE 7.1: Comparison of Simulated Voltages for the System Below Bromley and the Whole South Island Network

Busbar	250 Hz		850 Hz	
	South Island System	Test System	South Island System	Test System
Glenary	.87	1.21	.24	.16
Livingstone	.61	.78	.26	.13
Twizel	.56	.78	.11	.16
Tiwai	3.28	2.93	.50	.49

Data for the transmission lines connected to Manapouri was unsatisfactory. Although information on the different sections was available, the mountainous and forested terrain made accurate line parameters difficult to determine. These lines affect the sensitive parallel resonance at 17th harmonic, and therefore represent the most arduous conditions possible. The lack of acceptable data was overcome by lengthening the lines by 9 km and approximating the multitude of sections to one single section. This length was chosen to give correct resonance with measured impedance data at the 17th harmonic.

This represents a 6% increase in the length of the Manapouri to Invercargill lines and hence a similar increase in the line parameters. Commissioning tests on Line 2 showed an average difference in the measured and calculated impedance angles of 11% (New Zealand Electricity 1970). Measured data therefore supports the differences in line parameters found at harmonic frequencies.

Harmonic tests conducted by New Zealand Electricity, used for comparison with simulated data in this chapter refer to a test where the Tiwai aluminium smelter was operating on 7 rectiformers, with harmonic filters out of service (Hyland 1981). Maximum harmonic currents were thus injected and maximum voltage levels measured on the system. At Benmore the HVDC link between the South and North Islands was connected to the system in normal 12 pulse configuration. Filters at that site were in service and the effect of this source was thus minimised. Harmonic measurements were made simultaneously at six sites in the system. Yellow phase was used at all sites except at Tiwai where all three phases were measured.

The currents measured at Tiwai assuming 120 degrees between the phase voltages are documented in Table 7.2.

TABLE 7.2: Current Injections at Tiwai for 7 Rectiformer Operation (Amps)

Harmonic	Phase 1	Phase 2	Phase 3
5th	16.2 ∠-26	17.3 ∠-153	17.3 ∠84
7th	8.9 ∠-43	9.7 ∠-151	8.5 ∠94
11th	4.2 ∠59	5.1 ∠-51	5.1 ∠182
13th	2.4 ∠87	3.5 ∠-50	3.1 ∠206
17th	4.5 ∠11	4.6 ∠-97	4.6 ∠134
19th	3.0 ∠-40	3.8 ∠-148	2.9 ∠90
23rd	4.1 ∠-24	4.0 ∠-150	3.9 ∠75

7.3 MODEL SELECTION

To select system component models from the range available a comparison of measured and simulated impedances at Tiwai, the current injection busbar, is used.

Changing component models has the greatest effect on the magnitude and phase angles at the parallel resonant frequencies. Consequently, the measured values of the 5th and 17th harmonic impedances have been compared to the simulated values. The different generator, load and transformer models used in Table 7.3 are the same as those discussed in Chapter 4 and are summarised for clarity in Figure 7.2.

The effect of load modelling on harmonic impedances is indicated in cases 1-4, with load model A appearing the most satisfactory. The results using load models B and D are similar showing that the representation of frequency dependence in the reactance has only a small effect.

Transformer model variation is indicated in cases 5-8. There is little difference between transformer models A, D and E while the series RL models, B and C, are not as satisfactory.

The results of cases 9-11, where generator model B was introduced, show less acceptable agreement with the measured data than those of generator model A.

Case 1 models will be used in the examples of this chapter, although there is no single model combination that is substantially better than others. The models chosen give a best fit to the measured data for the test system used.

TABLE 7.3: Measured and Simulated Values of Harmonic Impedances at Tiwai with Different Generator, Load and Transformer Models (ohms)

Case	Trans-former Model	Gener-ator Model	Load Model	5th harmonic	17th harmonic
Measured			R Y B	138 - j 68 112 - j 73 150 - j109	491 + j 95 422 + j179 489 + j117
1	A	A	A	187 - j104 136 - j 66 168 - j 75	479 + j145 425 + j122 348 + j182
2	A	A	B	183 - j121 132 - j 80 164 - j 90	441 + j152 392 + j130 324 + j184
3	A	A	C	193 - j104 145 - j 68 173 - j 80	403 + j132 362 + j114 301 + j160
4	A	A	D	189 - j114 138 - j 75 169 - j 85	438 + j143 389 + j122 323 + j176
5	B	A	A	174 - j 89 130 - j 55 153 - j 62	411 + j 60 369 + j 57 326 + j114
6	C	A	A	192 - j 74 144 - j 48 169 - j 45	386 + j101 350 + j 91 300 + j136
7	D	A	A	173 - j 86 128 - j 54 151 - j 61	484 + j147 429 + j124 351 + j185
8	E	A	A	184 - j100 135 - j 63 165 - j 72	483 + j154 429 + j129 349 + j188
9	A	B	A	234 - j 90 164 - j 59 203 - j 54	415 + j201 381 + j175 297 + j208
10	C	B	A	228 - j 40 168 - j 29 190 - j 13	335 + j131 310 + j121 259 + j148
11	C	B	D	233 - j 50 173 - j 36 196 - j 21	322 + j125 298 + j115 250 + j145

FIGURE 7.2: Summary of Component Models

Transformer models:

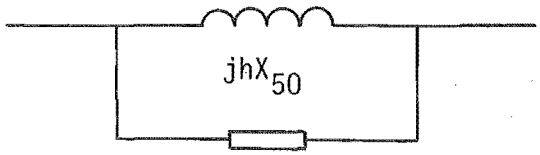

A.

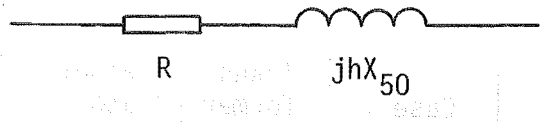

B.

C. As for B except R and X_{50} are scaled to 80% of the 50 Hz values.

D.

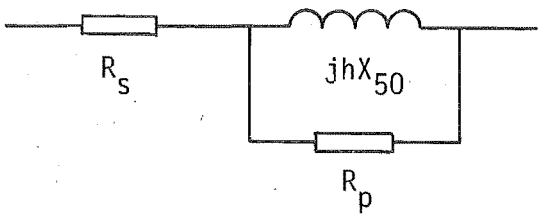

corresponding to a 30 MVA rating.

E. As for D but corresponding to a 100 MVA rating.

Synchronous Generator Models:

A. 100% of the subtransient reactance with a power factor of 0.2.

B. 80% of the subtransient reactance with a power factor of 0.2.

Load Models:

A. $\frac{jV^2}{kQ50}$

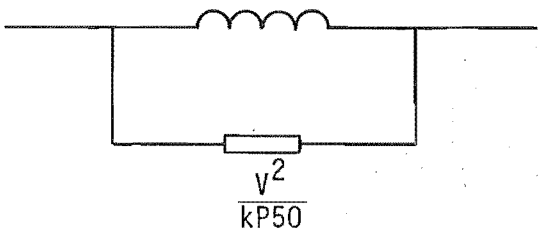

B. $\frac{jhV^2}{Q50}$

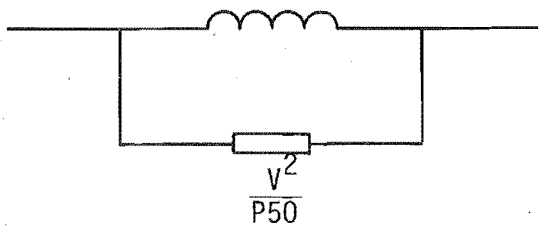

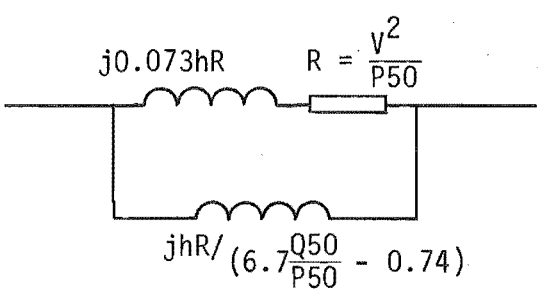

C.

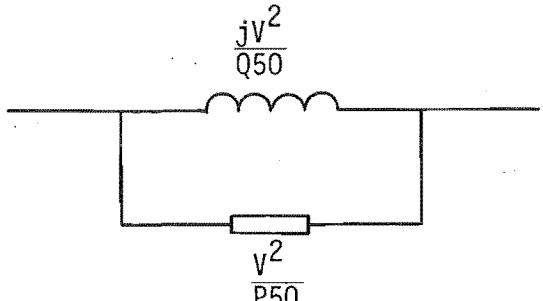

D.

When the models of case 1 are used to calculate impedances over the frequency range 50-1250 Hz, the plot of Figure 7.3 is obtained. Reasonable agreement with measured results is indicated for the characteristic harmonics.

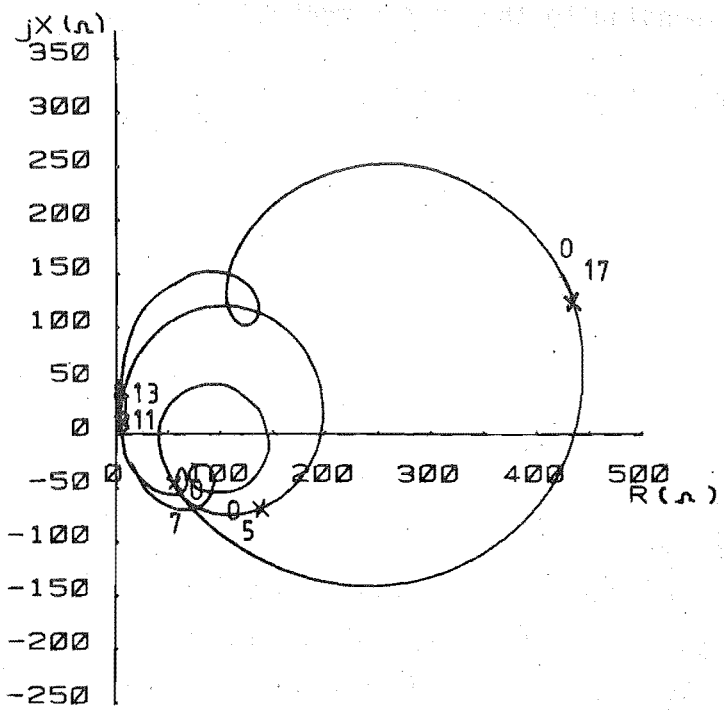

FIGURE 7.3: Measured and Simulated Yellow Phase Characteristic Harmonic Impedances for the South Island Transmission System from Tiwai 220 kV Busbar.

x simulated

0 measured

7.4 VOLTAGE SENSITIVITY TO INDIVIDUAL COMPONENT IMPEDANCES

7.4.1 Introduction

This section investigates the variation of system voltages in order to decide the accuracy of the component data necessary. Balanced current injections of 17 Amps 5th harmonic and 4.6 Amps 17th harmonic are used, corresponding to the levels measured at Tiwai.

To compare different results, the voltages at all the selected busbars will be summed, and the average referred to as the average voltage.

The larger the number of busbars used the more representative the average voltage will be of overall system conditions. Such an approach gives a simple and practical solution to the problem of comparing voltages at a number of busbars for different tests. By using a defined variation in component impedances, generally 10%, the average voltage enables a quantitative assessment of network sensitivity.

A map of the South Island is used to present results and associated with selected system busbars is a table containing four positions. The voltages for a particular study are placed in the same position at each busbar. The positions will be referred to by the numbers 1-4. The standard case using the models determined in the previous section and the current injection above will be placed in position 1.

7.4.2 Transformer Impedance Variation

All the transformer impedances are decreased and increased by 10%. The voltages obtained at the selected busbars, for the balanced current injection at Tiwai, are tabulated in Figure 7.4.

Features of the results include:

- both decreasing and increasing the impedances by 10% changes the average voltage by the same amount.
- with higher transformer impedance, higher voltages would be expected in a power flow program. This is the case for the 17th harmonic but not for the 5th harmonic.
- the sensitivity of the voltage to transformer impedance increases with frequency, i.e. the average voltage variation is 2% for the 5th and 5% for the 17th harmonic.

FIGURE 7.4(a): Percentage Voltage for Transformer Impedance Variation at 5th Harmonic

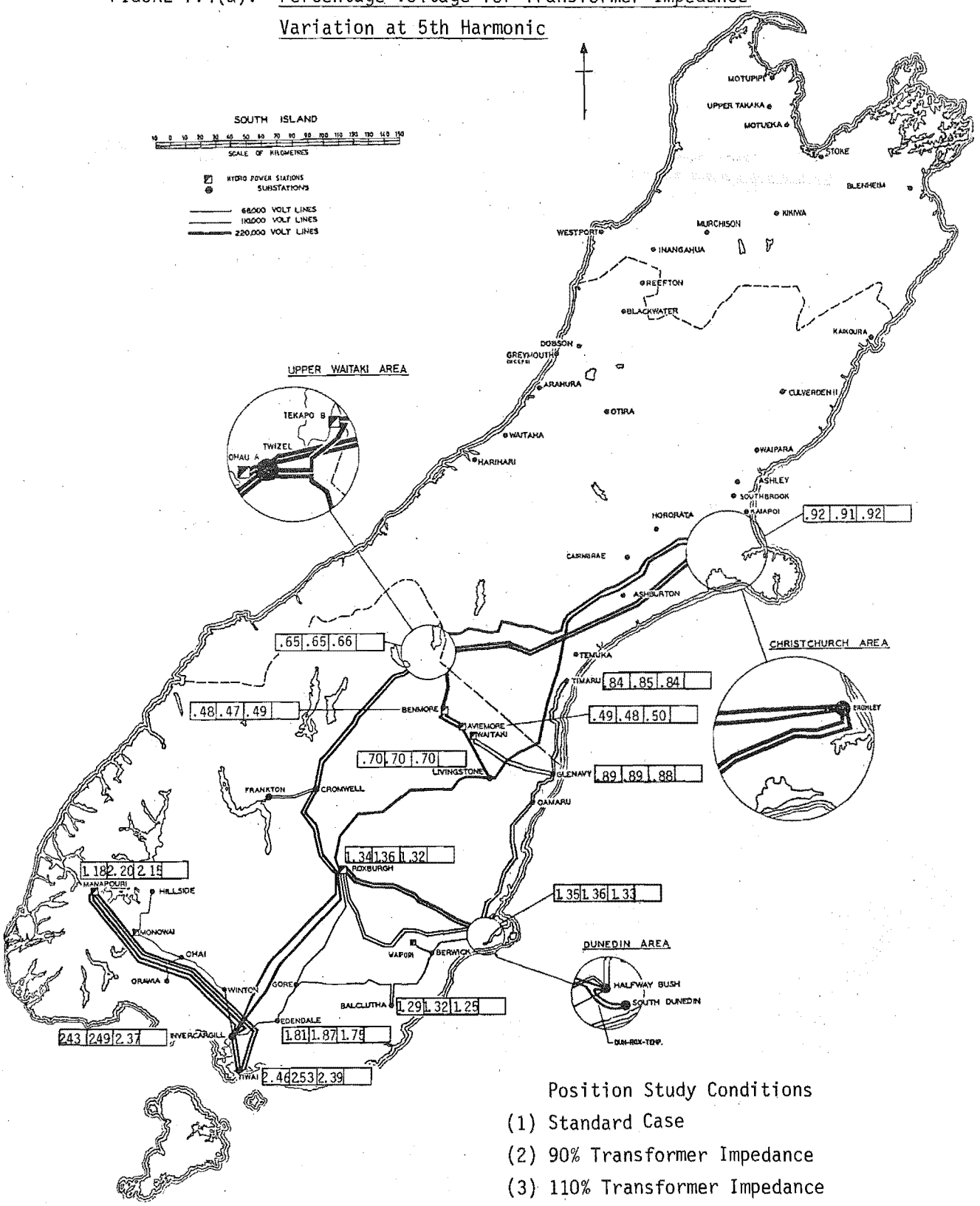

Position Study Conditions

(1) Standard Case

(2) 90% Transformer Impedance

(3) 110% Transformer Impedance

FIGURE 7.4(b): Percentage Voltage for Transformer Impedance Variation at 17th Harmonic

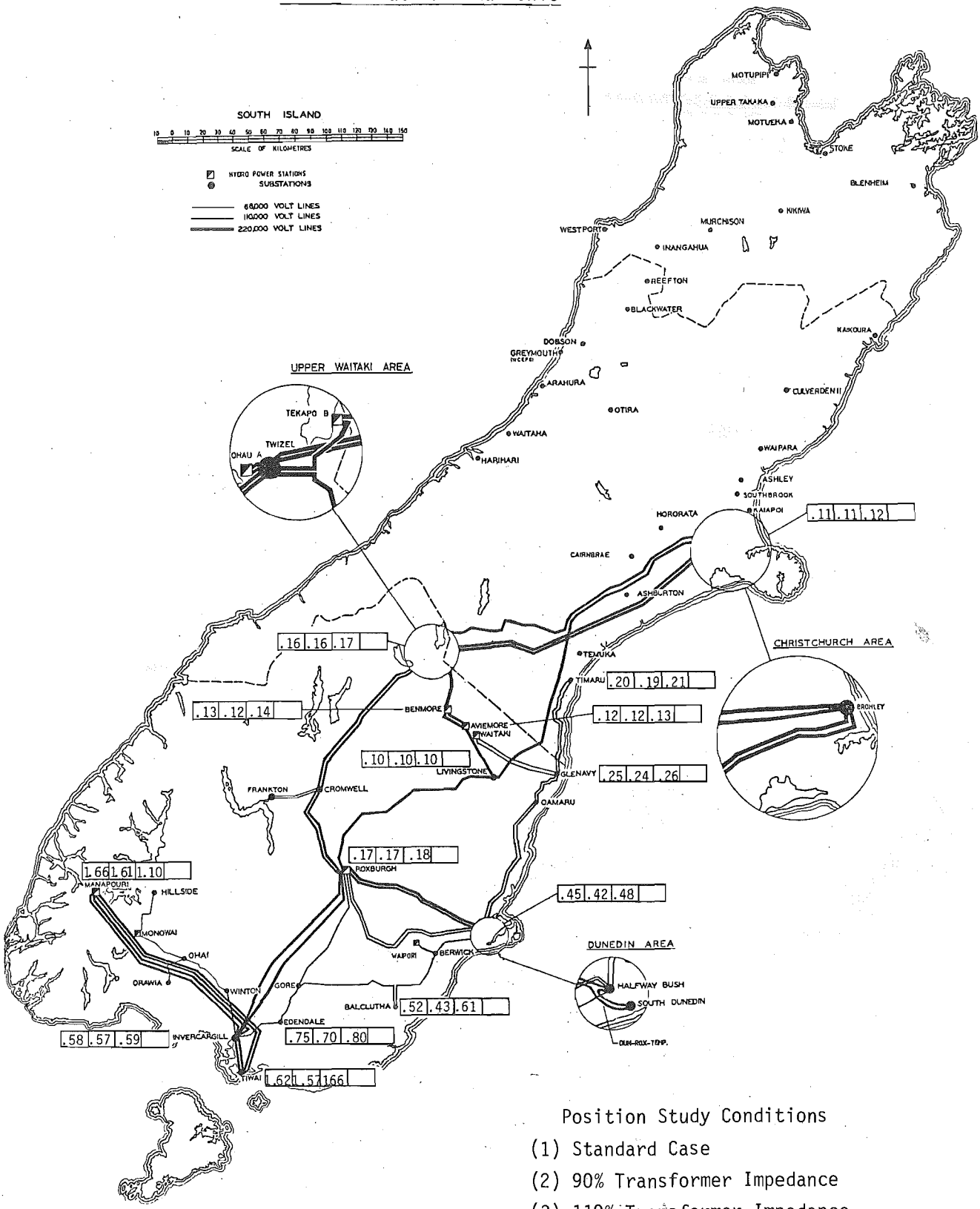

Position Study Conditions

(1) Standard Case

(2) 90% Transformer Impedance

(3) 110% Transformer Impedance

Even at the 17th harmonic system voltages are not sensitive to transformer impedance variation and therefore exact transformer data is not critical to program accuracy.

7.4.3 Generator Impedance Variation

Generator impedances are decreased and increased by 10% from the standard case, for both the 5th and 17th harmonics. The changes in voltage illustrated in Figure 7.5 show the following features:

- both increasing and decreasing generator impedance result in the same average voltage variations.
- with increased generator impedances, higher voltages would be expected. However this is not so for the 5th harmonic, indicating that harmonic voltages cannot be predicted using intuitive understanding.
- the sensitivity of voltage to generation changes decreases slightly as frequency increases, i.e. the average voltage changed 4% for the 5th harmonic and 3% for the 17th harmonic.

From the above observations generator data does not need to be known exactly. A generator unit within a station for instance, could be removed from the system without affecting the simulation validity.

FIGURE 7.5(a): Percentage Voltage for Generator Impedance Variation at 5th Harmonic

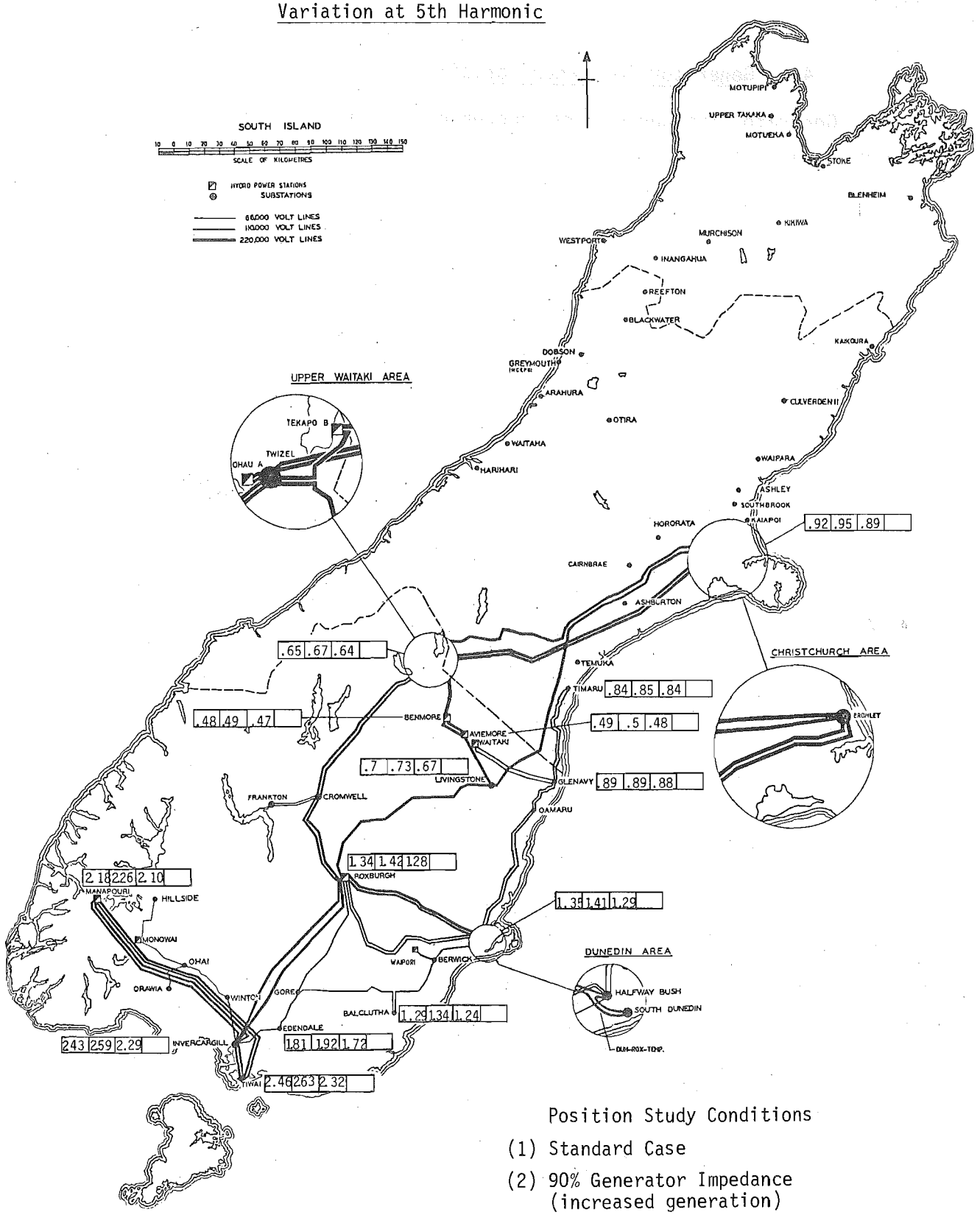

Position Study Conditions

(1) Standard Case

(2) 90% Generator Impedance (increased generation)

(3) 110% Generator Impedance (decreased generation)

FIGURE 7.5(b): Percentage Voltage for Generator Impedance Variation at 17th Harmonic

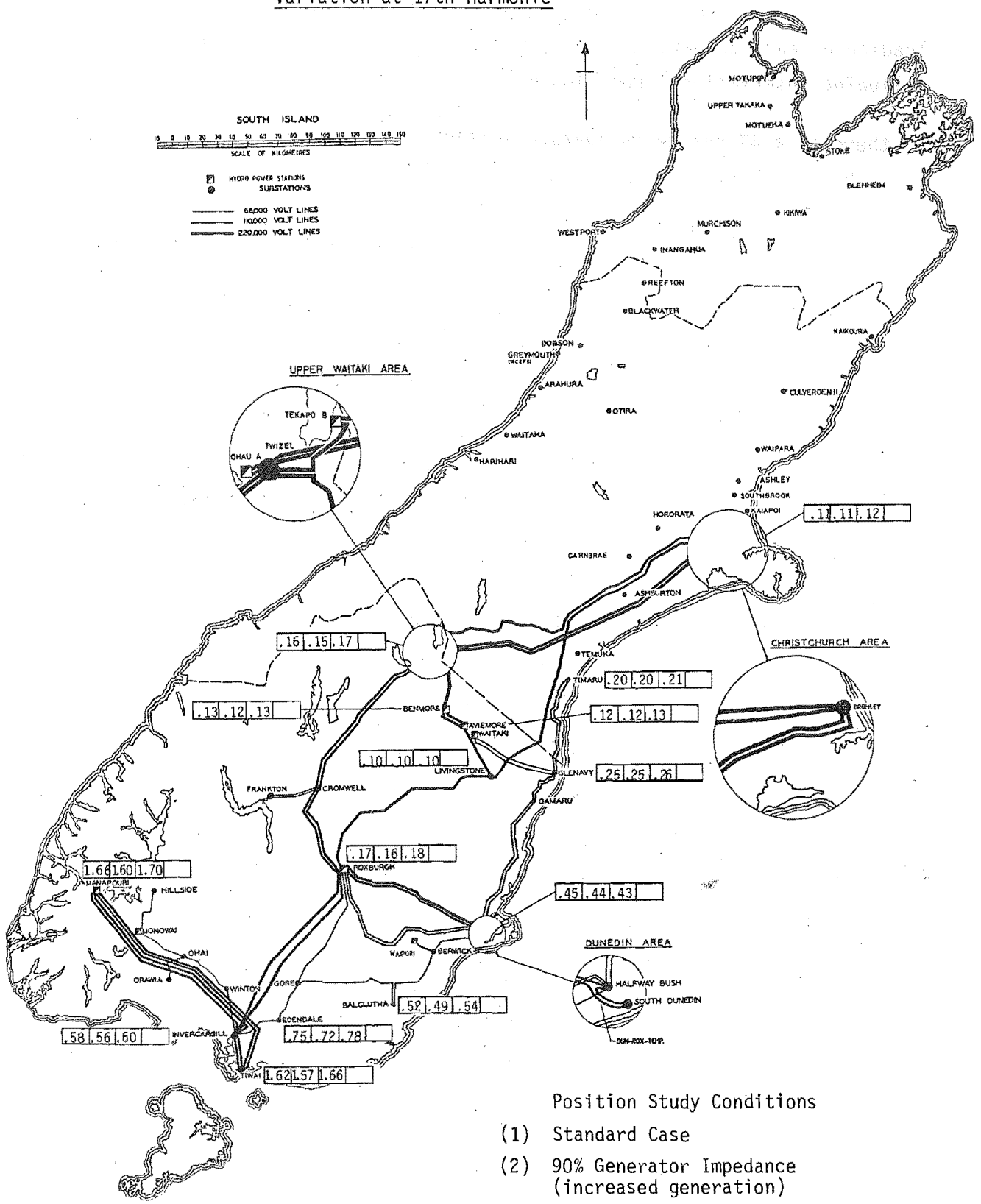

Position Study Conditions

(1) Standard Case

(2) 90% Generator Impedance (increased generation)

(3) 110% Generator Impedance (decreased generation)

7.4.4 Load Level Variation

The load level used in the standard case was 50% of the maximum loading on each busbar. Variations of 10% in this level lead to the following observations from Figure 7.6:

- there is a 4% change in average voltage at the 5th harmonic for both decreasing and increasing load levels.

- a decrease in load level (increasing load impedances) causes an increase in voltage levels. This is the opposite effect to transformer and generator impedance variation indicating the differences that occur between the component models.

- the average voltage at 17th harmonic is insensitive to load level variation, however, individual busbar voltages vary by percentages similar to the 5th harmonic.

The low sensitivity to load variation within a normal range makes the assumption of a constant percentage load for all busbars acceptable.

There is some controversy at present as to whether loads need be modelled at all, (Breuer et al 1982 and McGranaghan 1983). The no load case is simulated in Figure 7.7. Large variations, compared with the 50% load case, are observed for both the 5th and 17th harmonic voltages, i.e. 63% for the 5th harmonic and 36% for the 17th harmonic. The results are conclusive; load modelling should not be neglected.

FIGURE 7.6(a): Percentage Voltage for Load Level Variation at 5th Harmonic

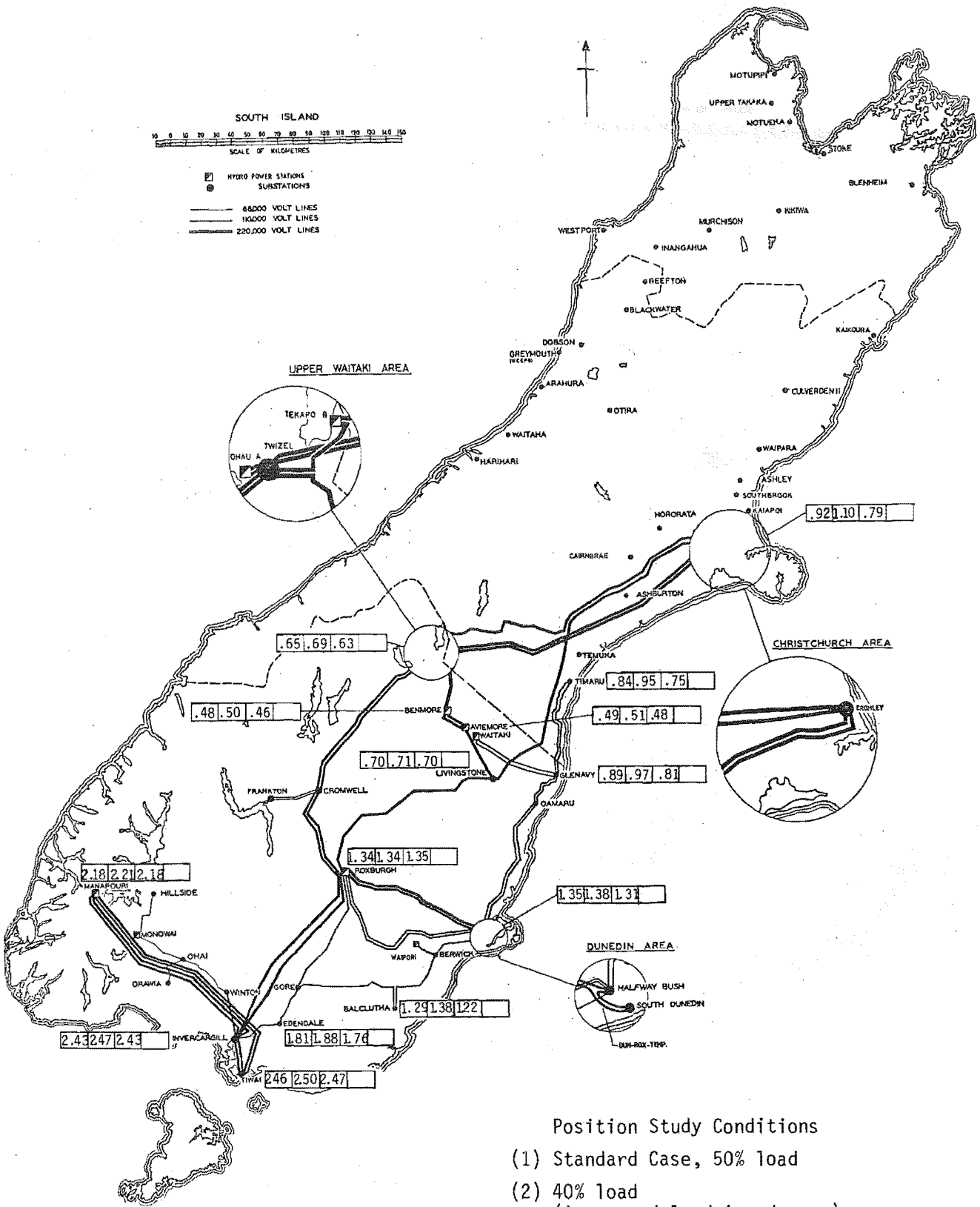

Position Study Conditions

(1) Standard Case, 50% load

(2) 40% load
(increased load impedances)

(3) 60% load
(decreased load impedances)

FIGURE 7.6(b): Percentage Voltage for Load Level Variation at 17th Harmonic

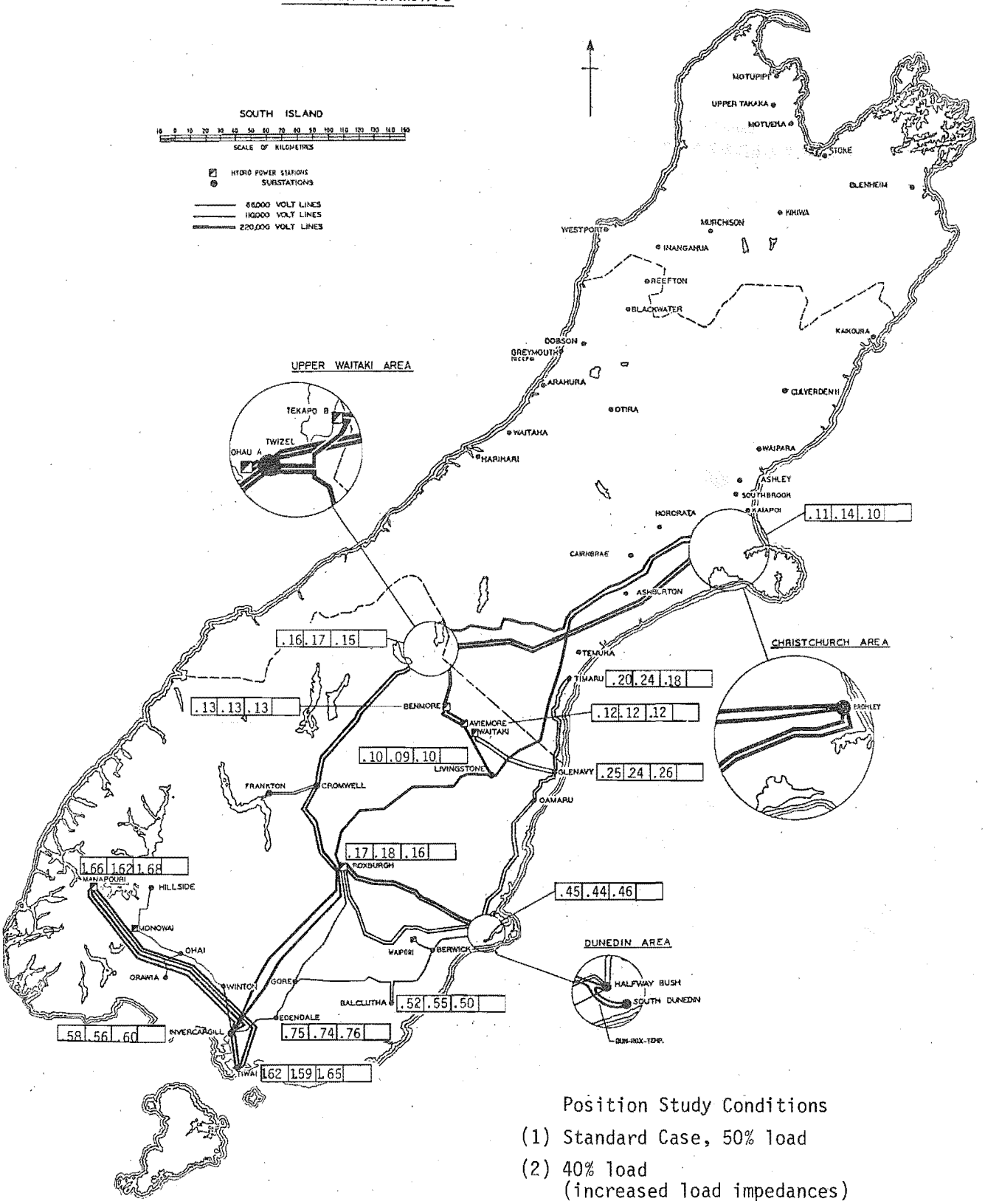

Position Study Conditions

(1) Standard Case, 50% load

(2) 40% load
(increased load impedances)

(3) 60% load
(decreased load impedances)

FIGURE 7.7(a): Percentage Voltage on No Load at 5th Harmonic

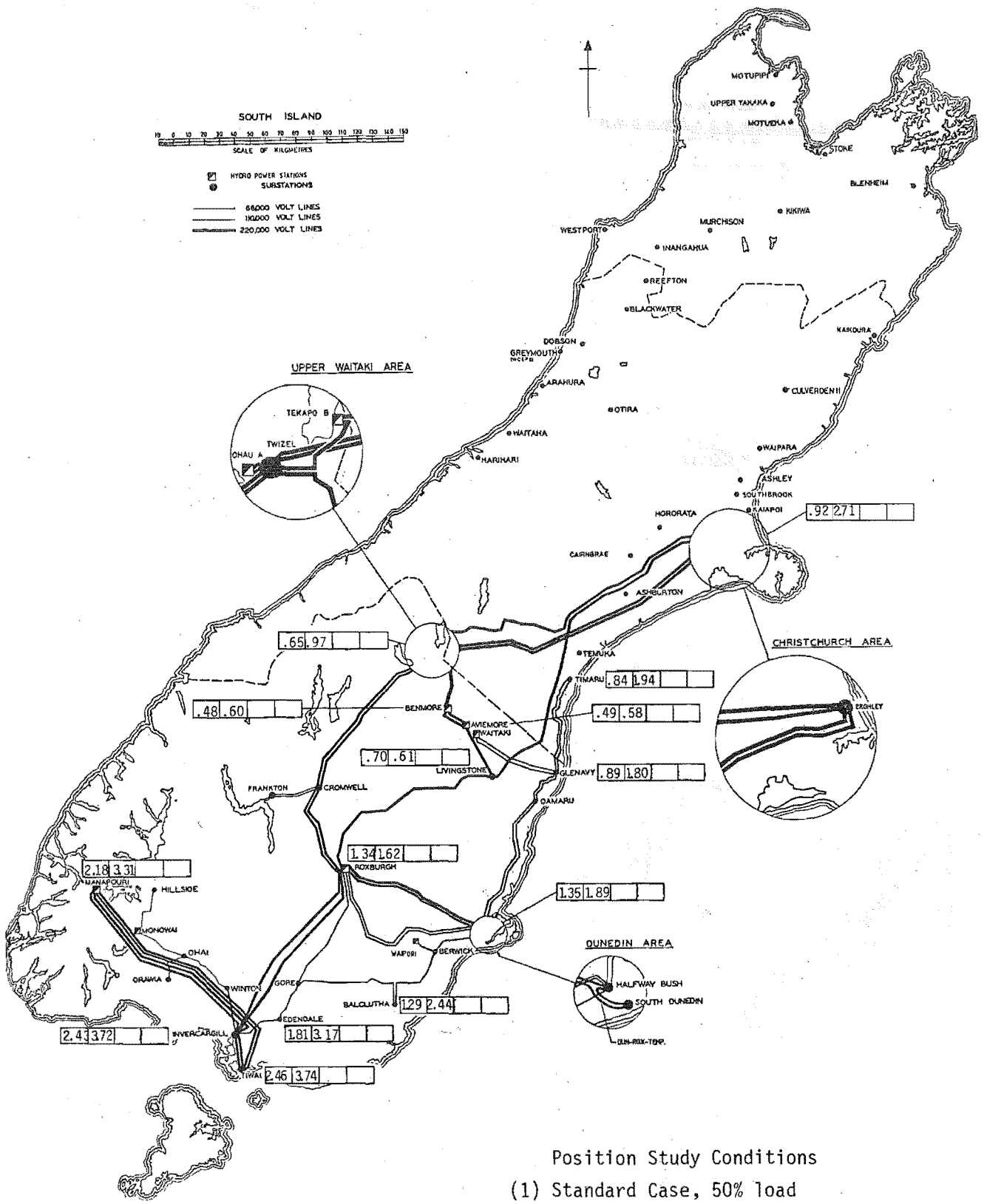

Position Study Conditions

(1) Standard Case, 50% load

(2) No load

FIGURE 7.7(b): Percentage Voltage on No Load at 17th Harmonic

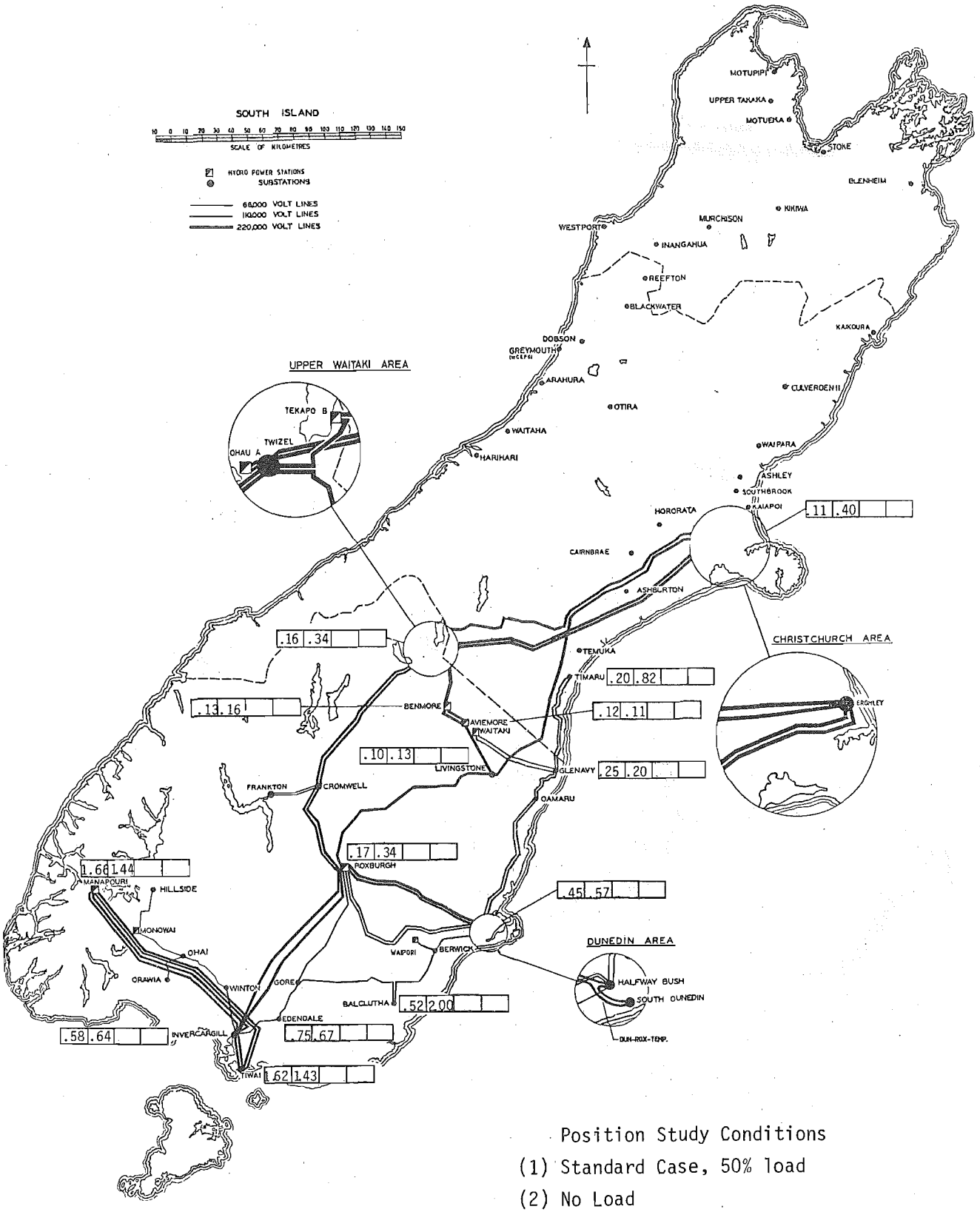

Position Study Conditions

(1) Standard Case, 50% load

(2) No Load

7.4.5 Line Parameter Variation

To vary the line parameters, all lines are shortened and lengthened by 1%. Figure 7.8 shows the sensitivity of voltage at the 5th and 17th harmonics to this variation.

Conclusions which can be drawn from these results are:

- shortening and lenghtening the lines by 1%, increases and decreases respectively the 5th harmonic average voltage by 2%.
- shortening the lines by 1% decreases the 17th harmonic average voltage by 39%. This is a very large variation.
- lengthening the lines by 1% increases the 17th harmonic average voltage by 9%. Some busbars show voltage decreases however.
- when the lines between Manapouri, Invercargill and Tiwai are shortened by 1% (the others remaining at their design length) there is little difference in the voltages compared with position 2 results.

Lines connected to the injection busbar affect the voltage levels more than lines further away and at the 17th harmonic vary uniformly with transmission line length.

From the above observations it is clear that the system is an order of magnitude more sensitive to changes in line parameters than to other component model variations, justifying the more detailed three phase transmission line model developed. The voltage sensitivity to line parameters is however beyond the accuracy capability of even this model. This represents a serious restriction on the ability of harmonic modelling to duplicate system results for the injection at the Tiwai Point Aluminium smelter.

FIGURE 7.8(a): Percentage Voltage for Line Length Variation at 5th Harmonic

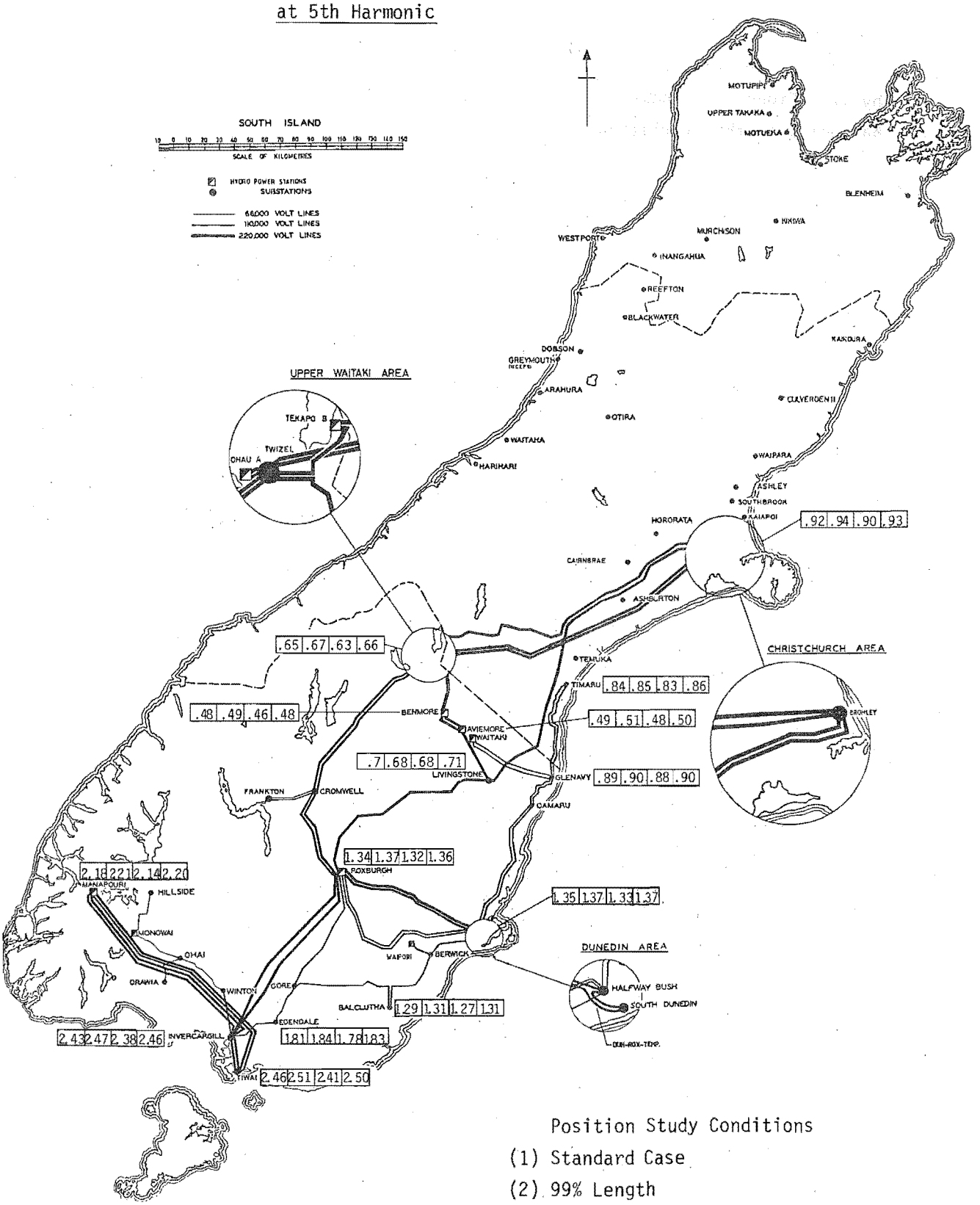

Position Study Conditions

(1) Standard Case

(2) 99% Length

(3) 101% Length

(4) 99% Length Manapouri Invercargill Tiwai lines

FIGURE 7.8(b): Percentage Voltage for Line Length Variation at 17th Harmonic

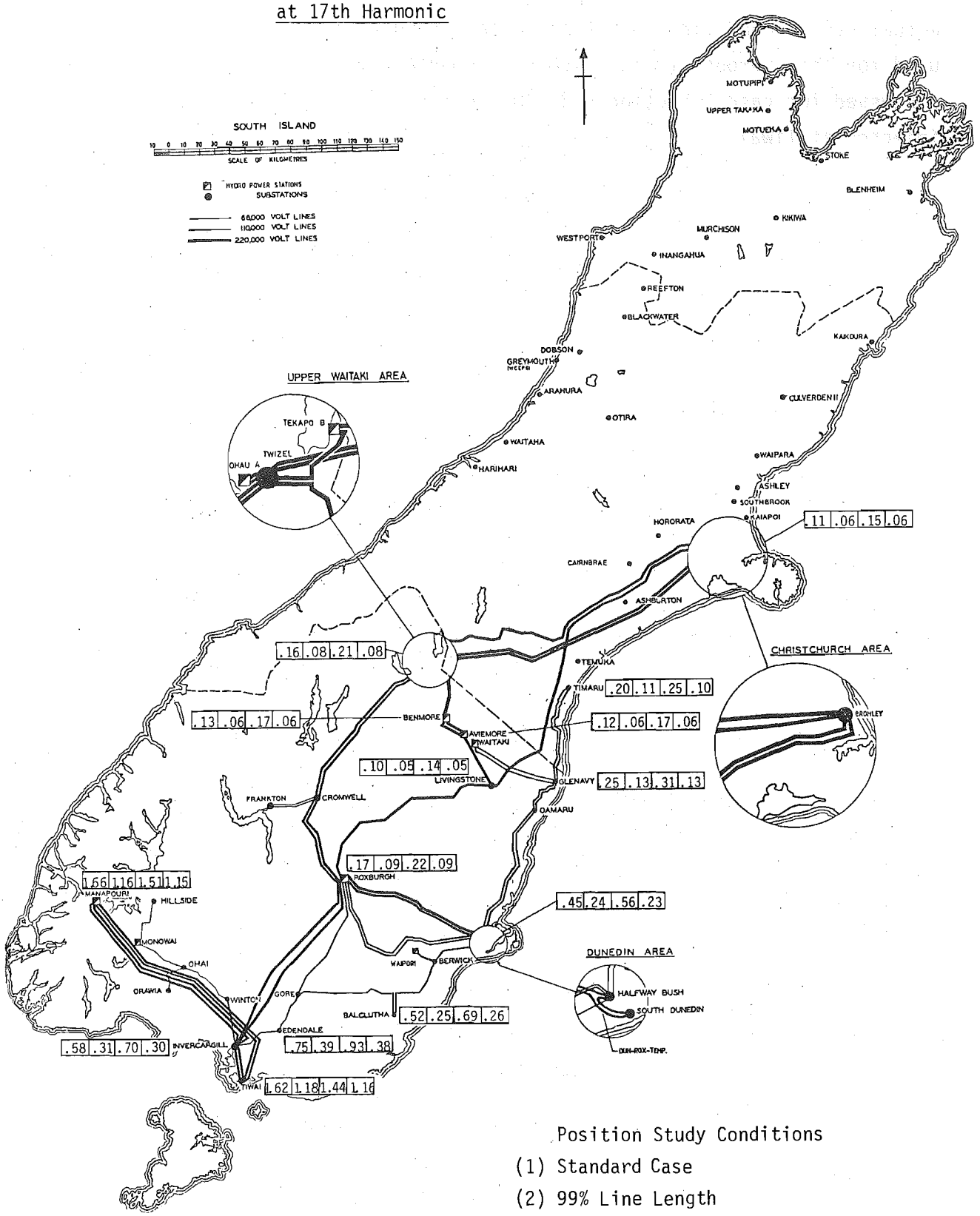

Position Study Conditions

(1) Standard Case

(2) 99% Line Length

(3) 101% Line Length

(4) 99% Line Length

Manapouri Invercargill Tiwai lines

7.5 COMPARISON OF MEASURED AND SIMULATED VOLTAGES

The validity of any computer model depends on its ability to match actual system conditions. Extensive test results available are used for this purpose (Hyland 1981). Component models are as previously discussed for case 1 Section 7.3, and current injections from Table 7.2 injected at Tiwai.

In Table 7.4 the measured voltages have been compared to the values obtained by the three phase harmonic simulation program. There is good agreement between the results for the 5th and 17th harmonics and the low measured values of the 11th and 13th harmonicsare verified. Values at busbars substantial distances from the injection point, namely Benmore and Bromley, show reasonable agreement, particularly when it is considered that modelling at Bromley is only approximate.

Simulated results for Halfway Bush are low at the 5th and 7th harmonics and at Manapouri there is considerable simulated voltage but almost none measured at these same frequencies.

At Tiwai there is poor agreement between measured and simulated phase values. The variation of voltage over the three phases is similar but the individual phase magnitudes do not show acceptable agreement.

Possible reasons for the inconsistencies experienced include:

- a second source of current injection was connected to the grid at Benmore. It is difficult to make accurate comparisons unless the current injections for all sources are known and can be modelled. No accurate information on the injection at Benmore was available.

- the accuracy of transducers and measuring instruments was suspect. The non-linearity of transducers, particularly voltage transducers, has been previously discussed. This is a possible source of error at Manapouri and Halfway Bush where CVTs were used.

- an insufficient number of parameters were measured. The three phase nature of harmonics dictates that 12 separate variables be measured at each bus. For each phase the magnitude of the current injection and voltage, and the angles of both quantities to a common reference are required. In the tests referred to only nine of these variables were recorded at Tiwai. Voltages on each phase were assumed to be separated by 120 degrees for the simulation studies.

TABLE 7.4: Comparison of Measured and Simulated Harmonic Voltages (percent of nominal phase to neutral voltage)

	5th		7th		11th		13th		17th		19th		23rd	
	M	S	M	S	M	S	M	S	M	S	M	S	M	S
TIWAI R	1.96	2.51	0.72	0.80	0.12	0.04	0.18	0.10	1.77	1.76	0.23	0.16	0.31	0.27
Y	1.83	2.34	0.71	1.09	0.05	0.05	0.09	0.11	1.66	1.58	0.17	0.23	0.27	0.22
B	2.52	2.46	0.63	0.47	0.03	0.07	0.08	0.19	1.75	1.48	0.11	0.10	0.27	0.31
INVERCARGILL	1.76	2.05	0.50	0.84	0.07	0.03	0.00	0.01	0.69	0.59	0.10	0.17	0.35	0.34
MANAPOURI	0.1	2.10	0.02	0.66	0.01	0.25	0.03	0.16	1.64	1.56	0.00	0.24	0.00	0.29
BENMORE	0.29	0.49	0.13	0.07	0.06	0.00	0.07	0.00	0.09	0.12	0.00	0.11	0.04	0.26
HALFWAY BUSH	1.78	1.34	0.77	0.38	0.23	0.02	0.00	0.03	0.85	0.47	0.20	0.21	0.00	0.19
BROMLEY	0.42	0.95	0.23	0.17	0.13	0.00	0.08	0.00	0.24	0.11	0.00	0.09	0.08	0.08

M - measured

S - simulated

- the single line diagram of the system at the time of the tests was incomplete. Because inadequate attention was paid to recording the connected generation it was necessary to assume that all generation was operating.

- transmission line data could not be obtained to the necessary accuracy for the lines to Manapouri.

7.6 IMPEDANCE IMBALANCE

In Figure 7.9 the complete system impedance loci for the three phases of the South Island system, as seen from Tiwai, is presented. Coupling between phases and circuits is responsible for the considerable imbalance which exists at various harmonic frequencies and particularly at the resonances near the 5th and 17th harmonics.

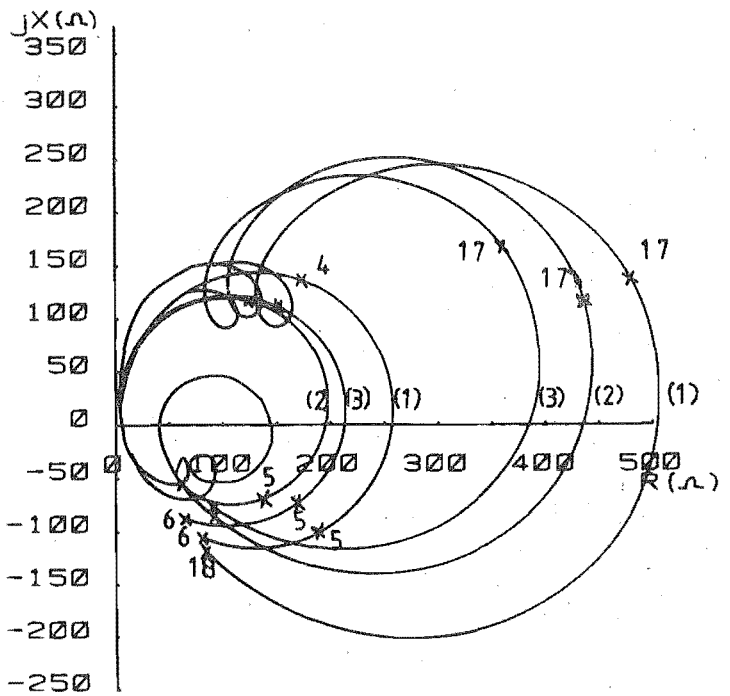

FIGURE 7.9: Equivalent Impedances for the South Island System
1) Red Phase 2) Yellow Phase 3) Blue Phase

The voltages at selected busbars in Figure 7.10, for a balanced current injection, illustrate the sequence components of the unbalanced system. Levels of negative and zero sequence voltage up to 20% of the positive sequence values are apparent. The generator busbars Roxburgh 1011, Manapouri 1014, Manapouri 2014 and Manapouri 3014; have reduced voltage levels caused by the voltage drop through the respective transformers. Also, these busbars have no zero sequence voltages because the generator transformers are star-g/delta connected and act as a short circuit on the primary to any zero sequence current flow.

The resonant frequencies of the zero sequence voltages do not always correspond to those of the positive sequence, and this is the case in Figure 7.10c where the zero sequence voltage is in fact resonating closer to the 6th harmonic.

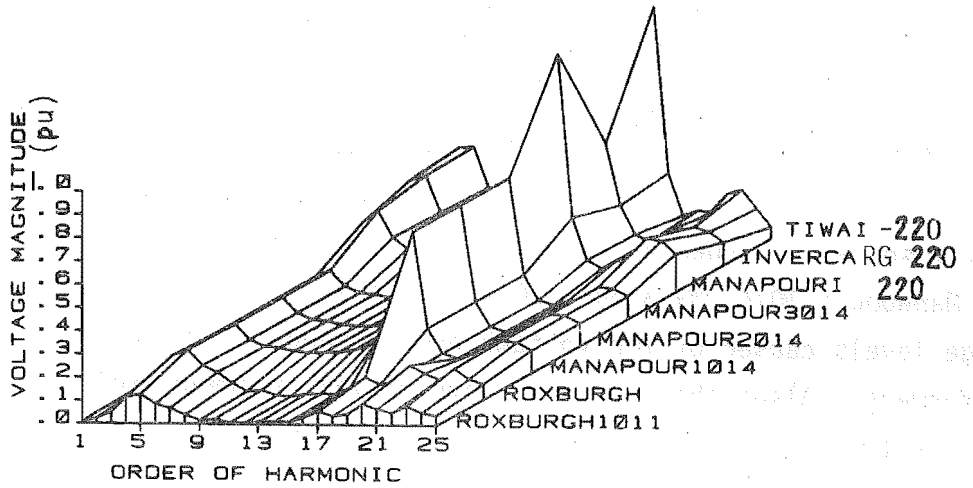

FIGURE 7.10: (a) Positive Sequence Voltages at Selected Busbars for Positive Sequence Current Injection at Tiwai Normalized to 1 p.u.

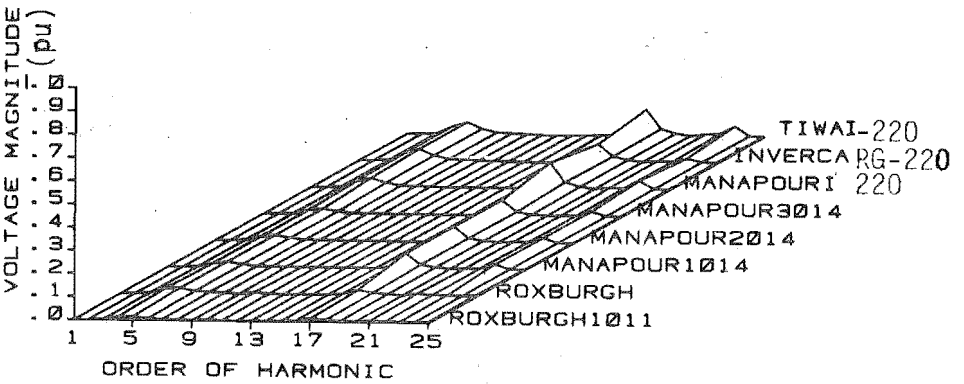

FIGURE 7.10: (b) Negative Sequence Voltages for Normalized Positive Sequence Current Injection at Tiwai

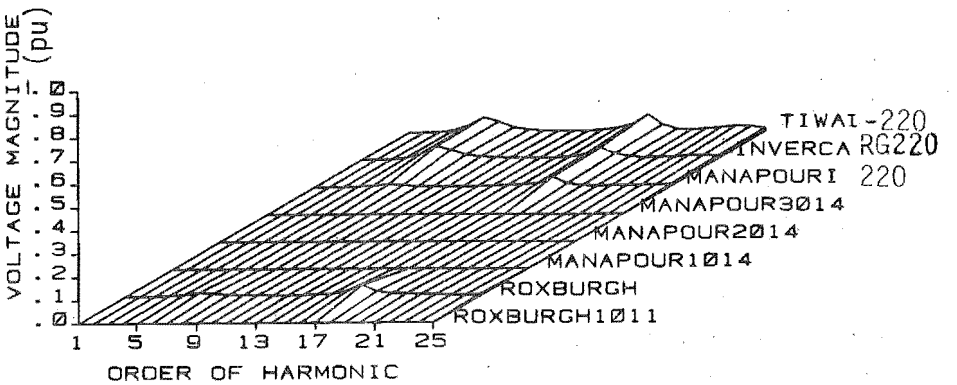

FIGURE 7.10: (c) Zero Sequence Voltages for Normalized Positive Sequence Current Injection at Tiwai

7.7 CIRCUIT COUPLING

When difficulty was found in obtaining accurate single phase simulations one hypothesis was that line coupling was responsible. To test this effect the off-diagonal 3x3 blocks in the series impedance and shunt admittance matrices for each line, are set to zero.

Figure 7.11 indicates the effect of removing circuit coupling for a network with a balanced current injection at Tiwai of 17 Amps 5th and 4.6 Amps 17th harmonic. The results in position 1 tabulate the positive sequence voltage with coupling, the standard case, and in position 2 the coupling has been removed. A 2% increase in 5th harmonic average voltage is observed while at the 17th harmonic the difference in the average voltage due to coupling increases to 8%.

The negative sequence voltages show considerably greater effects due to coupling. The ratio V-/V+ in percent is tabulated for the coupled lines in position 3 and for uncoupled lines in position 4. Levels generally increase when the coupling is removed and are higher at the 17th harmonic.

Certainly for single phase modelling lack of circuit coupling is not a major source of inaccuracy.

FIGURE 7.11(a): Percentage Voltage for Single Circuit Coupling at 5th Harmonic

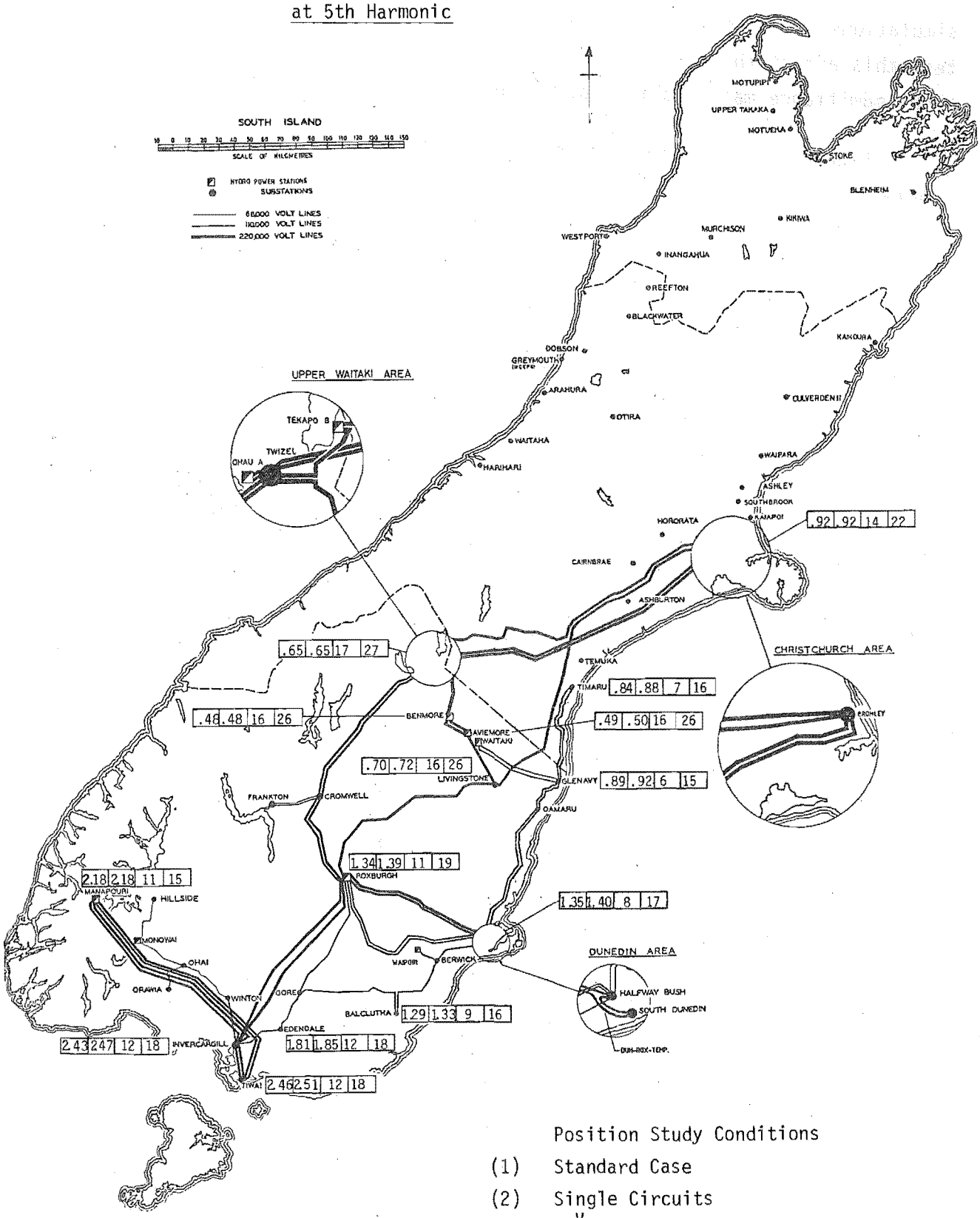

Position Study Conditions

(1) Standard Case

(2) Single Circuits

(3) $\% \frac{V-}{V+}$ Standard Case

(4) $\% \frac{V-}{V+}$ Single Circuits

FIGURE 7.11(b): Percentage Voltage for Single Circuit Coupling at 17th Harmonic

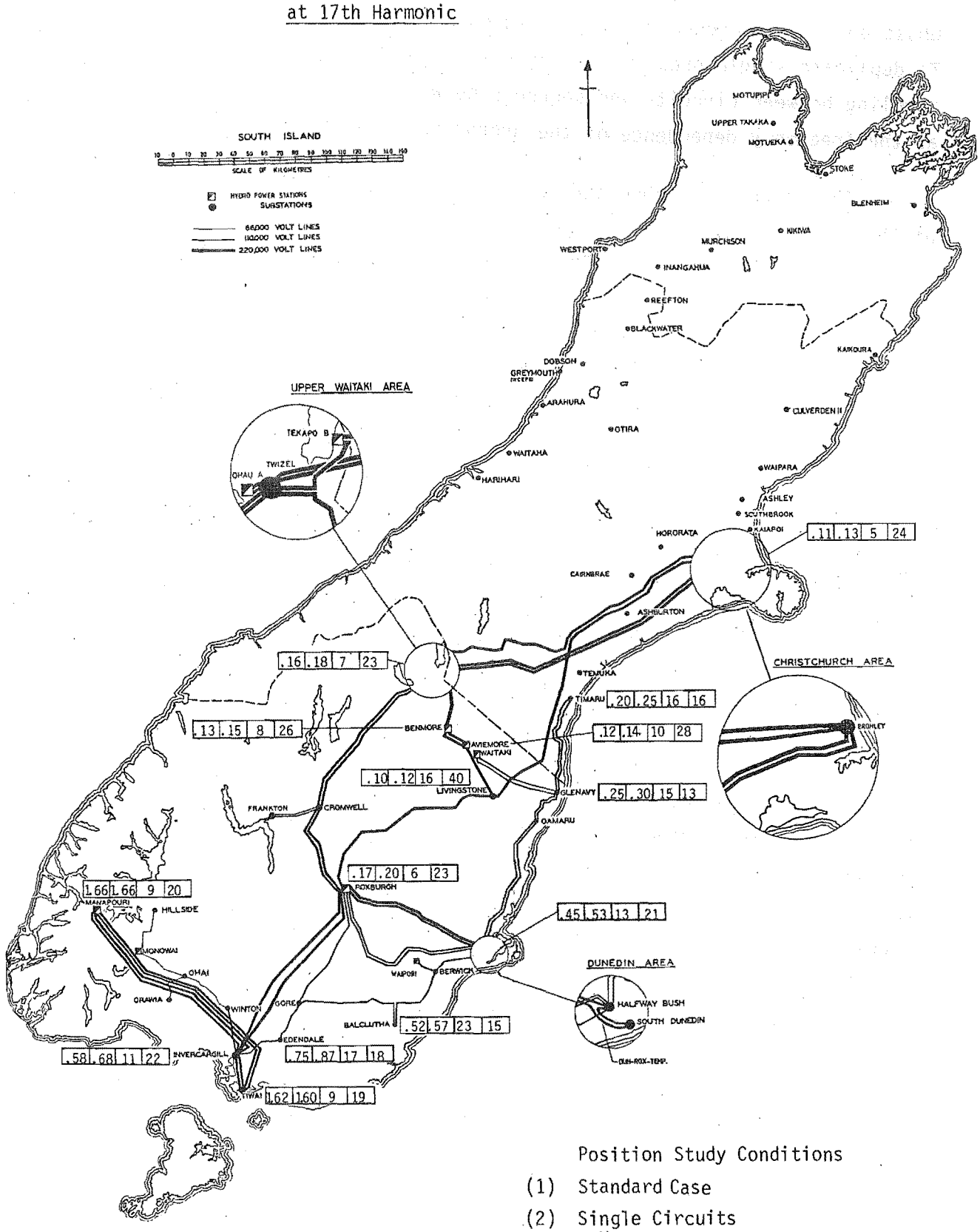

Position Study Conditions

(1) Standard Case

(2) Single Circuits

(3) % $\frac{V-}{V+}$ Standard Case

(4) % $\frac{V-}{V+}$ Single Circuits

7.8 SINGLE PHASE MODELLING

When the current injections can be considered balanced, a single phase positive sequence model is assumed accurate (Breuer et al 1982). To duplicate single phase modelling using the three phase program, the coupling between circuits and sequence networks is removed as well as the frequency dependence of the ground return model.

The series impedance and shunt admittance matrices for each line of the test system are converted to symmetrical components, and the off-diagonal terms set to zero. The diagonal matrices are then reconverted to phase components, the result being balanced lines with no circuit coupling.

The single phase model, ELAFANT, inputs self positive sequence impedances and admittances for each line calculated at fundamental frequency. To duplicate this the earth return parameters are set constant at the 50 Hz values in HARMAC. Skin effect can be modelled in single phase programs and so this is retained.

If only positive sequence currents are injected then the positive sequence voltages represent those obtained in a single phase program the negative and zero sequence quantities being zero.

The results of Figure 7.12 for 17 Amps 5th harmonic and 4.6 Amps 17th harmonic injections indicate a 2% increase in the average voltage for the 5th harmonic, compared to the standard three phase study, and 12% for the 17th harmonic. By comparing these results with those from the previous section, most of the voltage variation can be attributed to the removal of circuit coupling. As the frequency increases, so the coupling between sequence networks increases, indicating greater levels of imbalance. With balanced harmonic current injections the difference between single phase and three phase models does not account for the modelling inaccuracies experienced by Breuer et al (1982).

FIGURE 7.12(a): Percentage Voltage for Single Phase Modelling at 5th Harmonic

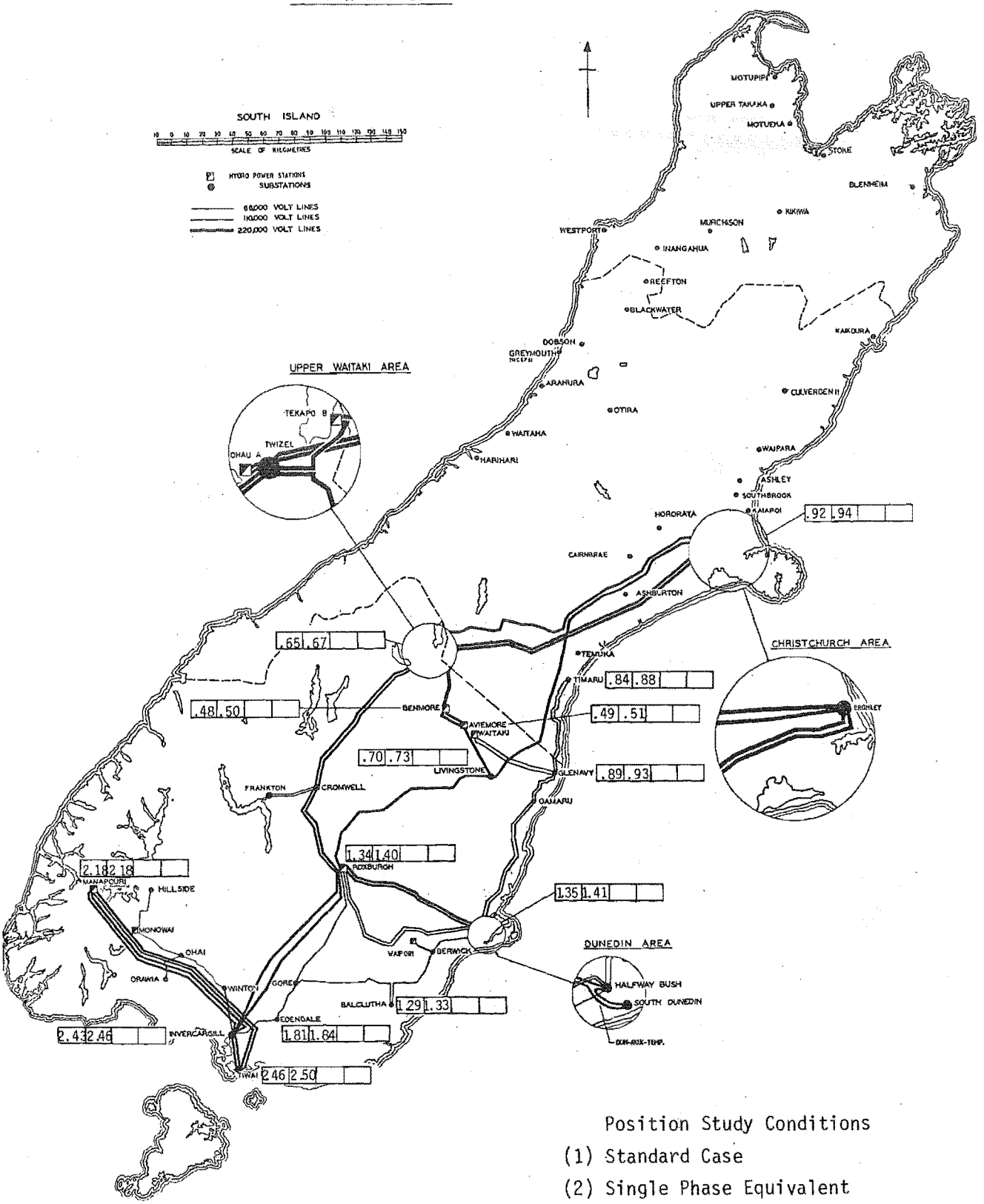

Position Study Conditions

(1) Standard Case

(2) Single Phase Equivalent

FIGURE 7.12(b): Percentage Voltage for Single Phase Modelling at 17th Harmonic

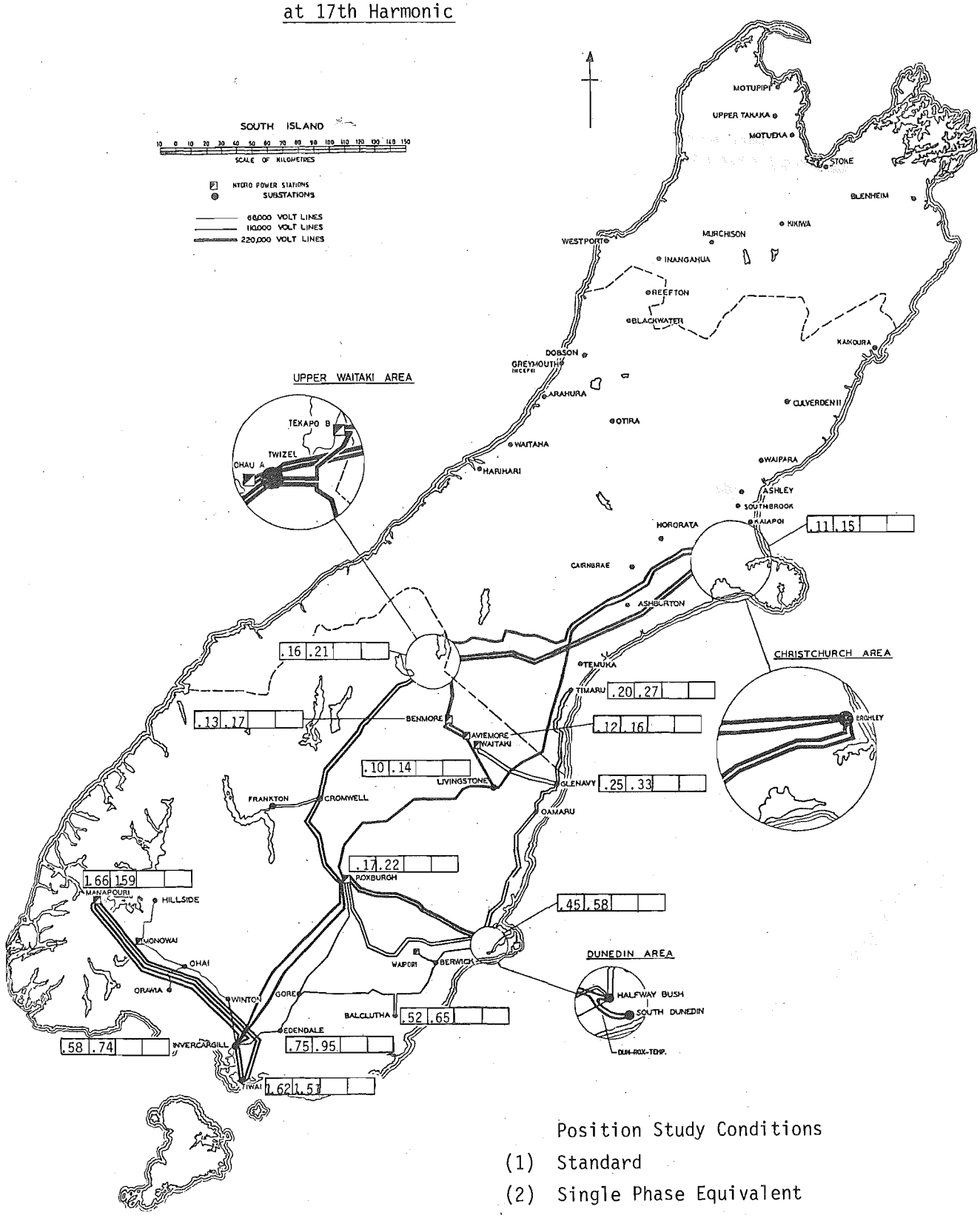

Position Study Conditions

(1) Standard

(2) Single Phase Equivalent

7.9 NETWORK ASSUMPTIONS

7.9.1 Temperature Variation

Transmission line resistances are generally not assumed to vary with temperature in harmonic penetration modelling. In a power system however, climatic and loading conditions cause the conductor temperatures to change. A 30 degree Centigrade increase is modelled by increasing the conductor resistances as discussed in Chapter 5.4.

With reference to Figure 7.13, the voltages caused by this increase in temperature are included in position 2 and can be compared with the standard case for normal 20 degree Centigrade conductor temperatures. At the 5th harmonic the average voltage reduces by less than 1% whereas at the 17th harmonic it decreases by 5%. The network is closer to a parallel resonance at the 17th harmonic, and the increased effect from the line resistance is expected.

7.9.2 Skin Effect

Skin effect ratios influence line resistance and increase with frequency. The importance of skin effect modelling is indicated in the results of position 3 in Figure 7.13. When this effect is removed from the line resistance, an increase in the positive sequence average voltage of 25%, at the 17th harmonic, is observed. Skin effect modelling has a greater influence than temperature variation and again the greatest influence is at the 17th harmonic resonance.

7.9.3 Earth Resistivity Variation

Earth resistivity is assumed constant over the whole network and independent of seasonal fluctuations; a value of 100 Ωm has been used throughout this thesis. Neither of these assumptions are accurate, considering the variation of ground soil types and water levels during any year.

Figure 7.14 shows the positive sequence voltages, for the case of ρ = 100 Ωm, the standard case. When the resistivity is increased to 1000 Ωm there is very little change in the positive sequence voltages, however, the levels of zero sequence voltage fluctuate. The position 2 results includes the percentage of V_0/V_+ for ρ = 100 Ωm while position 3 illustrates this ratio for ρ = 1000 Ωm.

FIGURE 7.13(a): Percentage Voltage for Temperature Variation and Skin Effect Modelling at 5th Harmonic

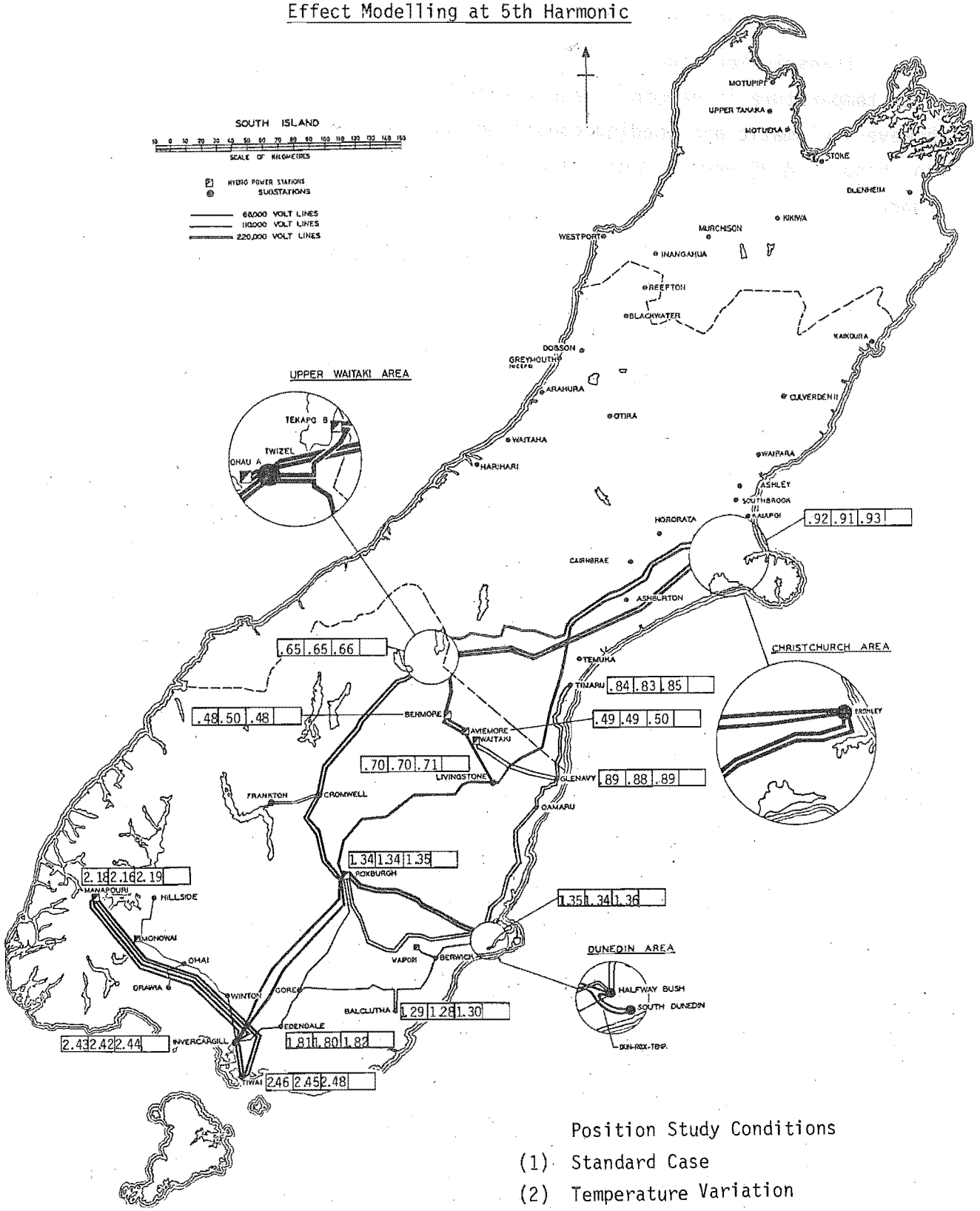

Position Study Conditions

(1) Standard Case

(2) Temperature Variation

(3) No Skin Effect Modelling

FIGURE 7.13(b): Percentage Voltage for Temperature Variation and Skin Effect Modelling at 17th Harmonic

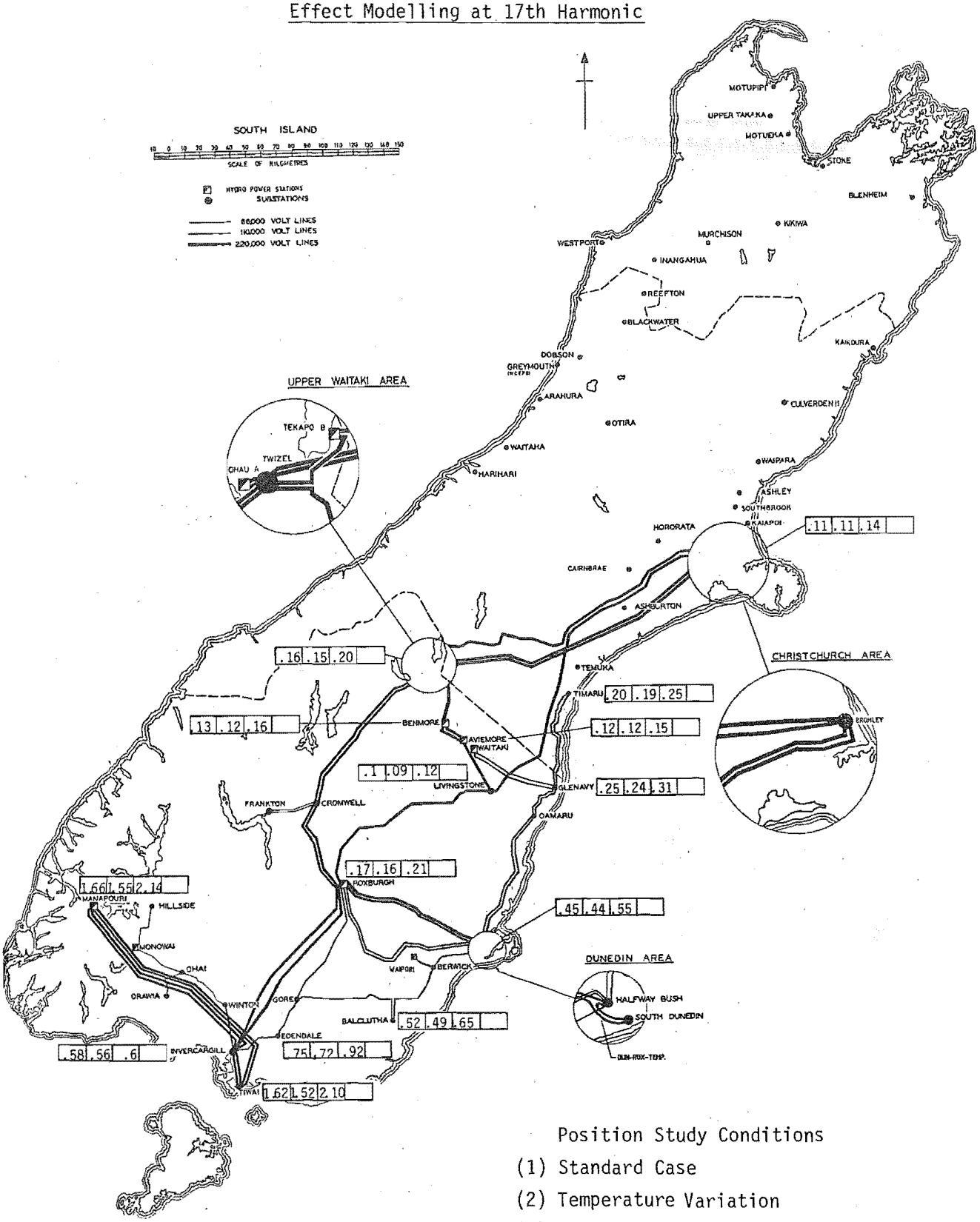

Position Study Conditions

(1) Standard Case

(2) Temperature Variation

(3) No Skin Effect Modelling

FIGURE 7.14(a): Percentage Voltage for Resistivity Variation at 5th Harmonic

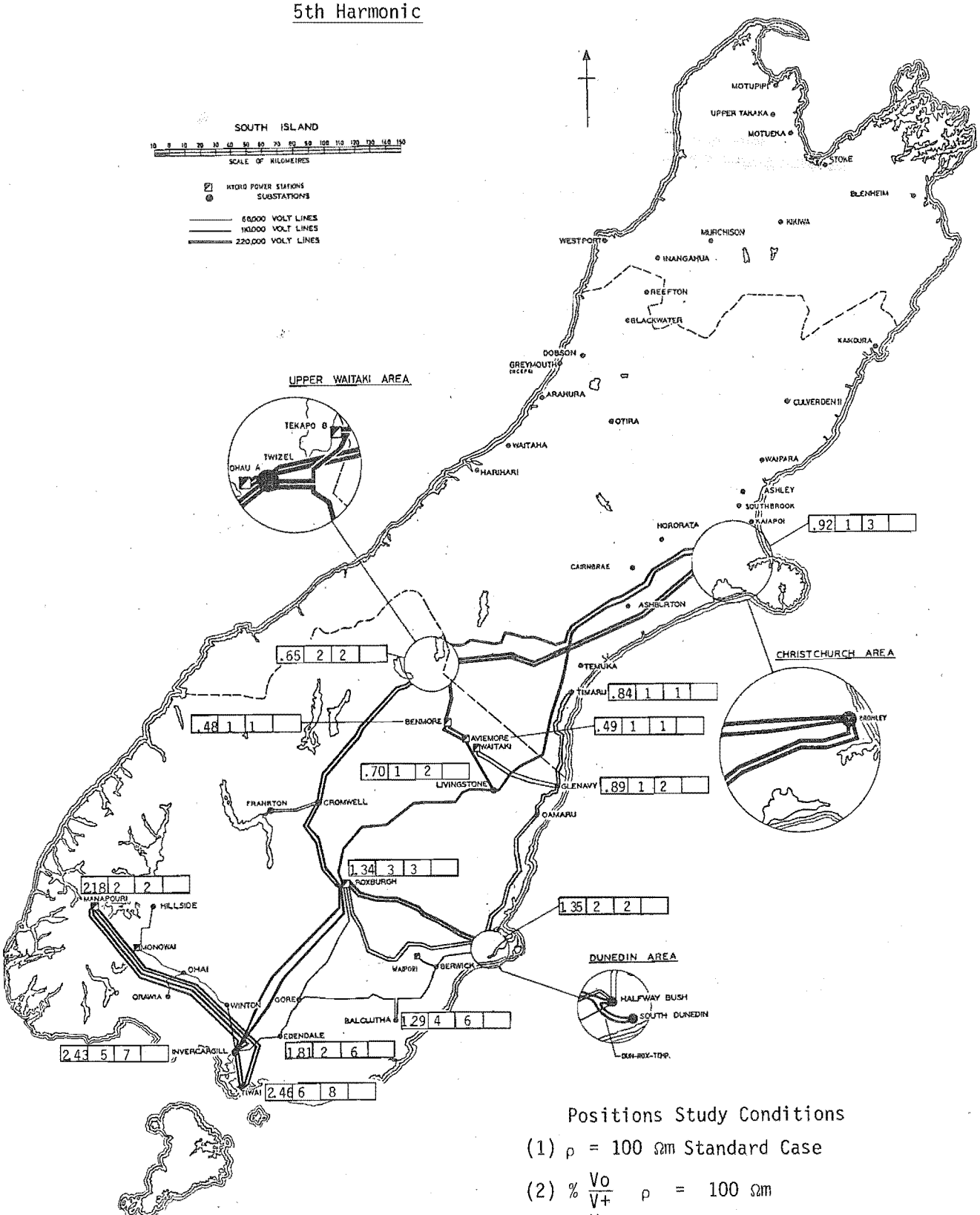

Positions Study Conditions

(1) ρ = 100 Ωm Standard Case

(2) % $\frac{Vo}{V+}$ ρ = 100 Ωm

(3) % $\frac{Vo}{V+}$ ρ = 1000 Ωm

FIGURE 7.14(b): Percentage Voltage for Resistivity Variation at 17th Harmonic

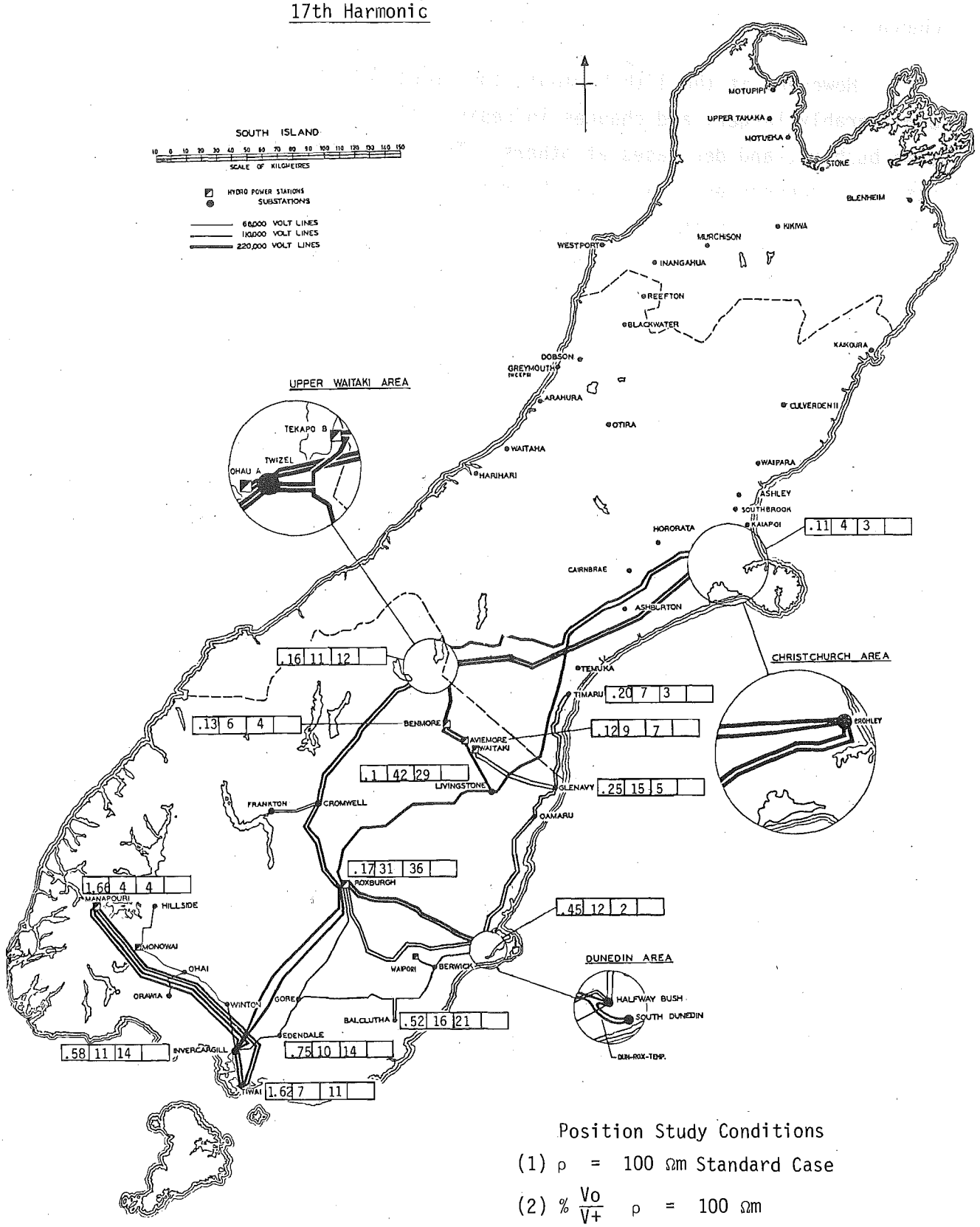

Position Study Conditions

(1) ρ = 100 Ωm Standard Case

(2) % $\frac{Vo}{V+}$ ρ = 100 Ωm

(3) % $\frac{Vo}{V+}$ ρ = 1000 Ωm

At the 5th harmonic, the ratios of zero sequence voltage to positive sequence voltage are less than 8% and the maximum variation with resistivity change is only 2%.

However, at the 17th harmonic the levels of zero sequence are considerably larger, and changes in resistivity cause increases in V_0 at some busbars, and decreases at others. This indicates the zero sequence resonant frequencies as well as the magnitudes are varying. While resistivity affects the zero sequence voltages in a network it is not important in improving the accuracy of positive sequence studies.

7.10 UNBALANCED HARMONIC CURRENT INJECTIONS

The harmonic currents injected into the AC system by a convertor are, in general, unbalanced between phases; the imbalance being more extreme for the case of non-characteristic harmonic orders. Only a three phase model, which includes coupling and impedance imbalance, can accurately assess the effect of unbalanced current injection.

Unbalanced currents of $1\angle 0^{o}$ pu, $0.65\angle -120^{o}$ pu and $0.65\angle 120^{o}$ pu were injected into the test system at the Tiwai bus. The three dimensional diagrams of Figure 7.15 show the positive, negative and zero sequence voltages for selected busbars in the system.

These can be compared with the balanced current injection case of Figure 7.10. With unbalanced current injection, the levels of negative and zero sequence voltage are considerably higher.

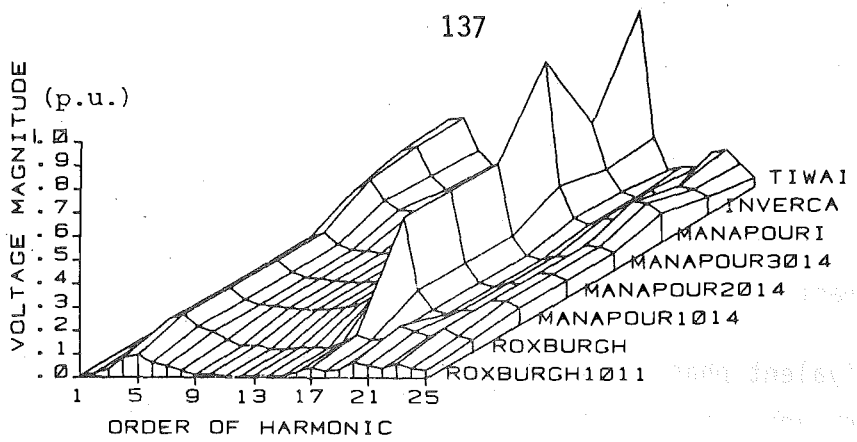

FIGURE 7.15: (a) Positive Sequence Voltages at Selected Busbars for Unbalanced Current Injection at Tiwai

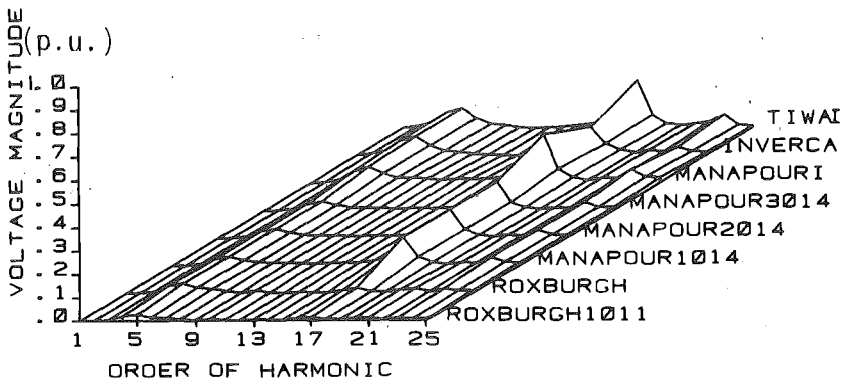

FIGURE 7.15: (b) Negative Sequence Voltages for Unbalanced Current Injection at Tiwai

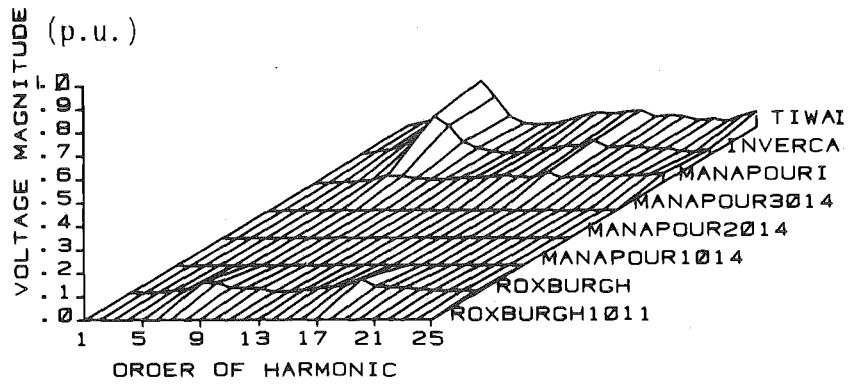

FIGURE 7.15: (c) Zero Sequence Voltages for Unbalanced Current Injection at Tiwai

7.11 SYSTEM CONFIGURATION CHANGE

Addition or removal of transmission lines is the result of routine maintenance, protection operation under fault conditions, or future system development.

The equivalent phase impedances for the 23rd harmonic are shown in Table 7.5 before and after the opening of a single line between Tiwai and Manapouri. This line remains coupled to the other circuits sharing the same right-of-way. While for this outage only a small change in impedance is observed, when the two lines between Tiwai and Manapouri are taken out of service, the high 24th harmonic response in Figure 7.16 is observed. The presence of 17th harmonic voltage on the busbars of the open circuit lines is evidence of the coupling between circuits.

TABLE 7.5: 23rd Harmonic Impedance Magnitudes at Tiwai for Single Circuit Outage (ohms)

		Measured Test Results	Simulated Results
Before line outage	R	96	96
	Y	86	79
	B	88	92
After line outage	R	127	128
	Y	95	109
	B	107	121

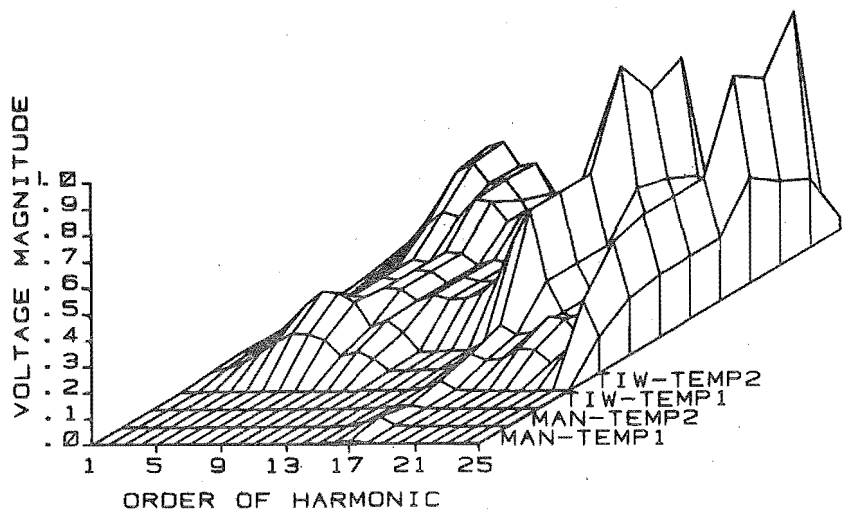

FIGURE 7.16: Positive Sequence Voltages at Selected Busbars with Both Lines from Tiwai to Manapouri Open Circuited. Current Injection at Tiwai normalized to 1 p.u.

7.12 CONCLUSIONS

The voltage sensitivity to transformer, generator and load impedance variation indicates that exact knowledge of the level or connection of these components is not required. However, load modelling should not be ignored.

Modelling transmission lines in forested and mountainous terrain using geometry and individual conductor data has been found unsatisfactory. In this situation the lines have been lengthened to give the measured resonant frequencies. The line parameters obtained in this manner involve a smaller correction than the difference between measured and calculated values reported during commissioning of the same lines.

Upon further investigation the sensitivity of simulated voltages have been found most susceptible to the transmission lines connected to the harmonic current injection busbar. The parameters of these lines are required to an accuracy of well below 1% at the parallel resonances, an assignment not possible with even the detailed line model in use.

Satisfactory comparisons between simulated and measured data on a number of busbars have been achieved, given the limitations of the available test data. Measurements of accurate phase angles relative to one reference angle were not available and to achieve agreement with simulation in individual phase voltages these will be required. Retrospectively determining a system configuration is unsatisfactory and a very accurate single line diagram of the system at the time of any tests will be necessary in future tests.

Circuit coupling and phase imbalance increases with frequency although ignoring coupling is not a major cause of program inaccuracy with balanced current injections.

Temperature change and the influence this has on line resistance causes variations in voltage of the same order as the transformer, generator or load impedance changes. This is difficult to compensate for in simulation studies. Of more importance at resonance is provision of accurate skin effect modelling, and fortunately this is possible.

Resistivity variation affects the levels of zero sequence but not the levels of positive sequence voltage. Thus, for the purpose of model validation a single resistivity over the entire network is satisfactory.

The three phase representation allows for analysis of unbalanced harmonic current injections, a condition which is most likely to be found in a practical system. Symmetrical component analysis using uncoupled sequence networks cannot provide the accuracy of the three phase techniques in this situation.

CHAPTER 8

RIPPLE CONTROL SPILLOVER

8.1 INTRODUCTION

This chapter is the result of a request from one of the local supply authorities, Central Canterbury Electric Power Board, to conduct ripple control spillover studies. Such investigations enable the determination of the likely consequences of a change in ripple control plant frequency. The extent to which three phase modelling is needed will also be investigated.

Ripple control is a technique used in load management where electrical supply authorities control customer load using coded pulses of current injected at a busbar called the point of injection. The current, I, propagates in the distribution network and operates receivers which switch the controllable loads (Ross 1972).

The signals injected onto the distribution network can "spillover" into the transmission system through the point of supply. These signals can propagate large distances on the transmission grid and be detected by other supply authorities, illustrated in Figure 8.1. If the spillover voltage level at the receiver is large enough and there is insufficient discrimination in the coded pulses, one supply authority may control another's customers. Since peak charges are expensive, high costs are incurred when load is switched at the wrong time.

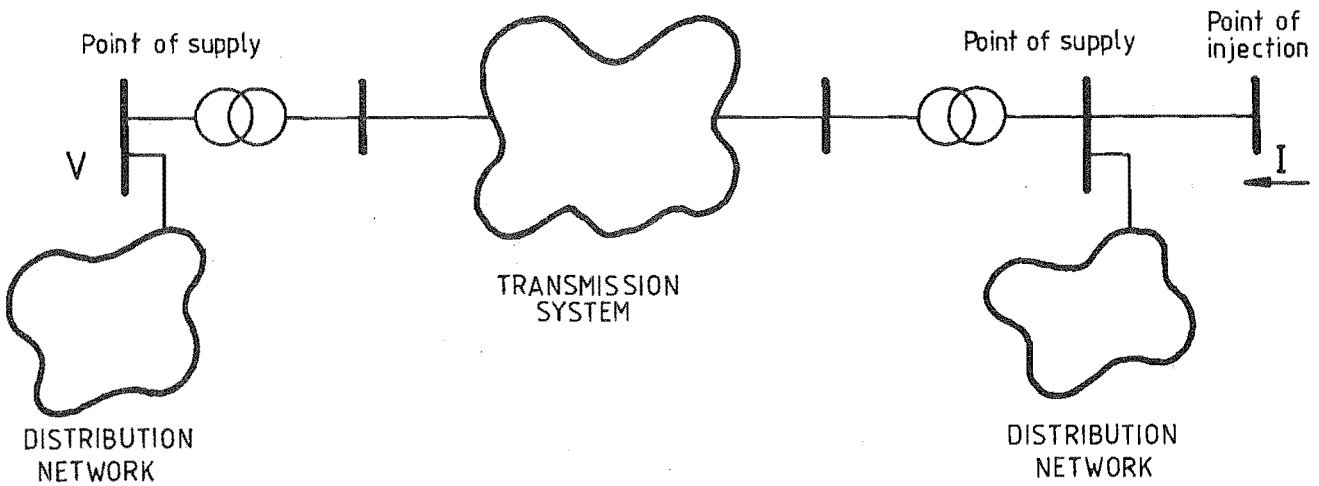

FIGURE 8.1: Schematic of Ripple Control Spillover

Areas and frequencies likely to cause spillover problems with the Central Canterbury Electric Power Board are marked on Figure 8.2. The control pulses injected by this authority use a carrier frequency of 510 Hz and have operated relays hundreds of kilometers from the injection point at Hornby. Increasing use of similar equipment and frequencies by different supply authorities has increased the possibility of interference.

If spillover voltage levels exceed .4% of nominal voltage at the point of supply to an authority with the same ripple control frequency, then interference between the two supply authorities can result. This will depend on the coding of the receivers and attenuation within the susceptible supply authority's area but levels above .4% have been found to require filtering. Generally no attempt is made to avoid propagating signals throughout the transmission grid and problems are dealt with by the supply authority affected. This is not an onerous problem because the plant used to inject each authority's ripple signals has a filter tuned to the injection frequency, and hence spillover frequency, which can be used as a shunt filter when the plant is not operating.

The sensitivity of voltage to individual component impedances and models is investigated further in this chapter with the complete South Island system documented in Appendix 3. The two single phase computer programs available in New Zealand and the three phase software discussed in this thesis are compared and guidelines to their usage and accuracy determined. Since three phase analysis is more complex the situations where it is justified need to be determined.

FIGURE 8.2: Ripple Control Spillover Areas for Central Canterbury Electric Power Board

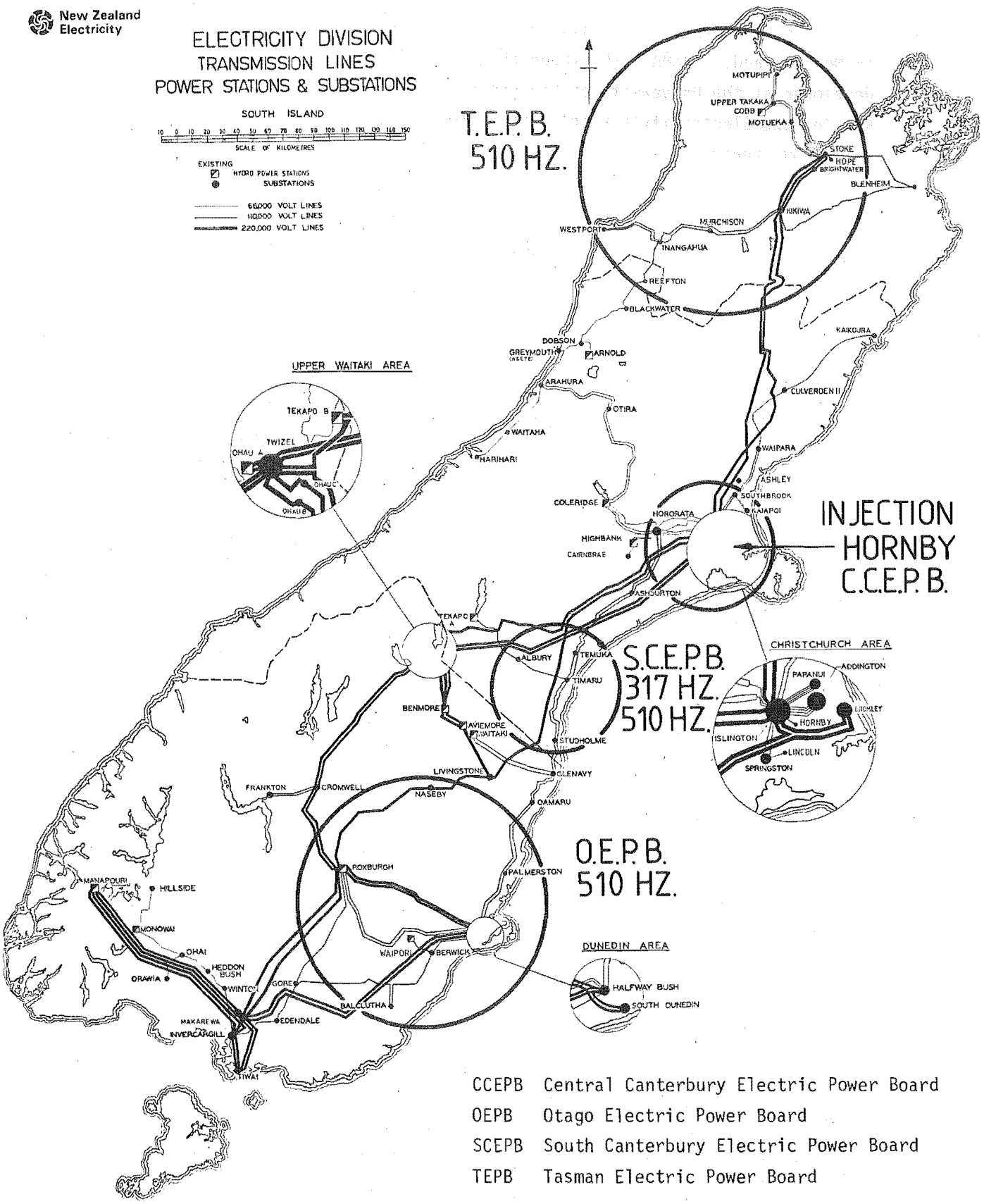

CCEPB Central Canterbury Electric Power Board
OEPB Otago Electric Power Board
SCEPB South Canterbury Electric Power Board
TEPB Tasman Electric Power Board

8.2 PROGRAM COMPARISON

Three different programs for harmonic penetration analysis exist in New Zealand; HARMAC, the three phase AC harmonic penetration program developed at the University of Canterbury (Densem et al 1983), ELAFANT, New Zealand Electricity's single phase program (Baird 1981), and AUDIOFLOW, Central Canterbury Electric Power Board's single phase program (Ross 1972). They are different software tools and Table 8.1 below indicates some of the main points.

TABLE 8.1: Features of the Three Harmonic Programs Available in New Zealand

HARMAC	ELAFANT	AUDIOFLOW
three phase	single phase	single phase
multiple frequencies	multiple frequencies	single frequency
multiple injections	single injection	multiple injections
line data independently calculated from tower and conductor geometry giving mutual coupling between phases and circuits	positive sequence line data in tabular form for each line calculated using geometric mean distances	positive sequence line data specified for a limited number of different line types

AUDIOFLOW is designed for distribution system ripple control studies. It has been used for transmission system studies but it has the following limitations:

- skin effect is not modelled.
- generators are not easily modelled. They are modelled as loads with a specified impedance at the ripple control frequency. This gives accurate results but the impedances need to be calculated by hand for each different frequency.
- line parameters are approximate. In New Zealand there are very few transmission lines that have the same geometry details and therefore a line type for almost each line is necessary. This is beyond the capabilities of the program at present and a number of line types approximately equal to 1/3 of the number of lines, is used. This assumption will be investigated to determine its accuracy.

ELAFANT is a flexible single phase program designed for transmission system studies. It has provision for skin effect modelling. The 50 Hz positive sequence line parameters are calculated using geometric mean distances and not from the self positive sequence quantities of a three phase program. The effect of this assumption will also be investigated.

HARMAC is a larger program and data preparation is an order of magnitude more complex. It is able to perform studies with unbalanced current injections. Skin effect is modelled and the coupling between phases and circuits accurately represented. The effects of multiple injection sources at different locations can also be determined.

While each program has been designed for different areas of investigation, all have the capability to model distributed parameter lines and other common components with balanced harmonic current injections. Using the same generator, transformer and load models, and with the same system configuration and balanced current injections, useful comparisons of the three programs can be made.

8.3 TEST SYSTEM

The full South Island network is used for the studies in this chapter. Details of the components and single line diagrams are included in Appendix 3.

The Central Canterbury Electric Power Board ripple injection is simulated with a steady state balanced injection of 50 Amps at 510 Hz, the present injection frequency, at the Hornby 33 kV busbar. This bus is not the point of supply and because of this the line between Hornby and the point of supply needs to be modelled, giving the configuration of Figure 8.3.

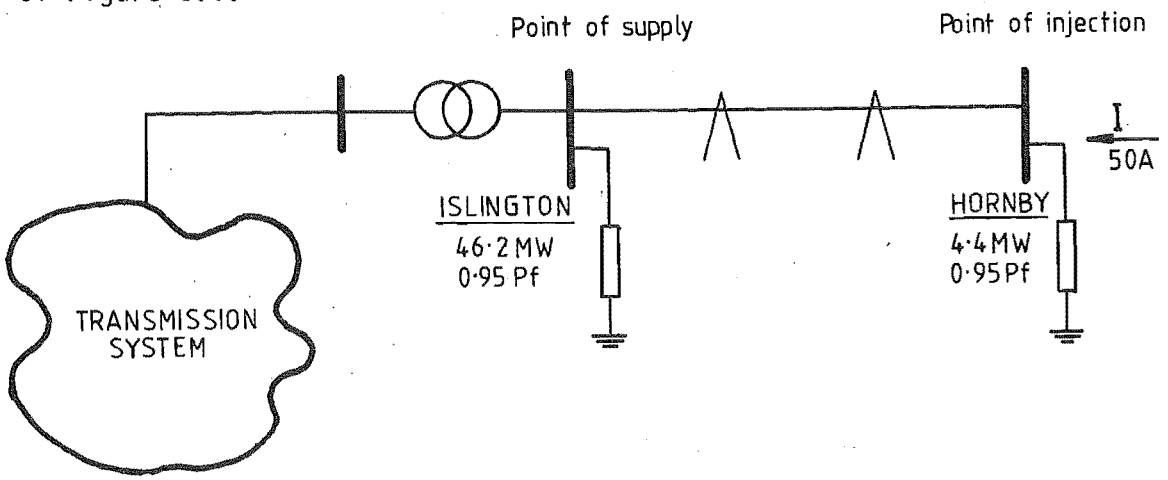

FIGURE 8.3: Central Canterbury Electric Power Board Ripple Control Injection at Hornby

Injections of 30 Amps at the Lincoln 33 kV bus and 10 Amps at the Hororata 33 kV bus are also used to simulate spillover from other Central Canterbury Electric Power Board injection equipment.

In 1985 Central Canterbury Electric Power Board is planning to reduce the ripple injection frequency to 317 Hz to give better coverage within their area. The difficulty in determining an accurate system configuration for 1985, and the wide variation of this configuration from hour to hour is resolved by using worst case conditions. These include:

- 20% of the maximum load at each busbar is used
- reduced generation approximating that of a typical summer evening is connected
- no synchronous condensors are modelled
- no shunt capacitors are modelled
- no filters are connected

Appendix 3 contains the relevant detail at individual busbars.

Models in this chapter use the same lettering references as Figure 7.2. The transformer and generator models chosen using the best fit to measured data in Chapter 7.3 have been retained. However, because of the inability to determine the scaling factor k in load model A, load model D was substituted. Results using these models and the system conditions above will be referred to as the standard case.

8.4 VOLTAGE SENSITIVITY TO INDIVIDUAL COMPONENT IMPEDANCES

8.4.1 Transformer Impedance Variation

In a similar manner to the previous chapter the sensitivity of system voltages to transformer impedance is obtained by reducing and increasing the impedances by 10%. In both cases of Figure 8.4 the average voltage varies by 4% and thus voltages are not sensitive to transformer impedance variation.

FIGURE 8.4: Percentage Voltage for Transformer Impedance Variation

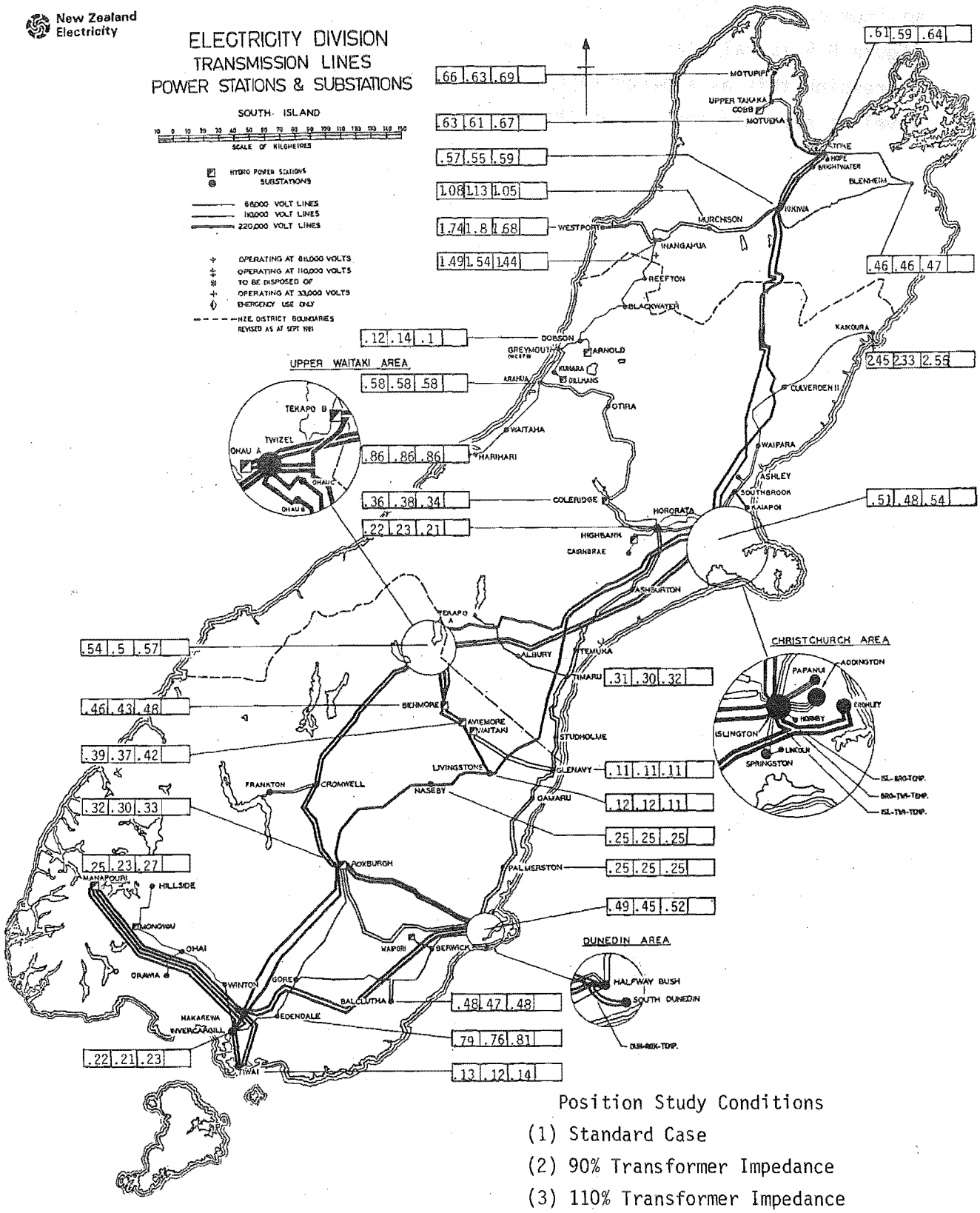

Position Study Conditions

(1) Standard Case

(2) 90% Transformer Impedance

(3) 110% Transformer Impedance

8.4.2 Generator Impedance Variation

Generator impedances are decreased and increased by 10% of the maximum capacity. The generation level of the standard case in Figure 8.5 is calculated by summing the connected generation and expressing this as a percentage of the maximum capacity. The generation level at each station is not the same.

Both increasing and decreasing impedances by 10% show the same average voltage variation, 4%.

This level indicates that detailed knowledge of connected generation is not necessary.

FIGURE 8.5: Percentage Voltage for Generator Impedance Variation

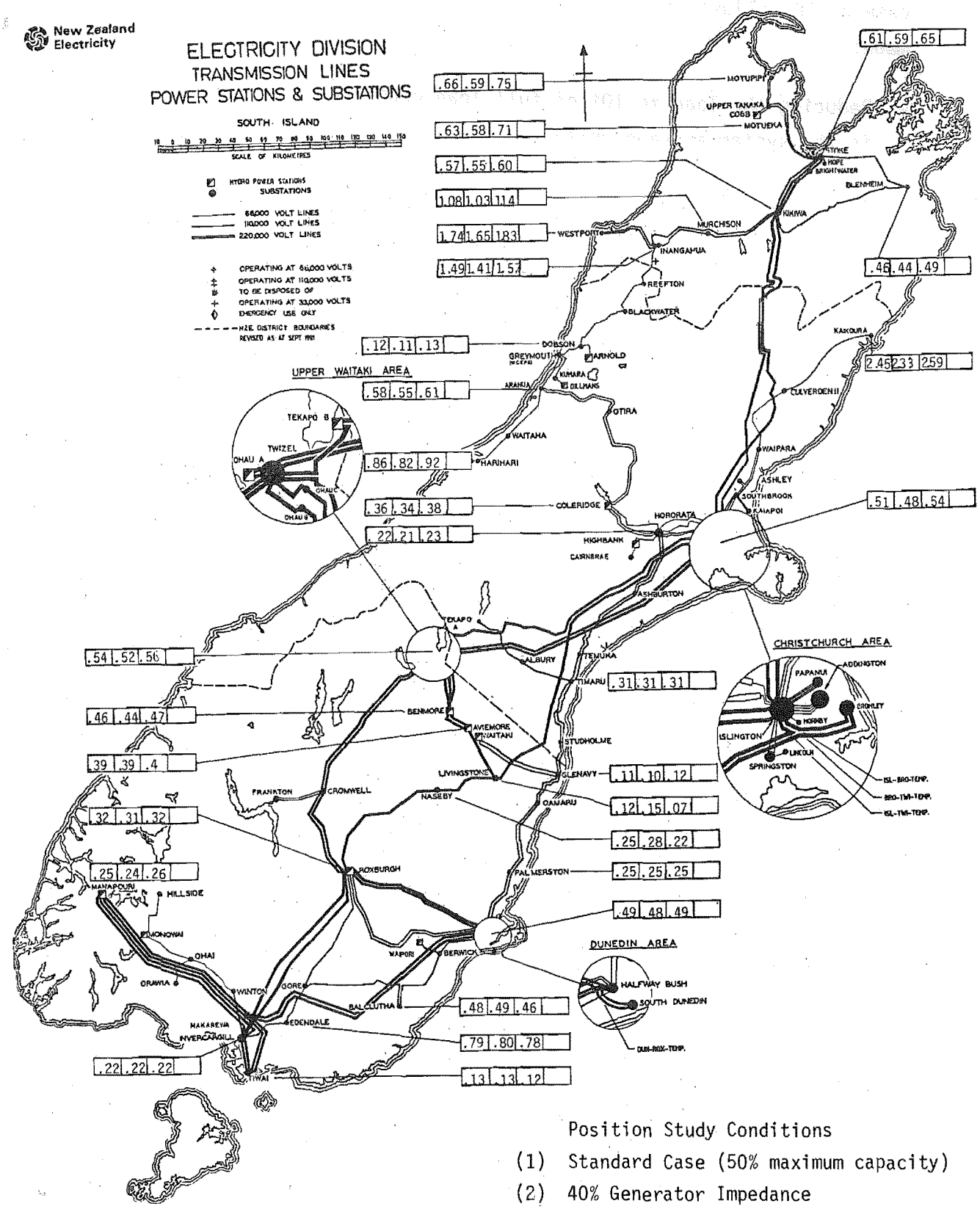

8.4.3 Load Level Variation

When the maximum load level is varied by 10%, from the standard case of 20% illustrated in Figure 8.6, the following observations are made:

- Reducing the load to 10% of full load caused a 30% increase in the system average voltage.
- Increasing the load to 30% of full load caused an 18% drop in the average voltage.

At low load, more accurate knowledge of the load level is required than under the high load conditions.

FIGURE 8.6: Percentage Voltage for Load Level Variation

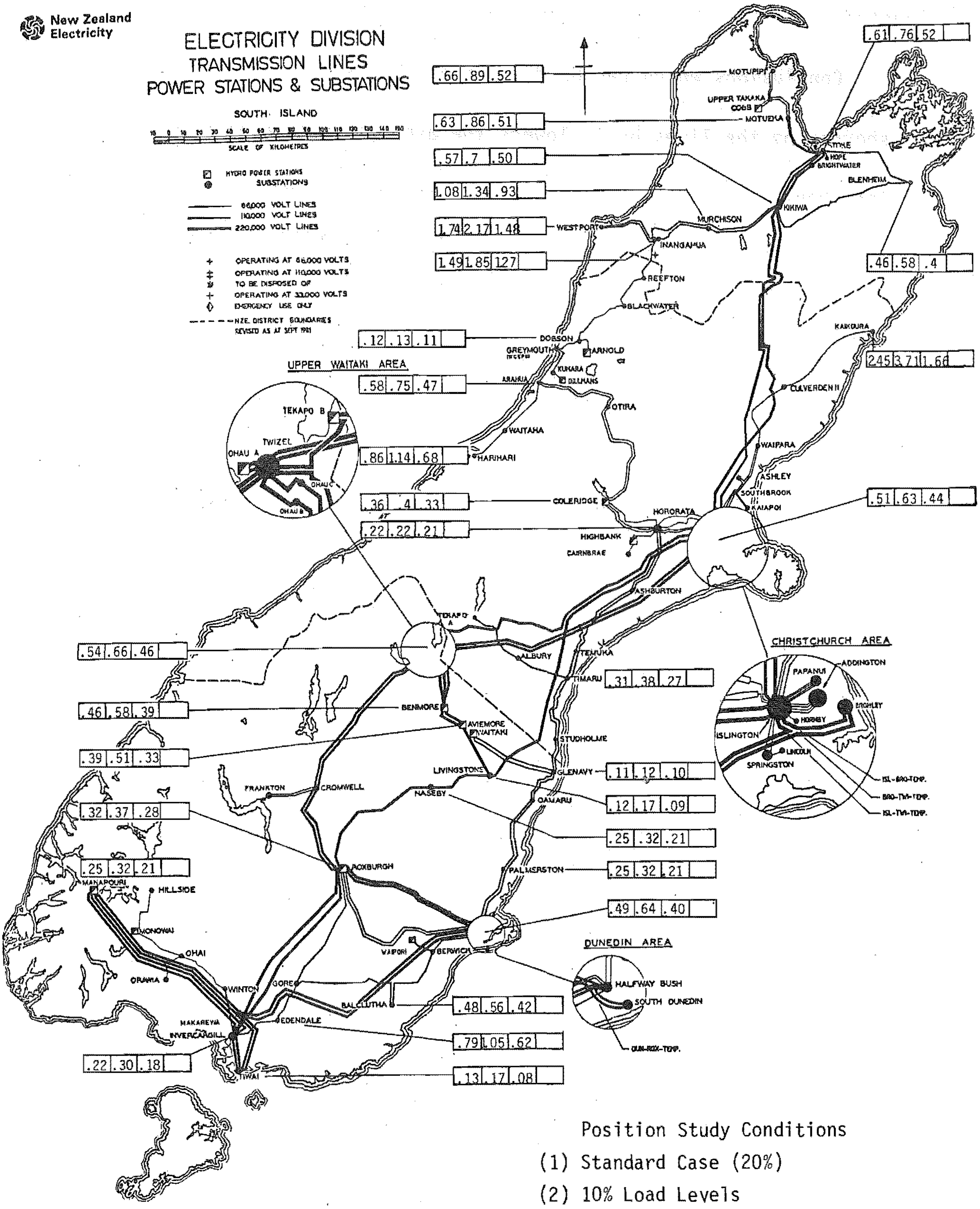

Position Study Conditions

(1) Standard Case (20%)

(2) 10% Load Levels

(3) 30% Load Levels

8.4.4 Line Parameter Variation

To vary the line parameters all lines are shortened and lengthened by 1%. Figure 8.7 shows the sensitivity of system voltages.

Conclusions which can be drawn from this are:

- shortening the lines by 1% lowers the average voltage by 5%.
- lengthening the lines by 1% increases the average voltage by 7%.

From the above observations the system voltages are more sensitive to line parameter variation than other component models, although the voltages are not as sensitive as the injection at Tiwai in Chapter 7.4.5. For this injection only transmission lines were connected to the Tiwai bus, whereas at Hornby considerable load is supplied from nearby buses. The system configuration near the point of injection affects the voltage sensitivity to component parameter variations.

FIGURE 8.7: Percentage Voltage for Line Length Variation

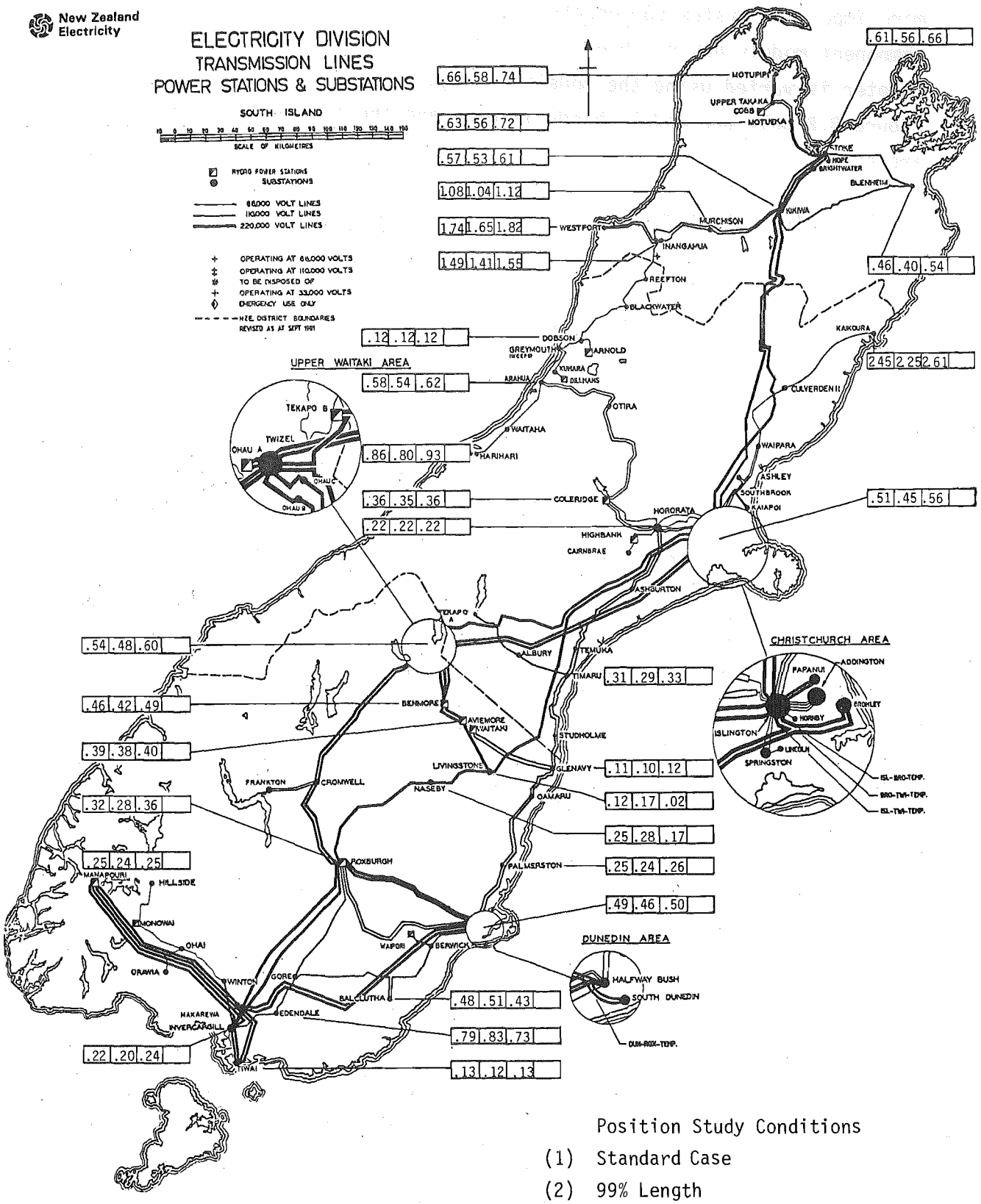

Position Study Conditions

(1) Standard Case

(2) 99% Length

(3) 101% Length

8.5 MODEL VARIATIONS

While impedance variations have been investigated indicating the more important system components, the effect on system voltages of the component models has not been determined. The standard case in this chapter is varied using the models of Figure 7.2. In each case of Figure 8.8 only one model change is made and the following conclusions are drawn:

- change to transformer model C with load and generator models unchanged, results in a decrease in the average voltage of 15%.

- transformer model E causes only small voltage variations, much the same as a 10% change in impedance.

- load model A causes a substantial drop in the average voltage of 25%.

- load model C causes an 8% increase in the average voltage.

- change to generator model B causes a 6% drop in the average voltage.

The above results indicate that there are considerable differences between the load and transformer models and further work is necessary to determine the best representations.

FIGURE 8.8(a): Percentage Voltage for Model Variation

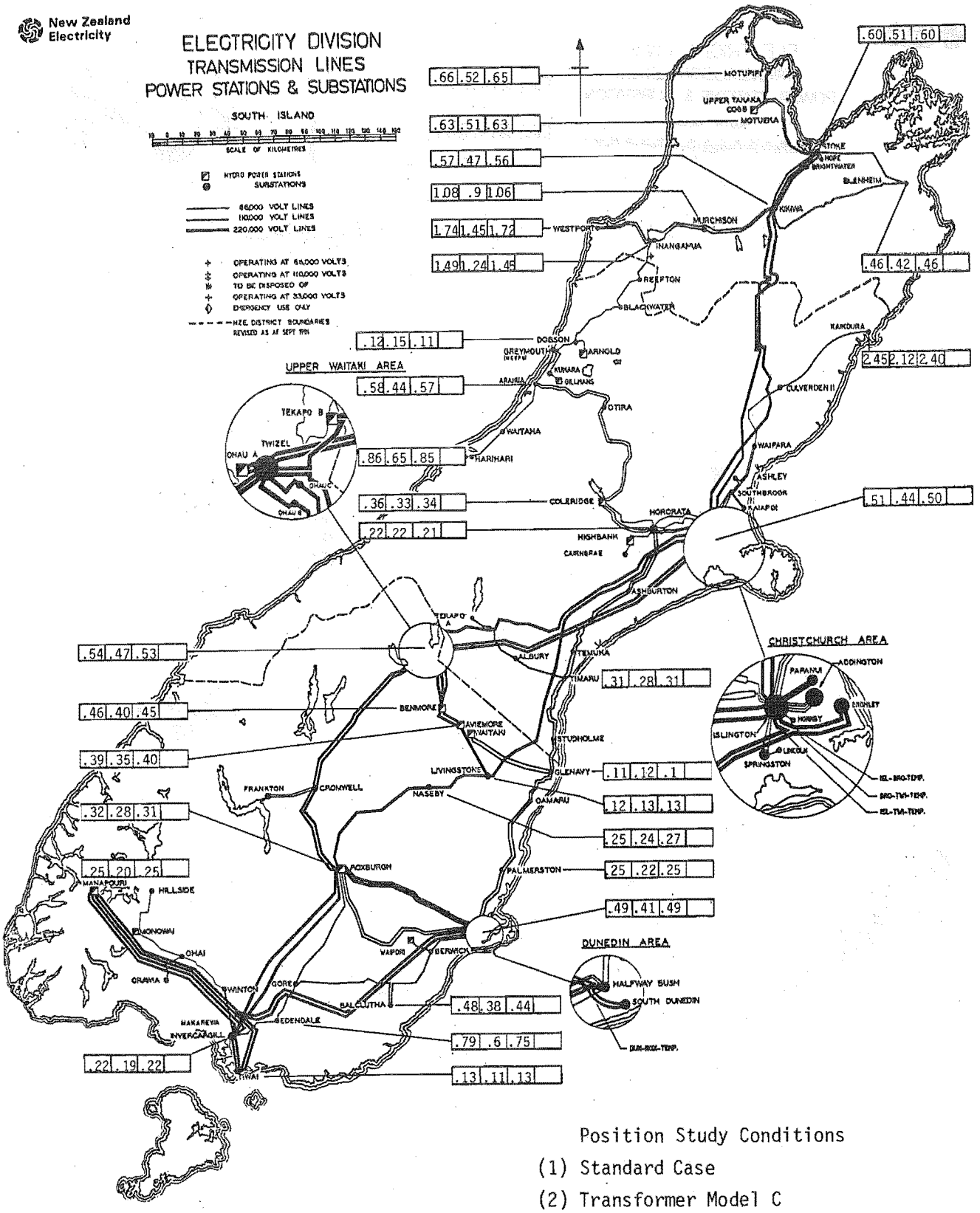

Position Study Conditions

(1) Standard Case

(2) Transformer Model C

(3) Transformer Model E

FIGURE 8.8(b): Percentage Voltage for Model Variation

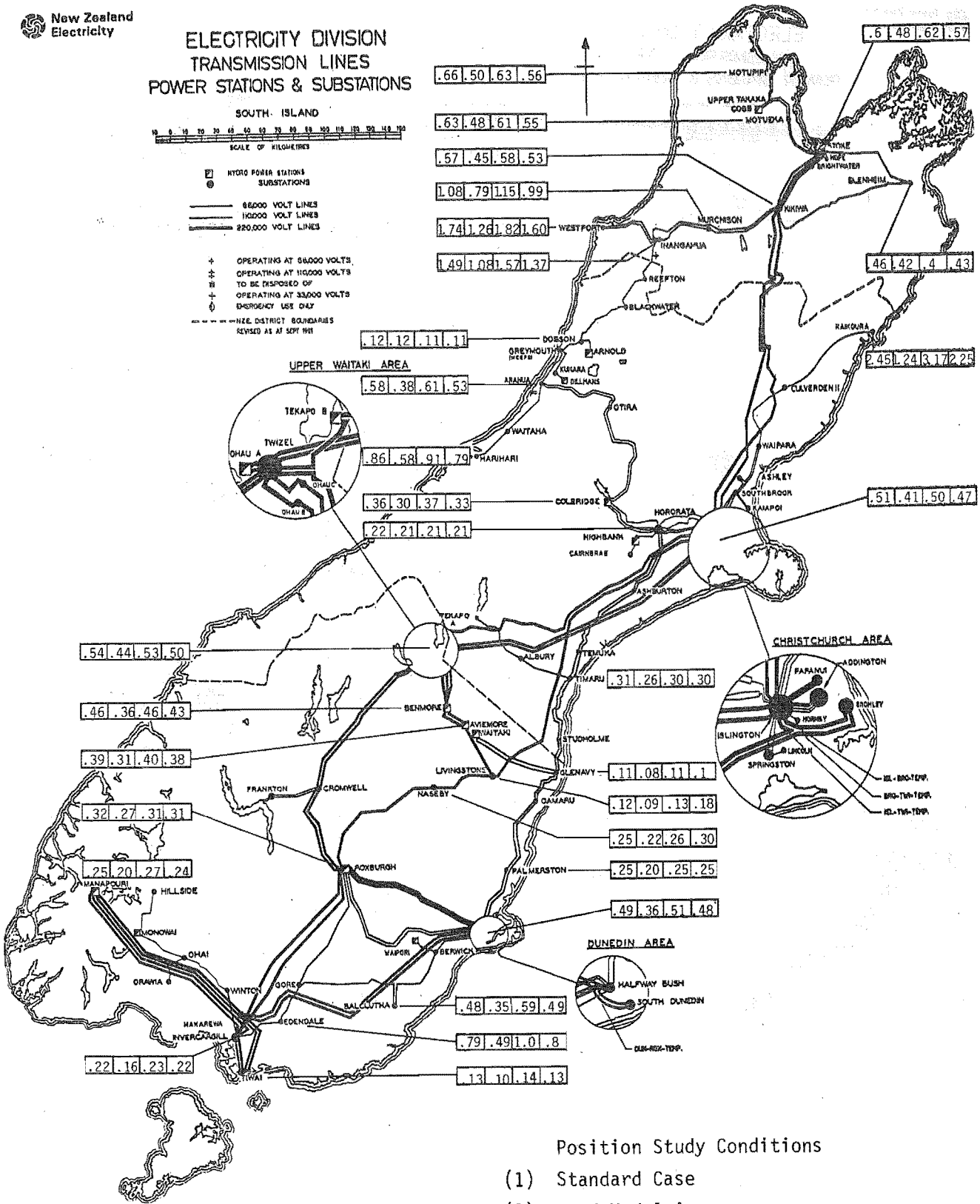

Position Study Conditions

(1) Standard Case

(2) Load Model A

(3) Load Model C

(4) Generator Model B

8.6 FILTERS AND SHUNT CAPACITORS

When the filters normally present at Tiwai are connected, very little change in system voltages are observed. However the filters at Benmore, position 3 Figure 8.9, lower the average voltage by 36%. When all the capacitor banks available are connected without the filters, the position 4 results show that the average voltage decreases from the standard case by 20%.

Neglecting filters and shunt capacitors substantially affects the voltage levels. The higher voltages without these elements represents the required worst case conditions for spillover studies.

FIGURE 8.9: Percentage Voltage due to Filters and Shunt Capacitors

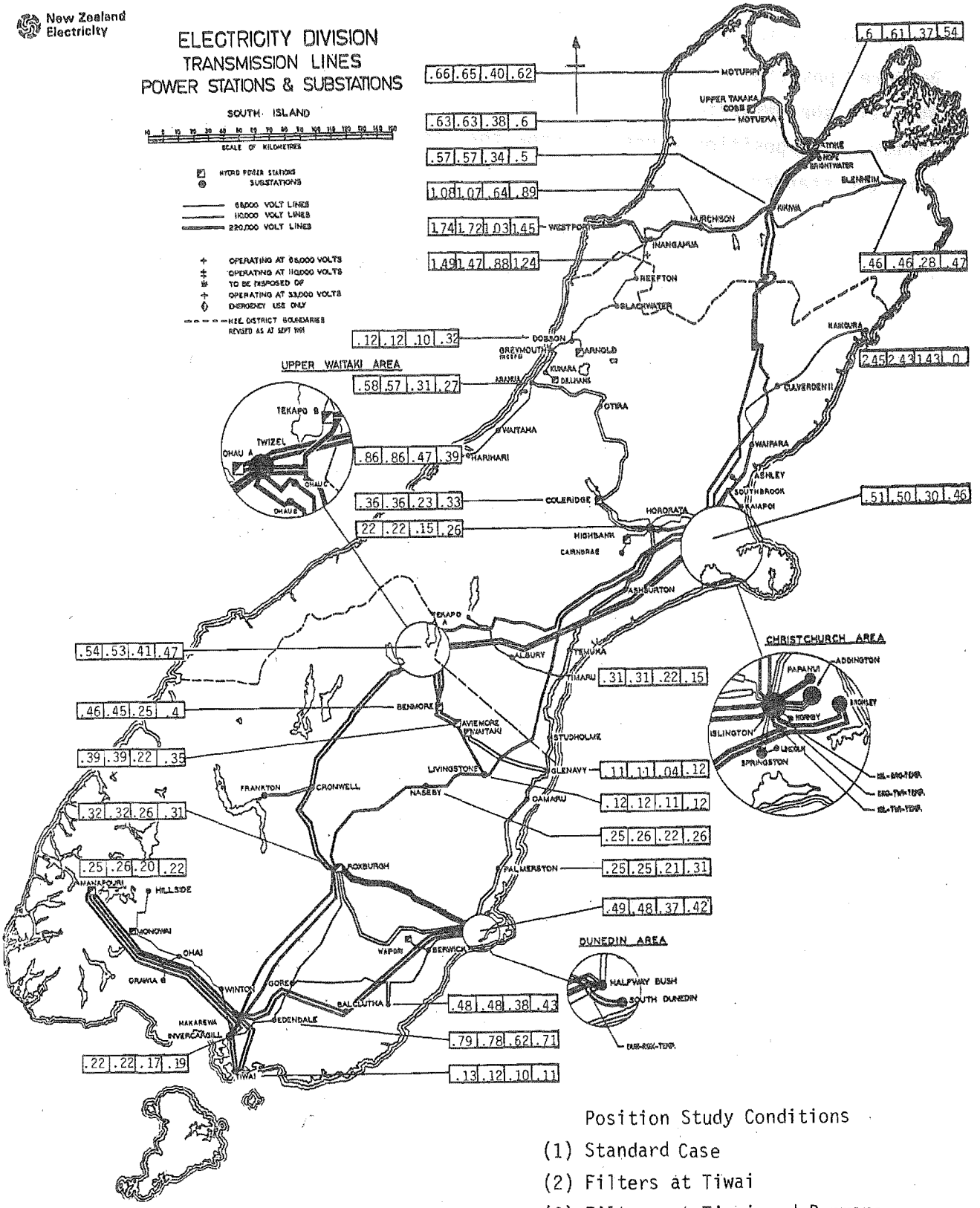

Position Study Conditions

(1) Standard Case

(2) Filters at Tiwai

(3) Filters at Tiwai and Benmore

(4) Shunt Capacitors Connected

8.7 SINGLE PHASE MODELLING

Single phase modelling has been duplicated in a similar manner to the previous chapter to determine if a different injection point affects system behaviour. The coupling between the sequence networks and circuits was removed for each line and the earth return connections set constant to the 50 Hz values. Figure 8.10 indicates that the positive sequence voltages are almost unaffected, the average voltage changes by only 1%, when single phase modelling is introduced. The coupling between sequence networks for this system and frequency is not significant. A single phase program could be used at this injection point for a balanced current injection, without undue inaccuracy.

The three programs previously described, ELAFANT, AUDIOFLOW and HARMAC, use different transmission line data. HARMAC uses three phase data obtained from individual conductor geometries, whereas ELAFANT inputs data comprising positive sequence parameters calculated using geometric mean distances. AUDIOFLOW uses similar data to ELAFANT except that not every line is given separate parameters. The effect of these approximations can be determined by comparing the three programs using the same component models, the same configuration and the same current injections. This is illustrated in Figure 8.11.

There is good agreement between the results from HARMAC and ELAFANT. Individual busbars show variations generally less than 10% and the average voltages are quite similar.

The position 3 voltages are calculated using AUDIOFLOW and the average voltage is 11% lower than HARMAC; not an unacceptable difference considering the uncertainty in planning studies.

The approximate line parameters used in ELAFANT and AUDIOFLOW are apparent, however, accurate studies require the use of three phase software.

FIGURE 8.10: Percentage Voltage Using Single Phase Modelling

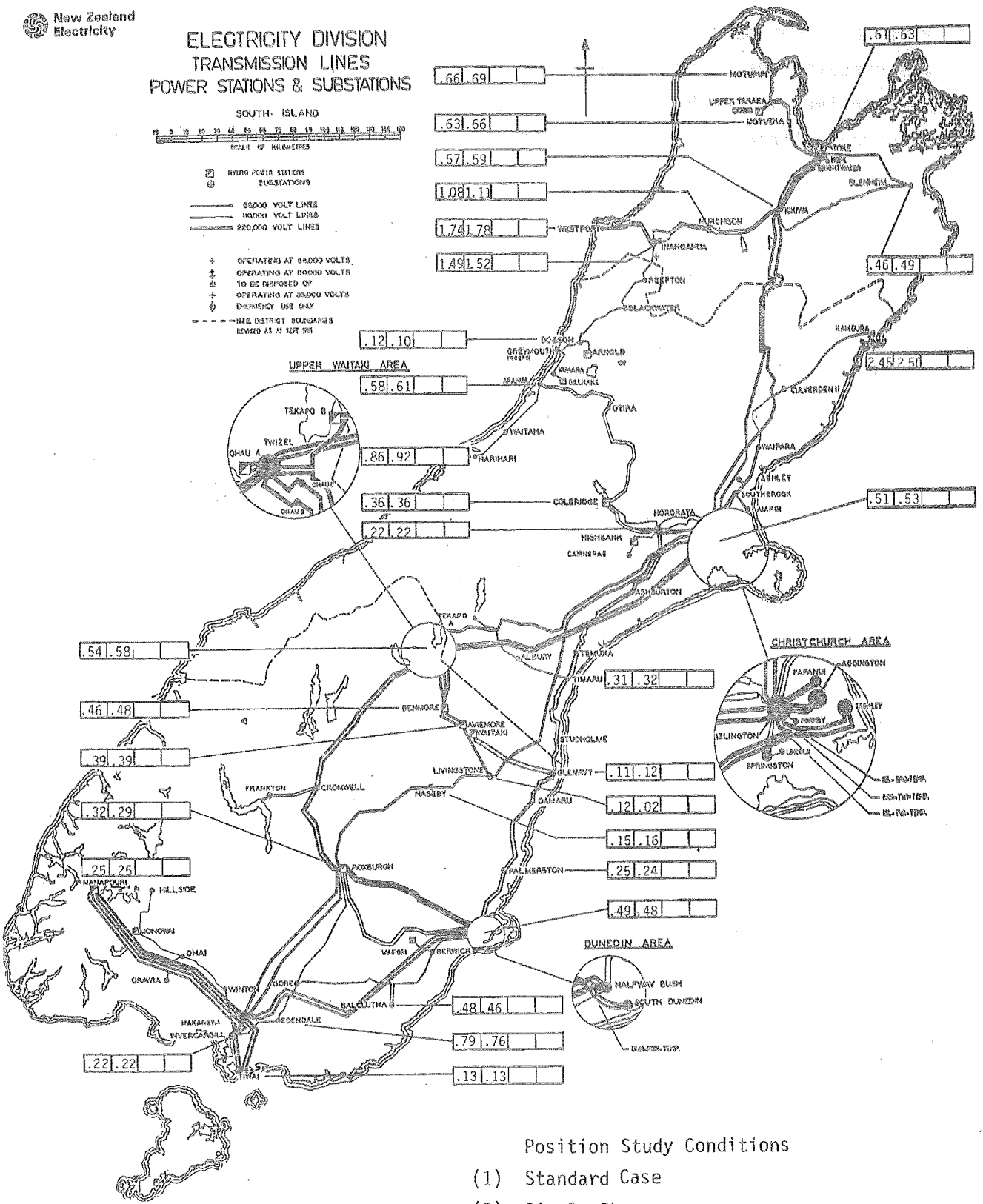

Position Study Conditions

(1) Standard Case

(2) Single Phase

FIGURE 8.11: Percentage Voltage using Three Different Harmonic Penetration Programs

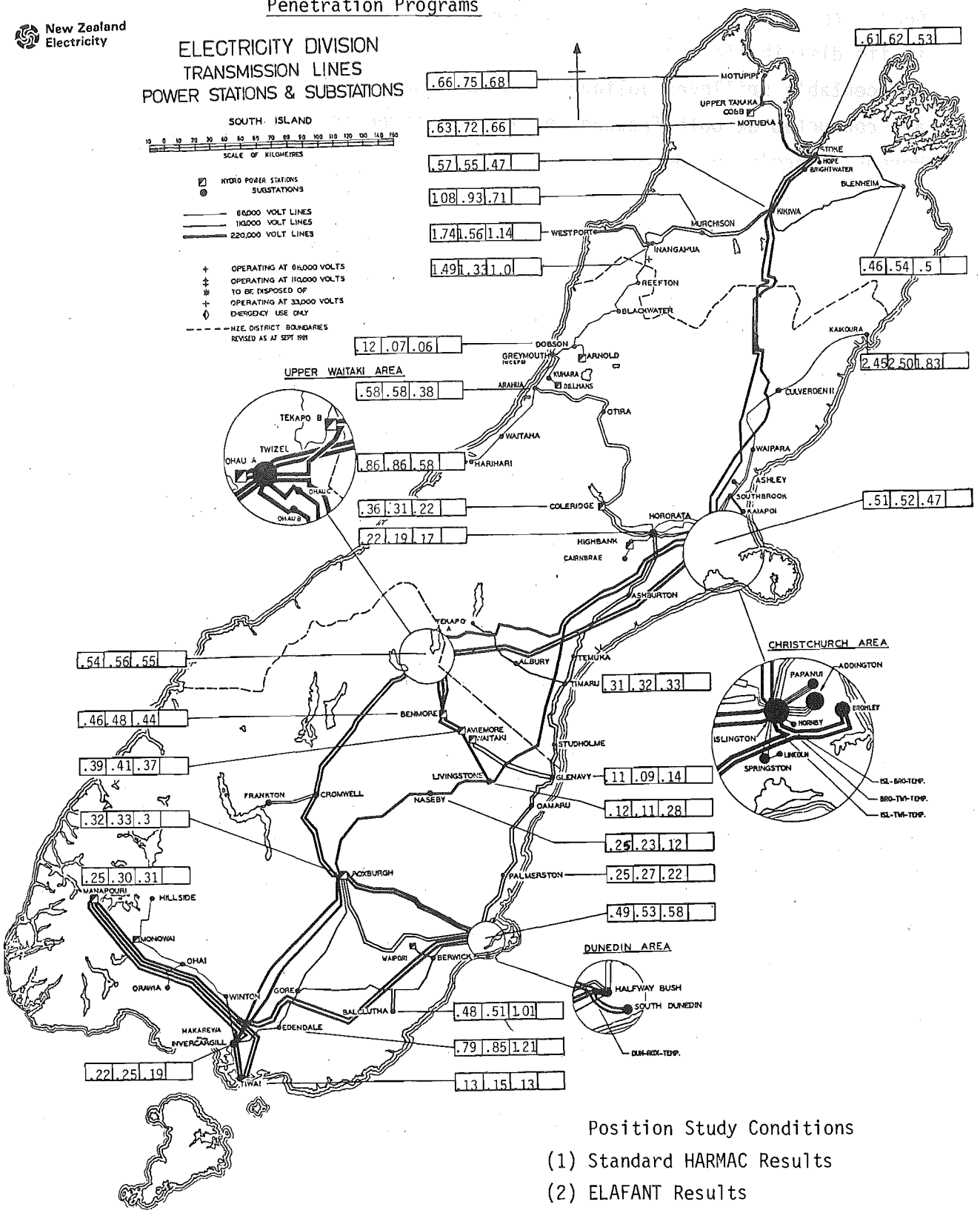

Position Study Conditions

(1) Standard HARMAC Results

(2) ELAFANT Results

(3) AUDIOFLOW Results

8.8 SPILLOVER VOLTAGES FOR DIFFERENT FREQUENCIES

The proposed frequency change by Central Canterbury Electric Power Board from 510 Hz to 317 Hz is designed to give better receiver levels in its distribution area. To know if the new frequency will cause unacceptable spillover voltages in other supply authority areas, studies are conducted at both frequencies for the three injection points at Hornby, Lincoln and Hororata.

At 510 Hz an injection from the Hornby and Lincoln plants causes unacceptable voltages (greater than .4%). The Lincoln plant interacts with Murchison while Hornby has unacceptable levels at Motueka, Murchison Stoke, Albany and Balclutha. There have been cases of spillover reported between Central Canterbury Electric Power Board and Murchison and Central Canterbury Electric Power Board and Naseby. Spillover has not been reported with the other areas.

This does not necessarily mean predicted spillover levels are inaccurate. The plant in each supply authority is designed with channel discrimination to enable increments of load to be switched. This discrimination also provides a degree of protection from the ripple signals of other authorities.

At the proposed frequency of 317 Hz injections at Hornby and Lincoln appear to give acceptable voltages in the South Canterbury area. Levels are approaching .4% however. At present this authority is the only other one with installed or planned 317 Hz plant. An injection at Hororata will cause spillover interaction at Albany, Studholm, Temuka and Timaru. This will require filtering at these busbars to avoid maloperation of relays.

TABLE 8.2: Spillover Voltage Levels for Central Canterbury Electric Power Board Injection Points at 510 Hz and 317 Hz (%)

	RECEPTION / INJECTION	KIKIWA 110	MOTUEKA 011	MURCHISON 011	STOKE 033	ALBURY 011	STUDHOLM 011	TEMUKA 011	TIMARU 011	BALCLUTHA 110	NASEBY 220	ISLINGTON 033	SPRINGSTON 033	HORORATA 033
510 Hz	HORNBY 033	.21	.59	1.04	.58	.42	.16	.30	.28	.48	.25	2.82	.34	.21
	LINCOLN 033	.14	.24	.50	.25	.28	.23	.16	.19	.17	.10	.20	4.02	.22
	HORORATA 033	.09	.08	.11	.03	.33	.39	.16	.22	.08	.09	.04	.07	2.79
317 Hz	HORNBY 033					.38	.32	.33	.32			1.47	.22	.19
	LINCOLN 033					.36	.28	.32	.31			.13	2.46	.25
	HORORATA 033					.88	.69	.77	.78			.04	.08	1.61

greater than .4% spillover interaction possible

8.9 CONCLUSIONS

Even if a simulation program could duplicate exactly the actual system voltages under known conditions, the variation in harmonic levels due to future system expansions is such that using a harmonic penetration model for planning purposes is difficult. Worst case analysis has been used including light load conditions with no capacitor compensation and filter plant disconnected.

As in the previous chapter system voltages are not sensitive to transformer and generator impedance variations. The connected capacity of these elements need not be known to the same accuracy as load levels and transmission line configuration. Load levels have been found more important in this chapter than in the test system of Chapter 7. This is due to the light load conditions and to the presence of considerable load at the injection bus and in close proximity to it.

Line parameter variation has a considerable but not unacceptable effect on system voltages. The data presently available is satisfactory. This is somewhat at variance with the conclusions of the previous chapter and is caused by the different characteristics of the system around the point of injection. Transmission line parameter modelling should be investigated at further injection locations to verify the accuracies possible.

Alternative component models have been demonstrated to have variable effects. Load and transformer models produce voltages that indicate more measurement and component model development is justified. Detailed measurements need to be made to determine the characteristics of rural systems with long distribution lines and ruban systems with high levels of underground cabling.

Ripple control uses balanced current injections and this chapter shows that a single phase model gives only small differences in voltages compared to those obtained using three phase software. Single phase modelling is thus an acceptable tool for spillover studies.

Results obtained for the Central Canterbury Electric Power Board injection at Hornby confirm some known spillover interactions and studies have been extended to a proposed frequency of 317 Hz. The need for filtering at the points of supply in the South Canterbury area to avoid spillover has been determined.

Measurement and comparison with simulated ripple control spillover levels needs to be performed. Measurement at distribution voltages levels is considerably simpler than at transmission voltages and the balanced nature of the harmonic injections at frequencies where there will only be one source provides an excellent opportunity to perform further program validation.

CHAPTER 9

CONCLUSIONS

The growth of system harmonic content due in particular, to the increased use of power electronic devices, has led to increasing concern among power engineers about the ability of a power system to function in the presence of the introduced distortion. Harmonic penetration modelling can play a vital role in the design of filter installations and convertor plant to minimize this distortion. A number of achievements towards this aim can be isolated from this thesis.

An algorithm for three phase harmonic studies including system and static convertor interaction has been developed. Problems including the quantity of data and presentation of results have been overcome.

A mathematical model for the assessment of harmonic penetration along three phase transmission lines and its application to the flow of zero sequence harmonic currents has been investigated. In particular the effects of transformer connection and filters on the harmonic levels along a transmission linehave been illustrated.

Three phase software has been developed capable of handling large systems for harmonic penetration studies. This software permits the calculation of unbalanced impedances, currents, and voltages at any frequency, not just characteristic harmonics orders. This is very useful for observing system behaviour at resonances and allows the different resonant frequencies of each phase to be isolated.

System component data for a sizable system has been assembled. This data has been used to compare measured and simulated harmonic levels for near balanced conditions with good agreement at a number of measurement locations and frequencies.

The effect of system component impedances on harmonic levels has been determined. Some uncertainty in the levels or accuracy of transformer, generator and load data can be tolerated but the accuracy of transmission line data at resonant frequencies, and particularly in rugged terrain, needs to be high.

The sensitivity of system voltage to individual component models has been calculated to determine the degree of representation required in each case.

Spillover voltage levels and interference with load management equipment is of real concern to the New Zealand Supply Authorities. Single phase modelling has been found satisfactory for such studies where balanced harmonic currents are injected and uncertain planning conditions exist. With the accurate three phase model developed the situations in which simplifying assumptions are valid have been determined.

Future endeavour can be focussed on the interaction of convertors connected to separate AC system busbars, and the effect of harmonics on the fundamental frequency operating state of such convertors. This is particularly important as the number of systems with multiple static convertor loads is rapidly increasing.

REFERENCES

Abramovich, B.J., Brewer, G.L., and Welch, I.M. (1982). "Cross Channel Power Link. Harmonic Filters for the Sellindge Converter Station", GEC Journal of Science and Technology, Vol. 48, No. 1, pp 35-38.

Abramowitz, M. and Stegun, I.A. (1968). "A Handbook of Mathematical Functions", Dover.

Adielson, T., Carlson, A., Margolis, H.B., and Halladay, J.A. (1981). "Resonant Overvoltages in EHV Transformer Modelling and Application", IEEE Trans., PAS-100, No. 7, pp 3563-3571.

Ainsworth, J.D. (1967). "Harmonic Instability Between Controlled Static Convertors and A.C. Networks", Proc. IEE, Vol. 114, No. 7, pp 949-957.

Alvarado, F.L. (1982). "Formation of Y-node Using the Primitive Y-node Concept", IEEE Trans., PAS-101, No. 12, pp 4563-4571.

Arrillaga, J. and Harker, B.J. (1978). "Fast Decoupled Three Phase Load Flow", Proc. IEE, Vol. 125, No. 8, pp 734-740.

Arrillaga, J. (1981). "Harmonic Elimination", International Conference on Harmonics in Power Systems, University of Manchester Institute of Science and Technology, pp 37-75.

Arrillaga, J. (1983). "High Voltage Direct Current Transmission", IEE Power Engineering Series 6, Peter Peregrinus.

Arrillaga, J., Arnold, C.P. and Harker, B.J. (1983a). "Computer Modelling of Electrical Power Systems", John Wiley.

Arrillaga, J., Densem, T.J. and Harker, B.J. (1983b). "Zero Sequence Harmonic Current Generation in Transmission Lines Connected to Large Convertor Plant", IEEE Trans., PAS-102, No. 7, pp 2357-2363.

Arseneau, R., Hill, E.F., Szabados, B. and Perry, D. (1979). "Synchronous Motor Impedances Measured at Harmonic Frequencies", IEEE Power Engineering Society Summer Meeting, Vancouver, Paper No. A79514-1.

Avila-Rosales, J. and Alvarado, F.L. (1982). "Nonlinear Frequency Dependent Transformer Model for Electromagnetic Transient Studies in Power Systems", IEEE Trans., PAS-101, No. 11, pp 4281-88.

Baggott, A.J. (1974). "The Effect of Waveshape Distortions on the Measurement of Energy by Tariff Meters", Conference on Sources and Effects of Power System Disturbances, IEE No. 110, pp 46-51.

Baird, J. (1981). "ELAFANT - Audio Frequency Analysis of a Power System", New Zealand Electricity.

Baker, W.P. (1981). "Measured Impedances of Power Systems", International Conference on Harmonics in Power Systems, University of Manchester Institute of Science and Technology, pp 141-158.

Barnes, H. and Kearley, S. (1981). "The Measurement of the Impedance Presented to Harmonic Current by Power Distribution Networks", CIRED International Conference on Electricity Distribution, IEE No. 197, pp 71-80.

Blommaent, J., De Vre, R. and Kniel, R. (1977). "Analysis of the Harmonics in Low Voltage Distribution Networks", CIRED International Conference on Electricity Distribution, IEE No. 151, pp 8-12.

Bowles, J.P. (1970). "A.C. System and Transformer Representation for H.V.-D.C. Transmission Studies", IEEE Trans., PAS-89, No. 7, pp 1603-1609.

Bowman, W.I. and McNamee, J.M. (1964). "Development of Equivalent Pi and T matrix Circuits for Long Untransposed Transmission Lines", IEEE Trans., PAS-84, pp 625-632.

Brameller, A., John, M.N, and Scott, M.R. (1969). "Practical Diakoptics for Electrical Networks", Chapman and Hall.

Brandwajn, V., Dommel, H.W. and Dommel, I.I. (1982). "Matrix Representation of Three Phase N-winding Transformers for Steady State and Transient Studies", IEEE Trans., PAS-101, No. 6, pp 1369-1378.

Breuer, G.D., Chow, J.A., Gentile, T.J., Lindh, C.B., Numrich, F.H., Lasseter, R.H., Addis, G. and Vithayathil, J.J. (1982). "HVDC-AC Harmonic Interaction, Parts I and II", IEEE Trans., PAS-101, No. 3, pp 701-718.

Breuer, G.D. (1983). "AC Filter Design Considerations", Panel Session on HVDC Convertor Station Design and Procurement Methods", IEEE Power Engineering Society Summer Meeting.

Brewer, G.L., Coates, R. and Clarke, C.D. (1974). "Initial Operating Experience with the Filters for the Kingsnorth D.C. Scheme", Conference on Sources and Effects of Power System Disturbances, IEE No. 110, pp 156-161.

Campbell, L.C. and Murray, N.S. (1970). "Harmonic Penetration into Power Systems", 5th Universities Power Engineering Conference, Swansea, Wales.

Carroll, D.P., Gareis, G.E., Ong, C.M. and Wood, P. (1977). "The Interaction of Batteries and Fuel Cells with Electrical Distribution Systems: Line Commutated Convertor Interface", IEEE Trans., PAS-96, pp 1202-1210.

Carson, J.R. (1926). "Wave Propagation in Overhead Wires with Ground Return", Bell Systems Technical Journal, Vol. 5, pp 539-54.

Chipman, R.A. (1968). "Theory and Problems of Transmission Lines", Schaums Outline Series, McGraw-Hill.

Clarke, E. (1943). "Circuit Analysis of AC Power Systems", John Wiley, New York.

Clarke, C.D. (1973). Discussion on Northcote-Green et al (1973a), High Voltage DC and/or AC Power Transmission, IEE No. 107, pp 100.

Coleman, D., Watts, F. and Shipley, R.B. (1958). "Digital Calculation of Overhead Transmission Line Constants", AIEE Trans., Vol. 77, pp 1266-68.

Comellini, E., Invernizzi, A. and Manzoni, G. (1972). "A Computer Program for Determining Electrical Resistance and Reactance of any Transmission Line", IEEE Trans., PAS-92, pp 308-314.

Concordia and Ihara (1982). "Load Representation in Power System Stability Studies", IEEE Trans., PAS-101, No. 4, pp 969-975.

Crevier, D. and Mercier, A. (1978). "Estimation of Higher Frequency Network Equivalent Impedances by Harmonic Analysis of Natural Waveforms", IEEE Trans., PAS-97, pp 424-431.

Degeneff, R.C., Neugebauer, W., Honey, C.C., McNutt, W.J., Panek, J. and McCallum, M.E. (1982). "Transformer Response to System Switching Voltages", IEEE Trans., PAS-101 No. 6, pp 1457-1470.

Densem, T.J., Bodger, P.S. and Arrillaga, J. (1983). "Three Phase Transmission System Modelling for Harmonic Penetration Studies", IEEE Power Engineering Society Summer Meeting, Los Angeles, Paper No. 83SM444-7.

Dillon, W.E. and Chen, M.S. (1972). "Transformer Modelling in Unbalanced Three Phase Networks", IEEE Power Engineering Society Summer Power Meeting, Vancouver, Paper No. C72 460-4.

Easton, V. (1966). "Turbo-Generator Operational Parameters on Rectifier Loads", Conference on High Voltage DC Transmission, IEE No. 22, pp 453-454.

Edison Electric Institute (1968). "EHV Transmission Line Reference Book", Edison Electric Institute, New York.

Edward, L.N.M., Arrillaga, J., Ross, N.W. and Baird, J.F. (1981). "Harmonic Measurement and the Selective Audio Frequency Power Analyser", CIRED, International Conference on Electricity Distribution, IEE No. 197, pp 81-85.

Elgerd, O. (1971). "Electric Energy Systems Theory: An Introduction", McGraw-Hill.

Evers, H.W. (1980). "Mains Pollution Caused by Domestic Appliances", Electronic Components and Applications, Vol. 2, No. 2, pp 83-96.

Frosch, S. and Schultz, W. (1978). "Digital Calculation of the Harmonic Load in Power Systems and Equipment", Siemens Review, XLV No. 6.

Galloway, R.H., Shorrocks, W.B., and Wedepohl, L.M. (1964). "Calculation of Electrical Parameters for Short and Long Polyphase Transmission Lines", Proc. IEE, Vol. III, No. 12, pp 2051-2059.

Gates, T.E. (1979). "A Case of Power System Harmonic Problems from Thyristor Drives", IEEE Conference Record, Paper No. PCI-79-6.

Gellen, S. (1982). "A Graphics Software Package for Harmonic Analysis", Final Year Project Report, Electrical and Electronic Engineering, University of Canterbury.

Gunn, H.R. (1966). "Commissioning and Early Operating Experience with the New Zealand Inter-Island Transmission Scheme", Conference on High Voltage D.C. Transmission, IEE No. 22, pp 30-38.

Harker, B.J. and Arrillaga, J. (1979). "Three Phase ac/dc Load Flow", Proc. IEE Vol. 126, No. 12, pp 1275-1281.

Harker, B.J. (1980). "Steady State Analysis of Integrated a.c. and d.c. Systems", Ph.D. Thesis, University of Canterbury, New Zealand.

Hesse, M.H. (1963). "Electromagnetic and Electrostatic Transmission Line Parameters by Digital Computer", Trans. IEEE, Vol. PAS-82, pp 282-291.

Hesse, M.H. (1966). "Circulating Currents in Parallel Untransposed Multicircuit Lines: I - Numerical Evaluations", IEEE Trans., PAS-85, pp 802-811.

Howroyd, D.C. (1977). "Public-Supply-System Distortion and Unbalance from Single-Phase AC Traction", Proc. Vol. 124, No. 10, pp 853-859.

Huddart, K.W. and Brewer, G.L. (1966). "Factors Influencing the Harmonic Impedance of a Power System", Conference on High Voltage DC Transmission, IEE No. 22, pp 450-452.

Hyland, P.R. (1981). "Report on Harmonics Test Conducted on July 8, 1981", New Zealand Electricity.

IEEE Power Systems Relaying Committee Working Group (1981). "EHV Protection Problems", IEEE Trans., PAS-100 No. 5, pp 2399-2406.

Jarrett, G.S.H. and Csuros, L. (1966). "The Performance of the Lydd Convertor of the Cross-Channel Connection", Conference of High Voltage D.C. Transmission, IEE No. 22, pp 17-20.

Kaban, I.H. and Parten, J.E. (1970). "Computation of the Flow of Harmonic Currents in Networks", 5th Universities Power Engineering Conference, Swansea, Wales.

Kauferle, J., Mey, R. and Rogowsky, Y. (1970). "HVDC Stations Connected to Weak AC Systems", IEEE Trans., PAS-89, No. 7, pp 1610-1617.

Kendall and Johnson (1977). "Limits for Harmonic Distortion in the U.K. Electricity Supply System", IEE No. 154, pp 174-178.

Kennelly, A.E., Laws, F.A. and Pierce, P.H. (1915). "Experimental Researches on Skin Effect in Conduction", AIEE Trans. Vol. 34, pp 1953-2018.

Kidd, W.I. and Duke, K.J. (1974). "Harmonic Voltage Distortion and Harmonic Currents in the British Distribution Network, Their Effects and Limitation", Conference on Sources and Effects of Power System Disturbances, IEE No. 110, pp 228-233.

Kimbark, E.W. (1950). "Electrical Transmission of Power and Signals", John Wiley, New York.

King, S.Y. (1970). "Electromagnetic Characteristics of Isolated Bundle Conductors", Proc. IEE, Vol. 117, No. 4, pp 753-60.

Kitchin, R.H. (1981). "New Method for Digital-Computer Evaluation of Convertor Harmonics in Power Systems Using State Variable Analysis", Proc. IEE, Vol. 128, Pt C No. 4, pp 196-207.

Klewe, H.R.J. (1958). "Interference Between Power Systems and Telecommunication Lines", Arnold, London.

Klingshirn, E.A. and Jordan, H.E. (1968). "Polyphase Induction Motor Performance and Losses on Non-sinusoidal Voltage Sources", IEEE Trans., PAS-87, No. 3, pp 624-631.

Kron, G. (1965). "Tensor Analysis of Networks", MacDonald, London.

Kuussaari, M., and Pesonen, A.J. (1976). "Measured Power-Line Harmonic Currents and Induced Telephone Noise Interference with Special Reference to Statistical Approach", CIGRE International Conference on Large High Voltage Electric Systems, Paris.

Laughton, M.A. (1968). "Analysis of Unbalanced Polyphase Networks by the Method of Phase Coordinates. Part I. System Representation in Phase Frame of Reference", Proc. IEE, Vol. 115, No. 8, pp 1163-1172.

Laurent, P.G., Gary, C. and Clade, J. (1962). "D.C. Interconnection Between France and Great Britain by Submarine Cables", Cigre, V. III, Paper No. 331.

Lewis, V.A. and Tuttle, P.D. (1958). "The Resistance and Reactance of Aluminium Conductors Steel Reinforced", AIEE Trans., PAS-77, pp 1189-1215.

Littler, G.E. (1977). "Power Transformer Delta Tertiary Windings and Their Influence on Telephone Line Induction", The Institution of Engineers Australia, Electrical Engineering Transactions, pp 31-37.

Littler, G.E. (1982). "The Effects of Thyristor Drive Harmonics in an Electrical Power System", Journal of Electrical and Electronics Engineering, Australia, Vol. 2, No. 4, pp 220-227.

Lopez, J.P., Mate, L.A. and Talukdar, S.N. (1977). "A Digital Method for Steady State Harmonic Analysis", CIRED International Conference on Electricity Distribution, IEE No. 151, pp 1-4.

Mahmoud, A.A. and Shultz, R.D. (1982). "A Method for Analyzing Harmonic Distribution in a.c. Power Systems", IEEE Trans., PAS-101, No. 6, pp 1815-1824.

McGranaghan, M.F., Dugan, R.C. and Spongler, W.L. (1981). "Digital Simulation of Distribution System Frequency-Response Characteristics", IEEE Trans., PAS-100, No. 3, pp 1362-1369.

McGranaghan, M.F. (1983). Discussion of Densem et al (1983), IEEE Power Engineering Society Winter Meeting.

Melvold, D.J. (1972). "Pacific HVDC Intertie System AC Side Harmonic Studies", IEE Power Engineering Society Summer Meeting, San Francisco, Paper No. T72523-9, pp 690-701.

Meyer, W.S. and Dommel, H.W. (1969). "Telephone-Interference Calculation for Multiconductor Power Lines", IEEE Trans., PAS-88, No. 1, pp 35-41.

New Zealand Electricity (1970). Dunedin District Test Report, 1021.

New Zealand Electricity (1983). "Limitation of Harmonic Levels", Issue 2.

Northcote-Green, J.E.D., Baron, J.A. and Vilks, P. (1973a). "The Computation of Impedance Frequency Loci and Harmonic Current Penetration for AC Systems Adjacent to HVDC Conversion Equipment", Conference on High Voltage DC and/or AC Power Transmission, IEE No. 107, pp 97-102.

Northcote-Green, J.E.D., Baron, J.A. and Vilks, P. (1973b). Reply to Northcote-Green et al 1973(a). Conference on High Voltage DC and/or AC Power Transmission, IEE No. 107, pp 102-103.

Orr, J.A., Emanuel, A.E., and Pileggi, D.G. (1982). "Current Harmonics, Voltage Distortion, and Power Associated with Battery Chargers", IEEE Trans., PAS-101, No. 8, pp 2703-2710.

Owen, R.E., McGranaghan, M.F., King, J.M., Vivirito, J.R. and Vincent, W.R. (1980). "Study of Distribution System Surge and Harmonic Characteristics", Final Report of EPRI Research Program 1024-1, McGraw-Edison Company.

Pesonen, M.A. (1981). "Harmonics, Characteristic Parameters, Methods of Study, Estimates of Existing Values in the Network", ELECTRA, ~~Vol.~~ no. 77, pp 35-54.

Phadke, A.G. and Harlow, J.H. (1966). "Unbalanced Convertor Operation", IEEE Trans., PAS-85, pp 233-239.

Phadke, A.G. and Harlow, J.H. (1968). "Generation of Abnormal Harmonics in High Voltage AC-DC Power Systems", IEEE Trans., PAS-87, No. 3, pp 873-882.

Pileggi, D.J., Chandra, N.H. and Emanuel, A.E. (1981). "Prediction of Harmonic Voltages in Distribution Systems", IEEE Trans., PAS-100, No. 3, pp 1307-1315.

Pileggi, D.J. and Emanuel, A.E. (1982). "Field Experience with Harmonics Injecting Equipment in Distribution Networks", IEEE PAS-101, No. 8, pp 2790-2798.

Reeve, J., and Krishnayya, P.C.S. (1968). "Unusual Current Harmonics Arising from High Voltage d.c. Transmission", IEEE Trans., PAS-87, No. 3, pp 883-893.

Reeve, J. and Baron, J.A. (1970). "Harmonic Interaction Between HVDC Converters and AC Power Systems", IEEE Power Engineering Society Winter Power Meeting, New York, Paper No. 71TP180-PWR, pp. 2785-2793.

Reeve, J., Baron, J.A. and Krishnayya, P.C.S. (1969). "A General Approach to Harmonic Current Generation by H.V.D.C. Convertors", IEEE Trans., PAS-88, No. 7, pp 989-995.

Robinson, G.H. (1966). "Harmonic Phenomena Associated with the Benmore-Haywards hvdc Transmission Scheme", New Zealand Engineering, 21(1), pp 16-29.

Roper, R.D. and Leedham, P.J. (1974). "A Review of the Causes and Effects of Distribution System Three-Phase Unbalance", Conference on Sources and Effects of Power System Disturbances, IEE No. 110, London, pp 83-92.

Ross, T.W. and Smith, R.M.A. (1948). "Centralised Ripple Control on High Voltage Networks", Proc. IEE, Vol. 95, Part II, pp 470-479.

Ross, N.W. (1972). "Modelling a Ripple Control System", The New Zealand Electrical Journal, pp 116-123.

Shipley, R.B., Coleman, D.W. and Holley, H.J. (1964). "Power Circuit Representation for Digital Studies", AIEE Trans., pp 376-380.

Silvester, P. (1969). "Impedance of Nonmagnetic Overhead Power Transmission Conductors", IEEE Trans., PAS-88, No. 5, pp 731-737.

Steeper, D.E. and Stratford, R.P. (1976). "Reactive Compensation and Harmonic Suppression for Industrial Power Systems using Thyristor Convertors", IEEE Trans. on Industrial Applications, Vol. IA-12 No. 3, pp 232-254.

Szabados, B. and Lee, J. (1981). "Harmonic Impedance Measurements on Transformers", IEEE Trans., PAS-100, No. 12, pp 5020-5026.

Szabados, B. (1982). "On the Interaction Between Power System Configuration and Industrial Rectifier Harmonic Interference: a Practical Case Study", IEEE Trans., PAS-101, No. 8, pp 2762-2769.

Thomas, A.O. (1959). "Calculation of Transmission-Line Impedances by Digital Computer", AIEE Trans., pp 1270-73.

Tschappu, F. (1981). "Problems of the Exact Measurement of Electrical Energy in Networks Having Harmonic Content in the Current", Landis and Gyr Review, 28-2, pp 8-15.

Vithayathil, J.J. (1973). "Experience with Harmonic Problems at Celilo HVDC Station", High Voltage DC and/or AC Power Transmission, IEE No. 107, pp 6-10.

Wedepohl, L.M. (1963). "Application of Matrix Methods to the Solution of Travelling-Wave Phenomena in Polyphase Systems. Proc. IEE, Vol. 110, No. 12, pp 2200-2212.

Westinghouse Electric Corporation (1950). "Electrical Transmission and Distribution Reference Book".

Whitehead, S. and Radley, W.G. (1949). "Generation and Flow of Harmonics in Transmission Systems", Proc. IEE, Vol. 96, pp 22-48.

Wilkinson, J.H. and Reinsch, C. (1971). "Handbook for Automatic Computations, Vol. II Linear Algebra", Springer-Verlag.

Winthrop, D.A. (1983). "Planning for a Railway Traction Load on the New Zealand Power System", IPENZ Conference, Paper No. 62.

Xia, D. and Heydt, G.T. (1982). "Harmonic Power Flow Studies - Parts I and II", IEEE Trans., PAS-101, No. 6, pp 1257-1270.

Yacamini, R. and de Oliveira, J.C. (1980a). "Harmonics in Multiple Convertor Systems: a Generalised Approach", IEE Proc., Vol. 127, Pt B, No. 2, pp 96-106.

Yacamini, R. and de Oliveira, J.C. (1980b). "Instability in h.v.d.c. Schemes at Low-Order Interger Harmonics", IEE Proc., Vol. 127, Pt C, No. 3, pp 179-188.

Yacamini, R. and Smith, W.J. (1983). "Third Harmonic Current from Unbalanced AC/DC Convertors", IEE Proc., Vol. 130 Pt C, No. 3, pp 122-126.

Zaborszky, J. (1953). "Skin and Spiralling Effect in Stranded Conductors", AIEE Trans., Vol. 72, pp 599-603.

Zollenkopf, K. (1970). "Bi-factorization-Basic Computational Algorithm and Programming Techniques", Conference on Large Sets of Sparse Linear Equations, Oxford, pp 75-96.

APPENDIX 1

DATA FOR THE REDUCED TEST SYSTEM

The data used in the harmonic penetration program HARMAC to calculate the results in Chapter 6 is included in Tables A1.1-A1.4. The last three numbers in each busbar name represent the voltage level in kV of that busbar. All double circuit lines are symmetrical about the tower axis and therefore conductor data for only one circuit is included.

Transformers have consistent star or delta connections depending on their location in the system, indicated in Figure A1.1.

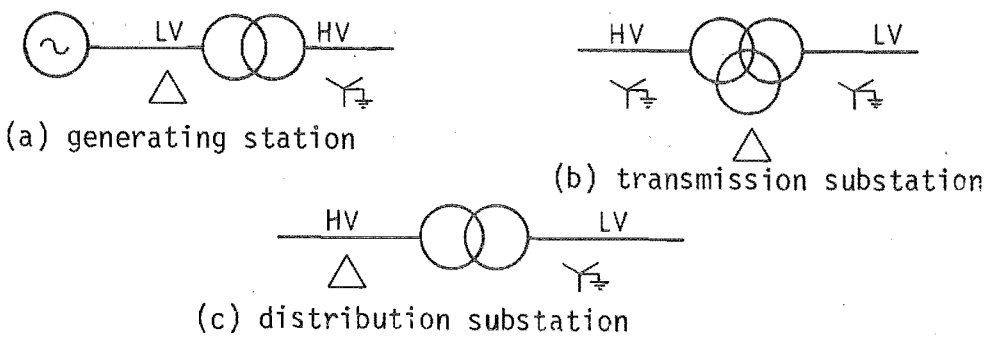

FIGURE A1.1: Transformer Connections

Generation transformers have deltas on the generator or low voltage side and grounded star connection on the HV side. Transmission substation transformers are grounded star on the HV and LV windings with delta connected tertiaries. Distribution transformers supplying the electrical supply authorities are delta connected on the HV and grounded star on the LV side. The connection is important in considering the flow of zero sequence currents. A delta winding will act as an open circuit and a star connected winding, with neutral point grounded, as a short circuit to the zero sequence currents. The zero sequence impedance of the system will thus be considerably different to that presented to positive or negative sequence currents.

TABLE A1.1: Reduced System Busbars and Loading

Busbar	P1(MW)	Q1(MVAR)	P2(MW)	Q2(MVAR)	P3(MW)	Q3(MVAR)
ROXBURGH-011	30.00	18.00	30.00	18.00	30.00	18.00
ROXBURGH-220	0.00	0.00	0.00	0.00	0.00	0.00
ROXBURGH1011	0.00	0.00	0.00	0.00	0.00	0.00
MANAPOURI220	0.00	0.00	0.00	0.00	0.00	0.00
MANAPOUR1014	0.00	0.00	0.00	0.00	0.00	0.00
MANAPOUR2014	0.00	0.00	0.00	0.00	0.00	0.00
TIWAI----220	0.00	0.00	0.00	0.00	0.00	0.00
INVERCARG033	45.00	12.00	45.00	12.00	45.00	12.00
INVERCARG220	0.00	0.00	0.00	0.00	0.00	0.00

TABLE A1.2: Reduced System Generation

Busbar	Subtransient Reactance at 50 Hz (pu)
MANAPOUR1014	0.0370
MANAPOUR2014	0.0740
ROXBURGH1011	0.0620

TABLE A1.3: Reduced System Transforms

Busbars		Leakage Reactance at 50 Hz (pu)	Type
ROXBURGH-220	ROXBURGH1011	0.03816000	4
ROXBURGH-011	ROXBURGH-220	0.03816000	4
MANAPOURI220	MANAPOUR1014	0.02690000	4
MANAPOURI220	MANAPOUR2014	0.05360000	4
INVERCARG033	INVERCARG220	0.10290000	4

Type 1 star-g/star-g

Type 4 star-g/delta

TABLE A1.4: Line Data for the Reduced System

Busbar Names				A	B	C	D	E	F	G	H	I	J	K	L	M	N	O	P	Q
INVERCARG220	INVERCARG220	MANAPOURI220	MANAPOURI220	1	1	152.90	2	0.46	2	6	1	32	4.80	12.50	6.33	17.99	4.42	23.50	0.00	28.94
INVERCARG220	ROXBURGH-220			1	1	132.20	1	0.00	1	5	2	31	6.47	12.50	0.00	12.50	-6.47	12.50	4.61	18.41
INVERCARG220	ROXBURGH-220			1	1	129.80	1	0.00	1	5	0	0	7.20	12.50	0.00	12.50	-7.20	12.50	0.00	0.00
INVERCARG220	INVERCARG220	TIWAI----220	TIWAI----220	1	1	24.30	2	0.46	2	6	2	36	4.77	12.50	6.29	17.95	4.41	23.41	1.52	28.26
MANAPOURI220	MANAPOURI220	TIWAI----220	TIWAI----220	1	1	175.60	2	0.45	2	6	1	32	4.80	12.50	6.34	18.00	4.42	23.50	0.00	29.00

KEY TO COLUMNS

A	section number
B	number of sections
C	Length (km)
D	Number of conductors in bundle
E	Bundle spacing (m)
F	Circuit type (1 single circuit, 2 double circuit)
G	Conductor type
H	Number of earth wires
I	Earth wire conductor type
J	Phase 1 horizontal distance (from the tower axis) (m)
K	Phase 1 vertical distance (from the ground) (m)
L	Phase 2 horizontal distance (m)
M	Phase 2 vertical distance (m)
N	Phase 3 horizontal distance (m)
O	Phase 3 vertical distance (m)
P	Earth wire horizontal distance (m)
Q	Earth wire vertical distance (m)

APPENDIX 2

DATA FOR THE NEW ZEALAND SOUTH ISLAND SYSTEM BELOW BROMLEY

The data used in the harmonic penetration program HARMAC to calculate the results in Chapter 7 is included in Tables A2.1-A2.4. The single line diagram of this system is illustrated in Figure A2.1.

Data for each line section is too extensive to use in the three phase studies. To obtain manageable file sizes line sections shorter than 5 km are concatenated with longer sections; the combined section having a length equal to the sum of the two sections with the geometry of the longer section. Mostly this is required on the 66 kV network and results in a halving of the data requirements. Little effect is noticed in system voltages.

Mutual coupling between lines at lower voltage levels can not be completely duplicated. Where lines are in the same right-of-way for small distances the coupling is often neglected. Temporary busbars are included where lines tee off at intermediate points between busbars. These buses have the form XXX-YYY-TEMP where XXX is a three letter abbreviation of the closer bus and YYY a three letter abbreviation of the more distant bus.

TABLE A2.1: Busbars and Loading for the South Island System below Bromley (MW and MVAR)

Busbar	P1	Q1	P2	Q2	P3	Q3
AVIEMORE-011	0.00	0.00	0.00	0.00	0.00	0.00
AVIEMORE-220	0.00	0.00	0.00	0.00	0.00	0.00
BALCLUTHA033	8.37	2.75	8.37	2.75	8.37	2.75
BALCLUTHA110	0.00	0.00	0.00	0.00	0.00	0.00
BENCG2001033	0.01	0.00	0.01	0.00	0.01	0.00
BENCG2002033	0.01	0.00	0.01	0.00	0.01	0.00
BENM-TEEBUS1	0.00	0.00	0.00	0.00	0.00	0.00
BENM-TEEBUS2	0.00	0.00	0.00	0.00	0.00	0.00
BENMORE--220	0.00	0.00	0.00	0.00	0.00	0.00
BENMORE-1016	0.00	0.00	0.00	0.00	0.00	0.00
BENMORE-2016	100.00	51.23	100.00	51.23	100.00	51.23
BERWICK--110	0.00	0.00	0.00	0.00	0.00	0.00
CROMWELL-033	2.17	0.63	2.17	0.63	2.17	0.63
CROMWELL1220	0.00	0.00	0.00	0.00	0.00	0.00
CROMWELL2220	0.00	0.00	0.00	0.00	0.00	0.00
DUN-ROX-TEMP	0.00	0.00	0.00	0.00	0.00	0.00
EDENDALE-011	0.00	0.00	0.00	0.00	0.00	0.00
EDENDALE-033	1.20	0.96	1.20	0.96	1.20	0.96
EDENDALE-110	0.00	0.00	0.00	0.00	0.00	0.00
FRANKTON-033	3.23	0.81	3.23	0.81	3.23	0.81
GLENAVY--110	0.00	0.00	0.00	0.00	0.00	0.00
GORE-----033	9.20	2.31	9.20	2.31	9.20	2.31
GORE-----110	0.00	0.00	0.00	0.00	0.00	0.00
HALEE0501011	0.00	0.00	0.00	0.00	0.00	0.00
HALEE0502011	0.00	0.00	0.00	0.00	0.00	0.00
HALF-TEEBUS1	0.00	0.00	0.00	0.00	0.00	0.00
HALF-TEEBUS2	0.00	0.00	0.00	0.00	0.00	0.00
HALF-TEEBUS3	0.00	0.00	0.00	0.00	0.00	0.00
HALFWAYB1033	21.80	4.43	21.80	4.43	21.80	4.43
HALFWAYB2033	19.93	4.05	19.93	4.05	19.93	4.05
HALFWAYBU110	0.00	0.00	0.00	0.00	0.00	0.00
HALFWAYBU220	0.00	0.00	0.00	0.00	0.00	0.00
HALSA1001011	0.01	0.00	0.01	0.00	0.01	0.00
HILLSIDE-033	0.00	0.00	0.00	0.00	0.00	0.00
HILLSIDE-066	0.00	0.00	0.00	0.00	0.00	0.00
INVBB0501011	0.01	0.00	0.01	0.00	0.01	0.00
INVE-TEEBUS2	0.00	0.00	0.00	0.00	0.00	0.00
INVERCARG033	26.50	5.38	26.50	5.38	26.50	5.38
INVERCARG110	0.00	0.00	0.00	0.00	0.00	0.00
INVERCARG220	0.00	0.00	0.00	0.00	0.00	0.00
ISLINGTON220	166.70	54.80	166.70	54.80	166.70	54.80
LIVINGSTN220	0.00	0.00	0.00	0.00	0.00	0.00
MANAPOUR1014	0.00	0.00	0.00	0.00	0.00	0.00
MANAPOUR2014	0.00	0.00	0.00	0.00	0.00	0.00
MANAPOUR3014	0.00	0.00	0.00	0.00	0.00	0.00
MANAPOURI220	0.00	0.00	0.00	0.00	0.00	0.00
MONOWAI--006	0.00	0.00	0.00	0.00	0.00	0.00
MONOWAI--011	0.00	0.00	0.00	0.00	0.00	0.00
MONOWAI--066	0.00	0.00	0.00	0.00	0.00	0.00
OAMARU---110	0.00	0.00	0.00	0.00	0.00	0.00
OHAI-----011	0.00	0.00	0.00	0.00	0.00	0.00
OHAI-----066	0.00	0.00	0.00	0.00	0.00	0.00
OHAU-A---013	0.00	0.00	0.00	0.00	0.00	0.00
OHAU-A---220	0.00	0.00	0.00	0.00	0.00	0.00
ORAWIA---011	0.00	0.00	0.00	0.00	0.00	0.00
ORAWIA---066	0.00	0.00	0.00	0.00	0.00	0.00
ROXB-TEEBUS1	0.00	0.00	0.00	0.00	0.00	0.00
ROXBB0501011	0.00	0.00	0.00	0.00	0.00	0.00
ROXBURGH-033	0.57	0.17	0.57	0.17	0.57	0.17
ROXBURGH-110	0.00	0.00	0.00	0.00	0.00	0.00
ROXBURGH-220	0.00	0.00	0.00	0.00	0.00	0.00
ROXBURGH1011	0.00	0.00	0.00	0.00	0.00	0.00
ROXBURGH2011	0.00	0.00	0.00	0.00	0.00	0.00
SOUTHDUN-033	22.53	0.00	22.53	0.00	22.53	0.00
SOUTHDUN-220	0.00	0.00	0.00	0.00	0.00	0.00
TEKAPO-B-011	0.00	0.00	0.00	0.00	0.00	0.00
TEKAPO-B-220	0.00	0.00	0.00	0.00	0.00	0.00
TIMARU---110	16.67	5.48	16.67	5.48	16.67	5.48
TIWAI----220	0.00	0.00	0.00	0.00	0.00	0.00
TWIZEL---033	1.53	0.50	1.53	0.50	1.53	0.50
TWIZEL---220	0.00	0.00	0.00	0.00	0.00	0.00
WAIPORI--110	0.00	0.00	0.00	0.00	0.00	0.00
WAITAKI--011	0.57	0.14	0.57	0.14	0.57	0.14
WAITAKI--033	0.20	0.05	0.20	0.05	0.20	0.05
WAITAKI--110	0.00	0.00	0.00	0.00	0.00	0.00
WAITAKI-1011	0.00	0.00	0.00	0.00	0.00	0.00
WAITAKI-2011	0.00	0.00	0.00	0.00	0.00	0.00
WINFE0151011	0.01	0.00	0.01	0.00	0.01	0.00
WINT-TEEBUS1	0.00	0.00	0.00	0.00	0.00	0.00
WINTON---011	2.33	0.58	2.33	0.58	2.33	0.58
WINTON---066	1.87	0.61	1.87	0.61	1.87	0.61
WINTON---110	0.00	0.00	0.00	0.00	0.00	0.00

Busbar	Subtransient reactance (pu)
AVIEMORE-011	0.0660
BENMORE-1016	0.0590
BENMORE-2016	0.0590
HALEE0501011	0.3900
HALEE0502011	0.3800
MANAPOUR1014	0.0370
MANAPOUR2014	0.1480
MANAPOUR3014	0.1480
MONOWAI--006	2.2650
OHAU-A---013	0.0471
ROXBURGH1011	0.0620
ROXBURGH2011	0.1040
TEKAPO-B-011	0.0731
WAIPORI--110	0.9350
WAITAKI-1011	0.5520
WAITAKI-2011	0.2130

Table A2.2: Generation for the South Island System below Bromley

TABLE A2.3: Transformers for the South Island System below Bromley

Busbars		Leakage reactance (pu)	Type
INVE-TEEBUS2	INVERCARG220	0.03310000	1
INVE-TEEBUS2	INVERCARG110	0.05610000	1
INVE-TEEBUS2	INVBB0501011	0.14730000	4
BENM-TEEBUS1	BENMORE--220	0.04600000	1
BENM-TEEBUS1	BENMORE-1016	0.02060000	4
BENM-TEEBUS1	BENCB2001033	-0.00450000	4
BENM-TEEBUS2	BENMORE--220	0.04600000	1
BENM-TEEBUS2	BENMORE-2016	0.02060000	4
BENM-TEEBUS2	BENCB2002033	-0.00450000	4
ROXB-TEEBUS1	ROXBURGH-220	0.21259999	1
ROXB-TEEBUS1	ROXBURGH-110	-0.05480000	1
ROXB-TEEBUS1	ROXBB0501011	0.38679999	4
WINT-TEEBUS1	WINTON---110	0.14170000	1
WINT-TEEBUS1	WINTON---066	-0.01030000	1
WINT-TEEBUS1	WINFE0151011	0.59969997	4
HALF-TEEBUS1	HALFWAYBU220	0.02290000	1
HALF-TEEBUS1	HALFWAYBU110	0.02360000	1
HALF-TEEBUS1	HALSA1001011	0.04460000	4
HALF-TEEBUS2	HALFWAYBU110	0.12300000	1
HALF-TEEBUS2	HALFWAYB1033	-0.00680000	1
HALF-TEEBUS2	HALEE0502011	0.07160000	4
HALF-TEEBUS3	HALFWAYBU110	0.11890000	1
HALF-TEEBUS3	HALFWAYB1033	-0.00790000	1
HALF-TEEBUS3	HALEE0501011	0.07450000	4
AVIEMORE-220	AVIEMORE-011	0.04180000	4
BALCLUTHA033	BALCLUTHA110	0.49750000	4
BALCLUTHA033	BALCLUTHA110	0.49649999	4
CROMWELL-033	CROMWELL2220	0.40050000	4
CROMWELL-033	CROMWELL1220	0.40050000	4
EDENDALE-011	EDENDALE-110	2.71059990	4
EDENDALE-033	EDENDALE-110	0.88400000	4
GORE-----033	GORE-----110	0.32969999	4
HALFWAYB2033	HALFWAYBU220	0.12590000	4
HILLSIDE-033	HILLSIDE-066	0.62500000	4
INVERCARG033	INVERCARG220	0.21920000	4
INVERCARG033	INVERCARG220	0.20580000	4
MANAPOURI220	MANAPOUR1014	0.02690000	4
MANAPOURI220	MANAPOUR2014	0.10720000	4
MANAPOURI220	MANAPOUR3014	0.10720000	4
MONOWAI--066	MONOWAI--006	1.00000000	4
MONOWAI--011	MONOWAI--006	7.19999981	4
OHAI-----011	OHAI-----066	2.13330007	4
OHAI-----011	OHAI-----066	2.13330007	4
OHAU-A---220	OHAU-A---013	0.03410000	4
ORAWIA---011	ORAWIA---066	1.49199998	4
ROXBB0501011	ROXBURGH-033	1.00399995	1
ROXBB0501011	ROXBURGH-033	1.00399995	1
ROXBURGH-110	ROXBURGH2011	0.06360000	4
ROXBURGH-220	ROXBURGH1011	0.03820000	4
SOUTHDUN-033	SOUTHDUN-220	0.12490000	4
TEKAPO-B-220	TEKAPO-B-011	0.03510000	4
TWIZEL---033	TWIZEL---220	0.40050000	4
WAITAKI--011	WAITAKI--110	5.55550003	4
WAITAKI--011	WAITAKI--110	5.55550003	4
WAITAKI--033	WAITAKI--110	0.97500002	4
WAITAKI--110	WAITAKI-2011	0.10710000	4
WAITAKI--110	WAITAKI-1011	0.27000001	4
WINTON---011	WINTON---110	1.06700003	4
WINTON---011	WINTON---110	1.06700003	4

TABLE A2.4: Transmission Line Data for the New Zealand South Island System Below Bromley

Busbar Names				A	B	C	D	E	F	G	H	I	J	K	L	M	N	O	P	Q
CROMWELL-033	CROMWELL-033	FRANKTON-033	FRANKTON-033	1	1	44.40	1	0.00	2	8	0	0	3.26	12.00	4.31	15.40	3.08	19.01	0.00	0.00
HILLSIDE-066	MONOWAI--066			1	1	41.50	1	0.00	1	17	0	0	1.21	11.50	0.00	11.83	-1.21	11.50	0.00	0.00
MONOWAI--066	OHAI-----066			1	1	29.80	1	0.00	1	27	0	0	1.74	11.50	0.00	12.02	-1.74	11.50	0.00	0.00
OHAI-----066	ORAWIA---066			1	1	22.00	1	0.00	1	17	0	0	1.74	11.50	0.00	12.02	-1.74	11.50	0.00	0.00
OHAI-----066	WINTON---066			1	1	41.60	1	0.00	1	27	0	0	1.76	11.50	0.00	12.02	-1.76	11.50	0.00	0.00
BALCLUTHA110	GORE-----110			1	1	80.20	1	0.00	1	21	0	0	3.83	12.00	0.00	12.00	-3.83	12.00	0.00	0.00
BALCLUTHA110	BERWICK--110			1	1	52.20	1	0.00	1	21	0	0	3.83	12.00	0.00	12.00	-3.83	12.00	0.00	0.00
BERWICK--110	HALFWAYBU110			1	1	36.60	1	0.00	1	21	0	0	3.83	12.00	0.00	12.00	-3.83	12.00	0.00	0.00
BERWICK--110	WAIPORI--110			1	1	7.20	1	0.00	1	21	0	0	3.83	12.00	0.00	12.00	-3.83	12.00	0.00	0.00
EDENDALE-110	GORE-----110			1	1	26.00	1	0.00	1	21	0	0	3.83	12.00	0.00	12.00	-3.83	12.00	0.00	0.00
EDENDALE-110	INVERCARG110			1	1	31.07	1	0.00	1	21	0	0	3.83	12.00	0.00	12.00	-3.83	12.00	0.00	0.00
GLENAVY--110	OAMARU---110			1	1	26.90	1	0.00	1	15	0	0	1.92	12.00	-1.92	12.00	1.92	14.73	0.00	0.00
GLENAVY--110	OAMARU---110			1	1	26.50	1	0.00	1	21	0	0	3.83	12.00	0.00	12.00	-3.83	12.00	0.00	0.00
GLENAVY--110	TIMARU---110			1	1	70.20	1	0.00	1	15	0	0	1.93	12.00	-1.93	12.00	1.93	14.73	0.00	0.00
GLENAVY--110	TIMARU---110			1	1	70.00	1	0.00	1	21	0	0	1.93	12.00	-1.93	12.00	1.93	14.73	0.00	0.00
GLENAVY--110	GLENAVY--110	WAITAKI--110	WAITAKI--110	1	1	60.80	1	0.00	2	8	0	0	3.03	12.00	3.94	15.33	3.03	18.66	0.00	0.00
GORE-----110	ROXBURGH-110			1	1	84.20	1	0.00	1	8	0	0	3.83	12.00	0.00	12.00	-3.83	12.00	0.00	0.00
HALFWAYBU110	OAMARU---110			1	1	100.80	1	0.00	1	8	0	0	3.83	12.00	0.00	12.00	-3.83	12.00	0.00	0.00
HALFWAYBU110	OAMARU---110			1	1	99.80	1	0.00	1	21	0	0	3.83	12.00	0.00	12.00	-3.83	12.00	0.00	0.00
HALFWAYBU110	HALFWAYBU110	ROXBURGH-110	ROXBURGH-110	1	1	126.20	1	0.00	2	8	0	0	2.88	12.00	3.94	16.55	2.88	21.10	0.00	0.00
INVERCARG110	WINTON---110			1	1	29.40	1	0.00	1	8	0	0	3.79	12.00	0.00	12.00	-3.79	12.00	0.00	0.00
AVIEMORE-220	AVIEMORE-220	BENMORE--220	BENMORE--220	1	1	17.44	1	0.00	2	6	2	29	3.56	12.50	3.56	19.17	3.56	25.80	1.20	32.20
AVIEMORE-220	LIVINGSTN220			1	1	39.80	1	0.00	1	6	0	0	7.58	12.50	0.00	12.50	-7.58	12.50	0.00	0.00
BENMORE--220	TWIZEL---220			1	1	46.10	2	0.36	1	6	2	29	6.97	12.50	0.00	12.50	-6.97	12.50	4.47	18.65
HALFWAYBU220	DUN-ROX-TEMP	ROXBURGH-220	ROXBURGH-220	1	1	104.50	2	0.46	2	5	0	0	5.10	12.50	6.60	18.00	4.60	23.50	0.00	0.00
HALFWAYBU220	DUN-ROX-TEMP	SOUTHDUN-220	SOUTHDUN-220	1	2	9.40	1	0.00	2	5	1	36	5.00	12.50	4.70	18.20	4.60	23.90	0.00	29.50
HALFWAYBU220	DUN-ROX-TEMP	SOUTHDUN-220	SOUTHDUN-220	2	2	2.60	1	0.00	2	5	1	36	3.78	12.50	3.78	18.00	3.78	23.50	0.00	29.00
INVERCARG220	INVERCARG220	MANAPOURI220	MANAPOURI220	1	1	143.90	2	0.46	2	6	1	32	4.80	12.50	6.33	17.99	4.42	23.50	0.00	28.94
INVERCARG220	ROXBURGH-220			1	1	132.20	1	0.00	1	5	2	31	6.47	12.50	0.00	12.50	-6.47	12.50	4.61	18.41
INVERCARG220	ROXBURGH-220			1	1	129.40	1	0.00	1	5	0	0	7.20	12.50	0.00	12.50	-7.20	12.50	0.00	0.00
INVERCARG220	INVERCARG220	TIWAI----220	TIWAI----220	1	1	24.30	2	0.46	2	6	2	36	4.77	12.50	6.29	17.95	4.41	23.41	1.52	28.26
BROMLEY--220	LIVINGSTN220			1	3	119.00	2	0.46	1	6	0	0	7.62	12.50	0.00	12.50	-7.62	12.50	0.00	0.00
BROMLEY--220	LIVINGSTN220			2	3	33.50	1	0.00	1	6	0	0	7.62	12.50	0.00	12.50	-7.62	12.50	0.00	0.00
BROMLEY--220	LIVINGSTN220			3	3	84.00	1	0.00	1	6	0	0	7.62	12.50	0.00	12.50	-7.62	12.50	0.00	0.00
BROMLEY--220	TEKAPO-B-220			1	1	213.50	2	0.36	1	6	2	29	6.97	12.50	0.00	12.50	-6.97	12.50	4.47	18.65
BROMLEY--220	BROMLEY--220	TWIZEL---220	TWIZEL---220	1	1	223.40	2	0.46	2	5	0	0	5.15	12.50	4.80	18.00	4.72	23.50	0.00	0.00
LIVINGSTN220	ROXBURGH-220			1	1	142.30	1	0.00	1	6	0	0	7.58	12.50	0.00	12.50	-7.58	12.50	0.00	0.00
MANAPOURI220	MANAPOURI220	TIWAI----220	TIWAI----220	1	1	166.60	2	0.45	2	6	1	32	4.80	12.50	6.34	18.00	4.42	23.50	0.00	29.00
OHAU-A---220	OHAU-A---220	TWIZEL---220	TWIZEL---220	1	1	7.93	1	0.00	2	5	0	0	5.10	12.50	6.60	18.00	4.60	23.50	0.00	0.00
ROXBURGH-220	ROXBURGH-220	CROMWELL1220	CROMWELL2220	1	1	53.02	1	0.00	2	5	0	0	4.80	12.50	6.33	17.99	4.42	23.48	0.00	0.00
CROMWELL1220	CROMWELL2220	TWIZEL---220	TWIZEL---220	1	1	118.60	1	0.00	2	5	0	0	4.80	12.50	6.33	17.99	4.42	23.48	0.00	0.00
TEKAPO-B-220	TWIZEL---220			1	1	24.80	2	0.36	1	6	2	29	6.97	12.50	0.00	12.50	-6.97	12.50	4.47	18.65

KEY TO COLUMNS

- A section number
- B number of sections
- C Length (km)
- D Number of conductors in bundle
- E Bundle spacing (m)
- F Circuit type (1 single circuit, 2 double circuit)
- G Conductor type
- H Number of earth wires
- I Earth wire conductor type
- J Phase 1 horizontal distance (from the tower axis) (m)
- K Phase 1 vertical distance (from the ground) (m)
- L Phase 2 horizontal distance (m)
- M Phase 2 vertical distance (m)
- N Phase 3 horizontal distance (m)
- O Phase 3 vertical distance (m)
- P Earth wire horizontal distance (m)
- Q Earth wire vertical distance (m)

FIGURE A2.1: Single Line Diagram for the South Island System Below Bromley

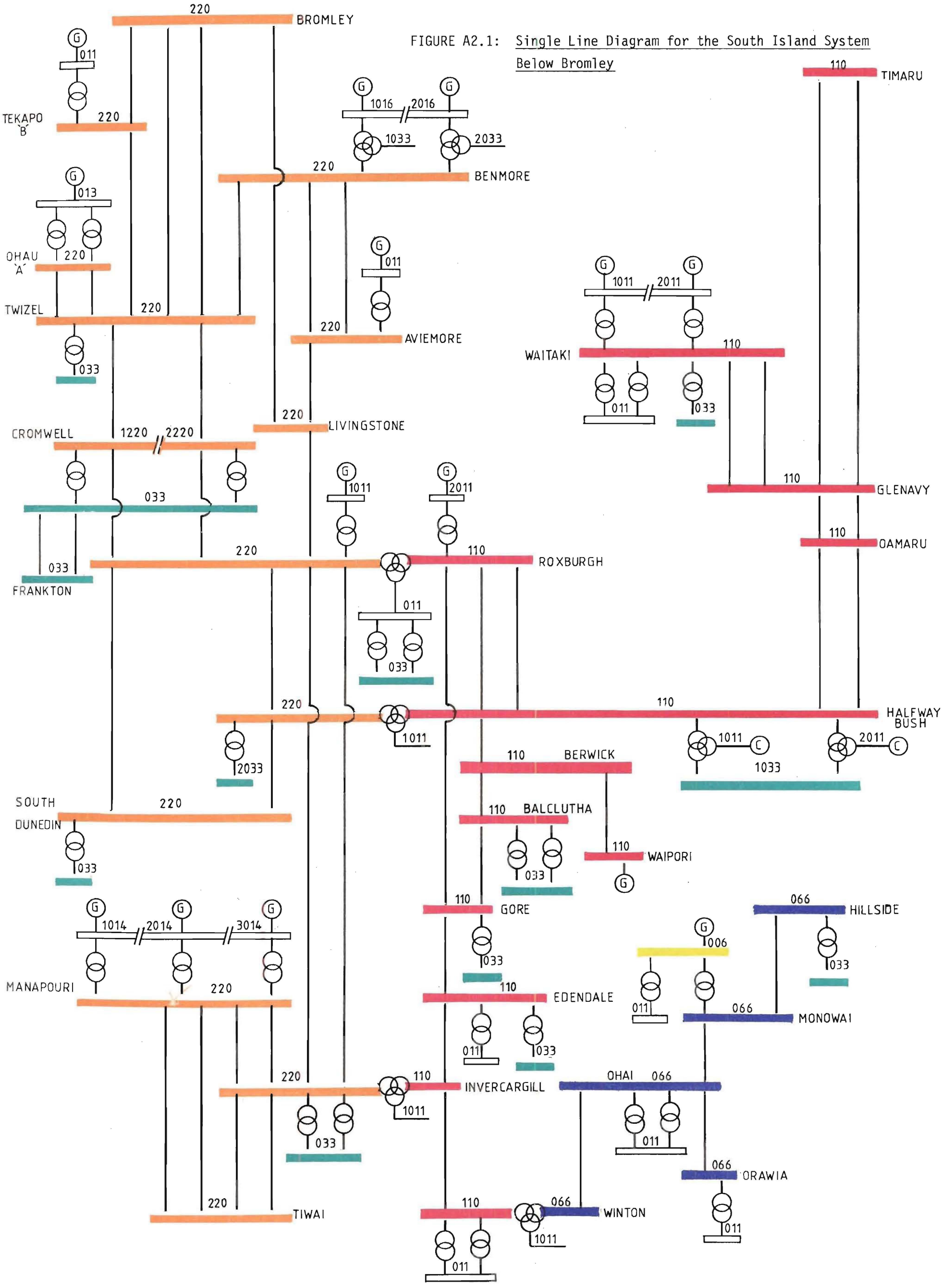

APPENDIX 3

DATA FOR THE NEW ZEALAND SOUTH ISLAND SYSTEM IN 1985

The data used in the harmonic penetration program HARMAC to calculate the results in Chapter 8 is included in Tables A3.1-A3.4. The single line diagrams of this system are illustrated in Figure A3.1.

TABLE A3.1: Busbars and Loading for the South Island System in 1985 (MW and MVAR)

Busbar	P1	Q1	P2	Q2	P3	Q3
AVIEMORE-011	0.00	0.00	0.00	0.00	0.00	0.00
AVIEMORE-220	0.00	0.00	0.00	0.00	0.00	0.00
BALCLUTHA033	8.63	2.16	8.63	2.16	8.63	2.16
BALCLUTHA110	0.00	0.00	0.00	0.00	0.00	0.00
BENCG2001033	0.01	0.00	0.01	0.00	0.01	0.00
BENCG2002033	0.01	0.00	0.01	0.00	0.01	0.00
BENM-TEEBUS1	0.00	0.00	0.00	0.00	0.00	0.00
BENM-TEEBUS2	0.00	0.00	0.00	0.00	0.00	0.00
BENMORE--220	0.00	0.00	0.00	0.00	0.00	0.00
BENMORE-1016	100.00	51.23	100.00	51.23	100.00	51.23
BENMORE-2016	100.00	51.23	100.00	51.23	100.00	51.23
BERWICK--110	0.00	0.00	0.00	0.00	0.00	0.00
CROMWELL-033	2.17	0.63	2.17	0.63	2.17	0.63
CROMWELL1220	0.00	0.00	0.00	0.00	0.00	0.00
CROMWELL2220	0.00	0.00	0.00	0.00	0.00	0.00
DUN-ROX-TEMP	0.00	0.00	0.00	0.00	0.00	0.00
EDENDALE-011	0.00	0.00	0.00	0.00	0.00	0.00
EDENDALE-033	1.13	0.51	1.13	0.51	1.13	0.51
EDENDALE-110	0.00	0.00	0.00	0.00	0.00	0.00
FRANKTON-033	3.23	0.81	3.23	0.81	3.23	0.81
GLENAVY--110	0.00	0.00	0.00	0.00	0.00	0.00
GORE-----033	10.40	2.60	10.40	2.60	10.40	2.60
GORE-----110	0.00	0.00	0.00	0.00	0.00	0.00
HALEE0501011	0.00	0.00	0.00	0.00	0.00	0.00
HALEE0502011	0.00	0.00	0.00	0.00	0.00	0.00
HALF-TEEBUS1	0.00	0.00	0.00	0.00	0.00	0.00
HALF-TEEBUS2	0.00	0.00	0.00	0.00	0.00	0.00
HALF-TEEBUS3	0.00	0.00	0.00	0.00	0.00	0.00
HALFWAYB1033	22.40	0.00	22.40	0.00	22.40	0.00
HALFWAYB2033	28.60	0.00	28.60	0.00	28.60	0.00
HALFWAYBU110	0.00	0.00	0.00	0.00	0.00	0.00
HALFWAYBU220	0.00	0.00	0.00	0.00	0.00	0.00
HALSA1001011	0.01	0.00	0.01	0.00	0.01	0.00
HILLSIDE-033	0.00	0.00	0.00	0.00	0.00	0.00
HILLSIDE-066	0.00	0.00	0.00	0.00	0.00	0.00
INVBB0501011	0.01	0.00	0.01	0.00	0.01	0.00
INVE-TEEBUS2	0.00	0.00	0.00	0.00	0.00	0.00
INVERCARG033	21.75	7.15	21.75	7.15	21.75	7.15
INVERCARG110	0.00	0.00	0.00	0.00	0.00	0.00
INVERCARG220	0.00	0.00	0.00	0.00	0.00	0.00
INVOPEN--110	0.00	0.00	0.00	0.00	0.00	0.00
LIVINGSTN220	0.00	0.00	0.00	0.00	0.00	0.00
MAKAREWA-033	6.50	2.14	6.50	2.14	6.50	2.14
MAKAREWA-220	0.00	0.00	0.00	0.00	0.00	0.00
MANAPOUR1014	0.00	0.00	0.00	0.00	0.00	0.00
MANAPOUR2014	0.00	0.00	0.00	0.00	0.00	0.00
MANAPOUR3014	0.00	0.00	0.00	0.00	0.00	0.00
MANAPOURI220	0.00	0.00	0.00	0.00	0.00	0.00
MONOWAI--006	0.00	0.00	0.00	0.00	0.00	0.00
MONOWAI--011	0.00	0.00	0.00	0.00	0.00	0.00
MONOWAI--066	0.00	0.00	0.00	0.00	0.00	0.00
NASEBY---033	0.99	0.00	0.99	0.00	0.99	0.00
NASEBY---220	0.00	0.00	0.00	0.00	0.00	0.00
OAMARU---011	12.20	1.73	12.20	1.73	12.20	1.73
OAMARU---110	0.00	0.00	0.00	0.00	0.00	0.00
OHAI-----011	0.00	0.00	0.00	0.00	0.00	0.00
OHAI-----066	0.00	0.00	0.00	0.00	0.00	0.00
OHAU-A---013	0.00	0.00	0.00	0.00	0.00	0.00
OHAU-A---220	0.00	0.00	0.00	0.00	0.00	0.00
OHAU-B---013	0.00	0.00	0.00	0.00	0.00	0.00
OHAU-B---220	0.00	0.00	0.00	0.00	0.00	0.00
OHAU-C---013	0.00	0.00	0.00	0.00	0.00	0.00
OHAU-C---220	0.00	0.00	0.00	0.00	0.00	0.00
ORAWIA---011	0.00	0.00	0.00	0.00	0.00	0.00
ORAWIA---066	0.00	0.00	0.00	0.00	0.00	0.00
PALMERSTN033	2.23	0.32	2.23	0.32	2.23	0.32
PALMERSTN110	0.00	0.00	0.00	0.00	0.00	0.00
ROXB-TEEBUS1	0.00	0.00	0.00	0.00	0.00	0.00
ROXBB0501011	0.00	0.00	0.00	0.00	0.00	0.00
ROXBURGH-033	0.57	0.17	0.57	0.17	0.57	0.17
ROXBURGH-110	0.00	0.00	0.00	0.00	0.00	0.00
ROXBURGH-220	0.00	0.00	0.00	0.00	0.00	0.00
ROXBURGH1011	0.00	0.00	0.00	0.00	0.00	0.00
ROXBURGH2011	0.00	0.00	0.00	0.00	0.00	0.00
SOUTHDUN-033	24.00	3.40	24.00	3.40	24.00	3.40
SOUTHDUN-220	0.00	0.00	0.00	0.00	0.00	0.00
TEKAPO-B-011	0.00	0.00	0.00	0.00	0.00	0.00
TEKAPO-B-220	0.00	0.00	0.00	0.00	0.00	0.00
TIWAI----220	0.00	0.00	0.00	0.00	0.00	0.00
TIWAI---1033	77.50	30.00	77.50	30.00	77.50	30.00

Busbar	P1	Q1	P2	Q2	P3	Q3
TIWAI---2033	77.50	30.00	77.50	30.00	77.50	30.00
TWIZEL---033	1.40	0.51	1.40	0.51	1.40	0.51
TWIZEL---220	0.00	0.00	0.00	0.00	0.00	0.00
WAIPORI--110	0.00	0.00	0.00	0.00	0.00	0.00
WAITAKI--011	1.53	0.56	1.53	0.56	1.53	0.56
WAITAKI--033	0.20	0.05	0.20	0.05	0.20	0.05
WAITAKI--110	0.00	0.00	0.00	0.00	0.00	0.00
WAITAKI-1011	0.00	0.00	0.00	0.00	0.00	0.00
WAITAKI-2011	0.00	0.00	0.00	0.00	0.00	0.00
WINFE0151011	0.01	0.00	0.01	0.00	0.01	0.00
WINT-TEEBUS1	0.00	0.00	0.00	0.00	0.00	0.00
WINTON---011	2.33	0.58	2.33	0.58	2.33	0.58
WINTON---066	1.87	0.61	1.87	0.61	1.87	0.61
WINTON---110	0.00	0.00	0.00	0.00	0.00	0.00
ADDINGTN1011	10.00	2.51	10.00	2.51	10.00	2.51
ADDINGTN2011	11.00	2.76	11.00	2.76	11.00	2.76
ADDINGTN3011	4.43	0.90	4.43	0.90	4.43	0.90
ADDINGTON066	20.33	5.10	20.33	5.10	20.33	5.10
ALBURY---011	0.70	0.20	0.70	0.20	0.70	0.20
ALBURY---110	0.00	0.00	0.00	0.00	0.00	0.00
ARAHURA--011	2.60	0.63	2.60	0.63	2.60	0.63
ARAHURA--066	0.00	0.00	0.00	0.00	0.00	0.00
ARNOLD---003	0.00	0.00	0.00	0.00	0.00	0.00
ARNOLD---066	0.00	0.00	0.00	0.00	0.00	0.00
ASHBURTON011	6.20	2.25	6.20	2.25	6.20	2.25
ASHBURTON110	0.00	0.00	0.00	0.00	0.00	0.00
ASHLEY---011	1.40	0.41	1.40	0.41	1.40	0.41
ASHLEY---066	0.00	0.00	0.00	0.00	0.00	0.00
BRO-TWI-TEMP	0.00	0.00	0.00	0.00	0.00	0.00
BROCB1002011	0.00	0.00	0.00	0.00	0.00	0.00
BROM-TEEBUS1	0.00	0.00	0.00	0.00	0.00	0.00
BROM-TEEBUS2	0.00	0.00	0.00	0.00	0.00	0.00
BROMLEY--011	20.00	6.57	20.00	6.57	20.00	6.57
BROMLEY--066	27.00	8.87	27.00	8.87	27.00	8.87
BROMLEY--220	0.00	0.00	0.00	0.00	0.00	0.00
BROSA1001011	0.00	0.00	0.00	0.00	0.00	0.00
CAIRNBRAE033	2.07	0.60	2.07	0.60	2.07	0.60
CAIRNBRAE066	0.00	0.00	0.00	0.00	0.00	0.00
COLERIDGE006	0.07	0.02	0.07	0.02	0.07	0.02
COLERIDGE066	0.00	0.00	0.00	0.00	0.00	0.00
CULVER-II033	1.13	0.33	1.13	0.33	1.13	0.33
CULVER-II066	0.00	0.00	0.00	0.00	0.00	0.00
DILLMANS-011	0.00	0.00	0.00	0.00	0.00	0.00
DILLMANS-066	0.00	0.00	0.00	0.00	0.00	0.00
DOBSON---011	4.80	1.59	4.80	1.59	4.80	1.59
DOBSON---066	0.00	0.00	0.00	0.00	0.00	0.00
GREYMOUTH011	3.60	1.19	3.60	1.19	3.60	1.19
GREYMOUTH066	0.00	0.00	0.00	0.00	0.00	0.00
HARIHARI-066	0.00	0.00	0.00	0.00	0.00	0.00
HARIHARI-011	0.72	0.43	0.72	0.43	0.72	0.43
HIGHBANK-011	0.00	0.00	0.00	0.00	0.00	0.00
HIGHBANK-066	2.20	0.55	2.20	0.55	2.20	0.55
HOREE0331011	0.00	0.00	0.00	0.00	0.00	0.00
HORGE0332011	0.00	0.00	0.00	0.00	0.00	0.00
HORNBY---033	1.46	0.48	1.46	0.48	1.46	0.48
HORO-TEEBUS1	0.00	0.00	0.00	0.00	0.00	0.00
HORO-TEEBUS2	0.00	0.00	0.00	0.00	0.00	0.00
HORO-TEEBUS3	0.00	0.00	0.00	0.00	0.00	0.00
HORORATA-033	1.17	0.29	1.17	0.29	1.17	0.29
HORORATA-066	0.00	0.00	0.00	0.00	0.00	0.00
HORORATA1110	0.00	0.00	0.00	0.00	0.00	0.00
HORORATA2110	0.00	0.00	0.00	0.00	0.00	0.00
ISL-TWI-TEMP	0.00	0.00	0.00	0.00	0.00	0.00
ISL-BRO-TEMP	0.00	0.00	0.00	0.00	0.00	0.00
ISL-T4---066	0.00	0.00	0.00	0.00	0.00	0.00
ISL-T5---066	0.00	0.00	0.00	0.00	0.00	0.00
ISLBB0504011	0.00	0.00	0.00	0.00	0.00	0.00
ISLBB0505011	0.00	0.00	0.00	0.00	0.00	0.00
ISLFE2003011	0.00	0.00	0.00	0.00	0.00	0.00
ISLFE2006011	0.00	0.00	0.00	0.00	0.00	0.00
ISLFE2007011	0.00	0.00	0.00	0.00	0.00	0.00
ISLI-TEEBUS3	0.00	0.00	0.00	0.00	0.00	0.00
ISLI-TEEBUS4	0.00	0.00	0.00	0.00	0.00	0.00
ISLI-TEEBUS5	0.00	0.00	0.00	0.00	0.00	0.00
ISLI-TEEBUS6	0.00	0.00	0.00	0.00	0.00	0.00
ISLI-TEEBUS7	0.00	0.00	0.00	0.00	0.00	0.00
ISLINGTON033	15.40	5.06	15.40	5.06	15.40	5.06
ISLINGTON066	19.30	2.75	19.30	2.75	19.30	2.75
ISLINGTON220	0.00	0.00	0.00	0.00	0.00	0.00
KAIAPOI--011	3.33	0.83	3.33	0.83	3.33	0.83
KAIAPOI--066	0.00	0.00	0.00	0.00	0.00	0.00
KAIKOURA-033	1.37	0.45	1.37	0.45	1.37	0.45
KAIKOURA-066	0.00	0.00	0.00	0.00	0.00	0.00

Busbar	P1	Q1	P2	Q2	P3	Q3
KUMARA---066	0.00	0.00	0.00	0.00	0.00	0.00
LINCOLN--033	1.67	0.55	1.67	0.55	1.67	0.55
OTIRA----011	0.80	0.16	0.80	0.16	0.80	0.16
OTIRA----066	0.00	0.00	0.00	0.00	0.00	0.00
PAPANUI--011	15.30	3.10	15.30	3.10	15.30	3.10
PAPANUI--066	6.67	1.35	6.67	1.35	6.67	1.35
SOUTHBRK-011	5.30	1.74	5.30	1.74	5.30	1.74
SOUTHBRK-066	0.00	0.00	0.00	0.00	0.00	0.00
SPRINGSTN033	3.30	1.08	3.30	1.08	3.30	1.08
SPRINGSTN066	0.00	0.00	0.00	0.00	0.00	0.00
STUDHOLM-011	1.97	0.57	1.97	0.57	1.97	0.57
STUDHOLM-110	0.00	0.00	0.00	0.00	0.00	0.00
TEKAPO---011	0.00	0.00	0.00	0.00	0.00	0.00
TEKAPO---110	0.00	0.00	0.00	0.00	0.00	0.00
TEKAPO---033	0.53	0.11	0.53	0.11	0.53	0.11
TEMUKA---011	2.87	0.84	2.87	0.84	2.87	0.84
TEMUKA---110	0.00	0.00	0.00	0.00	0.00	0.00
TIMARU---011	14.10	4.60	14.10	4.60	14.10	4.60
TIMARU---110	0.00	0.00	0.00	0.00	0.00	0.00
WAIPARA--033	2.43	0.71	2.43	0.71	2.43	0.71
WAIPARA--066	0.00	0.00	0.00	0.00	0.00	0.00
BLACKWATR066	0.00	0.00	0.00	0.00	0.00	0.00
BLENHEIM-033	6.75	1.98	6.75	1.98	6.75	1.98
BLENHEIM-110	0.00	0.00	0.00	0.00	0.00	0.00
BRIGHTWAT220	0.00	0.00	0.00	0.00	0.00	0.00
BRIGHTWAT033	19.50	6.40	19.50	6.40	19.50	6.40
COBB-----006	0.00	0.00	0.00	0.00	0.00	0.00
COBB-----066	0.00	0.00	0.00	0.00	0.00	0.00
HOPE-----033	6.25	2.26	6.25	2.26	6.25	2.26
INAN-TEEBUS1	0.00	0.00	0.00	0.00	0.00	0.00
INANGAHUA066	0.00	0.00	0.00	0.00	0.00	0.00
INANGAHUA110	0.00	0.00	0.00	0.00	0.00	0.00
INASI0201011	4.41	1.45	4.41	1.45	4.41	1.45
KIKEE0501011	0.43	0.14	0.43	0.14	0.43	0.14
KIKI-TEEBUS1	0.00	0.00	0.00	0.00	0.00	0.00
KIKIWA---110	0.00	0.00	0.00	0.00	0.00	0.00
KIKIWA---220	0.00	0.00	0.00	0.00	0.00	0.00
MOTUEKA--011	4.00	1.45	4.00	1.45	4.00	1.45
MOTUEKA-1066	0.00	0.00	0.00	0.00	0.00	0.00
MOTUEKA-2066	0.00	0.00	0.00	0.00	0.00	0.00
MOTUPIPI-033	2.83	0.93	2.83	0.93	2.83	0.93
MOTUPIPI-066	0.00	0.00	0.00	0.00	0.00	0.00
MURCHISON011	0.43	0.14	0.43	0.14	0.43	0.14
MURCHISON110	0.00	0.00	0.00	0.00	0.00	0.00
REEFTON--066	0.47	0.20	0.47	0.20	0.47	0.20
STOAE1002011	0.00	0.00	0.00	0.00	0.00	0.00
STOK-TEEBUS1	0.00	0.00	0.00	0.00	0.00	0.00
STOK-TEEBUS2	0.00	0.00	0.00	0.00	0.00	0.00
STOKE----033	11.67	4.23	11.67	4.23	11.67	4.23
STOKE----066	0.00	0.00	0.00	0.00	0.00	0.00
STOKE----110	0.00	0.00	0.00	0.00	0.00	0.00
STOKE----220	0.00	0.00	0.00	0.00	0.00	0.00
STOSI0201011	0.00	0.00	0.00	0.00	0.00	0.00
UPPERTAKA011	0.00	0.00	0.00	0.00	0.00	0.00
UPPERTAKA066	0.00	0.00	0.00	0.00	0.00	0.00
WESTPORT-011	2.00	0.66	2.00	0.66	2.00	0.66
WESTPORT1110	0.00	0.00	0.00	0.00	0.00	0.00
WESTPORT2110	0.00	0.00	0.00	0.00	0.00	0.00

TABLE A3.2: Transformers for the South Island System in 1985

Busbars		leakage reactance (pu)	Type
ASHBURTON011	ASHBURTON110	0.95099998	4
ASHBURTON011	ASHBURTON110	0.95899999	4
ASHLEY---011	ASHLEY---066	1.02400005	4
BROMLEY--011	BROMLEY--066	0.33309999	4
BROMLEY--011	BROMLEY--066	0.31490001	4
BROMLEY--011	BROMLEY--066	0.32229999	4
BROM-TEEBUS1	BROMLEY--220	0.03830000	1
BROM-TEEBUS1	BROMLEY--066	0.04170000	1
BROM-TEEBUS1	BROSA1001011	0.06270000	4
BROM-TEEBUS2	BROMLEY--220	0.03970000	1
BROM-TEEBUS2	BROMLEY--066	0.04120000	1
BROM-TEEBUS2	BROCG1002011	0.04420000	4
CAIRNBRAE033	CAIRNBRAE066	1.00000000	4
CAIRNBRAE033	CAIRNBRAE066	1.00000000	4
COLERIDGE066	COLERIDGE006	0.25400001	4
CULVER-II033	CULVER-II066	1.00000000	4
DILLMANS-066	DILLMANS-011	0.83329999	4
DOBSON---011	DOBSON---066	0.48400000	4
GREYMOUTH011	GREYMOUTH066	0.48400000	4
HARIHARI-011	HARIHARI-066	0.97039998	4
HIGHBANK-066	HIGHBANK-011	0.30460000	4
HORORATA-033	HORORATA-066	0.79100001	4
HORORATA-033	HORORATA-066	0.79100001	4
HORO-TEEBUS1	HORORATA2110	0.03950000	1
HORO-TEEBUS1	HORORATA-066	-0.00450000	1
HORO-TEEBUS1	HOREE0331011	0.19599999	4
HORO-TEEBUS2	HORORATA1110	0.06910000	1
HORO-TEEBUS2	HORORATA-066	0.00240000	1
HORO-TEEBUS2	HORGE0332011	0.38609999	4
HORO-TEEBUS3	HORORATA1110	0.06910000	1
HORO-TEEBUS3	HORORATA-066	0.00240000	1
HORO-TEEBUS3	HORGE0332011	0.38609999	4
ISLI-TEEBUS4	ISLINGTON220	0.07430000	1
ISLI-TEEBUS4	ISL-T4---066	0.08210000	1
ISLI-TEEBUS4	ISLBB0504011	0.21670000	4
ISLI-TEEBUS5	ISLINGTON220	0.07430000	1
ISLI-TEEBUS5	ISL-T5---066	0.08210000	1
ISLI-TEEBUS5	ISLBB0505011	0.21670000	4
ISLI-TEEBUS3	ISLINGTON220	0.08080000	1
ISLI-TEEBUS3	ISLINGTON066	-0.00510000	1
ISLI-TEEBUS3	ISLFE2003011	0.05580000	4
ISLI-TEEBUS7	ISLINGTON220	0.08320000	1
ISLI-TEEBUS7	ISLINGTON066	-0.00480000	1
ISLI-TEEBUS7	ISLFE2007011	0.05520000	4
ISLI-TEEBUS6	ISLINGTON220	0.08320000	1
ISLI-TEEBUS6	ISLINGTON066	-0.00480000	1
ISLI-TEEBUS6	ISLFE2006011	0.05520000	4
ISLINGTON033	ISLINGTON220	0.18170001	4
ISLINGTON033	ISLINGTON220	0.19300000	4
KAIAPOI--011	KAIAPOI--066	0.48019999	4
KAIKOURA-033	KAIKOURA-066	1.00000000	4
OTIRA----011	OTIRA----066	2.29749990	4
PAPANUI--011	PAPANUI--066	0.35130000	4
PAPANUI--011	PAPANUI--066	0.48350000	4
PAPANUI--011	PAPANUI--066	0.48350000	4
PAPANUI--011	PAPANUI--066	0.33360001	4
SOUTHBRK-011	SOUTHBRK-066	0.98350000	4
SOUTHBRK-011	SOUTHBRK-066	0.97109997	4
SPRINGSTN033	SPRINGSTN066	0.33219999	4
SPRINGSTN033	SPRINGSTN066	0.33219999	4
STUDHOLM-011	STUDHOLM-110	0.95899999	4
TEKAPO---110	TEKAPO---011	0.36960000	4
TEKAPO---033	TEKAPO---011	1.00010002	4
TEMUKA---011	TEMUKA---110	1.51800001	4
TEMUKA---011	TEMUKA---110	1.51800001	4
TEMUKA---011	TEMUKA---110	1.56599998	4
TIMARU---011	TIMARU---110	0.51300001	4
TIMARU---011	TIMARU---110	0.51450002	4
WAIPARA--033	WAIPARA--066	0.95109999	4
WAIPARA--033	WAIPARA--066	0.95109999	4
BLENHEIM-033	BLENHEIM-110	0.33270001	4
BLENHEIM-033	BLENHEIM-110	0.49750000	4
BRIGHTWAT033	BRIGHTWAT220	0.19000000	4
BRIGHTWAT033	BRIGHTWAT220	0.19000000	4
COBB-----066	COBB-----006	0.25400001	4
INAN-TEEBUS1	INANGAHUA110	0.11750000	1
INAN-TEEBUS1	INANGAHUA066	-0.01000000	1
INAN-TEEBUS1	INASI0201011	0.41400000	4
KIKI-TEEBUS1	KIKIWA---220	0.02900000	1
KIKI-TEEBUS1	KIKIWA---110	0.09520000	1
KIKI-TEEBUS1	KIKEE0501011	0.09760000	4
MOTUEKA--011	MOTUEKA-1066	0.97020000	4
MOTUEKA--011	MOTUEKA-2066	0.97020000	4

Busbars		Leakage reactance (pu)	Type
INVE-TEEBUS2	INVERCARG220	0.03310000	1
INVE-TEEBUS2	INVERCARG110	0.05610000	1
INVE-TEEBUS2	INVBB0501011	0.14730000	4
BENM-TEEBUS1	BENMORE--220	0.04600000	1
BENM-TEEBUS1	BENMORE-1016	0.02060000	4
BENM-TEEBUS1	BENCG2001033	-0.00450000	4
BENM-TEEBUS2	BENMORE--220	0.04600000	1
BENM-TEEBUS2	BENMORE-2016	0.02060000	4
BENM-TEEBUS2	BENCG2002033	-0.00450000	4
ROXB-TEEBUS1	ROXBURGH-220	0.21259999	1
ROXB-TEEBUS1	ROXBURGH-110	-0.05480000	1
ROXB-TEEBUS1	ROXBB0501011	0.38679999	4
WINT-TEEBUS1	WINTON---110	0.14170000	1
WINT-TEEBUS1	WINTON---066	-0.01030000	1
WINT-TEEBUS1	WINFE0151011	0.59969997	4
HALF-TEEBUS1	HALFWAYBU220	0.02290000	1
HALF-TEEBUS1	HALFWAYBU110	0.02360000	1
HALF-TEEBUS1	HALSA1001011	0.04460000	4
HALF-TEEBUS2	HALFWAYBU110	0.12300000	1
HALF-TEEBUS2	HALFWAYB1033	-0.00680000	1
HALF-TEEBUS2	HALEE0502011	0.07160000	4
HALF-TEEBUS3	HALFWAYBU110	0.11890000	1
HALF-TEEBUS3	HALFWAYB1033	-0.00790000	1
HALF-TEEBUS3	HALEE0501011	0.07450000	4
AVIEMORE-220	AVIEMORE-011	0.04180000	4
BALCLUTHA033	BALCLUTHA110	0.49750000	4
BALCLUTHA033	BALCLUTHA110	0.49649999	4
CROMWELL-033	CROMWELL2220	0.40050000	4
CROMWELL-033	CROMWELL1220	0.40050000	4
EDENDALE-011	EDENDALE-110	2.71059990	4
EDENDALE-033	EDENDALE-110	0.88400000	4
GORE-----033	GORE-----110	0.32969999	4
HALFWAYB2033	HALFWAYBU220	0.12590000	4
HILLSIDE-033	HILLSIDE-066	0.62500000	4
INVERCARG033	INVERCARG220	0.21920000	4
INVERCARG033	INVERCARG220	0.20580000	4
MAKAREWA-033	MAKAREWA-220	0.05000000	4
MAKAREWA-033	MAKAREWA-220	0.05000000	4
MANAPOURI220	MANAPOUR1014	0.02690000	4
MANAPOURI220	MANAPOUR2014	0.10720000	4
MANAPOURI220	MANAPOUR3014	0.10720000	4
MONOWAI--066	MONOWAI--006	1.00000000	4
MONOWAI--011	MONOWAI--006	7.19999981	4
NASEBY---033	NASEBY---220	0.50040001	4
OAMARU---011	OAMARU---110	0.33140001	4
OHAI-----011	OHAI-----066	2.13330007	4
OHAI-----011	OHAI-----066	2.13330007	4
OHAU-A---220	OHAU-A---013	0.03410000	4
OHAU-A---220	OHAU-A---013	0.03410000	4
OHAU-B---220	OHAU-B---013	0.03410000	4
OHAU-B---220	OHAU-B---013	0.03410000	4
OHAU-C---220	OHAU-C---013	0.03410000	4
OHAU-C---220	OHAU-C---013	0.03410000	4
ORAWIA---011	ORAWIA---066	1.49199998	4
PALMERSTN033	PALMERSTN110	0.88099998	4
ROXBB0501011	ROXBURGH-033	1.00399995	1
ROXBB0501011	ROXBURGH-033	1.00399995	1
ROXBURGH-110	ROXBURGH2011	0.06360000	4
ROXBURGH-220	ROXBURGH1011	0.03820000	4
SOUTHDUN-033	SOUTHDUN-220	0.12490000	4
TEKAPO-B-220	TEKAPO-B-011	0.03510000	4
TIWAI---1033	TIWAI----220	0.08220000	4
TIWAI---2033	TIWAI----220	0.08220000	4
TWIZEL---033	TWIZEL---220	0.40050000	4
WAITAKI--011	WAITAKI--110	5.55550003	4
WAITAKI--011	WAITAKI--110	5.55550003	4
WAITAKI--033	WAITAKI--110	0.97500002	4
WAITAKI--110	WAITAKI-2011	0.10710000	4
WAITAKI--110	WAITAKI-1011	0.27000001	4
WINTON---011	WINTON---110	1.06700003	4
WINTON---011	WINTON---110	1.06700003	4
ADDINGTN1011	ADDINGTON066	0.32640001	4
ADDINGTN1011	ADDINGTON066	0.32240000	4
ADDINGTN1011	ADDINGTONC66	0.31889999	4
ADDINGTN1011	ADDINGTON066	0.31639999	4
ADDINGTN2011	ADDINGTON066	0.35299999	4
ADDINGTN2011	ADDINGTON066	0.35260001	4
ADDINGTN3011	ADDINGTON066	0.33550000	4
ALBURY---011	ALBURY---110	1.40799999	4
ARAHURA--011	ARAHURA--066	1.42149997	4
ARAHURA--011	ARAHURA--066	1.32480001	4
ARNOLD---066	ARNOLD---003	1.34249997	4
ASHBURTON011	ASHBURTON110	0.96200001	4

Busbars		Leakage reactance (pu)	Type
MOTUPIPI-033	MOTUPIPI-066	0.39410001	4
MURCHISON011	MURCHISON110	1.99399996	4
STOK-TEEBUS1	STOKE-----220	0.02600000	1
STOK-TEEBUS1	STOKE-----110	0.02690000	1
STOK-TEEBUS1	STOAE1002011	0.07940000	4
STOK-TEEBUS2	STOKE-----110	0.11750000	1
STOK-TEEBUS2	STOKE-----066	-0.01000000	1
STOK-TEEBUS2	STOSI0201011	0.41400000	4
STOKE-----033	STOKE-----220	0.18920000	4
STOKE-----033	STOKE-----220	0.19520000	4
UPPERTAKA011	UPPERTAKA066	21.00000000	4
WESTPORT-011	WESTPORT1110	0.66700000	4
WESTPORT-011	WESTPORT2110	0.66700000	4

TABLE A3.3: Generation for the South Island System in 1985

Busbar	Subtransient reactance (pu)
AVIEMORE-011	0.1320
BENMORE-1016	0.0885
BENMORE-2016	0.0885
MANAPOUR1014	0.0370
MANAPOUR2014	0.1480
MANAPOUR3014	0.1480
MONOWAI--006	2.2650
OHAU-A---013	0.0942
ROXBURGH1011	0.1240
ROXBURGH2011	0.2080
TEKAPO-B-011	0.0731
WAITAKI-1011	1.1020
WAITAKI-2011	0.4260
ARNOLD---003	4.0010
COLERIDGE006	0.6900
DILLMANS-011	1.8910
COBB-----006	0.9000

TABLE A3.4: Transmission Line Data for New Zealand South Island System in 1985 (Nelson District)

Busbar Names			A	B	C	D	E	F	G	H	I	J	K	L	M	N	O	P	Q
HOPE-----033	HOPE-----033	STOKE----033 STOKE----033	1	1	9.66	1	0.00	2	22	0	0	2.12	11.50	1.97	13.32	1.74	15.14	0.00	0.00
COBB-----066	UPPERTAKA066		1	1	10.40	1	0.00	1	10	0	0	4.75	11.50	0.00	11.50	-4.75	11.50	0.00	0.00
COBB-----066	UPPERTAKA066		1	1	10.60	1	0.00	1	14	0	0	2.75	11.50	0.00	11.50	-2.75	11.50	0.00	0.00
DOBSON---066	BLACKWATR066		1	1	43.00	1	0.00	1	26	0	0	1.59	11.50	1.59	13.32	-1.59	13.32	0.00	0.00
BLACKWATR066	REEFTON--066		1	1	25.20	1	0.00	1	10	0	0	3.84	12.00	0.00	12.00	-3.84	12.00	0.00	0.00
REEFTON--066	INANGAHUA066		1	1	28.80	1	0.00	1	10	0	0	4.18	12.00	0.00	12.00	-4.18	12.00	0.00	0.00
MOTUEKA-1066	STOKE----066		1	2	19.30	1	0.00	1	14	0	0	2.75	11.50	0.00	11.50	-2.75	11.50	0.00	0.00
MOTUEKA-1066	STOKE----066		2	2	16.70	1	0.00	1	10	0	0	2.75	11.50	0.00	11.50	-2.75	11.50	0.00	0.00
MOTUEKA-2066	STOKE----066		1	2	19.60	1	0.00	1	10	0	0	2.75	11.50	0.00	11.50	-2.75	11.50	0.00	0.00
MOTUEKA-2066	STOKE----066		2	2	16.80	1	0.00	1	14	0	0	2.75	11.50	0.00	11.50	-2.75	11.50	0.00	0.00
MOTUEKA-1066	UPPERTAKA066		1	1	23.62	1	0.00	1	14	0	0	2.75	11.50	0.00	11.50	-2.75	11.50	0.00	0.00
MOTUEKA-2066	UPPERTAKA066		1	1	22.46	1	0.00	1	10	0	0	2.75	11.50	0.00	11.50	-2.75	11.50	0.00	0.00
MOTUPIPI-066	UPPERTAKA066		1	1	19.50	1	0.00	1	14	0	0	2.75	11.50	0.00	11.50	-2.75	11.50	0.00	0.00
MOTUPIPI-066	UPPERTAKA066		1	1	19.47	1	0.00	1	17	0	0	2.75	11.50	0.00	11.50	-2.75	11.50	0.00	0.00
BLENHEIM-110	KIKIWA---110		1	1	107.70	1	0.00	1	10	0	0	3.87	12.00	0.00	12.00	-3.87	12.00	0.00	0.00
BLENHEIM-110	STOKE----110		1	1	76.40	1	0.00	1	6	2	32	2.58	12.00	2.58	15.14	2.58	18.30	1.54	21.80
INANGAHUA110	KIKIWA---110		1	2	88.50	1	0.00	1	5	0	0	3.78	12.50	3.78	18.00	3.78	23.50	0.00	0.00
INANGAHUA110	KIKIWA---110		2	2	9.10	2	0.46	1	5	1	36	5.10	12.50	6.60	18.00	4.60	23.50	0.00	32.21
INANGAHUA110	MURCHISON110		1	1	34.90	1	0.00	1	10	0	0	4.73	12.00	0.00	12.00	-4.73	12.00	0.00	0.00
INANGAHUA110	WESTPORT1110		1	4	9.10	2	0.46	1	5	1	36	5.10	12.50	6.60	18.00	4.60	23.50	0.00	32.21
INANGAHUA110	WESTPORT1110		2	4	6.53	1	0.00	1	1	0	0	7.15	12.50	0.00	12.50	-7.15	12.50	0.00	0.00
INANGAHUA110	WESTPORT1110		3	4	14.19	1	0.00	1	8	1	36	3.10	12.00	-2.95	13.85	2.95	15.70	0.00	21.00
INANGAHUA110	WESTPORT1110		4	4	24.61	1	0.00	1	8	1	36	3.27	12.00	3.08	15.55	3.08	19.10	0.00	24.15
INANGAHUA110	WESTPORT2110		1	2	26.21	1	0.00	1	10	2	34	4.73	12.00	0.00	12.00	-4.73	12.00	3.36	15.29
INANGAHUA110	WESTPORT2110		2	2	23.38	1	0.00	1	12	0	0	4.18	12.00	0.00	12.00	-4.18	12.00	0.00	0.00
KIKIWA---110	MURCHISON110		1	1	54.70	1	0.00	1	10	0	0	4.73	12.00	0.00	12.00	-4.73	12.00	0.00	0.00
KIKIWA---110	STOKE----110		1	2	14.60	1	0.00	1	10	0	0	4.73	12.00	0.00	12.00	-4.73	12.00	0.00	0.00
KIKIWA---110	STOKE----110		2	2	38.30	1	0.00	1	10	0	0	3.78	12.00	0.00	12.00	-3.78	12.00	0.00	0.00
BRIGHTWAT220	KIKIWA---220		1	1	36.10	1	0.00	1	5	1	32	5.15	12.50	4.55	17.95	3.94	23.41	1.82	27.35
BRIGHTWAT220	STOKE----220		1	1	19.50	1	0.00	1	5	1	32	5.15	12.50	4.55	17.95	3.94	23.41	1.82	27.35
KIKIWA---220	STOKE----220		1	1	52.64	1	0.00	1	5	1	32	5.15	12.50	4.55	17.95	3.94	23.41	1.82	27.35
ISLINGTON220	KIKIWA---220		1	1	229.70	1	0.00	1	5	0	0	7.58	12.50	0.00	12.50	-7.58	12.50	0.00	0.00
ISLINGTON220	KIKIWA---220		1	1	236.00	1	0.00	1	5	0	0	5.10	12.50	6.60	18.00	4.60	23.50	0.00	0.00

KEY TO COLUMNS

A section number
B number of sections
C Length (km)
D Number of conductors in bundle
E Bundle spacing (m)
F Circuit Type (1 single circuit, 2 double circuit)
G Conductor Type
H Number of Earth wires
I Earth conductor type
J Phase 1 horizontal distance (from the tower axis) (m)
K Phase 1 vertical distance (from the ground) (m)
L Phase 2 horizontal distance (m)
M Phase 2 vertical distance (m)
N Phase 3 horizontal distance (m)
O Phase 3 vertical distance (m)
P Earth wire horizontal distance (m)
Q Earth wire vertical distance (m)

TABLE A3.4: Christchurch District

Busbar Names				A	B	C	D	E	F	G	H	I	J	K	L	M	N	O	P	Q
HORNBY---033	ISLINGTON033			1	1	3.22	1	0.00	1	22	0	0	2.12	11.50	1.97	13.32	1.74	15.14	0.00	0.00
LINCOLN--033	SPRINGSTN033			1	1	4.40	1	0.00	1	22	0	0	2.12	11.50	1.97	13.32	1.74	15.14	0.00	0.00
ADDINGTON066	ADDINGTON066	ISLINGTON066	ISLINGTON066	1	1	8.46	2	0.46	2	5	0	0	1.74	11.50	2.65	13.77	1.74	16.05	0.00	0.00
ADDINGTON066	ADDINGTON066	ISLINGTON066	ISLINGTON066	1	1	8.50	2	0.46	2	5	0	0	1.74	11.50	2.65	13.77	1.74	16.05	0.00	0.00
ARAHURA--066	GREYMOUTH066			1	1	32.61	1	0.00	1	14	0	0	3.03	12.00	2.85	15.27	2.79	18.54	0.00	0.00
ARAHURA--066	HARIHARI-066			1	2	46.80	1	0.00	1	14	0	0	3.23	11.50	0.00	11.50	-3.23	11.50	0.00	0.00
ARAHURA--066	HARIHARI-066			2	2	28.00	1	0.00	1	14	0	0	3.23	11.50	0.00	11.50	-3.23	11.50	0.00	0.00
ARAHURA--066	ARAHURA--066	OTIRA----066	OTIRA----066	1	1	65.50	1	0.00	2	22	0	0	2.12	11.50	1.97	13.32	1.74	15.14	0.00	0.00
ARNOLD---066	DOBSON---066			1	1	14.44	1	0.00	1	28	0	0	1.82	11.50	0.00	11.50	-1.82	11.50	0.00	0.00
ASHLEY---066	SOUTHBRK-066			1	1	12.02	1	0.00	1	8	0	0	2.05	11.50	2.53	14.38	2.05	17.26	0.00	0.00
ASHLEY---066	WAIPARA--066			1	1	27.92	1	0.00	1	8	0	0	2.05	11.50	2.53	14.38	2.05	17.26	0.00	0.00
CAIRNBRAE066	HIGHBANK-066			1	1	12.30	1	0.00	1	25	0	0	1.82	11.50	0.00	11.50	-1.82	11.50	0.00	0.00
COLERIDGE066	HORORATA-066			1	2	7.40	1	0.00	1	23	0	0	0.91	11.50	-0.91	11.50	0.00	13.08	0.00	0.00
COLERIDGE066	HORORATA-066			2	2	44.00	1	0.00	1	21	0	0	0.91	11.50	-0.91	11.50	0.00	13.08	0.00	0.00
COLERIDGE066	COLERIDGE066	HORORATA-066	HORORATA-066	1	2	32.90	1	0.00	2	21	0	0	7.58	11.50	5.76	11.50	6.67	13.08	0.00	0.00
COLERIDGE066	COLERIDGE066	HORORATA-066	HORORATA-066	2	2	14.00	1	0.00	2	21	0	0	1.97	11.50	2.88	14.53	1.97	17.56	0.00	0.00
COLERIDGE066	COLERIDGE066	OTIRA----066	OTIRA----066	1	3	66.00	1	0.00	2	22	0	0	1.35	11.50	1.80	13.32	1.35	15.14	0.00	0.00
COLERIDGE066	COLERIDGE066	OTIRA----066	OTIRA----066	2	3	5.40	1	0.00	2	12	0	0	1.35	11.50	1.80	13.32	1.35	15.14	0.00	0.00
COLERIDGE066	COLERIDGE066	OTIRA----066	OTIRA----066	3	3	11.80	1	0.00	2	22	0	0	2.57	11.50	2.57	14.23	2.57	16.96	0.00	0.00
CULVER-II066	KAIKOURA-066			1	1	84.50	1	0.00	1	14	0	0	2.90	11.50	0.00	11.50	-2.90	11.50	0.00	0.00
CULVER-II066	WAIPARA--066			1	1	39.00	1	0.00	1	5	0	0	5.10	12.50	6.60	18.00	4.60	23.50	0.00	0.00
DOBSON---066	GREYMOUTH066			1	1	8.00	1	0.00	1	14	0	0	3.03	12.00	2.85	15.27	2.79	18.54	0.00	0.00
DILLMANS-066	KUMARA---066			1	1	8.00	1	0.00	1	13	0	0	1.74	11.50	0.02	12.02	-1.74	11.50	0.00	0.00
GREYMOUTH066	KUMARA---066			1	1	23.38	1	0.00	1	26	0	0	1.59	11.50	1.59	13.32	-1.59	11.50	0.00	0.00
HIGHBANK-066	HORORATA-066			1	2	13.87	1	0.00	1	18	0	0	0.91	11.50	0.00	13.08	-0.91	11.50	0.00	0.00
HIGHBANK-066	HORORATA-066			2	2	7.68	1	0.00	1	18	0	0	2.89	11.50	0.00	14.80	-2.89	11.50	0.00	0.00
HORORATA-066	ISLINGTON066			1	3	23.68	1	0.00	1	21	0	0	1.82	11.50	0.00	11.50	-1.82	11.50	0.00	0.00
HORORATA-066	ISLINGTON066			2	3	20.92	1	0.00	1	21	0	0	2.85	11.50	0.00	11.50	-2.85	11.50	0.00	0.00
HORORATA-066	ISLINGTON066			3	3	6.03	1	0.00	1	6	0	0	3.03	11.50	2.85	14.77	2.79	18.04	0.00	0.00
HORORATA-066	ISLINGTON066			1	3	21.72	1	0.00	1	21	0	0	1.59	11.50	0.00	13.62	-1.59	11.50	0.00	0.00
HORORATA-066	ISLINGTON066			2	3	20.48	1	0.00	1	21	0	0	1.82	11.50	0.00	11.50	-1.82	11.50	0.00	0.00
HORORATA-066	ISLINGTON066			3	3	6.03	1	0.00	1	6	0	0	3.03	11.50	2.85	14.77	2.79	18.04	0.00	0.00
HORORATA-066	ISLINGTON066			1	1	45.13	1	0.00	1	21	0	0	1.82	11.50	0.00	11.50	-1.82	11.50	0.00	0.00
HORORATA-066	ISLINGTON066			1	1	45.23	1	0.00	1	21	0	0	1.82	11.50	0.00	11.50	-1.82	11.50	0.00	0.00
ISLINGTON066	ISLINGTON066	PAPANUI--066	PAPANUI--066	1	1	8.71	2	0.46	2	5	0	0	2.73	11.50	3.48	14.23	3.33	16.95	0.00	0.00
ISLINGTON066	ISLINGTON066	PAPANUI--066	PAPANUI--066	1	1	8.71	2	0.46	2	5	0	0	2.73	11.50	3.48	14.23	3.33	16.95	0.00	0.00
ISLINGTON066	ISLINGTON066	SOUTHBRK-066	SOUTHBRK-066	1	2	11.26	1	0.00	2	8	0	0	1.74	11.50	2.65	14.22	1.74	16.05	0.00	0.00
ISLINGTON066	ISLINGTON066	SOUTHBRK-066	SOUTHBRK-066	2	2	14.20	1	0.00	2	8	0	0	2.09	11.50	2.88	14.38	2.09	17.26	0.00	0.00
ISLINGTON066	SOUTHBRK-066			1	2	14.00	2	0.46	1	5	0	0	5.10	12.50	6.60	18.00	4.60	23.50	0.00	0.00
ISLINGTON066	SOUTHBRK-066			2	2	19.07	1	0.00	1	8	0	0	3.10	12.00	-2.95	13.85	2.95	15.70	0.00	0.00
ISLINGTON066	ISLINGTON066	SPRINGSTN066	SPRINGSTN066	1	1	12.80	1	0.00	2	8	0	0	1.74	11.50	2.65	14.22	1.74	16.05	0.00	0.00
KAIAPOI--066	KAIAPOI--066	SOUTHBRK-066	SOUTHBRK-066	1	1	7.10	1	0.00	2	12	0	0	1.74	11.50	2.65	14.22	1.74	16.05	0.00	0.00
SOUTHBRK-066	WAIPARA--066			1	1	34.60	1	0.00	1	8	0	0	2.05	11.50	2.53	14.38	2.05	17.26	0.00	0.00
ALBURY---110	TEKAPO---110			1	1	39.40	1	0.00	1	21	0	0	3.85	12.00	0.00	12.00	-3.85	12.00	0.00	0.00
ALBURY---110	TIMARU---110			1	1	39.50	1	0.00	1	21	0	0	1.90	12.00	0.00	14.73	-1.90	12.00	0.00	0.00
ASHBURTON110	HORORATA1110			1	2	43.66	1	0.00	1	21	0	0	1.90	12.00	1.90	14.73	-1.90	14.73	0.00	0.00
ASHBURTON110	HORORATA1110			2	2	5.16	1	0.00	1	15	0	0	1.90	12.00	1.90	14.73	-1.90	14.73	0.00	0.00
ASHBURTON110	HORORATA2110			1	2	6.27	1	0.00	1	21	0	0	1.90	12.00	1.90	14.73	-1.90	14.73	0.00	0.00
ASHBURTON110	HORORATA2110			2	2	42.76	1	0.00	1	15	0	0	1.90	12.00	1.90	14.73	-1.90	14.73	0.00	0.00
ASHBURTON110	TEMUKA---110			1	2	22.30	1	0.00	1	15	0	0	9.09	12.00	5.30	12.00	9.09	14.73	0.00	0.00
ASHBURTON110	TEMUKA---110			2	2	34.20	1	0.00	1	21	0	0	9.09	12.00	5.30	12.00	9.09	14.73	0.00	0.00
ASHBURTON110	TIMARU---110			1	3	45.10	1	0.00	1	15	0	0	9.09	12.00	5.30	12.00	9.09	14.73	0.00	0.00
ASHBURTON110	TIMARU---110			2	3	11.50	1	0.00	1	21	0	0	9.09	12.00	5.30	12.00	9.09	14.73	0.00	0.00
ASHBURTON110	TIMARU---110			3	3	18.80	1	0.00	1	21	0	0	9.09	12.00	5.30	12.00	9.09	14.73	0.00	0.00
STUDHOLM-110	TIMARU---110			1	1	48.50	1	0.00	1	15	0	0	1.93	12.00	-1.93	12.00	1.93	14.73	0.00	0.00
TEMUKA---110	TIMARU---110			1	1	18.20	1	0.00	1	21	0	0	9.09	12.00	5.30	12.00	9.09	14.73	0.00	0.00
BROMLEY--220	BROMLEY--220	BRO-TWI-TEMP	ISL-BRO-TEMP	1	1	20.37	2	0.46	2	5	0	0	5.15	12.50	4.80	18.00	4.72	23.50	0.00	0.00
ISLINGTON220	ISLINGTON220	ISL-TWI-TEMP	ISL-BRO-TEMP	1	1	7.58	2	0.46	2	5	0	0	5.15	12.50	4.80	18.00	4.72	23.50	0.00	0.00

TABLE A3.4: Dunedin District

Busbar Names				A	B	C	D	E	F	G	H	I	J	K	L	M	N	O	P	Q
CROMWELL-033	CROMWELL-033	FRANKTON-033	FRANKTON-033	1	1	44.40	1	0.00	2	8	0	0	3.26	12.00	4.31	15.40	3.08	19.01	0.00	0.00
HILLSIDE-066	MONOWAI--066			1	1	41.50	1	0.00	1	17	0	0	1.21	11.50	0.00	11.83	-1.21	11.50	0.00	0.00
MONOWAI--066	OHAI-----066			1	1	29.80	1	0.00	1	27	0	0	1.74	11.50	0.00	12.02	-1.74	11.50	0.00	0.00
OHAI-----066	ORAWIA---066			1	1	22.00	1	0.00	1	17	0	0	1.74	11.50	0.00	12.02	-1.74	11.50	0.00	0.00
OHAI-----066	WINTON---066			1	1	41.60	1	0.00	1	27	0	0	1.76	11.50	0.00	12.02	-1.76	11.50	0.00	0.00
BALCLUTHA110	GORE-----110			1	1	80.20	1	0.00	1	21	0	0	3.83	12.00	0.00	12.00	-3.83	12.00	0.00	0.00
BALCLUTHA110	BERWICK--110			1	1	52.20	1	0.00	1	21	0	0	3.83	12.00	0.00	12.00	-3.83	12.00	0.00	0.00
BERWICK--110	HALFWAYBU110			1	1	36.60	1	0.00	1	21	0	0	3.83	12.00	0.00	12.00	-3.83	12.00	0.00	0.00
BERWICK--110	WAIPORI--110			1	1	7.20	1	0.00	1	21	0	0	3.83	12.00	0.00	12.00	-3.83	12.00	0.00	0.00
EDENDALE-110	GORE-----110			1	1	26.00	1	0.00	1	21	0	0	3.83	12.00	0.00	12.00	-3.83	12.00	0.00	0.00
EDENDALE-110	INVOPEN--110			1	1	31.07	1	0.00	1	21	0	0	3.83	12.00	0.00	12.00	-3.83	12.00	0.00	0.00
GLENAVY--110	OAMARU---110			1	1	26.90	1	0.00	1	15	0	0	1.92	12.00	-1.92	12.00	1.92	14.73	0.00	0.00
GLENAVY--110	OAMARU---110			1	1	26.50	1	0.00	1	21	0	0	3.83	12.00	0.00	12.00	-3.83	12.00	0.00	0.00
GLENAVY--110	STUDHOLM-110			1	1	21.70	1	0.00	1	15	0	0	1.93	12.00	-1.93	12.00	1.93	14.73	0.00	0.00
GLENAVY--110	TIMARU---110			1	1	70.00	1	0.00	1	21	0	0	1.93	12.00	-1.93	12.00	1.93	14.73	0.00	0.00
GLENAVY--110	GLENAVY--110	WAITAKI--110	WAITAKI--110	1	1	60.80	1	0.00	2	8	0	0	3.03	12.00	3.94	15.33	3.03	18.66	0.00	0.00
GORE-----110	ROXBURGH-110			1	1	84.20	1	0.00	1	8	0	0	3.83	12.00	0.00	12.00	-3.83	12.00	0.00	0.00
HALFWAYBU110	OAMARU---110			1	1	99.80	1	0.00	1	8	0	0	3.83	12.00	0.00	12.00	-3.83	12.00	0.00	0.00
HALFWAYBU110	PALMERSTN110			1	1	45.80	1	0.00	1	8	0	0	3.83	12.00	0.00	12.00	-3.83	12.00	0.00	0.00
HALFWAYBU110	HALFWAYBU110	ROXBURGH-110	ROXBURGH-110	1	1	126.20	1	0.00	2	8	0	0	2.88	12.00	3.94	16.55	2.88	21.10	0.00	0.00
INVERCARG110	WINTON---110			1	1	29.40	1	0.00	1	8	0	0	3.79	12.00	0.00	12.00	-3.79	12.00	0.00	0.00
PALMERSTN110	OAMARU---110			1	1	55.00	1	0.00	1	21	0	0	3.83	12.00	0.00	12.00	-3.83	12.00	0.00	0.00
AVIEMORE-220	AVIEMORE-220	BENMORE--220	BENMORE--220	1	1	17.44	1	0.00	2	6	2	29	3.56	12.50	3.56	19.17	3.56	25.80	1.20	32.20
AVIEMORE-220	LIVINGSTN220			1	1	39.80	1	0.00	1	6	0	0	7.58	12.50	0.00	12.50	-7.58	12.50	0.00	0.00
BENMORE--220	OHAU-B---220			1	1	34.10	2	0.36	1	6	2	29	6.97	12.50	0.00	12.50	-6.97	12.50	4.47	18.65
BENMORE--220	OHAU-C---220			1	1	36.70	2	0.36	1	6	2	29	6.97	12.50	0.00	12.50	-6.97	12.50	4.47	18.65
BENMORE--220	TWIZEL---220			1	1	46.10	2	0.36	1	6	2	29	6.97	12.50	0.00	12.50	-6.97	12.50	4.47	18.65
HALFWAYBU220	DUN-ROX-TEMP	ROXBURGH-220	ROXBURGH-220	1	1	104.50	2	0.46	2	5	0	0	5.10	12.50	6.60	18.00	4.60	23.50	0.00	0.00
HALFWAYBU220	DUN-ROX-TEMP	SOUTHDUN-220	SOUTHDUN-220	1	2	9.40	1	0.00	2	5	1	36	5.00	12.50	4.70	18.20	4.60	23.90	0.00	29.50
HALFWAYBU220	DUN-ROX-TEMP	SOUTHDUN-220	SOUTHDUN-220	2	2	2.60	1	0.00	2	5	1	36	3.78	12.50	3.78	18.00	3.78	23.50	0.00	29.00
HALFWAYBU220	HALFWAYBU220	MAKAREWA-220	MAKAREWA-220	1	1	208.00	2	0.45	2	6	1	32	4.80	12.50	6.34	18.00	4.42	23.50	0.00	29.00
INVERCARG220	INVERCARG220	MANAPOURI220	MANAPOURI220	1	1	145.90	2	0.46	2	6	1	32	4.80	12.50	6.33	17.99	4.42	23.50	0.00	28.94
INVERCARG220	ROXBURGH-220			1	1	132.20	1	0.00	1	5	2	31	6.47	12.50	0.00	12.50	-6.47	12.50	4.61	18.41
INVERCARG220	ROXBURGH-220			1	1	129.40	1	0.00	1	5	0	0	7.20	12.50	0.00	12.50	-7.20	12.50	0.00	0.00
INVERCARG220	INVERCARG220	TIWAI----220	TIWAI----220	1	1	24.30	2	0.46	2	6	2	36	4.77	12.50	6.29	17.95	4.41	23.41	1.52	28.26
ISLINGTON220	LIVINGSTN220			1	3	119.00	2	0.46	1	6	0	0	7.62	12.50	0.00	12.50	-7.62	12.50	0.00	0.00
ISLINGTON220	LIVINGSTN220			2	3	33.50	1	0.00	1	6	0	0	7.62	12.50	0.00	12.50	-7.62	12.50	0.00	0.00
ISLINGTON220	LIVINGSTN220			3	3	84.00	1	0.00	1	6	0	0	7.62	12.50	0.00	12.50	-7.62	12.50	0.00	0.00
ISLINGTON220	TEKAPO-B-220			1	1	213.50	2	0.36	1	6	2	29	6.97	12.50	0.00	12.50	-6.97	12.50	4.47	18.65
ISL-TWI-TEMP	BRO-TWI-TEMP	TWIZEL---220	TWIZEL---220	1	1	215.84	2	0.46	2	5	0	0	5.15	12.50	4.80	18.00	4.72	23.50	0.00	0.00
LIVINGSTN220	NASEBY---220			1	1	48.20	1	0.00	1	6	0	0	7.58	12.50	0.00	12.50	-7.58	12.50	0.00	0.00
MAKAREWA-220	MAKAREWA-220	TIWAI----220	TIWAI----220	1	1	38.20	2	0.45	2	6	1	32	4.80	12.50	6.34	18.00	4.42	23.50	0.00	29.00
MAKAREWA-220	MAKAREWA-220	MANAPOURI220	MANAPOURI220	1	1	128.10	2	0.45	2	6	1	32	4.80	12.50	6.34	18.00	4.42	23.50	0.00	29.00
NASEBY---220	ROXBURGH-220			1	1	94.10	1	0.00	1	6	0	0	7.58	12.50	0.00	12.50	-7.58	12.50	0.00	0.00
OHAU-A---220	OHAU-A---220	TWIZEL---220	TWIZEL---220	1	1	7.93	1	0.00	2	5	0	0	5.10	12.50	6.60	18.00	4.60	23.50	0.00	0.00
OHAU-B---220	TWIZEL---220			1	1	4.80	2	0.46	1	5	0	0	5.40	12.50	7.25	18.90	5.00	25.30	0.00	0.00
OHAU-C---220	TWIZEL---220			1	1	12.20	2	0.46	1	5	0	0	5.40	12.50	7.25	18.90	5.00	25.30	0.00	0.00
ROXBURGH-220	ROXBURGH-220	CROMWELL1220	CROMWELL2220	1	1	53.02	1	0.00	2	5	0	0	4.80	12.50	6.33	17.99	4.42	23.48	0.00	0.00
CROMWELL1220	CROMWELL2220	TWIZEL---220	TWIZEL---220	1	1	118.60	1	0.00	2	5	0	0	4.80	12.50	6.33	17.99	4.42	23.48	0.00	0.00
TEKAPO-B-220	TWIZEL---220			1	1	24.80	2	0.36	1	6	2	29	6.97	12.50	0.00	12.50	-6.97	12.50	4.47	18.65

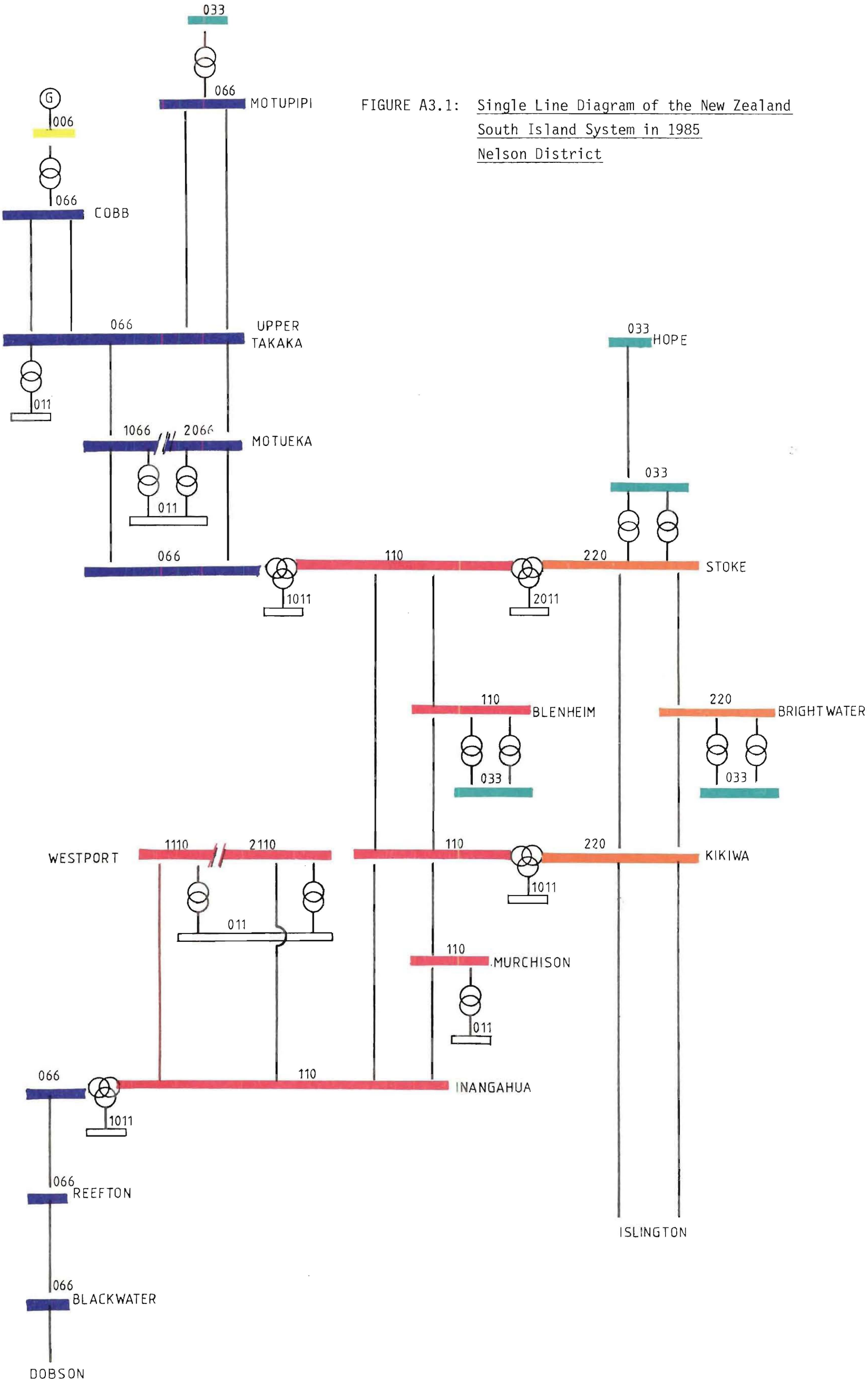

FIGURE A3.1: Single Line Diagram of the New Zealand South Island System in 1985 Nelson District

FIGURE A3.1: Single Line Diagram of the New Zealand South Island System in 1985 Christchurch District

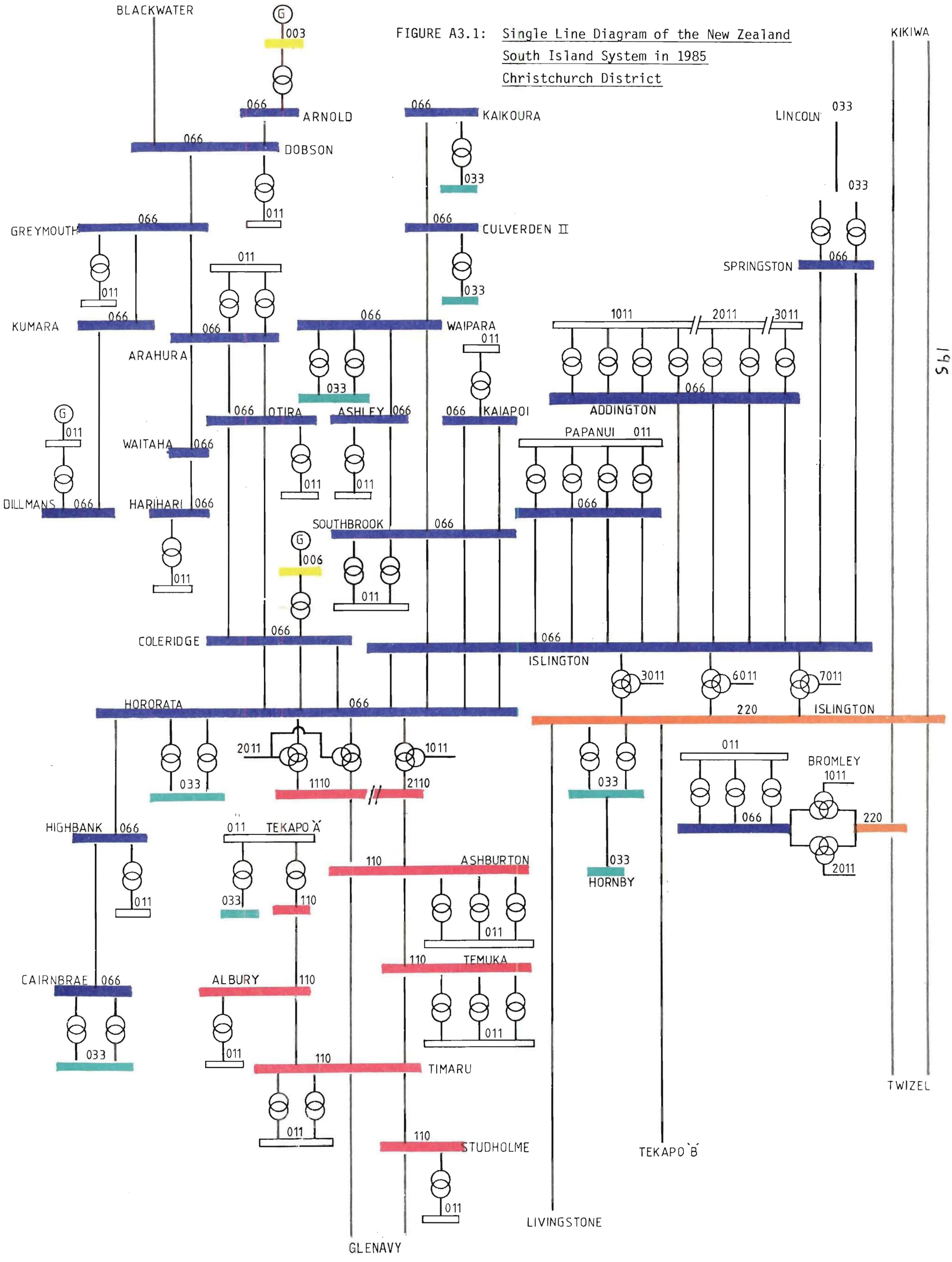

FIGURE A3.1: Single Line Diagram of the New Zealand South Island System in 1985. Dunedin District

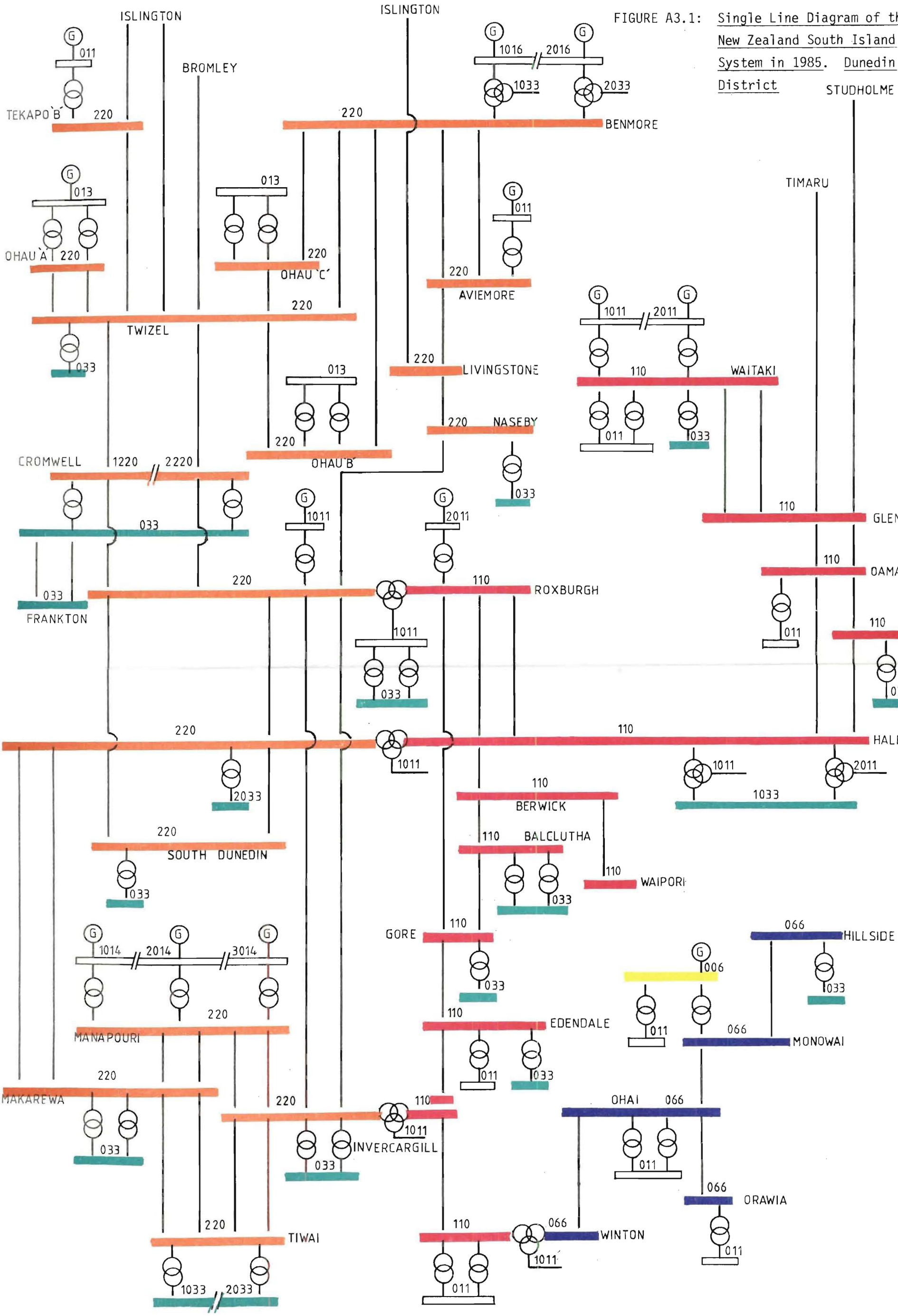

APPENDIX 4

83 WM 168-2

ZERO SEQUENCE HARMONIC CURRENT GENERATION IN TRANSMISSION LINES CONNECTED TO LARGE CONVERTOR PLANT

J. Arrillaga, Non Member
University of Canterbury,
Christchurch, New Zealand

T.J. Densem, Student Member

B.J. Harker, Non Member
New Zealand Electricity

Abstract - Although the bridge-type convertor produces only positive and negative sequence harmonic currents, the coupling between sequence networks resulting from ac transmission asymmetries can cause considerable zero sequence interference in nearby power or communications lines. This paper discusses the modelling of ac system and convertor plant components needed to assess the level of zero sequence harmonic current generation in transmission lines connected to large convertor plant.

INTRODUCTION

The decision as to whether line transpositions should be used in a particular transmission line is normally made purely in terms of power frequency voltage unbalance. However, owing to the high cost of transpositions the levels of asymmetry permitted are often high. While this policy may be acceptable in cases of lines loaded exclusively by conventional ac power plant, the effect of line asymmetry on the behaviour of convertor plant requires special consideration, both at fundamental and harmonic frequencies.

In fundamental frequency ac/dc power flow the effect of line asymmetry can only be assessed by detailed representation of the ac transmission network in the phase frame of reference, with mutual effects included, as well as three-phase analysis of the convertor operation.[1][2] Even when the analysis is restricted to purely sinusoidal voltages the line and convertor voltage asymmetry is shown to produce phase currents of varying widths containing uncharacteristic harmonic frequencies for which filtering is not normally provided.

Measurements of the harmonic currents at the rectifier end of the New Zealand dc link have shown deviations between phases of up to 56% (at 450 Hz) with an average deviation of 35%. The combined effect of the current unbalance and any system impedance unbalance is reflected in the phase voltages, which are shown in Table I for the Benmore 220 kV busbar [3]. All harmonic voltages are unbalanced with the most severe unbalance occurring at the non-characteristic third and ninth harmonics. Although unbalanced, the current injections at the convertor itself consist purely of positive and negative sequence components as there is no zero sequence path for the convertor currents.

On the other hand, the level of electromagnetic interference from power transmission lines is mainly determined by the zero sequence current components of the interfering source, which in the case of a bridge convertor loaded line must be entirely due asymmetric conditions on the ac system.

While the line distance may not be sufficient to cause unacceptable fundamental frequency zero-sequence voltage unbalance, the 'electrical distance' at harmonic frequencies will increase proportionally to their orders. Consequently the line asymmetry is expected to have a greater effect at harmonic frequencies.

83 WM 168-2 A paper recommended and approved by the IEEE Transmission and Distribution Committee of the IEEE Power Engineering Society for presentation at the IEEE/PES 1983 Winter Meeting, New York, New York, January 30-February 4, 1983. Manuscript submitted September 3, 1982; made available for printing January 6, 1983.

Table I - Harmonic Measurements during Back-to-Back Testing of the New Zealand dc Link

Harmonic	400 A dc (one third full load current) Phase-to-neutral voltages At Benmore 220 kV		
	Red phase (%)	Yellow phase (%)	Blue phase (%)
1	100	100	100
2	0.5	0.7	1.0
3	2.9	0.3	1.0
4	0.6	0.3	0.4
5	0.25	0.15	0.25
6	0.25	0.30	0.35
7	0.15	0.15	0.1
8	0	0.05	0.1
9	0.05	0.05	0.15
10	0.05	0.05	0.05
11	0.1	0.15	0.1
12	0.15	0.05	0.15
13	0.05	0.05	0.05
14	0.05	0.05	0.05
15	0.15	0	0.2
16	0	0.1	0.15
17	0.3	0.3	0.3
18	0	0.05	0.1
19	0.3	0.3	0.7

The results of tests carried out in an out-of-service 220 kV transmission line (between Islington and Kikiwa in the New Zealand system) are shown in Table II. The induced harmonic voltages were caused by electromagnetic coupling with a parallel transmission line which was in service at the time of measurement; this line is over one hundred km away from the nearest convertor station. The zero sequence harmonic currents in the in-service line are also listed in Table II.

These currents and voltages were measured using existing station current transformers, which are considered reasonably accurate at the frequencies measured (i.e. within 1.5%), and a Selective Audio Frequency Power Analyser [4]. The Phase to Phase voltages were very small indicating that the induced voltages were of zero sequence.

Table II - Measurements of Induced Voltages in Parallel Transmission Line

Harmonic Order	Zero Sequence Current (In-Service Line) (Amps)	Induced Voltages (Volts) (Out-of-Service)		
		VR	VY	VB
1	2.186	170	165	170
3	0.45	9	9	9
5	0.106	38	38	38
7	0.186	9	9	9
9	0.30	10	10	10

In the following sections this paper describes a mathematical model for the assessment of harmonic penetration along transmission lines and its application to the determination of the zero sequence harmonic currents developed along transmission lines as a result of positive or negative sequence current injection from large static convertors.

CONVERTOR PLANT MODELS AT HARMONIC FREQUENCIES

The convertor bridge produces varying degrees of harmonic currents and can be represented as a source of positive and negative sequence harmonic currents. Although the convertor cannot generate zero sequence currents, any asymmetries in the ac system parameters will give rise to interaction between the sequence networks. Therefore in harmonic penetration studies the ac plant components at the convertor terminals must be modelled in detail as part of the ac system.

Convertor Transformers

The transformer models developed at fundamental frequency can also be used in harmonic studies, except for the values of damping resistance and leakage reactance.

In general a two-winding three-phase transformer has a primitive, or unconnected, network consisting of six coupled coils and is thus modelled as a six by six admittance matrix. Considering the reciprocal nature of the mutual couplings, the complete model requires twenty one short-circuit tests. If the magnetic asymmetry is ignored only two tests are required, i.e. a positive-sequence and a zero-sequence short-circuit tests.

The transformer nodal admittance matrix is in each case derived from the primitive admittance by the expression

$$[Y]_{node} = [C]^t\,[Y]_{PRIM}\,[C]$$

where [C], the connection matrix, is derived from consideration of the actual transformer connections.

Of the two common convertor transformer connections only the star-g/delta provides a path for any zero sequence currents developed in the ac system. The node admittance matrix for this transformer connection (on the assumption of single phase units) is

$$[Y]_{node} = \begin{bmatrix}
\frac{Y_{t1}}{a_1^2} & & & -\frac{Y_{t1}}{\sqrt{3}\,a_1} & \frac{Y_{t1}}{\sqrt{3}\,a_1} & \\
 & \frac{Y_{t2}}{a_2^2} & & & -\frac{Y_{t2}}{\sqrt{3}\,a_2} & \frac{Y_{t2}}{\sqrt{3}\,a_2} \\
 & & \frac{Y_{t3}}{a_3^2} & \frac{Y_{t3}}{\sqrt{3}\,a_3} & & -\frac{Y_{t3}}{\sqrt{3}\,a_3} \\
\frac{-Y_{t1}}{\sqrt{3}\,a_1} & & \frac{Y_{t3}}{\sqrt{3}\,a_3} & \frac{Y_{t1}+Y_{t3}}{3} & -\frac{Y_{t1}}{3} & -\frac{Y_{t3}}{3} \\
\frac{Y_{t1}}{\sqrt{3}\,a_1} & \frac{-Y_{t2}}{\sqrt{3}\,a_2} & & -\frac{Y_{t1}}{3} & \frac{Y_{t2}+Y_{t1}}{3} & -\frac{Y_{t2}}{3} \\
 & \frac{Y_{t2}}{\sqrt{3}\,a_2} & \frac{-Y_{t3}}{\sqrt{3}\,a_3} & -\frac{Y_{t3}}{3} & -\frac{Y_{t2}}{3} & \frac{Y_{t2}+Y_{t3}}{3}
\end{bmatrix}$$

which is sufficiently general to investigate the effect of small asymmetries in the single-phase transformer units due either to leakage admittances (Y) or off-nominal taps (a). If the three single phase units are perfectly symmetrical the equivalent circuit for the star-g/delta connection (unity tap ratio) is as shown in Fig. 1.

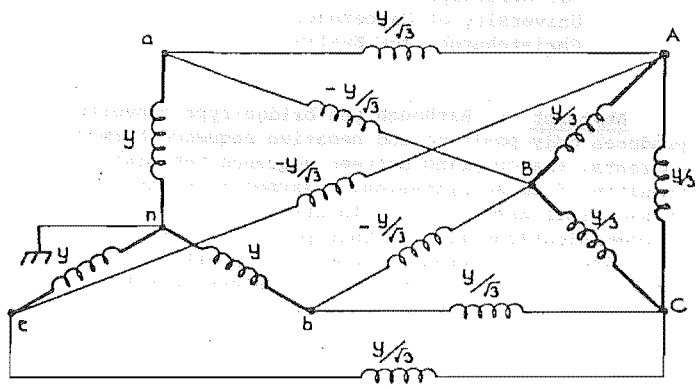

Fig. 1. Equivalent circuit for symmetrical star-g/delta transformer (unity tap ratio)

At harmonic frequencies it is recommended that the leakage inductance component of the admittance matrix is paralleled by a resistance. A recent CIGRE Working Group [5] has suggested the following range to match experimental results:

$$13 < \frac{S_N\,R_P}{U_N^2} < 30$$

where R_P is the parallel resistance in ohms

S_N is the power rating

and U_N is the voltage rating

The resistance variation with frequency, shown in Fig. 2, increases significantly with frequency while the inductance decreases only slightly with frequency.

Convertor Filters

The ac filter branches contribute to the shunt admittance of the convertor busbar to which they are connected. Moreover they are often the cause of parallel resonances at non characteristic convertor harmonic frequencies and therefore must be represented in detail.

Typical equivalent circuits, for each phase, of single-tuned and high-pass filters are illustrated in Fig. 3.

TRANSMISSION LINE MODELS AT HARMONIC FREQUENCIES

Nominal π models are of general use in fundamental frequency studies to represent single phase transmission

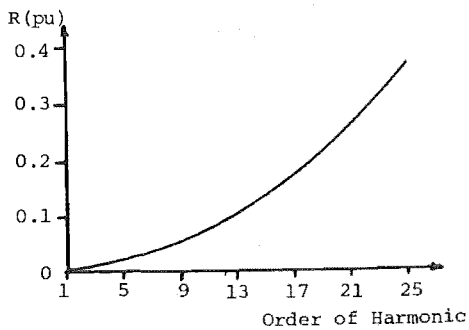

Fig. 2. Frequency dependence of transformer model

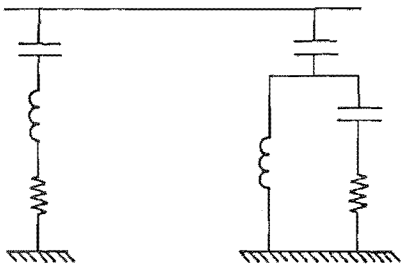

Fig. 3. HVDC shunt filter types

lines.

For a given transmission distance the number of π sections to be used will depend on the level of accuracy required at the line terminals: e.g. a three-section model provides 1.2% accuracy for a quarter wave-length line.

As the frequency increases the number of Nominal π sections to maintain a particular accuracy increases proportionally; e.g. a 300 km long line requires 30 nominal π sections to maintain the above accuracy for the 50th harmonic.

The computational effort can be greatly reduced and the accuracy improved with the use of an Equivalent π model derived from the solution of the second order linear differential equations describing wave propagation along transmission lines [6]. Such a model, illustrated in Fig. 4, is obtained from the Nominal π model by using two correction factors, i.e.

$$\frac{\sinh(x\sqrt{Z'Y'})}{x\sqrt{Z'Y'}} \quad \text{for the series impedance}$$

$$\frac{\tanh(x\sqrt{Z'Y'}/2}{x\sqrt{Z'Y'}/2} \quad \text{for the shunt admittance}$$

where Z' and Y' are the series impedance and shunt admittance per km respectively.

Multiconductor Transmission Lines

In the case of multiconductor transmission lines the Nominal π series impedance and shunt admittance matrices per km, $[Z']$ and $[Y']$ respectively are square, their size being fixed by the number of mutually coupled conductors.

The formulation used in the derivation of the series and shunt matrix elements [7][8] is described in Appendix (i).

The derivation of the Equivalent π model from the Nominal π matrices involves the evaluation of hyperbolic functions of a matrix. For such evaluation the matrix must be diagonal.

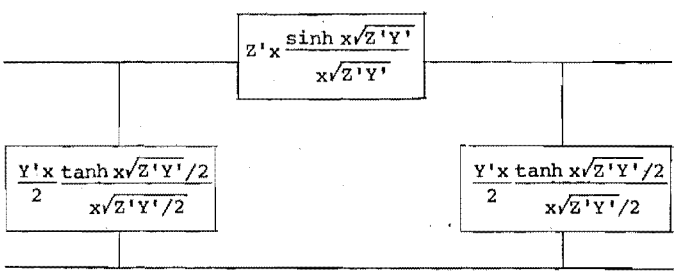

Fig. 4. The equivalent PI model

However the matrix involved:

$$\psi = ([Y'][Z'])^{\frac{1}{2}}$$

is not diagonal and therefore a transformation is required. The use of eigenvalue analysis results in the following expressions for the Equivalent π Model [9]:

$$[Z]_{EPM} = x[Z'][M]\left[\frac{\sinh(\gamma x)}{(\gamma x)}\right][M]^{-1}$$

where x is the transmission line length

$[Z]_{EPM}$ is the Equivalent π series impedance matrix

$[M]$ is the matrix of normalized eigenvectors

$$\left[\frac{\sinh(\gamma x)}{(\gamma x)}\right] = \begin{array}{|c|c|c|}\hline \frac{\sinh(\gamma_1 x)}{(\gamma_1 x)} & 0 & 0 \\ \hline 0 & \frac{\sinh(\gamma_2 x)}{(\gamma_2 x)} & 0 \\ \hline 0 & 0 & \frac{\sinh(\gamma_3 x)}{(\gamma_3 x)} \\ \hline \end{array}$$

and γ_j is the jth eigenvalue

Similarly

$$[Y]_{EPM} = x[M]\left[\frac{\tanh(\gamma x/2)}{\gamma x/2}\right][M]^{-1}[Y']$$

where $[Y]_{EPM}$ is the Equivalent π shunt admittance matrix.

A clear illustration of the relative accuracies achieved by the Equivalent and Nominal π equivalent circuits is displayed in Fig. 5. The figure shows the per unit positive sequence voltages of a 230 km 220 kV line (for parameter information refer to Appendix (iii). The line, when open-circuited, has a half-wavelength frequency close to 650 Hz; the standing wave effect at this frequency clearly shows the different accuracies provided by the two models, with the voltage magnitudes approaching those of the Equivalent π model as the Nominal π model increases from 10 to 20 sections.

The difference is larger than expected because of the accumulation of round-off error over a number of sections and the sensitivity of the physical system near resonance.

The derivation of correction factors for conversion from Nominal π to Equivalent π and their incorporation into the series impedance and shunt admittance matrices

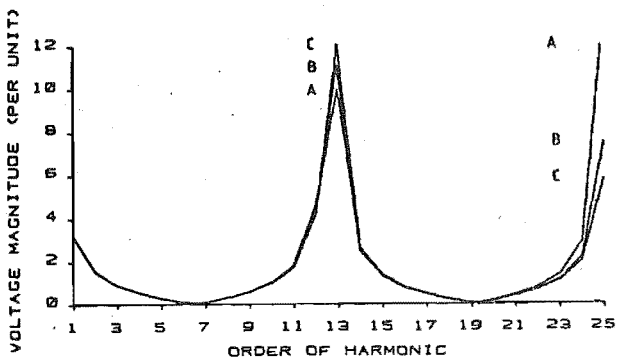

Fig. 5. Comparison of Equivalent and Nominal 'π' models

A - 10 Nominal 'π' Sections C - Equivalent 'π'

B - 20 Nominal 'π' Sections

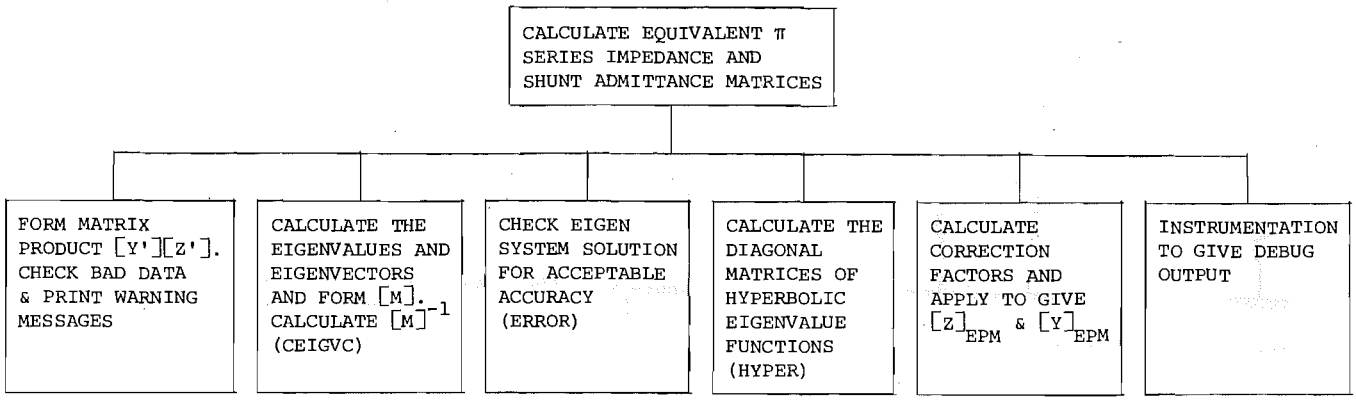

Fig. 6. Structure diagram

is carried out as indicated in the structure diagram of Fig. 6. The LRs algorithm of Wilkinson and Reinsch [10] is used with due regard for accurate calculations in the derivation of the eigenvalues and eigenvectors.

Earth Resistivity and Skin Effects

Although the value of earth resistivity remains a source of considerable conjecture, the phase voltage magnitudes are not sensitive to changes in this parameter under normal steady state loading conditions.

The formulation of the skin effect, as derived by Chipman [11] has been included in the programme and the effect of its incorporation in the model of the test line (Appendix (iii)) is illustrated in Fig. 7. Due to the relatively small value of the series resistance, the skin effect is insignificant at non-resonant frequencies. At frequencies close to resonance, however, the real and imaginary components of the line parameters are of the same order of magnitude and modelling skin effect is important.

The presence of mutual coupling between phases affects the resonant peak levels and each phase has a different resonant frequency. In Fig. 7. the ratio of the open circuit voltages without and with skin effect representation at 650 Hz is 1.1 on phase 3. This ratio appears to be significantly lower than the skin effect ratio of 1.83 predicted by consideration of the conductor resistance alone. The reason is that the resonant frequency of the line and phase under investigation is closer to 637 Hz. By altering the line length from 230 to 225 km the resonant frequency for phase 3 gets closer to 650 Hz and comparative results, illustrated in Fig. 8, show the different effect of phases 1 (ratio 1.63) and 3 (ratio 1.80).

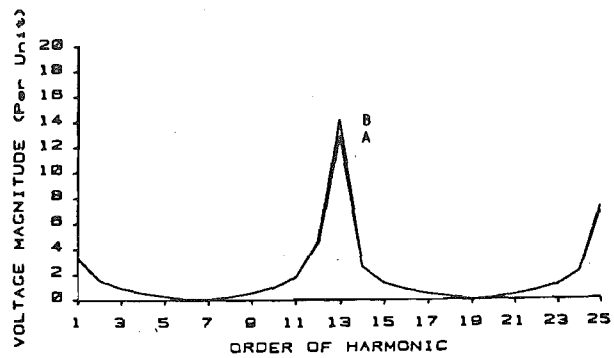

Fig. 7. Phase-3 voltages with (A) and without (B) skin effect

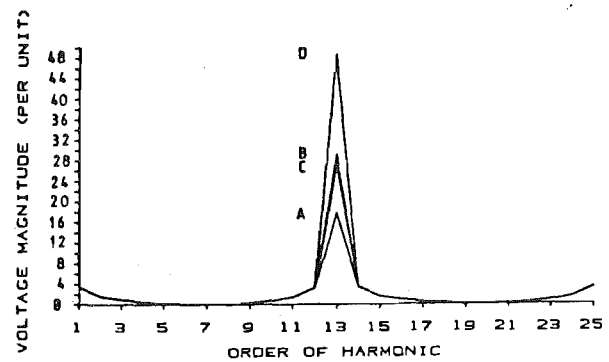

Fig. 8. Skin effect on different phases of open-ended line

Phase 1	Phase 3
A - with skin effect	C - with skin effect
B - without skin effect	D - without skin effect

APPLICATION OF THE COMPUTER MODEL

Zero Sequence Harmonic Currents Generated in Transmission Lines

The Islington-Kikiwa line of the New Zealand system, described in Appendix (iii), has been used to test the computer model described in previous sections.

A three-dimensional graphic representation has been developed to provide simultaneous information of the harmonic levels along the line; at each frequency one per unit current of positive sequence (up to the 25th harmonic) is injected at the Islington end of the line.

Figs. 9 and 10 illustrate the effect of two extreme cases of line termination (at Kikiwa), i.e. with the line open-circuited and short-circuited respectively. The differences in positive sequence current harmonic magnitudes along the line are remarkable; these are due to standing wave effects and shifting of the resonant frequencies caused by the line termination.

However it is the zero sequence, rather than the positive sequence penetration, that provides relevant information for the assessment of possible harmonic interference in neighbouring telephone systems at various locations.

The zero sequence harmonic currents produced by the coupling of sequence networks along the line are illustrated in Figs. 11 and 12; these are produced by the same positive sequence current injections (i.e. one p.u.) as in Figs. 9 and 10.

The locations of maximum zero sequence current appear to coincide with those of the positive sequence, and the highest level produced in the test line, about 10% of the injected positive current, occurs at the 19th harmonic at the far end of the short-circuited line.

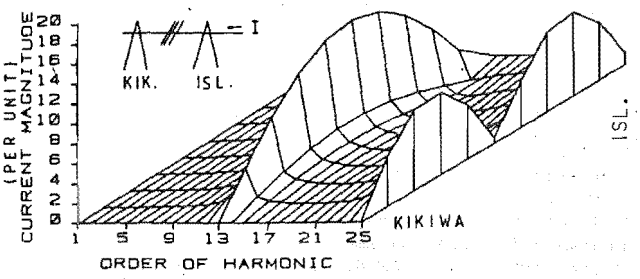

Fig. 9. Positive sequence currents along the open-ended line

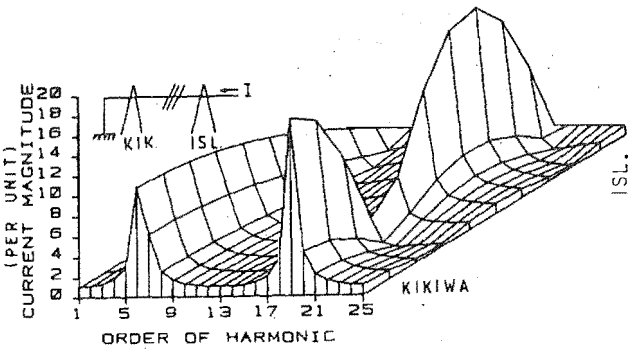

Fig. 10. Positive sequence currents along the short-circuited line

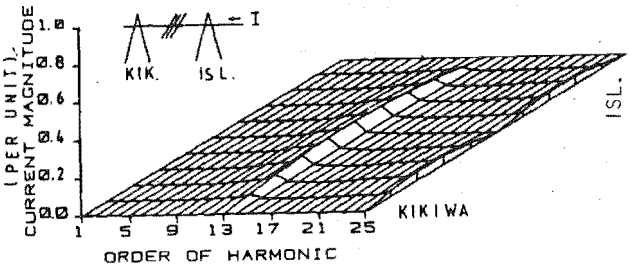

Fig. 11. Zero sequence currents along the open-ended line

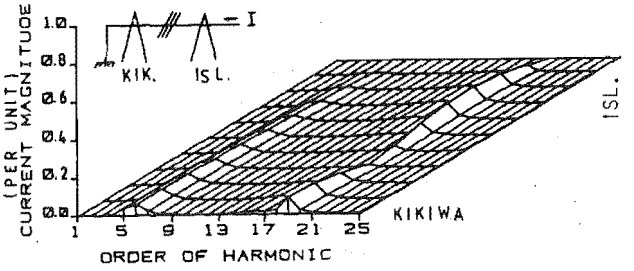

Fig. 12. Zero sequence currents along the short-circuited line

Zero Sequence Harmonics in Transmission Lines Connected to Static Convertors

As indicated earlier the presence of zero sequence in a transmission line connected to a convertor bridge is entirely due to asymmetries in either the convertor ac plant components or the transmission line itself.

The results in this section illustrate the generation of zero sequence currents along the test line when the line is connected to a convertor station which includes a star-delta convertor transformer and harmonic filters. The transformer and filter models of Figures 1 and 3 are used together with the transmission line and the one per unit positive sequence harmonic current is now injected by the convertor bridge into the secondary (valve side) of the transformer.

In the absence of filters, the zero-sequence harmonic current distribution along the transmission line is illustrated in Fig. 13.

The effect of the convertor transformer can be assessed by comparing the results of Figures 11 and 13. The transformer has little effect on the positive and zero sequence harmonic voltages produced by the positive sequence current injection. However, the provision of a low impedance zero sequence path, due to the transformer delta connection, increases substantially the generation of zero sequence harmonic current. This is illustrated by the larger content of 13th harmonic current in Fig. 13.

In practical convertor installations the filters reduce the harmonic current injection into the system considerably. The smaller current injections thus produce considerably less zero sequence in the ac system. This can be observed in Fig. 14, where filters for the characteristic harmonics have been connected to the Islington bus. The levels are particularly low at 5th, 7th, 11th, 13th and above the 17th harmonic, corresponding to the filter design frequencies.

By adjusting the terminating impedance at the Kikiwa end of the line it is possible to excite a parallel resonance at a low frequency between the line (inductive) and the filters (capacitive). In the test case this effect can only be shown at second harmonic (Fig. 15).

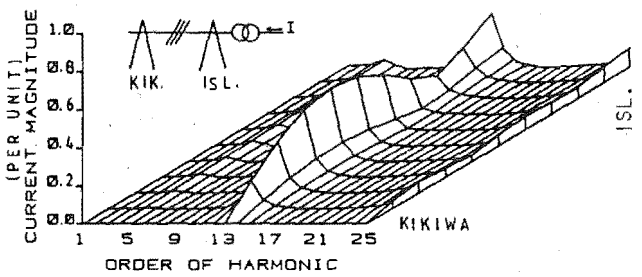

Fig. 13. Zero sequence currents, open-ended line fed from convertor transformer

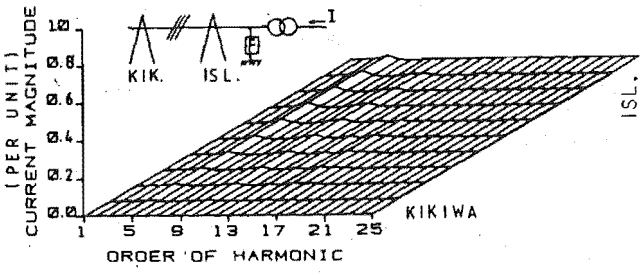

Fig. 14. Zero sequence currents in the presence of convertor transformer and filters

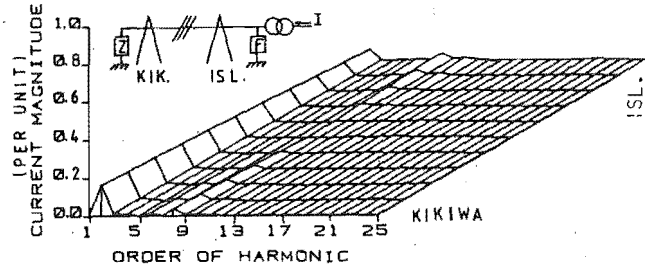

Fig. 15. Zero sequence currents with parallel resonance at 2nd harmonic between line and filters

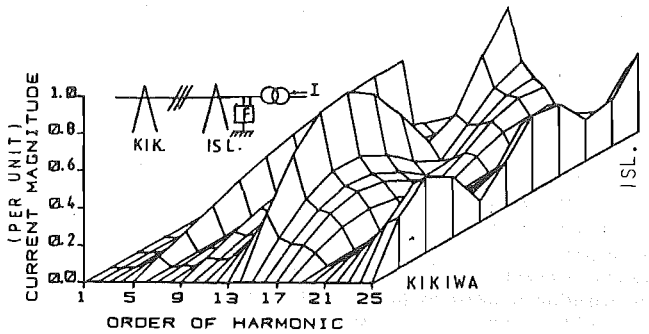

Fig. 16. Zero sequence currents, open-ended line and one filter phase disconnected

Finally, Fig. 16 illustrates the effect of a large unbalance, e.g. an open circuited phase in the filter bank. The pronounced coupling between sequence networks, in this case, gives rise to considerable levels of zero sequence harmonic currents, with the highest level occurring at the 14th harmonic.

CONCLUSIONS

A computer model has been developed to investigate the coupling between the positive and zero sequence circuits of asymmetrical transmission lines and the generation of zero sequence currents from convertor-injected harmonic currents.

Depending on line distance and standing wave effects the levels of zero sequence harmonic currents generated need to be given detailed consideration to calculate interference levels at various locations along the line.

Considering the difficulty and cost of harmonic monitoring at intermediate locations, this programme can be of assistance in the determination of interfering harmonic levels at different locations when telephone systems are being considered. It has been shown that skin effect has considerable influence in the harmonic levels under resonant conditions.

Particular importance has been given to the presentation of results in a three-dimensional graphical form to obtain the necessary information simultaneously.

Although the discussion has been confined to single circuit lines, the model has provision for multiple circuits, multiple sections and any system configuration.

The difficulties and uncertainty associated with harmonic investigations should not be underestimated; in particular the lack of reliable three phase system data at harmonic frequencies and the inaccurate assessment of three-phase harmonic injections.

ACKNOWLEDGEMENTS

The authors wish to acknowledge the advice received from Professor H.W. Dommel and the technical assistance of Mr. S. Gellen with the software needed to obtain the graphic results. The authors are also grateful to Mr. K. McCool, General Manager of New Zealand Electricity and to Mr. J.F. Baird of Systems Software and Instrumentation for their help.

REFERENCES

[1] J. Arrillaga and B.J. Harker, "Fast decoupled three phase load flow", Proc. IEE, vol. 125, no. 8, pp. 734-740, August 1978.

[2] B.J. Harker and J. Arrillaga, "3-phase ac/dc load flow", Proc. IEE, vol. 126, no. 12, pp. 1275-1281, December 1979.

[3] G.H. Robinson, "Harmonic phenomena associated with the Benmore-Haywards hvdc transmission scheme", New Zealand Engineering, 21(1) Jan. 1966, pp. 16-29.

[4] L.N.M. Edward et al, "Harmonic measurement and the selective audio frequency power analyser", IEE Publication No. 197, CIRED, 1981, pp. 81-85.

[5] M.A. Pesonen, "Harmonics, characteristic parameters, methods of study, estimates of existing values in the network", ELECTRA, vol. 77, pp. 35-54.

[6] E.W. Kimbark, "Electrical transmission of power and signals", John Wiley, New York, 1949, chapter 6,15,9.

[7] M.H. Hesse, "Electromagnetic and electrostatic transmission line parameters by digital computer", Trans. IEEE, vol. PAS-82, pp. 282-291, June 1963.

[8] D. Coleman, F. Watts, and R.B. Shipley, "Digital calculation of overhead transmission line constants", Trans. AIEE, vol. 77, pp. 1266-68, 1958.

[9] W.I. Bowman and J.M. McNamee, "Development of equivalent Pi and T matrix circuits for long untransposed transmission lines", Trans. IEEE, vol. PAS-84, pp. 625-632, June 1964.

[10] J.H. Wilkinson and C. Reinsch, "Handbook for automatic computations, Vol. II Linear algebra", Springer-Verlag, 1971.

[11] R.A. Chipman, "Theory and problems of transmission lines", Schaums Outline Series McGraw-Hill, 1968.

[12] E. Clarke, "Circuit analysis of A-C power systems", John Wiley, New York, 1943, chapter 6.

[13] J.R. Carson, "Wave propagation in overhead wires with ground return", Bell Systems Technical Journal, vol. 5, pp. 539-54, 1926.

[14] V.A. Lewis and P.D. Tuttle, "The resistance and reactance of aluminium conductors steel reinforced" Trans. AIEE, PAS-77, pp. 1189-1215, 1958.

APPENDICES

(i) Formulation of Line Parameters

Series elements:

The total series inductance of a single phase circuit is:

$$L = L_1 + L_2 - 2M$$

where

$$L_1 = L_2 = \frac{\mu_o}{2\pi} \ln \frac{1}{GMR}$$

$$M = \frac{\mu_o}{2\pi} \ln \frac{1}{d}$$

L_1 = self inductance of conductor 1

L_2 = self inductance of conductor 2

M = mutual inductance between conductors 1 and 2

d = distance between conductor centres

μ_o = permeability of free space

GMR = effective geometric mean distance or the radius of an infinitely thin tube that gives the same inductance as the two terms of the self inductance.

The self impedance per kilometer of conductor a with earth return (Zaa), and the mutual impedance per kilometer between conductors a and b (Zab) are expressed [12]:

$$Z'_{aa} = R'_a + R'_g + j(X'_{aa} + X'_g)$$

$$Z'_{ab} = R'_g + j(X'_{ab} + X'_g)$$

R'_d = ac resistance of conductor a

X'_{aa} = self reactance of conductor a

X'_{ab} = mutual reactance between conductors a and b

R'_g, X'_g = Carson's earth return corrections [13]

The effect of earth resistivity on the self reactance X'_{aa} at 50 Hz can be assessed from the approximate expression:

$$X'_{aa} = .00289\ f \log\ (\frac{660\sqrt{\rho/f}}{GMR})\ \Omega/km$$

Shunt Elements:

The following approximate relationships can be written for the potential coefficients:

$$P'_{aa} = \frac{1}{2\pi\varepsilon_o} \ln\ (\frac{2H}{R})\ km/F$$

$$P'_{ab} = \frac{1}{2\pi\varepsilon_o} \ln\ (\frac{D_{ab}}{d_{ab}})\ km/F$$

where

P'_{aa} = potential coefficient of conductor a
P'_{ab} = potential coefficient between conductors a and b
H = average height of the conductor above ground in m
R = conductor radius
d_{ab} = distance between conductors a and b in m
D_{ab} = distance between conductor a and the image of conductor b in m
ε_o = permeativity of free space

(ii) Skin Effect Formulation

The development of skin effect relationships is as follows [11]

$$J_z(r) = \sigma E_z(r)$$

where $J_z(r)$ is the current density and $E_z(r)$ is the electric field intensity at radius r. Using Faraday's law:

$$\int \bar{E}\cdot d\bar{\ell} = \frac{-\partial}{\partial t} \int_s \bar{B}\cdot d\bar{s}$$

where B is the magnetic flux density, and solving gives

$$\frac{\partial^2 J_z(r)}{\partial r^2} + \frac{1}{r}\frac{\partial J_z(r)}{\partial r} - j\omega\mu\sigma J_z(r) = 0$$

The solution for $J_z(r)$ is:

$$J_z(r) = A_1 J_o\ [(\sqrt{-j\omega\mu\sigma})r] + A_2\ Y_o\ [(\sqrt{-j\omega\mu\sigma})r]$$

where J_o and Y_o are Bessel functions of the first and second kinds respectively, of order zero. These functions can be broken into real and imaginary parts:

$$ber(x) = REAL\ [J_o(\sqrt{-j}\ x)]$$
$$bei(x) = IMAGINARY\ [J_o(\sqrt{-j}\ x)]$$
$$ker(x) = REAL\ [Y_o(\sqrt{-j}\ x)]$$
$$kei(x) = IMAGINARY\ [Y_o(\sqrt{-j}\ x)]$$

Hence

$$J_z(r) = A_1\ (ber(\sqrt{\omega\mu\sigma}\ r) + jbei(\sqrt{\omega\mu\sigma}\ r)) + A_2(ker(\sqrt{\omega\mu\sigma}\ r) + jkei\ (\sqrt{\omega\mu\sigma}\ r))$$

If the internal impedance Z is

$$Z(r) = \frac{J_z(r)}{\sigma I_z(r)}$$

and from Maxwell's equations

$$\frac{\partial E_z(r)}{\partial r} = j\omega\mu H_\theta(r)$$

and Ampere's Law

$$I_z(r) = 2\pi r H_\theta(r)$$

gives

$$R = REAL\ (\frac{j\mu\omega}{2\pi a}\frac{J_z(r)}{\partial J_z(r)/\partial r|_{r=a}})$$

where a is the outside radius of the conductor.

Using the computer realizable relationships [13] and assuming that the ACSR cable can be approximated to tubes that just enclose the aluminium strands, gives:

$$\frac{R}{Rdc} = \frac{ma}{2}\frac{(a^2-q^2)}{a^2}\ \frac{(KN-ML)}{M^2+N^2}$$

N = J + bei' ma
L = H + bei ma
M = I + bei' ma
K = G + ber ma
J = F ker' ma + E kei' ma
I = E ker' ma - F kei' ma
H = F ker ma + kei ma
G = E ker ma - F kei ma

$$F = -\frac{(ker'\ mq)\ (bei'\ mq) - (kei'\ mq)\ (ber'\ mq)}{(ker'\ mq)^2 + (kei'\ mq)^2}$$

$$E = -\frac{(ber'\ mq)\ (ker'\ mq) + (bei'\ mq)\ (kei'\ mq)}{(ker'\ mq)^2 + (kei'\ mq)^2}$$

$$m = \sqrt{\frac{8\pi^2 f}{\rho}}$$

t = a-q
t is the thickness and q the inside radius of the conductor.

(iii) Transmission Line Data

All the results discussed in the paper relate to the 220 kV line of flat configuration between Islington and Kikiwa (of the New Zealand system). The main parameters of this line are as follows:

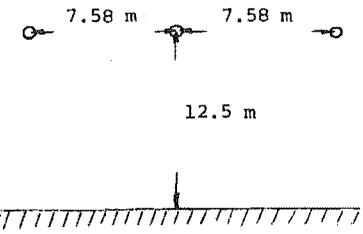

Conductor type Zebra (54/3.18 + 7/3.18)
Length = 230 km

THREE PHASE TRANSMISSION SYSTEM MODELLING FOR HARMONIC PENETRATION STUDIES

T.J. Densem, Student Member
New Zealand Electricity

P.S. Bodger, Non Member
J. Arrillaga, Non Member
University of Canterbury,
Christchurch, New Zealand

Abstract - Three phase modelling of an a.c. transmission system is presented for harmonic penetration studies. Circuit coupling and impedance unbalance are incorporated in a simulation programme which models an 86 bus equivalent of the New Zealand South Island system. A comparison of measured and simulated results at the current injection busbar is used to select system component models; then results of impedances and sequence voltages are presented for selected busbars when the system is subjected to current unbalance and circuit configuration changes.

INTRODUCTION

The use of impedances and sequence voltages at harmonic frequencies are convenient methods of presenting the complexity of an electric power system network in a simple form. Given this information the engineer can design for the inclusion of filters or observe the effect of the addition of harmonic sources such as high power d.c. convertors, in the form of industrial loads or HVDC transmission schemes. A knowledge can also be gained of the system harmonic response under varying daily load curves as well as normal daily circuit switching due to maintenance or faults.

Harmonic impedances, calculated from the measured values of voltage and current of practical tests, only represent the system at the time of the test and assume a single source of harmonic current.

Harmonic network modelling on the other hand, uses known system components such as transmission lines, generators, loads and transformers, along with the interconnections and couplings of each component, with which the total network can be modelled and the system impedances calculated. Modelling enables these impedances to be calculated for any point in the system.

An impedance-frequency characteristic curve was obtained by Laurent [1] using a reduced scale model of the French 225 kV system. It was possible to measure system node voltages and observe the effects of the inclusion of filters. Hingorani [2] used this curve to calculate an equivalent LRC circuit for which filter design studies at an HVDC terminal were undertaken.

This type of equivalent circuit is similar to results obtained by practical measurement in that the impedance-frequency curve represents a single snapshot of the system and therefore suffers the same restriction of use.

Digital computer network models at harmonic frequencies have been developed, which represent the system as individual elements connected in the manner of the physical network. Campbell [3] used balanced circuit parameters and loads, and reduced the transmission system to a single phase equivalent represented by the positive sequence values. Network elements were linear and passive, allowing analysis at individual harmonic frequencies. Breuer [4] compares a single phase positive sequence equivalent impedance of a balanced three phase network with measured test data. There are frequencies where the comparison of these is poor. The balanced impedance model does not allow for presentation of unbalanced impedances as reported in the measured test data. A further paper [5] also covers the use of a single phase network model, evaluated for characteristic harmonics.

Harmonic penetration studies have also been undertaken for distribution systems [6,7]. In the former, low order balanced and unbalanced characteristic harmonics are injected from a convertor load. Symmetrical component matrix analysis is used to obtain harmonic voltages at specific network buses. In the latter paper, multiphase analysis is applied where coupling exists between double circuits. Again, characteristic harmonic responses are analysed. The transmission system is represented as a short circuit equivalent at the high side of the substation transformer.

While representation of three phase unbalanced impedance networks in harmonic analysis has been reported; it has been confined to distribution networks and to the study of characteristic harmonics. Actual presentation of results and the significance of these, as compared to single phase harmonic modelling, has not been adequately conveyed.

It is thus the subject of this paper to present the 3Ø impedance characteristics and sequence voltages of an a.c. transmission system for any harmonic, and to discuss the effect of unbalanced current injection along with circuit configuration changes.

THREE PHASE HARMONIC NETWORK MODELLING

For the three phase network, unbalanced self and mutual impedances of network elements can be modelled as well as circuit coupling. It is assumed that the a.c. system is linear and passive and therefore the principle of superposition may be applied to enable each harmonic to be considered independently.

In a multibranch interconnected network, an admittance matrix $[Y_h]$ is formed from the individual elements, for any particular harmonic frequency h. Harmonic currents are injected into the bus under consideration and the voltages throughout the system are calculated from the solution of

$$[I_h] = [Y_h][V_h]$$

where for the three phase system, the elements of the admittance matrix are formed from the 3 x 3 matrix of self and transfer impedances.

Using Gaussian elimination and back-substitution, advantage is taken of the symmetry and sparsity of the admittance matrix [8]. Row ordering techniques reduce the amount of off-diagonal element build-up during the triangulation of $[Y_h]$. It is possible to keep storage down to approximately ten times that of the single phase representation.

The injected currents at most a.c. busbars will be zero, since the sources of the harmonics considered are generally from d.c. convertors. To calculate the impedances, it is necessary to form the admittance matrix with those buses at which harmonic current injection occurs, ordered last. The matrix is then triangulated using Gaussian elimination, down to but

83 SM 444-7 A paper recommended and approved by the IEEE Transmission and Distribution Committee of the IEEE Power Engineering Society for presentation at the IEEE/PES 1983 Summer Meeting, Los Angeles, California, July 17-22, 1983. Manuscript submitted January 28, 1983; made available for printing May 10, 1983.

excluding the rows of the specified buses. The resulting matrix equation is

$$\begin{bmatrix} 0 \\ \vdots \\ 0 \\ \hline I_j \\ \vdots \\ I_N \end{bmatrix} = \begin{bmatrix} & & \\ & 0 & \\ & & \\ \hline & Y_{jj} \cdots Y_{jN} & \\ & \vdots \quad \ddots \quad \vdots & \\ & Y_{Nj} \cdots Y_{NN} & \end{bmatrix} \cdot \begin{bmatrix} V_1 \\ \vdots \\ V_{j-1} \\ \hline V_j \\ \vdots \\ V_N \end{bmatrix}$$

As a consequence, $I_j \ldots I_N$ remain unchanged since the currents above these in the current vector are zero.

The reduced matrix equation is

$$\begin{bmatrix} I_j \\ \vdots \\ I_N \end{bmatrix} = \begin{bmatrix} Y_{jj} \cdots Y_{jN} \\ \vdots \quad \ddots \quad \vdots \\ Y_{Nj} \cdots Y_{NN} \end{bmatrix} \cdot \begin{bmatrix} V_j \\ \vdots \\ V_N \end{bmatrix}$$

where the admittance matrix is of order equal to 3 times the number of injection busbars. The elements are the self and transfer admittances of the reduced total system as viewed from the injection busbars.

This reduced matrix is particularly useful for studies of interaction between two or more sources of harmonics and provides complete flexibility to considering unbalanced (both in magnitude and phase) current injections.

To compare measured and simulated impedances for a current injection busbar, it is necessary to define equivalent phase impedances, derived from the 3 x 3 admittance matrix. If I_1 = 1 p.u. $\angle 0^\circ$, I_2 = 1 p.u. $\angle -120^\circ$ and I_3 = 1 p.u. $\angle 120^\circ$, then the matrix equation

$$\begin{bmatrix} I_1 \\ I_2 \\ I_3 \end{bmatrix} = \begin{bmatrix} Y_{11} & Y_{12} & Y_{13} \\ Y_{21} & Y_{22} & Y_{23} \\ Y_{31} & Y_{32} & Y_{33} \end{bmatrix} \cdot \begin{bmatrix} V_1 \\ V_2 \\ V_3 \end{bmatrix}$$

can be solved for V_1, V_2 and V_3. The equivalent phase impedances are then

$$Z_1 = \frac{V_1}{I_1}, \quad Z_2 = \frac{V_2}{I_2}, \quad Z_3 = \frac{V_3}{I_3}$$

Finally, the impedances can be plotted in their cartesian co-ordinates over the range of frequencies of interest. This has previously been presented for single phase impedance-frequency data in refs. [1, 2, 3, 5].

NETWORK ELEMENT MODELS

Models of network elements have been developed which are useful for both single phase and three phase harmonic studies. Where relevant, coupling between circuits and impedance unbalance due to network configurations must be taken into account for the three phase analysis. However, there is disagreement as to which models are best for generators, loads and transformers [9]. As a consequence, the models used have been derived from a comparison of measured test results and those given by the three phase modelling.

Transmission Lines

In general, the lumped parameter or nominal π approximation commonly used for fundamental frequency analysis, where most lines may be considered electrically short, cannot be applied when higher harmonic frequencies are being considered. Also, cascading nominal π's has computational, storage and accuracy problems for large systems. Instead, a multi-conductor equivalent π model [10], which incorporates skin effect, using eigenvalue analysis and modal transformations, considerably reduces the above problems.

Filters

Single tuned and high pass shunt filters are usually connected to the a.c. terminal busbars of high power d.c. convertor installations. These are represented as uncoupled LRC branches in three phase modelling, allowing for unbalanced parameters which may be due to capacitor failure.

Synchronous Generator Models

In general, it may be assumed that the synchronous generators produce no harmonic currents and they may therefore be modelled simply by a shunt connected impedance at their terminal busbar. The two generator models compared are [11]

A. 100% of the subtransient reactance with a power factor of 0.2.

B. 80% of the subtransient reactance with a power factor of 0.2.

Load Models

By using the specified values of real and reactive power demand at 50 Hz, P_{50} and Q_{50}, an impedance can be evaluated for each frequency. The load models considered are:

A. $R = \frac{V^2}{P_{50}}$, $X = \frac{V^2}{Q_{50}}$

and $\frac{1}{Z_n} = k\left(\frac{1}{R} + \frac{1}{jX}\right)$

where $k = 0.1\,h + 0.9$

h is the harmonic number while V is the nominal voltage. This model is based on that of ref. [9].

B. $R = \frac{V^2}{P_{50}}$, $X = \frac{V^2}{Q_{50}}$

and $\frac{1}{Z_n} = \frac{1}{R} + \frac{1}{jhX}$

C. The load is represented by a reactance X_s in series with a resistance R, both connected in parallel with a reactance X_p such that [9]

$$R = \frac{V^2}{P_{50}}$$

$$X_s = 0.073\,hR$$

$$X_p = hR/\left(6.7\,\frac{Q_{50}}{P_{50}} - 0.74\right)$$

D. $R = \frac{V^2}{P_{50}}$, $X = \frac{V^2}{Q_{50}}$

and $\frac{1}{Z_n} = \frac{1}{R} + \frac{1}{jX}$

Transformer Modelling

Transformer models developed for fundamental frequency are also used in harmonic studies except for the values of damping resistance and leakage reactance. A primitive, six by six admittance matrix is formed for a two winding, 3Ø transformer and the nodal admittance

matrix derived from this [10].

The transformer models compared are:

A.

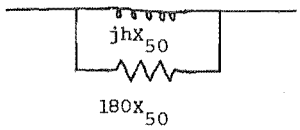

where X_{50} is the leakage reactance at 50 Hz [12].

B.

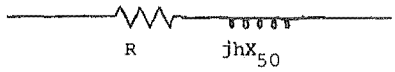

where $R = .1026\ Kh\ X_{50}(J+h)$ [13]

and J is the ratio of hysteresis to eddy current losses taken as 3 for silicon steels.

$$k = \frac{1}{J+1}$$

C. As for B except R and X are scaled to 80% of the 50 Hz values [13].

D.

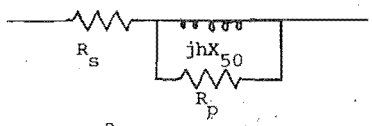

where, $90 < V^2/SR_s < 110$

$13 < SR_p/V^2 < 30$

with S being the rated power of the transformer [9]. For this case, R_s = 0.04 p.u. and R_p = 60 p.u. which corresponds to a 30 MVA rating.

E. As for D but with R_s = 0.01 p.u. and R_p = 20 p.u., corresponding to a 100 MVA rating.

Choice of Component Models

The main interconnections for the New Zealand South Island electric power transmission system below Bromley, are presented in Fig. 1. The results used for comparison in this paper refer to the test where at Tiwai, the site of a large aluminium smelter, 7 rectiformers were in operation, however, harmonic filters were out of service.[14] At Benmore, the interisland HVDC link was connected to the system and filters at that site were in service. This test gave maximum harmonic current injection at Tiwai, and hence maximum measurable voltage levels on the system. However, with the HVDC connected at Benmore, another source of harmonic current injection was present on the system.

The impedances for the system, as measured at one instant of time from the Tiwai 220 kV busbar, are presented in Fig. 2 for characteristic harmonics.

Using an 86 bus computer simulation model of the system, 3Ø impedances were calculated and then compared to the measured values.

It was observed that the calculated impedances were most sensitive to changes in the transmission system. In practice, the exact length of conductors is not known and it is usual to calculate approximate lengths from map profiles of a circuit. Thus it is possible that small line length errors may arise due to conductor sag and terrain unevenness. Additional to this, uncertainty in the spacing between circuits and different conductor configurations along the lines, add errors that are difficult to assess. While this is not significant at fundamental frequency, it is important at higher order harmonics. The combination of the

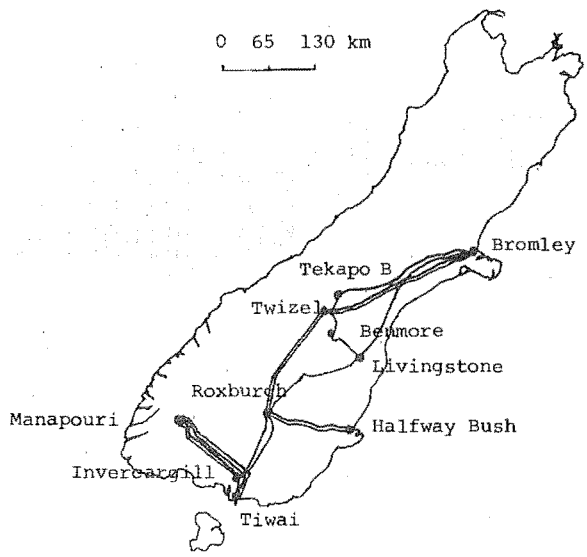

Fig. 1. New Zealand South Island 220 kV transmission system as used in the simulation studies. (Lower voltage interconnections not shown).

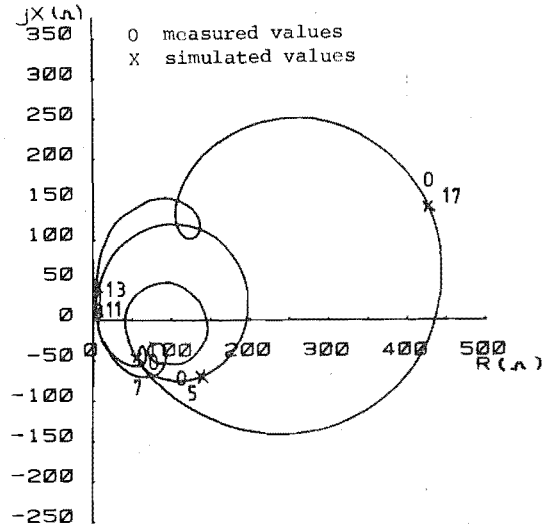

Fig. 2. Measured and simulated yellow phase characteristic harmonic impedances for the South Island transmission system as measured from Tiwai 220 kV busbar.

above inaccuracies required that the lines connected to Manapouri needed to be increased in length by 9 km to give the correct resonant frequencies.

Changing the other component models was seen to have the greatest effect on the magnitude and phase angles at the points of parallel resonance. Consequently, the measured values of 5th and 17th harmonic impedances have been compared to the simulated values for the generator, load and transformer models discussed and are presented in Table I. Using generator model A gave better magnitudes at the 5th harmonic, load model A gave closer magnitudes at the 17th harmonic, and transformer model A gave closest agreement with the 17th harmonic impedance.

The sensitivity of the results is however not high, as a number of similar results were obtained. There is no single model combination that is substantially better than the others. The models above are used as the basis for comparison of measured and simulated results for selected busbars throughout the South Island system, discussed in the next section.

Table I. Measured and Simulated Values of Harmonic Impedances at Tiwai to Determine Generator, Load and Transformer Models (ohms).

Case	Transformer Model	Generator Model	Load Model		5th harmonic	17th harmonic
Measured				R	138 - j 68	491 + j 95
				Y	112 - j 73	422 + j179
				B	150 - j109	489 + j117
					187 - j104	479 + j145
1	A	A	A		136 - j 66	425 + j122
					168 - j 75	348 + j182
					183 - j121	441 + j152
2	A	A	B		132 - j 80	392 + j130
					164 - j 90	324 + j184
					193 - j104	403 + j132
3	A	A	C		145 - j 68	362 + j114
					173 - j 80	301 + j160
					189 - j114	438 + j143
4	A	A	D		138 - j 75	389 + j122
					169 - j 85	323 + j176
					174 - j 89	411 + j 60
5	B	A	A		130 - j 55	369 + j 57
					153 - j 62	326 + j114
					192 - j 74	386 + j101
6	C	A	A		144 - j 48	350 + j 91
					169 - j 45	300 + j136
					173 - j 86	484 + j147
7	D	A	A		128 - j 54	429 - j124
					151 - j 61	351 + j185
					184 - j100	483 + j154
8	E	A	A		135 - j 63	429 + j129
					165 - j 72	349 + j188
					234 - j 90	415 + j201
9	A	B	A		164 - j 59	381 + j175
					203 - j 54	297 + j208
					228 - j 40	335 + j131
10	C	B	A		168 - j 29	310 + j121
					190 - j 13	259 + j148
					233 - j 50	322 + j125
11	C	B	D		173 - j 36	298 + j115
					196 - j 21	250 + j145

COMPARISON OF MEASURED TEST DATA AND SIMULATION RESULTS

Harmonic measurements were made simultaneously at six sites in the system. Yellow phase was used at all sites except at Tiwai where all three phases were measured. In Table II these have been compared to values obtained by the 3Ø harmonic simulation programme, which has component models as previously discussed, and with currents as for the tests at Tiwai.

There is good agreement between the results for the 5th and 17th harmonics and the low measured values of the 11th and 13th harmonic have been simulated. Values at busbars which are at substantial distances from the injection point, namely Benmore and Bromley, show acceptable agreement over all frequencies.

Simulated results for Halfway Bush are low at the 5th and 7th harmonics (1.34%, 0.39% compared with the measured values of 1.78% and 0.77%), and at Manapouri, there is a substantial difference between simulated and measured results at the 5th and 7th harmonic.

In general, it can be said that agreement between the simulated and measured results was acceptable for this case of balanced characteristic harmonic currents. However, there are three possible areas of inaccuracy in the results.

1. The presence of multiple harmonic sources - Tiwai and Benmore in this case. It is difficult to make accurate comparisons unless the current injections for all sources are known and can be modelled.
2. Accuracy of transducers and measuring instruments. The non-linearity of transducers, particularly voltage transducers, has previously been recognized [9]. This is a possible source of error at Manapouri and Halfway Bush where CVT's were used.
3. Measurement of an insufficient number of parameters. The three phase nature of harmonics, dictates that accurate simulation and test comparisons require 12 separate variables to be measured at each bus. For each phase, the magnitude of the current injections, the voltage, and the angles of both quantities to some reference, are required. In the tests referred to, only nine of these variables were recorded at Tiwai. Currents on each phase were assumed to be separated by 120° for the simulation studies.

VERSATILITY OF 3Ø HARMONIC MODELLING

It has been established that a reasonable agreement exists between measured test data and simulated data using 3Ø modelling of the transmission system. In this section, different practical considerations are discussed which show the versatility of the 3Ø modelling.

Circuit Coupling and Impedance Unbalance

It can be observed from Fig. 1 that many of the 220 kV circuits in the S.I. transmission system share common rights of way. A reduced portion of the 86 bus system is presented in Fig. 3.

A feature of Fig. 3 is the inclusion of 120 km of 2 double circuit towers coupled together from Manapouri. The geometry of each circuit is such that mutual impedance unbalance exists between phases. Thus, to have a more realistic representation of the system, coupling between these circuits as well as impedance unbalance between phases was represented in the 3Ø modelling. This is not possible in 1Ø modelling. In Fig. 4 the complete system impedance-frequency loci for the three phases of the S.I. system as seen from Tiwai is presented, along with sequence voltages at selected busbars. The impedance plot clearly indicates the considerable unbalance which exists at various harmonic frequencies

Table II. Comparison of Measured and Simulated Harmonic Voltages (percent of nominal phase to neutral voltage)

		5th		7th		11th		13th		17th		19th		23rd	
		M	S	M	S	M	S	M	S	M	S	M	S	M	S
TIWAI	R	1.96	2.51	0.72	0.80	0.12	0.04	0.18	0.10	1.77	1.76	0.23	0.16	0.31	0.27
	Y	1.83	2.34	0.71	1.09	0.05	0.05	0.09	0.11	1.66	1.58	0.17	0.23	0.27	0.22
	B	2.52	2.46	0.63	0.47	0.03	0.07	0.08	0.19	1.75	1.48	0.11	0.10	0.27	0.31
INVERCARGILL		1.76	2.05	0.50	0.84	0.07	0.03	0.00	0.01	0.69	0.59	0.10	0.17	0.35	0.34
MANAPOURI		0.1	2.10	0.02	0.66	0.01	0.25	0.03	0.16	1.64	1.56	0.00	0.24	0.00	0.29
BENMORE		0.29	0.49	0.13	0.07	0.06	0.00	0.07	0.00	0.09	0.12	0.00	0.11	0.04	0.26
HALFWAY BUSH		1.78	1.34	0.77	0.38	0.23	0.02	0.00	0.03	0.85	0.47	0.20	0.21	0.00	0.19
BROMLEY		0.42	0.95	0.23	0.17	0.13	0.00	0.08	0.00	0.24	0.11	0.00	0.09	0.08	0.08

M - measured
S - simulated

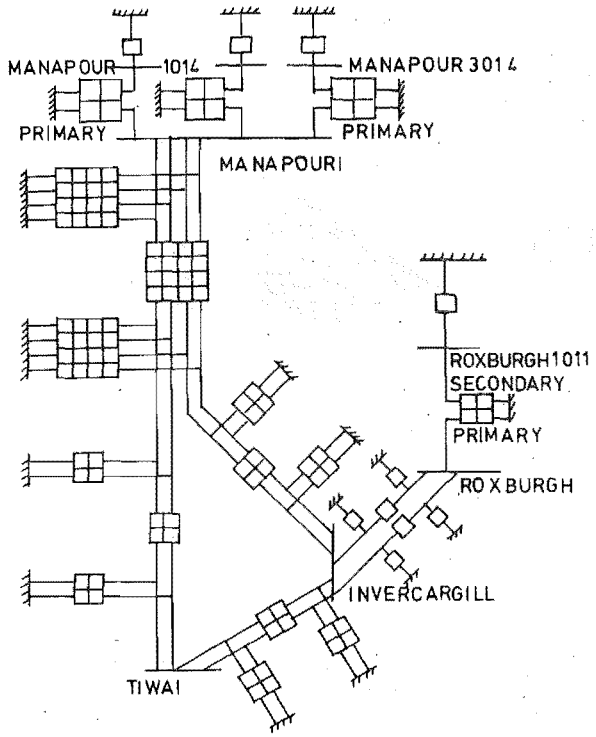

Fig. 3. South Island system close to Tiwai busbar showing circuit coupling with each 3 x 3 matrix block represented.

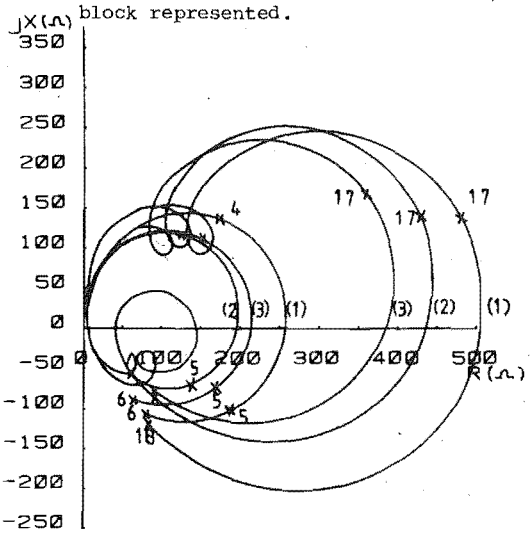

Fig. 4. (a) Impedances for the South Island system 1) Red Phase 2) Yellow Phase 3) Blue Phase

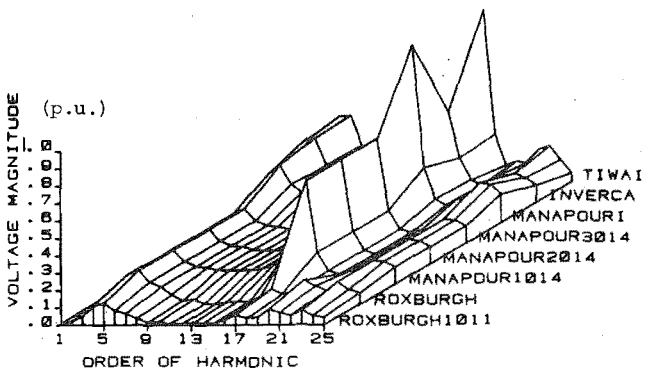

Fig. 4. (b) Positive sequence voltages at selected busbars for positive sequence current injection at Tiwai normalized to 1 p.u.

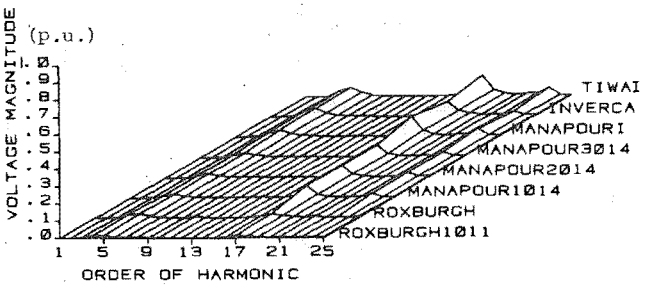

Fig. 4. (c) Negative sequence voltages for normalized positive sequence current injection at Tiwai.

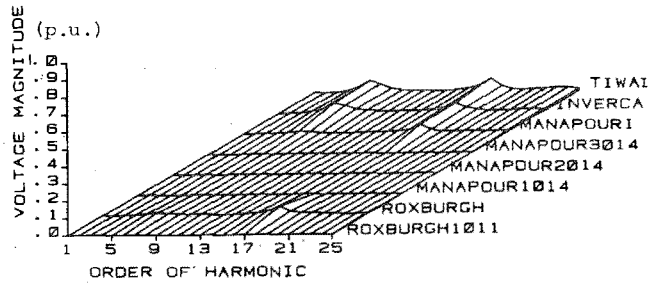

Fig. 4. (d) Zero sequence voltages for normalized positive sequence current injection at Tiwai.

and particularly at the resonant points, even though the system is reasonably balanced at fundamental frequency.

Unbalanced Harmonic Current Injections

The major source of harmonics which are troublesome in the a.c. system is the high power d.c. convertor. The harmonic currents injected into the a.c. system by the convertor are, in general, unbalanced between phases; the unbalance being more extreme for the case of non-characteristic harmonic orders. Measurements of the harmonic currents at the rectifier end of the N.Z. d.c. link have shown an average deviation between phases of 35% [15]. Also, similar unbalances are reported at Tiwai in the tests [14]. Only a 3Ø model, which includes coupling and impedance unbalance, can accurately assess the effect of current injection unbalance.

Unbalanced currents of 1 p.u. $\angle 0^\circ$, 0.65 p.u. $\angle -120^\circ$ and 0.65 p.u. $\angle 120^\circ$ were injected into the system at the Tiwai bus. The three dimensional diagrams of Fig. 5 show the positive, negative and zero sequence voltages for some of the busbars of Fig. 1.

These should be compared to the balanced current injection case of Fig. 4(b)-4(d). With unbalanced current injection, the zero sequence resonant frequencies do not correspond with those of the positive sequence. There is considerable 6th harmonic compared to the 5th harmonic of the positive sequence.

Busbars not at the injected bus voltage level, Roxburgh 1011, Manapouri 1014, Manapouri 2014 and Manapouri 3014, have reduced voltage levels caused by the voltage drop through the respective transformers. Also, these busbars have no zero sequence voltage. The transformers are STAR-G DELTA and act as a short circuit on the primary to any zero sequence current flow.

System Configuration Change

The addition or removal of transmission lines are the result of routine maintenance, protection operation under fault conditions, or future system development. The equivalent phase impedances for the 23rd harmonic are shown in Table III for a single line open circuited

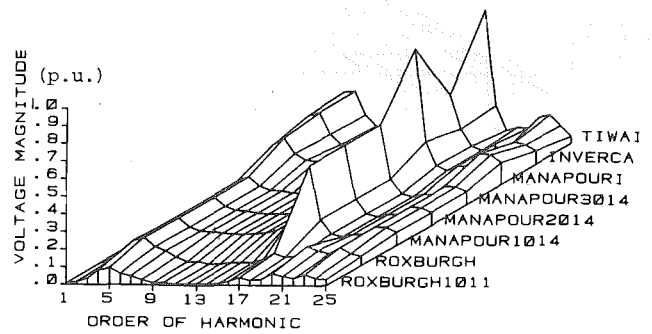

Fig. 5. (a) Positive sequence voltages at selected busbars for unbalanced current injection at Tiwai.

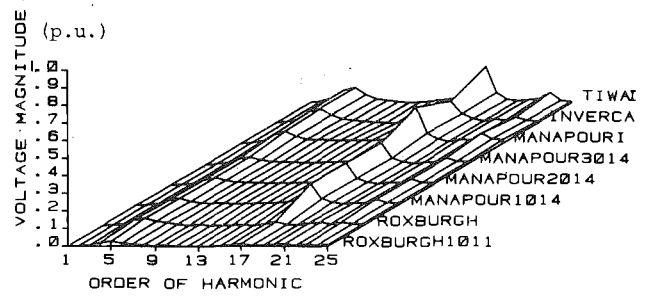

Fig. 5. (b) Negative sequence voltages for unbalanced current injection at Tiwai.

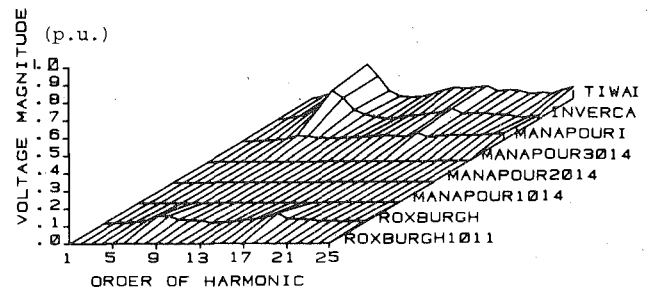

Fig. 5. (c) Zero sequence voltages for unbalanced current injection at Tiwai.

Table III. 23rd Harmonic Impedance Magnitudes at Tiwai for Single Circuit Outage (ohms).

		Measured Test Results	Simulated Results
Before line outage	R	96	96
	Y	86	79
	B	88	92
After line outage	R	127	128
	Y	95	109
	B	107	121

between Tiwai and Manapouri. This line remains coupled to the other circuits sharing the same right of way. While for this outage only a small change in bus voltages was observed, when two lines are open circuited, a high 24th harmonic response is apparent as observed in Fig. 6. The presence of 17th harmonic on the temporary

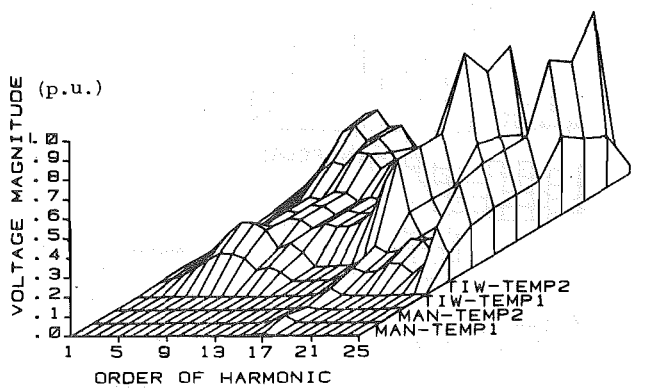

Fig. 6. Positive sequence voltages at selected busbars with both lines from Tiwai to Manapouri open circuited. Current injection at Tiwai normalized to 1 p.u.

busbars of the open circuit lines is evidence of the coupling between circuits.

CONCLUSIONS

While a symmetric transmission system can be modelled by a 1Ø representation in harmonic penetration studies, it is necessary to expand to a 3Ø representation when unsymmetrical conditions such as circuit coupling and impedance unbalance are taken into account. Moreover, the 3Ø representation allows for analysis of unbalanced harmonic current injection, a condition which is most likely to be found in a practical system.

It has been shown that by taking the unbalance into account, satisfactory comparisons between simulated and measured data can be achieved. It was observed that the sensitivity of simulated impedance results was most susceptible to the transmission lines connected to the harmonic current injection busbar and that models of generators, loads and transformers had less significant effects. Selection of the latter was achieved from a best fit between measured and simulated impedances for specific harmonics.

The models were then used to provide sequence voltages at other system busbars, and impedances at the current injection busbar. These agreed well with measured data.

In this way the simulation method can be seen to be complementary to test methods in that once a model has been established, it can be used to provide the above information for any point in the system; a task very difficult to achieve by simultaneous measurement. The model also allows for easy investigation into the effects of system line changes due to daily operational considerations or future development strategies. Although not reported here, load changes have been modelled. However these appear to have little effect on system voltages and impedances.

A facility of the 3Ø modelling is that impedances and voltages at any frequency can be obtained, not just those for characteristic harmonics. This allows for the study of non-harmonic ripple frequency overspill from one distribution system into another via the transmission system, as a result of direct load management activities. Further, more than one source of harmonics can be included in the system as occurs in practice, and the interactions between these sources can be investigated. Both of these topics are areas of ongoing research.

ACKNOWLEDGEMENTS

The authors are grateful to Mr. K. McCool, General Manager of New Zealand Electricity, for his support.

REFERENCES

[1] P.G. Laurent, "D.C. interconnection between France and Great Britain by submarine cables", Cigre, v. III, 1962, paper: 331.

[2] N.G. Hingorani and M.F. Burberry, "Simulation of A.C. system impedance in HVDC system studies", IEEE Trans., PAS-89, no. 5/6, May/June 1970, pp. 820-828.

[3] L.C. Campbell and N.S. Murray, "Harmonic penetration into power systems", 5th Universities Power Engineering Conference, Swansea, Wales, 1970.

[4] G.D. Breuer, et al, "HVDC-AC harmonic interaction, Parts I and II", IEEE Trans., PAS-101, no. 3, March 1982, pp. 701-718.

[5] A.A. Mahmoud, "A method for analyzing harmonic distribution in a.c. power systems", IEEE Trans., PAS-101, no. 6, June 1982, pp. 1815-1824.

[6] D.J. Pileggi, et al, "Prediction of harmonic voltages in distribution systems", IEEE Trans., PAS-100, No. 3, March 1981, pp. 1307-1315.

[7] M.F. McGranaghan, et al, "Digital simulation of distribution system frequency-response characteristics", IEEE Trans., PAS-100, no. 3, March 1981, pp. 1362-1369.

[8] K. Zollenkopf, "Bi-factorization-basic computational algorithm and programming techniques", Conference on Large Sets of Sparse Linear Equations, Oxford, 1970, pp. 75-96.

[9] Cigre, "Harmonics, characteristic parameters, methods of study, estimates of existing values in the network", ELECTRA, no. 77, July 1981, pp. 35-54. *Pesaran, M.A.

[10] J. Arrillaga, et al, "Zero sequence harmonic current generation in transmission lines connected to large convertor plant", Accepted for publication, PES Winter Power Meeting, N.Y., February 1983.

[11] T.W. Ross and R.M.A. Smith, "Centralized ripple control on high voltage networks", Proc. IEE, vol. 95, pt. III, Oct. 1948, pp. 470-479.

[12] B.J. Harker, "Steady state analysis of integrated a.c. and d.c. systems", Ph.D. Thesis, University of Canterbury, New Zealand, 1980.

[13] J. Baird, "Elafant - audio frequency analysis of a power system", New Zealand Electricity, 1981.

[14] P.R. Hyland, "Report on Harmonics Test conducted on July 8, 1981", New Zealand Electricity.

[15] G.H. Robinson, "Harmonic phenomena associated with the Benmore-Haywards hvdc transmission scheme", New Zealand Engineering, 21(1), Jan. 1966, pp. 16-29.